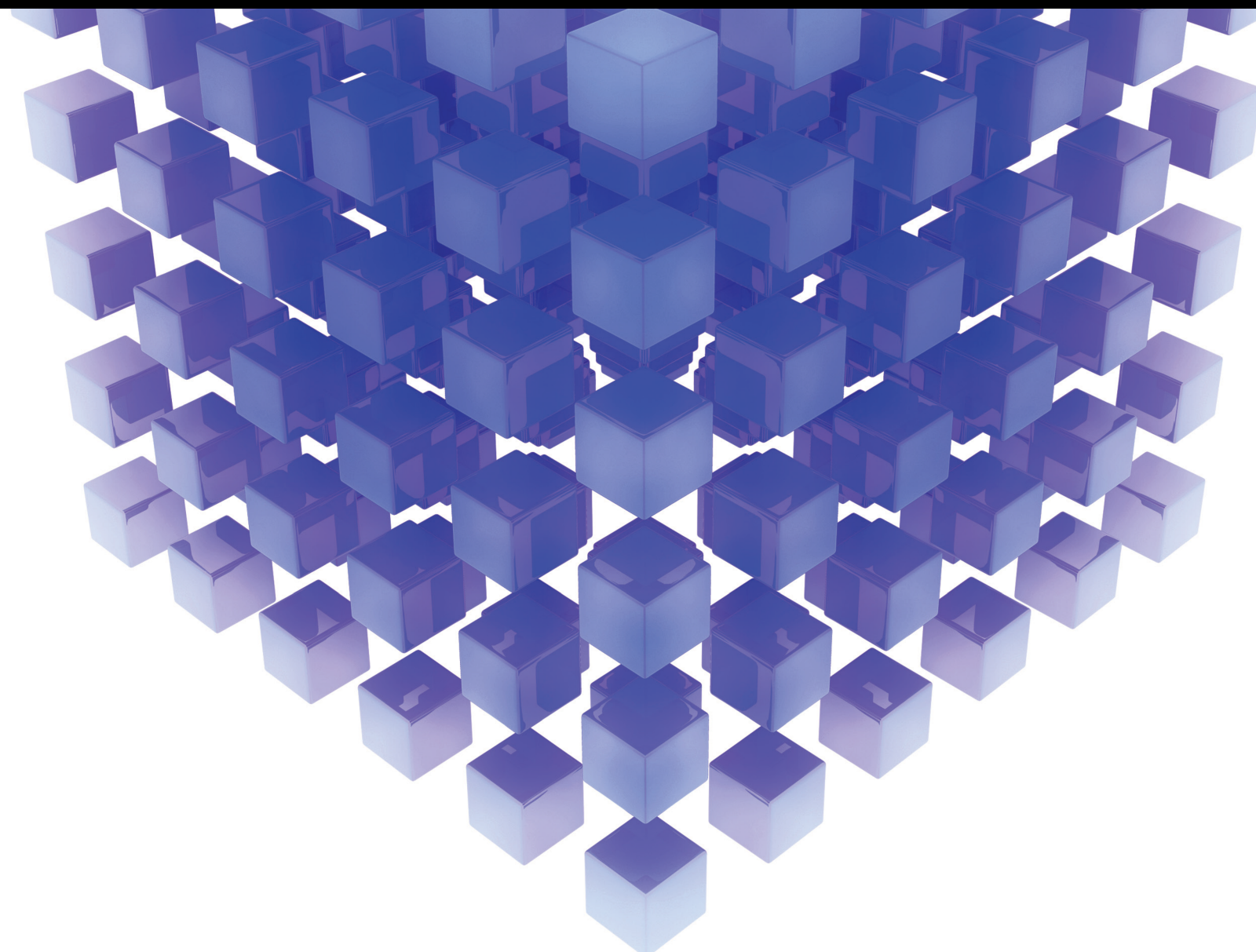


Discrete Fractional-Order Systems with Applications in Engineering and Natural Sciences 2021

Lead Guest Editor: Abdelalim A. Elsadany

Guest Editors: Abdulrahman Al-khedhairi, Hamdy N. Agiza, Baogui Xin,
and Amr Elsonbaty





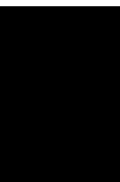
**Discrete Fractional-Order Systems with
Applications in Engineering and Natural
Sciences 2021**

Mathematical Problems in Engineering

**Discrete Fractional-Order Systems with
Applications in Engineering and Natural
Sciences 2021**

Lead Guest Editor: Abdelalim A. Elsadany


Guest Editors: Abdulrahman Al-khedhairi, Hamdy
N. Agiza, Baogui Xin, and Amr Elsonbaty



Copyright © 2022 Hindawi Limited. All rights reserved.

This is a special issue published in “Mathematical Problems in Engineering.” All articles are open access articles distributed under the Creative Commons Attribution License, which permits unrestricted use, distribution, and reproduction in any medium, provided the original work is properly cited.

Chief Editor

Guangming Xie , China

Academic Editors

Kumaravel A , India
Waqas Abbasi, Pakistan
Mohamed Abd El Aziz , Egypt
Mahmoud Abdel-Aty , Egypt
Mohammed S. Abdo, Yemen
Mohammad Yaghoub Abdollahzadeh
Jamalabadi , Republic of Korea
Rahib Abiyev , Turkey
Leonardo Acho , Spain
Daniela Addessi , Italy
Arooj Adeel , Pakistan
Waleed Adel , Egypt
Ramesh Agarwal , USA
Francesco Aggogeri , Italy
Ricardo Aguilar-Lopez , Mexico
Afaq Ahmad , Pakistan
Naveed Ahmed , Pakistan
Elias Aifantis , USA
Akif Akgul , Turkey
Tareq Al-shami , Yemen
Guido Ala, Italy
Andrea Alaimo , Italy
Reza Alam, USA
Osamah Albahri , Malaysia
Nicholas Alexander , United Kingdom
Salvatore Alfonzetti, Italy
Ghous Ali , Pakistan
Nouman Ali , Pakistan
Mohammad D. Aliyu , Canada
Juan A. Almendral , Spain
A.K. Alomari, Jordan
José Domingo Álvarez , Spain
Cláudio Alves , Portugal
Juan P. Amezcua-Sanchez, Mexico
Mukherjee Amitava, India
Lionel Amodeo, France
Sebastian Anita, Romania
Costanza Arico , Italy
Sabri Arik, Turkey
Fausto Arpino , Italy
Rashad Asharabi , Saudi Arabia
Farhad Aslani , Australia
Mohsen Asle Zaem , USA

Andrea Avanzini , Italy
Richard I. Avery , USA
Viktor Avrutin , Germany
Mohammed A. Awadallah , Malaysia
Francesco Aymerich , Italy
Sajad Azizi , Belgium
Michele Baccocchi , Italy
Seungik Baek , USA
Khaled Bahlali, France
M.V.A Raju Bahubalendruni, India
Pedro Balaguer , Spain
P. Balasubramaniam, India
Stefan Balint , Romania
Ines Tejado Balsera , Spain
Alfonso Banos , Spain
Jerzy Baranowski , Poland
Tudor Barbu , Romania
Andrzej Bartoszewicz , Poland
Sergio Baselga , Spain
S. Caglar Baslamisli , Turkey
David Bassir , France
Chiara Bedon , Italy
Azeddine Beghdadi, France
Andriette Bekker , South Africa
Francisco Beltran-Carbajal , Mexico
Abdellatif Ben Makhlof , Saudi Arabia
Denis Benasciutti , Italy
Ivano Benedetti , Italy
Rosa M. Benito , Spain
Elena Benvenuti , Italy
Giovanni Berselli, Italy
Michele Betti , Italy
Pietro Bia , Italy
Carlo Bianca , France
Simone Bianco , Italy
Vincenzo Bianco, Italy
Vittorio Bianco, Italy
David Bigaud , France
Sardar Muhammad Bilal , Pakistan
Antonio Bilotta , Italy
Sylvio R. Bistafa, Brazil
Chiara Boccaletti , Italy
Rodolfo Bontempo , Italy
Alberto Borboni , Italy
Marco Bortolini, Italy

Paolo Boscariol, Italy
Daniela Boso , Italy
Guillermo Botella-Juan, Spain
Abdesselem Boulkroune , Algeria
Boulaïd Boulkroune, Belgium
Fabio Bovenga , Italy
Francesco Braghin , Italy
Ricardo Branco, Portugal
Julien Bruchon , France
Matteo Bruggi , Italy
Michele Brun , Italy
Maria Elena Bruni, Italy
Maria Angela Butturi , Italy
Bartłomiej Błachowski , Poland
Dhanamjayulu C , India
Raquel Caballero-Águila , Spain
Filippo Cacace , Italy
Salvatore Caddemi , Italy
Zuowei Cai , China
Roberto Caldelli , Italy
Francesco Cannizzaro , Italy
Maosen Cao , China
Ana Carpio, Spain
Rodrigo Carvajal , Chile
Caterina Casavola, Italy
Sara Casciati, Italy
Federica Caselli , Italy
Carmen Castillo , Spain
Inmaculada T. Castro , Spain
Miguel Castro , Portugal
Giuseppe Catalanotti , United Kingdom
Alberto Cavallo , Italy
Gabriele Cazzulani , Italy
Fatih Vehbi Celebi, Turkey
Miguel Cerrolaza , Venezuela
Gregory Chagnon , France
Ching-Ter Chang , Taiwan
Kuei-Lun Chang , Taiwan
Qing Chang , USA
Xiaoheng Chang , China
Prasenjit Chatterjee , Lithuania
Kacem Chehdi, France
Peter N. Cheimets, USA
Chih-Chiang Chen , Taiwan
He Chen , China

Kebing Chen , China
Mengxin Chen , China
Shyi-Ming Chen , Taiwan
Xizhong Chen , Ireland
Xue-Bo Chen , China
Zhiwen Chen , China
Qiang Cheng, USA
Zeyang Cheng, China
Luca Chiapponi , Italy
Francisco Chicano , Spain
Tirivanhu Chinyoka , South Africa
Adrian Chmielewski , Poland
Seongim Choi , USA
Gautam Choubey , India
Hung-Yuan Chung , Taiwan
Yusheng Ci, China
Simone Cinquemani , Italy
Roberto G. Citarella , Italy
Joaquim Ciurana , Spain
John D. Clayton , USA
Piero Colajanni , Italy
Giuseppina Colicchio, Italy
Vassilios Constantoudis , Greece
Enrico Conte, Italy
Alessandro Contento , USA
Mario Cools , Belgium
Gino Cortellessa, Italy
Carlo Cosentino , Italy
Paolo Crippa , Italy
Erik Cuevas , Mexico
Guozeng Cui , China
Mehmet Cunkas , Turkey
Giuseppe D'Aniello , Italy
Peter Dabnichki, Australia
Weizhong Dai , USA
Zhifeng Dai , China
Purushothaman Damodaran , USA
Sergey Dashkovskiy, Germany
Adiel T. De Almeida-Filho , Brazil
Fabio De Angelis , Italy
Samuele De Bartolo , Italy
Stefano De Miranda , Italy
Filippo De Monte , Italy



























José António Fonseca De Oliveira
Correia , Portugal
Jose Renato De Sousa , Brazil
Michael Defoort, France
Alessandro Della Corte, Italy
Laurent Dewasme , Belgium
Sanku Dey , India
Gianpaolo Di Bona , Italy
Roberta Di Pace , Italy
Francesca Di Puccio , Italy
Ramón I. Diego , Spain
Yannis Dimakopoulos , Greece
Hasan Dinçer , Turkey
José M. Domínguez , Spain
Georgios Dounias, Greece
Bo Du , China
Emil Dumic, Croatia
Madalina Dumitriu , United Kingdom
Premraj Durairaj , India
Saeed Eftekhari Azam, USA
Said El Kafhali , Morocco
Antonio Elipse , Spain
R. Emre Erkmen, Canada
John Escobar , Colombia
Leandro F. F. Miguel , Brazil
FRANCESCO FOTI , Italy
Andrea L. Facci , Italy
Shahla Faisal , Pakistan
Giovanni Falsone , Italy
Hua Fan, China
Jianguang Fang, Australia
Nicholas Fantuzzi , Italy
Muhammad Shahid Farid , Pakistan
Hamed Faruqi, Iran
Yann Favennec, France
Fiorenzo A. Fazzolari , United Kingdom
Giuseppe Fedele , Italy
Roberto Fedele , Italy
Baowei Feng , China
Mohammad Ferdows , Bangladesh
Arturo J. Fernández , Spain
Jesus M. Fernandez Oro, Spain
Francesco Ferrise, Italy
Eric Feulvarch , France
Thierry Floquet, France

Eric Florentin , France
Gerardo Flores, Mexico
Antonio Forcina , Italy
Alessandro Formisano, Italy
Francesco Franco , Italy
Elisa Francomano , Italy
Juan Frausto-Solis, Mexico
Shujun Fu , China
Juan C. G. Prada , Spain
HECTOR GOMEZ , Chile
Matteo Gaeta , Italy
Mauro Gaggero , Italy
Zoran Gajic , USA
Jaime Gallardo-Alvarado , Mexico
Mosè Gallo , Italy
Akemi Gálvez , Spain
Maria L. Gandarias , Spain
Hao Gao , Hong Kong
Xingbao Gao , China
Yan Gao , China
Zhiwei Gao , United Kingdom
Giovanni Garcea , Italy
José García , Chile
Harish Garg , India
Alessandro Gasparetto , Italy
Stylianos Georgantzinou, Greece
Fotios Georgiades , India
Parviz Ghadimi , Iran
Ştefan Cristian Gherghina , Romania
Georgios I. Giannopoulos , Greece
Agathoklis Giaralis , United Kingdom
Anna M. Gil-Lafuente , Spain
Ivan Giorgio , Italy
Gaetano Giunta , Luxembourg
Jefferson L.M.A. Gomes , United Kingdom
Emilio Gómez-Déniz , Spain
Antonio M. Gonçalves de Lima , Brazil
Qunxi Gong , China
Chris Goodrich, USA
Rama S. R. Gorla, USA
Veena Goswami , India
Xunjie Gou , Spain
Jakub Grabski , Poland

Antoine Grall , France
George A. Gravvanis , Greece
Fabrizio Greco , Italy
David Greiner , Spain
Jason Gu , Canada
Federico Guarracino , Italy
Michele Guida , Italy
Muhammet Gul , Turkey
Dong-Sheng Guo , China
Hu Guo , China
Zhaoxia Guo, China
Yusuf Gurefe, Turkey
Salim HEDDAM , Algeria
ABID HUSSANAN, China
Quang Phuc Ha, Australia
Li Haitao , China
Petr Hájek , Czech Republic
Mohamed Hamdy , Egypt
Muhammad Hamid , United Kingdom
Renke Han , United Kingdom
Weimin Han , USA
Xingsi Han, China
Zhen-Lai Han , China
Thomas Hanne , Switzerland
Xinan Hao , China
Mohammad A. Hariri-Ardebili , USA
Khalid Hattaf , Morocco
Defeng He , China
Xiao-Qiao He, China
Yanchao He, China
Yu-Ling He , China
Ramdane Hedjar , Saudi Arabia
Jude Hemanth , India
Reza Hemmati, Iran
Nicolae Herisanu , Romania
Alfredo G. Hernández-Díaz , Spain
M.I. Herreros , Spain
Eckhard Hitzer , Japan
Paul Honeine , France
Jaromir Horacek , Czech Republic
Lei Hou , China
Yingkun Hou , China
Yu-Chen Hu , Taiwan
Yunfeng Hu, China

Can Huang , China
Gordon Huang , Canada
Linsheng Huo , China
Sajid Hussain, Canada
Asier Ibeas , Spain
Orest V. Iftime , The Netherlands
Przemyslaw Ignaciuk , Poland
Giacomo Innocenti , Italy
Emilio Insfran Pelozo , Spain
Azeem Irshad, Pakistan
Alessio Ishizaka, France
Benjamin Ivorra , Spain
Breno Jacob , Brazil
Reema Jain , India
Tushar Jain , India
Amin Jajarmi , Iran
Chiranjibe Jana , India
Łukasz Jankowski , Poland
Samuel N. Jator , USA
Juan Carlos Jáuregui-Correa , Mexico
Kandasamy Jayakrishna, India
Reza Jazar, Australia
Khalide Jbilou, France
Isabel S. Jesus , Portugal
Chao Ji , China
Qing-Chao Jiang , China
Peng-fei Jiao , China
Ricardo Fabricio Escobar Jiménez , Mexico
Emilio Jiménez Macías , Spain
Maolin Jin, Republic of Korea
Zhuo Jin, Australia
Ramash Kumar K , India
BHABEN KALITA , USA
MOHAMMAD REZA KHEDMATI , Iran
Viacheslav Kalashnikov , Mexico
Mathiyalagan Kalidass , India
Tamas Kalmar-Nagy , Hungary
Rajesh Kaluri , India
Jyottheswara Reddy Kalvakurthi, India
Zhao Kang , China
Ramani Kannan , Malaysia
Tomasz Kapitaniak , Poland
Julius Kaplunov, United Kingdom
Konstantinos Karamanos, Belgium
Michal Kawulok, Poland

Irfan Kaymaz , Turkey
Vahid Kayvanfar , Qatar
Krzysztof Kecik , Poland
Mohamed Khader , Egypt
Chaudry M. Khalique , South Africa
Mukhtaj Khan , Pakistan
Shahid Khan , Pakistan
Nam-Il Kim, Republic of Korea
Philipp V. Kiryukhantsev-Korneev ,
Russia
P.V.V Kishore , India
Jan Koci , Czech Republic
Ioannis Kostavelis , Greece
Sotiris B. Kotsiantis , Greece
Frederic Kratz , France
Vamsi Krishna , India
Edyta Kucharska, Poland
Krzysztof S. Kulpa , Poland
Kamal Kumar, India
Prof. Ashwani Kumar , India
Michal Kunicki , Poland
Cedrick A. K. Kwuimy , USA
Kyandoghere Kyamakya, Austria
Ivan Kyrchei , Ukraine
Márcio J. Lacerda , Brazil
Eduardo Lalla , The Netherlands
Giovanni Lancioni , Italy
Jaroslaw Latalski , Poland
Hervé Laurent , France
Agostino Lauria , Italy
Aimé Lay-Ekuakille , Italy
Nicolas J. Leconte , France
Kun-Chou Lee , Taiwan
Dimitri Lefebvre , France
Eric Lefevre , France
Marek Lefik, Poland
Yaguo Lei , China
Kauko Leiviskä , Finland
Ervin Lenzi , Brazil
ChenFeng Li , China
Jian Li , USA
Jun Li , China
Yueyang Li , China
Zhao Li , China






























Zhen Li , China
En-Qiang Lin, USA
Jian Lin , China
Qibin Lin, China
Yao-Jin Lin, China
Zhiyun Lin , China
Bin Liu , China
Bo Liu , China
Heng Liu , China
Jianxu Liu , Thailand
Lei Liu , China
Sixin Liu , China
Wanquan Liu , China
Yu Liu , China
Yuanchang Liu , United Kingdom
Bonifacio Llamazares , Spain
Alessandro Lo Schiavo , Italy
Jean Jacques Loiseau , France
Francesco Lolli , Italy
Paolo Lonetti , Italy
António M. Lopes , Portugal
Sebastian López, Spain
Luis M. López-Ochoa , Spain
Vassilios C. Loukopoulos, Greece
Gabriele Maria Lozito , Italy
Zhiguo Luo , China
Gabriel Luque , Spain
Valentin Lychagin, Norway
YUE MEI, China
Junwei Ma , China
Xuanlong Ma , China
Antonio Madeo , Italy
Alessandro Magnani , Belgium
Toqeer Mahmood , Pakistan
Fazal M. Mahomed , South Africa
Arunava Majumder , India
Sarfranz Nawaz Malik, Pakistan
Paolo Manfredi , Italy
Adnan Maqsood , Pakistan
Muazzam Maqsood, Pakistan
Giuseppe Carlo Marano , Italy
Damijan Markovic, France
Filipe J. Marques , Portugal
Luca Martinelli , Italy
Denizar Cruz Martins, Brazil

Francisco J. Martos , Spain
Elio Masciari , Italy
Paolo Massioni , France
Alessandro Mauro , Italy
Jonathan Mayo-Maldonado , Mexico
Pier Luigi Mazzeo , Italy
Laura Mazzola, Italy
Driss Mehdi , France
Zahid Mehmood , Pakistan
Roderick Melnik , Canada
Xiangyu Meng , USA
Jose Merodio , Spain
Alessio Merola , Italy
Mahmoud Mesbah , Iran
Luciano Mescia , Italy
Laurent Mevel , France
Constantine Michailides , Cyprus
Mariusz Michta , Poland
Prankul Middha, Norway
Aki Mikkola , Finland
Giovanni Minafò , Italy
Edmondo Minisci , United Kingdom
Hiroyuki Mino , Japan
Dimitrios Mitsotakis , New Zealand
Ardashir Mohammadzadeh , Iran
Francisco J. Montáns , Spain
Francesco Montefusco , Italy
Gisele Mophou , France
Rafael Morales , Spain
Marco Morandini , Italy
Javier Moreno-Valenzuela , Mexico
Simone Morganti , Italy
Caroline Mota , Brazil
Aziz Moukrim , France
Shen Mouquan , China
Dimitris Mourtzis , Greece
Emiliano Mucchi , Italy
Taseer Muhammad, Saudi Arabia
Ghulam Muhiuddin, Saudi Arabia
Amitava Mukherjee , India
Josefa Mula , Spain
Jose J. Muñoz , Spain
Giuseppe Muscolino, Italy
Marco Mussetta , Italy

Hariharan Muthusamy, India
Alessandro Naddeo , Italy
Raj Nandkeolyar, India
Keivan Navaie , United Kingdom
Soumya Nayak, India
Adrian Neagu , USA
Erivelton Geraldo Nepomuceno , Brazil
AMA Neves, Portugal
Ha Quang Thinh Ngo , Vietnam
Nhon Nguyen-Thanh, Singapore
Papakostas Nikolaos , Ireland
Jelena Nikolic , Serbia
Tatsushi Nishi, Japan
Shanzhou Niu , China
Ben T. Nohara , Japan
Mohammed Nouari , France
Mustapha Nourelfath, Canada
Kazem Nouri , Iran
Ciro Núñez-Gutiérrez , Mexico
Włodzimierz Ogryczak, Poland
Roger Ohayon, France
Krzysztof Okarma , Poland
Mitsuhiro Okayasu, Japan
Murat Olgun , Turkey
Diego Oliva, Mexico
Alberto Olivares , Spain
Enrique Onieva , Spain
Calogero Orlando , Italy
Susana Ortega-Cisneros , Mexico
Sergio Ortobelli, Italy
Naohisa Otsuka , Japan
Sid Ahmed Ould Ahmed Mahmoud , Saudi Arabia
Taoreed Owolabi , Nigeria
EUGENIA PETROPOULOU , Greece
Arturo Pagano, Italy
Madhumangal Pal, India
Pasquale Palumbo , Italy
Dragan Pamučar, Serbia
Weifeng Pan , China
Chandan Pandey, India
Rui Pang, United Kingdom
Jürgen Pannek , Germany
Elena Panteley, France
Achille Paolone, Italy

George A. Papakostas , Greece
Xosé M. Pardo , Spain
You-Jin Park, Taiwan
Manuel Pastor, Spain
Pubudu N. Pathirana , Australia
Surajit Kumar Paul , India
Luis Payá , Spain
Igor Pažanin , Croatia
Libor Pekař , Czech Republic
Francesco Pellicano , Italy
Marcello Pellicciari , Italy
Jian Peng , China
Mingshu Peng, China
Xiang Peng , China
Xindong Peng, China
Yuxing Peng, China
Marzio Pennisi , Italy
Maria Patrizia Pera , Italy
Matjaz Perc , Slovenia
A. M. Bastos Pereira , Portugal
Wesley Peres, Brazil
F. Javier Pérez-Pinal , Mexico
Michele Perrella, Italy
Francesco Pesavento , Italy
Francesco Petrini , Italy
Hoang Vu Phan, Republic of Korea
Lukasz Pieczonka , Poland
Dario Piga , Switzerland
Marco Pizzarelli , Italy
Javier Plaza , Spain
Goutam Pohit , India
Dragan Poljak , Croatia
Jorge Pomares , Spain
Hiram Ponce , Mexico
Sébastien Poncet , Canada
Volodymyr Ponomaryov , Mexico
Jean-Christophe Ponsart , France
Mauro Pontani , Italy
Sivakumar Poruran, India
Francesc Pozo , Spain
Aditya Rio Prabowo , Indonesia
Anchasa Pramuanjaroenkij , Thailand
Leonardo Primavera , Italy
B Rajanarayan Prusty, India

Krzysztof Puszynski , Poland
Chuan Qin , China
Dongdong Qin, China
Jianlong Qiu , China
Giuseppe Quaranta , Italy
DR. RITU RAJ , India
Vitomir Racic , Italy
Carlo Rainieri , Italy
Kumbakonam Ramamani Rajagopal, USA
Ali Ramazani , USA
Angel Manuel Ramos , Spain
Higinio Ramos , Spain
Muhammad Afzal Rana , Pakistan
Muhammad Rashid, Saudi Arabia
Manoj Rastogi, India
Alessandro Rasulo , Italy
S.S. Ravindran , USA
Abdolrahman Razani , Iran
Alessandro Reali , Italy
Jose A. Reinoso , Spain
Oscar Reinoso , Spain
Haijun Ren , China
Carlo Renno , Italy
Fabrizio Renno , Italy
Shahram Rezapour , Iran
Ricardo Rianza , Spain
Francesco Riganti-Fulginei , Italy
Gerasimos Rigatos , Greece
Francesco Ripamonti , Italy
Jorge Rivera , Mexico
Eugenio Roanes-Lozano , Spain
Ana Maria A. C. Rocha , Portugal
Luigi Rodino , Italy
Francisco Rodríguez , Spain
Rosana Rodríguez López, Spain
Francisco Rossomando , Argentina
Jose de Jesus Rubio , Mexico
Weiguo Rui , China
Rubén Ruiz , Spain
Ivan D. Rukhlenko , Australia
Dr. Eswaramoorthi S. , India
Weichao SHI , United Kingdom
Chaman Lal Sabharwal , USA
Andrés Sáez , Spain

Bekir Sahin, Turkey
Laxminarayan Sahoo , India
John S. Sakellariou , Greece
Michael Sakellariou , Greece
Salvatore Salamone, USA
Jose Vicente Salcedo , Spain
Alejandro Salcido , Mexico
Alejandro Salcido, Mexico
Nunzio Salerno , Italy
Rohit Salgotra , India
Miguel A. Salido , Spain
Sinan Salih , Iraq
Alessandro Salvini , Italy
Abdus Samad , India
Sovan Samanta, India
Nikolaos Samaras , Greece
Ramon Sancibrian , Spain
Giuseppe Sanfilippo , Italy
Omar-Jacobo Santos, Mexico
J Santos-Reyes , Mexico
José A. Sanz-Herrera , Spain
Musavarah Sarwar, Pakistan
Shahzad Sarwar, Saudi Arabia
Marcelo A. Savi , Brazil
Andrey V. Savkin, Australia
Tadeusz Sawik , Poland
Roberta Sburlati, Italy
Gustavo Scaglia , Argentina
Thomas Schuster , Germany
Hamid M. Sedighi , Iran
Mijanur Rahaman Seikh, India
Tapan Senapati , China
Lotfi Senhadji , France
Junwon Seo, USA
Michele Serpilli, Italy
Silvestar Šesnić , Croatia
Gerardo Severino, Italy
Ruben Sevilla , United Kingdom
Stefano Sfarra , Italy
Dr. Ismail Shah , Pakistan
Leonid Shaikhet , Israel
Vimal Shanmuganathan , India
Prayas Sharma, India
Bo Shen , Germany
Hang Shen, China

Xin Pu Shen, China
Dimitri O. Shepelsky, Ukraine
Jian Shi , China
Amin Shokrollahi, Australia
Suzanne M. Shontz , USA
Babak Shotorban , USA
Zhan Shu , Canada
Angelo Sifaleras , Greece
Nuno Simões , Portugal
Mehakpreet Singh , Ireland
Piyush Pratap Singh , India
Rajiv Singh, India
Seralathan Sivamani , India
S. Sivasankaran , Malaysia
Christos H. Skiadas, Greece
Konstantina Skouri , Greece
Neale R. Smith , Mexico
Bogdan Smolka, Poland
Delfim Soares Jr. , Brazil
Alba Sofi , Italy
Francesco Soldovieri , Italy
Raffaele Solimene , Italy
Yang Song , Norway
Jussi Sopanen , Finland
Marco Spadini , Italy
Paolo Spagnolo , Italy
Ruben Specogna , Italy
Vasilios Spitas , Greece
Ivanka Stamova , USA
Rafał Stanisławski , Poland
Miladin Stefanović , Serbia
Salvatore Strano , Italy
Yakov Strelniker, Israel
Kangkang Sun , China
Qiuqin Sun , China
Shuaishuai Sun, Australia
Yanchao Sun , China
Zong-Yao Sun , China
Kumarasamy Suresh , India
Sergey A. Suslov , Australia
D.L. Suthar, Ethiopia
D.L. Suthar , Ethiopia
Andrzej Swierniak, Poland
Andras Szekrenyes , Hungary
Kumar K. Tamma, USA




Yong (Aaron) Tan, United Kingdom
Marco Antonio Taneco-Hernández , Mexico
Lu Tang , China
Tianyou Tao, China
Hafez Tari , USA
Alessandro Tasora , Italy
Sergio Teggi , Italy
Adriana del Carmen Téllez-Anguiano , Mexico
Ana C. Teodoro , Portugal
Efstathios E. Theotokoglou , Greece
Jing-Feng Tian, China
Alexander Timokha , Norway
Stefania Tomasiello , Italy
Gisella Tomasini , Italy
Isabella Torricollo , Italy
Francesco Tornabene , Italy
Mariano Torrisi , Italy
Thang nguyen Trung, Vietnam
George Tsiatas , Greece
Le Anh Tuan , Vietnam
Nerio Tullini , Italy
Emilio Turco , Italy
Ilhan Tuzcu , USA
Efstratios Tzirtzilakis , Greece
FRANCISCO UREÑA , Spain
Filippo Ubertini , Italy
Mohammad Uddin , Australia
Mohammad Safi Ullah , Bangladesh
Serdar Ulubeyli , Turkey
Mati Ur Rahman , Pakistan
Panayiotis Vafeas , Greece
Giuseppe Vairo , Italy
Jesus Valdez-Resendiz , Mexico
Eusebio Valero, Spain
Stefano Valvano , Italy
Carlos-Renato Vázquez , Mexico
Martin Velasco Villa , Mexico
Franck J. Vernerey, USA
Georgios Veronis , USA
Vincenzo Vespri , Italy
Renato Vidoni , Italy
Venkatesh Vijayaraghavan, Australia

Anna Vila, Spain
Francisco R. Villatoro , Spain
Francesca Vipiana , Italy
Stanislav Vitek , Czech Republic
Jan Vorel , Czech Republic
Michael Vynnycky , Sweden
Mohammad W. Alomari, Jordan
Roman Wan-Wendner , Austria
Bingchang Wang, China
C. H. Wang , Taiwan
Dagang Wang, China
Guoqiang Wang , China
Huaiyu Wang, China
Hui Wang , China
J.G. Wang, China
Ji Wang , China
Kang-Jia Wang , China
Lei Wang , China
Qiang Wang, China
Qingling Wang , China
Weiwei Wang , China
Xinyu Wang , China
Yong Wang , China
Yung-Chung Wang , Taiwan
Zhenbo Wang , USA
Zhibo Wang, China
Waldemar T. Wójcik, Poland
Chi Wu , Australia
Qihong Wu, China
Yuqiang Wu, China
Zhibin Wu , China
Zhizheng Wu , China
Michalis Xenos , Greece
Hao Xiao , China
Xiao Ping Xie , China
Qingzheng Xu , China
Binghan Xue , China
Yi Xue , China
Joseph J. Yame , France
Chuanliang Yan , China
Xinggang Yan , United Kingdom
Hongtai Yang , China
Jixiang Yang , China
Mijia Yang, USA
Ray-Yeng Yang, Taiwan



Zaoli Yang , China
Jun Ye , China
Min Ye , China
Luis J. Yebra , Spain
Peng-Yeng Yin , Taiwan
Muhammad Haroon Yousaf , Pakistan
Yuan Yuan, United Kingdom
Qin Yuming, China
Elena Zaitseva , Slovakia
Arkadiusz Zak , Poland
Mohammad Zakwan , India
Ernesto Zambrano-Serrano , Mexico
Francesco Zammori , Italy
Jessica Zangari , Italy
Rafal Zdunek , Poland
Ibrahim Zeid, USA
Nianyin Zeng , China
Junyong Zhai , China
Hao Zhang , China
Haopeng Zhang , USA
Jian Zhang , China
Kai Zhang, China
Lingfan Zhang , China
Mingjie Zhang , Norway
Qian Zhang , China
Tianwei Zhang , China
Tongqian Zhang , China
Wenyu Zhang , China
Xianming Zhang , Australia
Xuping Zhang , Denmark
Yinyan Zhang, China
Yifan Zhao , United Kingdom
Debao Zhou, USA
Heng Zhou , China
Jian G. Zhou , United Kingdom
Junyong Zhou , China
Xueqian Zhou , United Kingdom
Zhe Zhou , China
Wu-Le Zhu, China
Gaetano Zizzo , Italy
Mingcheng Zuo, China

Contents




On the Solution of Fractional Order KdV Equation and Its Periodicity on Bounded Domain Using Radial Basis Functions

Marjan Uddin , Hameed Ullah Jan , and Muhammad Usman 
Research Article (10 pages), Article ID 8924450, Volume 2022 (2022)




On Discrete Fractional Complex Gaussian Map: Fractal Analysis, Julia Sets Control, and Encryption Application

Amr Elsonbaty , A. Elsadany, and Fatma Kamal 
Research Article (18 pages), Article ID 8148831, Volume 2022 (2022)

Qualitative Behavior of Solutions of Tenth-Order Recursive Sequence Equation

E. M. Elsayed , B. S. Alofi , and Abdul Qadeer Khan 
Research Article (10 pages), Article ID 5242325, Volume 2022 (2022)

On the Dynamics of a Discrete Fractional-Order Cournot–Bertrand Competition Duopoly Game

Abdulrahman Al-Khedhairi , Abdelalim A. Elsadany , and Amr Elsonbaty 
Research Article (13 pages), Article ID 8249215, Volume 2022 (2022)



Bifurcation Analysis of a Discrete Food Chain Model with Harvesting

Abdul Qadeer Khan  and Shahid Mehmood Qureshi
Research Article (31 pages), Article ID 5987435, Volume 2021 (2021)

On a Unified Mittag-Leffler Function and Associated Fractional Integral Operator

Yanyan Zhang , Ghulam Farid , Zabidin Salleh , and Ayyaz Ahmad
Research Article (9 pages), Article ID 6043769, Volume 2021 (2021)


Some New Kinds of Fractional Integral Inequalities via Refined $(\alpha, h - m)$ -Convex Function

Moquddsa Zahra, Muhammad Ashraf, Ghulam Farid , and Kamsing Nonlaopon 
Research Article (15 pages), Article ID 8331092, Volume 2021 (2021)

Novel Stability Results for Caputo Fractional Differential Equations

Abdellatif Ben Makhlouf  and El-Sayed El-Hady 
Research Article (6 pages), Article ID 9817668, Volume 2021 (2021)

Dynamics and Solutions' Expressions of a Higher-Order Nonlinear Fractional Recursive Sequence

Abeer Alshareef, Faris Alzahrani, and Abdul Qadeer Khan 
Research Article (12 pages), Article ID 1902473, Volume 2021 (2021)

Research Article

On the Solution of Fractional Order KdV Equation and Its Periodicity on Bounded Domain Using Radial Basis Functions

Marjan Uddin ¹, Hameed Ullah Jan ¹, and Muhammad Usman ²

¹Department of Basics Sciences, University of Engineering and Technology Peshawar, Peshawar, Pakistan

²Department of Mathematics, University of Dayton, Dayton, OH, USA

Correspondence should be addressed to Marjan Uddin; marjan@uetpeshawar.edu.pk, Hameed Ullah Jan; huj@uetpeshawar.edu.pk, and Muhammad Usman; musman1@udayton.edu

Received 9 July 2021; Revised 23 February 2022; Accepted 11 April 2022; Published 18 May 2022

Academic Editor: Abdelalim Elsadany

Copyright © 2022 Marjan Uddin et al. This is an open access article distributed under the Creative Commons Attribution License, which permits unrestricted use, distribution, and reproduction in any medium, provided the original work is properly cited.

The Coimbra concept of fractional order derivative is used to build a numerical approach using radial functions in this paper. The Coimbra derivative is capable of modelling a dynamic system with varying fractional order behaviour over time. The proposed scheme's stability and convergence are investigated. In one and two space dimensions, the developed approach is validated for the given model. By applying a periodic boundary condition on a bounded domain, the model's periodicity is shown statistically. The acquired findings demonstrate the new numerical scheme's potency and, as a result, its high order accuracy.

1. Introduction

The Korteweg-De Vries (KdV) equation is first derived by Boussinesq in the year 1870. Later on in 1895, the same model was retrieved by Korteweg and de Vries [1] with the presumption of compact amplitude and huge wave length. In many nonlinear dispersive physical systems, the evolution of long wave can be expressed by the KdV type equation (see [2–5] and the references therein). In mathematical sciences and engineering, evolutionary nonlinear equations play a major role to model physical phenomena [2, 6]. In the theory of shallow water waves, the KdV equation is one of the most essential equations in nonlinear evolution developed in [4] and the references therein. Some of the important aspects of solutions of these dispersive equations discovered through observations are their long-time behaviour and known periodicity in time [7]. The important event of eventual periodicity has been presented previously in [8], and in more recent work [9, 10], a new solution is reestablished corresponding to the KdV equation. In addition, the forced oscillations and the stability of the KdV equation have been carried out in a very recent work [11–14]. In applied mathematics, physics, and other related fields, a rich filed of research has evolved within the last century because of

computational and analytic research on fractional and classical KdV equation [15–19].

Both the theory and application of fractional calculus have advanced dramatically in the previous two decades. The nonlocal quality of fractional calculus and its effectiveness in reproducing anomalous diffusion that happens in transport dynamics in complex systems, such as fluid motion in viscoelastic medium, are the most important advantages [20], anomalous transfer in biology [21] and porous materials [22], etc. Control theory, entropy theory, image processing, and wave propagation phenomena all employing fractional calculus can be found in [23–26]. The creation of tools to offer a mathematical structure for sophisticated physical systems and processes has been aided by breakthroughs in current variable order (VO) fractional calculus [27]. As a result of its appropriateness for modelling in a wide range of subjects, including science, engineering, and a variety of other disciplines, variable order fractional differential equations (VO-FDEs) have gained prominence [28–31]. Physical modelling utilizing VO-FDE models has been the subject of a large-scale investigation. For example, Kobelev et al. [32] highlighted the dynamical and statistical systems with varying memory difficulties where the fractal dimension changes with coordinate and time. Coimbra et al.

[33] used VO-fractional operators to investigate the visco-elasticity oscillator. Al-Mekhlafi and Sweilam [34] proposed a new multistrain TB model based on the VO-fractional derivative as a nonlinear ordinary differential equation extension. Due to the enormous number of applications, analytical and numerical techniques for solving variable order fractional order differential equations (VO-FDEs) have increased substantially in the last year. The analytical solution of VO-FDEs, on the other hand, is frequently difficult to obtain. Therefore, numerical approaches are used as sophisticated methods for numerical approximation of VO-FDEs in general [29, 35–38].

The Caputo, the Liouville, the Marchaud, the Grunwald, and the Coimbra definitions are some of the recent variable order operator definitions suggested in the literature [33, 39]. Samko et al. [39] analyzed that the Riemann variable order definitions lost some features, meaning that the Marchaud operator is better than the Riemann-Liouville type operator. Ramirez et al. [40] also compared the variable order operators such as operators due to Riemann-Liouville, Marchaud, Caputo, and Coimbra using a simple criterion: the variable order operator must return the correct fractional derivative that corresponds to the argument of the functional order. Only the operator due to Coimbra and the Marchaud satisfy the aforementioned elementary condition [40], as well as the Coimbra variable order operator is more efficient numerically. Soon et al. [41] also demonstrated that the Coimbra variable order operator satisfies a mapping requirement and that it is the only formulation that returns the necessary derivatives as a function of $x(t)$ for transitions between elastic and viscous regimes. Ramirez [40] demonstrated that the Coimbra concept is the most appropriate for physical modelling since it has essential properties that are desirable.

The numerical solution of the KdV problem of order $0 < \tau(t) < 1$ and its eventual periodicity over confined domain is achieved using RBF with Coimbra variable order derivative. The following equations represent the proposed models in both one-dimensional and two-dimensional space:

$$D_t^{\tau(t)} w(x, t) + \varepsilon w(x, t) w_x(x, t) + \nu w_{xxx}(x, t) = f(x, t), \quad t > 0, \quad x \in \Omega, \quad (1)$$

with the following initial condition

$$w(x, t) = g(x), \quad t = 0, \quad x \in \Omega, \quad (2)$$

and the boundary conditions given by

$$w(x, t) = h(x, t), \quad t \geq 0, \quad x \in \partial\Omega, \quad (3)$$

where $0 < \tau(t) < 1$.

$$D_t^{\tau(t)} w(x, y, t) + \varepsilon w^2(x, y, t) w_x(x, y, t) + w_{xxx}(x, y, t) + w_{xyy}(x, y, t) = f(x, y, t), \quad (4)$$

where $(x, y) \in \Omega$, with the following boundary and initial conditions

$$\begin{aligned} w(x, y, t) &= h(x, y, t) \in \partial\Omega, \quad t \geq 0, \quad w(x, y, 0), \\ &= g(x, y), \quad (x, y) \in \Omega. \end{aligned} \quad (5)$$

The models in the above form are selected for the sake of comparison given in [42]. The Coimbra variable order derivative is defined by (7) in the next section.

1.1. The KdV Equation. Suppose that a wave propagates along a horizontal channel of the uniform width along the positive direction of x -axis alone. Let the depth of the channel be d , t be the time, and x be the horizontal coordinate and let $w(x, t)$ be the vertical distance of the fluid surface in equilibrium position. Let the amplitude of the wave be small enough, then the irrotational wave propagation can be modelled by the following equation known as the KdV equation

$$w(x, y)_t + \varepsilon w(x, y) w_x(x, y) + \nu w_{xxx}(x, y) = 0, \quad (6)$$

where the first term u_t represents the uniform wave translation, and the other two terms $\varepsilon w(x, t) w_x(x, t)$ and $\nu w_{xxx}(x, t)$ serve for the modification of the wave under the influences of nonlinear term $w w_x$ and dispersive term w_{xxx} , respectively.

1.2. Coimbra Variable Order Derivative. Modelling physical problems is better using the Coimbra concept. Variable order differentials are a useful tool for studying systems where the order changes with regard to one or more parameters, such as the management of a nonlinear visco-elasticity oscillator.

$$D_t^{\tau(t)} w(t) = \frac{1}{\Gamma(1 - \alpha(t))} \int_0^t \frac{w'(s) ds}{(t - s)^{\alpha(t)}} + \frac{\beta t^{-\tau(t)}}{\Gamma(1 - \tau(t))}. \quad (7)$$

$0 < \tau(t) < 1$, $\beta = w(0_+) - w(0_-)$, and the above operator require only one initial condition $w(0_+)$. The integer order derivative with respect to the variable t is denoted by $w'(t)$ [33].

2. Analysis of RBF Approximation Method for Fractional Order KdV Equations

In the theory of multivariate approximation, the radial basis functions (RBF) method is the most extensively used tool. A generalized refinement of the multiquadric approach is RBF approximation methods. The MQ has a long history of application and theoretical research can be found in [43, 44]. The MQ approach is widely used in geology, geodesy, geophysics, and other domains, see [44]. Franke [45] conducted a comparative study in the field of MQ. Meanwhile, a key period in RBF history occurred, see for example [46], when Charles Micchelli refined the theory of the MQ method by establishing requirements that guarantee the system matrix nonsingularity for MQ methods. Schoenberg [47] is attribute with the results that generate the invertibility of the system matrix. Micchelli went on to say that Schoenberg's constraints could be relaxed to allow many more functions to be included and that adequate conditions for functions could be applied to make the system matrix nonsingular. In 1990, physicist Kansa [48] discovery quickly disseminated the study, and RBF is used in a systematic

approach for numerically solving partial differential equations and is meshless [49]. In numerous branches of applied areas [50, 51], a huge amount of mathematical applications of RBF are employed. In numerical techniques for solving PDEs with reasonable accuracy in multidimensions, Madych exposed the convergence rate of spectral order for MQ interpolation in [52]. In comparison to other state-of-the-art methodologies, these findings propelled RBF research forward swiftly, and the RBF methods drew appreciable attention in the literature as mesh-free approaches and their capacity to attain spectral accuracy for PDE numerical solutions on irregular domains [53]. In this work, a numerical scheme based on RBF and Coimbra derivative is constructed for fractional order KdV equations (1)–(5) defined in the following form:

$$D_t^\tau w(t, x) = f(t, x) + \mathcal{L}w(t, x), \quad 0 \leq t \leq T, \quad x \in \Omega \subset \mathbb{R}^d, \quad d \geq 1, \quad (8)$$

with the following boundary and initial conditions

$$\mathcal{B}w(t, x) = g(t, x), \quad x \in \partial\Omega, \quad w(t = 0, x) = w_0(x), \quad x \in \Omega, \quad (9)$$

with $0 < \tau(t) < 1$.

3. Variable Order Differential Operator Approximation

There are numerous definitions of varying order operators in the literature [54], but in the current study, we are using the definition due to Coimbra [33]. Because this variable order derivative has a great capability to model many complicated

mechanical problems with accuracy, the Coimbra variable order operator has the capability to investigate and analyze the dynamics behaviour of many physical models, for example, the fractional forces which cannot be approximated accurately with constant order fractional operator or some other variable order derivatives. In the work [40], the authors performed a comparative study for solving a dynamical system and demonstrated that the Coimbra variable order derivative produced better results in many aspects than the nine definitions of variable order derivatives used in this study.

Now, for the numerical approximation of the Coimbra variable order derivative, we consider for $t \in [0, T]$, and let $t_n = (n - 1)\delta t$, where $n = 1, \dots, M + 1$, then at time level t_n , the Coimbra variable order derivative defined in (7) can be given by the following equation:

$$D_{t_n}^{\tau(t_n)} w = \frac{1}{\Gamma(1 - \tau(t_n))} \int_0^{t_n} (t_n - s)^{-\tau(t_n)} w'(x, s) ds + \frac{\beta t^{-\tau(t_n)}}{\Gamma(1 - \tau(t_n))}. \quad (10)$$

Let us denote the last term of this equation by h_n , then we have

$$h_n = t^{-\tau(t_n)} \frac{\beta}{\Gamma(1 - \tau(t_n))}. \quad (11)$$

By using (11) in (10), we get the following form:

$$D_n^{\tau(t_n)} w(x, t_n) = C_n \sum_{k=1}^{n-1} \int_{t_k}^{t_{k+1}} (t_n - s)^{-\tau(t_n)} ds \left[\frac{w(x, t_{k+1}) - w(x, t_k)}{\delta t} \right] + h_n, \quad (12)$$

where $C_n = (1/\Gamma(1 - \tau(t_n)))$; after further simplification, we get

$$D_n^{\tau(t_n)} w(x, t_n) = C_n \sum_{k=1}^{n-1} \left[\frac{w(x, t_{k+1}) - w(x, t_k)}{\delta t} \right] \int_{t_k}^{t_{k+1}} (t_n - s)^{-\tau(t_n)} ds + h_n, \quad (13)$$

and by simplifying the integral involved, we have

$$D_n^{\tau(t_n)} w(x, t_n) = C_n \sum_{k=1}^{n-1} \left[\frac{(t_n - t_k)^{1-\tau(t_n)} - (t_n - t_{k+1})^{1-\tau(t_n)}}{(1 - \tau(t_n))} \right] \left[\frac{w(x, t_{k+1}) - w(x, t_k)}{\delta t} \right] + h_n. \quad (14)$$

Denoting the quantity $(t_n - t_k)^{1-\tau(t_n)} - (t_n - t_{k+1})^{1-\tau(t_n)}$ by the b_{k+1} , we get

$$D_n^{\tau(t_n)} w(x, t_n) = \frac{(\delta t)^{-1} C_n}{\Gamma(1-\tau(t_n))} \sum_{k=1}^{n-1} b_{k+1} [w(x, t_{k+1}) - w(x, t_k)] + h_n, \quad (15)$$

and assuming the value $(\delta t)^{-1} C_n / \Gamma(1-\tau(t_n))$ be denoted by a_n , we get

$$D_n^{\tau(t_n)} w(x, t_n) = a_n \sum_{k=1}^{n-2} b_k [w(x, t_{k+1}) - w(x, t_k)] + a_n b_n [w(x, t_n) - w(x, t_{n-1})] + h_n. \quad (17)$$

Assuming $S_n = a_n \sum_{k=1}^{n-2} b_k [w(x, t_{k+1}) - w(x, t_k)] + h_n$, the approximation of Coimbra variable order derivative can be represented in the more simplified form

$$D_n^{\alpha(t_n)} w(x, t_n) = a_n b_n [w^n(x) - w^{n-1}(x)] + S_n, \quad (18)$$

which is the Coimbra variable order differential operator's finite-difference approximation.

4. RBF Approximation Scheme

The RBF interpolant can be characterized as a linear combination of radial basis functions, as seen in the equation below. For a set of N scattered nodes $x_i \in \Omega \subset \mathbb{R}^d$, $d \geq 1$,

$$w(x, t_n) = \sum_{x_j \in \Omega} \lambda^n \kappa_j (\|x - x_j\|), x \in \Omega, \quad (19)$$

where λ^n denotes the expansion coefficients at any time t_n , κ_j denotes an RBF centred at $x_j \in \Omega$, and $\|\cdot\|$ denotes a distance norm in \mathbb{R}^d , $d \geq 1$. It is possible to obtain the matrix form of (19) by

$$w^n = A \lambda^n, \quad (20)$$

where A is a square matrix termed a system matrix, and the entries are $A_{ij} = \kappa_j (\|x_i - x_j\|)$. If \mathcal{L} is a spatial operator and \mathcal{B} is a boundary operator, then (19) is obtained.

$$\begin{aligned} \mathcal{L}w(x, t_n) &= \sum_{x_j \in \Omega} \lambda^n \mathcal{L}\kappa_j (\|x - x_j\|), x \in \Omega, \\ \mathcal{B}w(x, t_n) &= \sum_{x_j \in \Omega} \lambda^n \mathcal{B}\kappa_j (\|x - x_j\|), x \in \partial\Omega. \end{aligned} \quad (21)$$

The above two equations can be expressed in matrix form by

$$\begin{pmatrix} \mathcal{L}w^n(x) \\ \mathcal{B}w^n(x) \end{pmatrix} = \begin{pmatrix} \mathcal{L}\kappa_j (\|x - x_j\|), x \in \Omega \\ \mathcal{B}\kappa_j (\|x - x_j\|), x \in \partial\Omega \end{pmatrix} \lambda^n. \quad (22)$$

We obtain it in a more compressed form

$$M_{LB} w^n(x) = D \lambda^n, \quad (23)$$

$$D_n^{\tau(t_n)} w(x, t_n) = a_n \sum_{k=1}^{n-1} b_{k+1} [w(x, t_{k+1}) - w(x, t_k)] + h_n. \quad (16)$$

Splitting the first term of this series and rewriting in the form, we have

In case of identity operators \mathcal{L} , \mathcal{B} , the equation above can be written as

$$w^n(x) = B \lambda^n. \quad (24)$$

Model equations (1)–(5) can be approximated in the following way employing the θ -weighted scheme, VODO finite-difference approximation, and RBF spatial operator approximation

$$a_n b_n [w^n(x) - w^{n-1}(x)] + S_n = \theta M_{LB} w^n(x) + (1-\theta) M_{LB} w^{n-1}(x) + f^n(x). \quad (25)$$

Substituting the values of from (19) and (20), we get

$$\begin{aligned} [a_n b_n B \lambda^n - a_n b_n B \lambda^{n-1}] + S_n &= (1-\theta) D \lambda^{n-1} + \theta D \lambda^n + f^n(x), \\ [b_n a_n B - \theta D] \lambda^n &= [(1-\theta) D + a_n b_n B] \lambda^{n-1} + f^n(x) - S_n. \end{aligned} \quad (26)$$

This numerical strategy based on RBF can be solved at any point in time t_n to acquire the value of λ^n , for which we can use (20). Using equation (20) to remove the value of λ^n , we get

$$[b_n a_n B - \theta D] A^{-1} w^n = [(1-\theta) D + b_n a_n B] A^{-1} w^{n-1} + f^n(x) - S_n. \quad (27)$$

The amplification matrix of the numerical scheme (27) is the following matrix E :

$$E = A [b_n a_n B - \theta D]^{-1} [(1-\theta) D + b_n a_n B] A^{-1}. \quad (28)$$

In fact, the matrices A and B are identical, as shown by (20) and (24), because matrix B is a special instance of matrix D for identity operators. It is evident from the definitions of a_n and b_n that they are positive real integers, hence $\eta = a_n b_n > 0$. As a result, (28) amplification matrix can be represented in a more basic form as follows:

$$E = [a_n b_n A A^{-1} - \theta D A^{-1}]^{-1} [a_n b_n A A^{-1} + (1-\theta) D A^{-1}]. \quad (29)$$

Now, for $\theta = (1/2)$, and denoting $(1/2) D A^{-1}$ by Q , we obtain

$$E = [\eta I - Q]^{-1} [\eta I + Q]. \quad (30)$$

Lemma 1. *If Q is a square matrix of rank $N \times N$ with negative eigenvalues, then the estimate for any $\eta > 0$ is*

$$\|(\eta I - Q)^{-1}(\eta I + Q)\| \leq 1. \quad (31)$$

This is also true for the Euclidean norm.

Proof: Let the eigenvectors of the matrix Q be $\{u^i\}_{i=1}^N$ with the corresponding eigenvalues ν_i , thus we have the following equation:

$$(\eta I - Q)^{-1}(\eta I + Q)u^i = \frac{\eta + \nu_i}{\eta - \nu_i}u^i, \quad i = 1, \dots, N. \quad (32)$$

Suppose the vectors be orthonormal eigensystem for the matrix $(\eta I - Q)^{-1}(\eta I + Q)$, since $\eta > 0$ and all the eigenvalues of the matrix Q are negative, so we obtain

$$\|(\eta I - Q)^{-1}(\eta I + Q)\| = \left\| \frac{\eta + \nu_i}{\eta - \nu_i} \right\| \leq 1, \quad \forall i = 1, \dots, N. \quad (33)$$

□

5. The Numerical Scheme's Error Analysis

The VODO numerical scheme of order in time is $\mathcal{O}((\delta t)^{2-\tau})$, whereas RBF numerical scheme is mostly dependent on the RBF utilized for the derivation of other differentiation matrices and the RBF system matrix, as demonstrated in the previous work discussion. The order of convergence of several forms of RBF has been determined in [51]. Let the spatial numerical approximation corresponding to the present numerical scheme for a given RBF be of order $\mathcal{O}(h^q)$, $q \geq 0$, and h be the separation distance between the scattered nodes utilized for RBF interpolant. For the numerical scheme specified in (22), let w^n be the approximate solution, w be the precise solution, and $\Theta_n = w^n - w$ be the error at time t_n :

$$\Theta_n = E\Theta_{n-1} + \mathcal{O}((\delta t)^{2-\tau} + h^q). \quad (34)$$

The above numerical technique's amplification matrix, E , is mostly determined by the type of RBF and the scale factor used. Assume that when the condition of Lemma 1 holds for a given optimal shape parameter value and optimal RBF option, then

$$\|E\| \leq 1, \quad (35)$$

is a criterion for the numerical scheme's stability in (27). Assuming that both the initial solution value and the solution are sufficiently smooth along with $\delta t \rightarrow 0$,

$$\|\Theta_n\| \leq \|E\| \|\Theta_{n-1}\| + C_1(h^q + (\delta t)^{2-\tau}), \quad n = 1: M + 1, \quad (36)$$

where C_1 stands for a constant. At time $t = 0$, the error $\|\Theta_n\|$ always fulfils the initial as well as the boundary condition via mathematical induction.

$$\|\Theta_n\| \leq C_1 \left(1 + \sum_{i=1}^{n-1} \|E\|^i \right) ((\delta t)^{h^q+2-\tau}), \quad n = 1: M + 1, \quad (37)$$

when the condition (35) holds, then

$$\|\Theta_n\| \leq nC_1((\delta t)^{2-\tau} + h^q), \quad n = 1: M + 1, \quad (38)$$

This demonstrates that the current numerical method for VODO is convergent.

6. The Numerical Methodology for Variable Order Diffusion Models

Problem 1. We consider the KdV equation defined in (1)–(3) for the following value of function f :

$$f(x, t) = \frac{t^5 e^{-x^2}}{25} \left[\frac{t^{-\tau}}{\Gamma(6-\tau)} - \frac{t^2 x e^{-x^2}}{180000} + \frac{x}{10} - \frac{x^3}{15} \right], \quad (39)$$

with the following initial condition

$$w(x, 0) = 0, \quad a \leq x \leq b, \quad (40)$$

where the boundary conditions can be extracted from the exact solution

$$w(x, t) = \frac{t^5 e^{-x^2}}{3000}, \quad (41)$$

where $0 < \tau < 1$ is the fractional order. The compactly supported radial basis function defined as $\kappa(r, \varepsilon) = (35(\varepsilon r)^2 + 18\varepsilon r + 3)(1 - \varepsilon r)_+^6$, with a support size of $\varepsilon = 0.5$, is used to solve this issue across the spatial domain $[-4, 4]$ and the number of points $N = 100$ are used. For various settings of order τ , step size δt , and collocation points N , the results are presented in Figures 1 and 2 and Table 1, where the accuracy is quantified in terms of maximum error norm. When we gave a periodic boundary condition at $x = -1$, like $w(a, t) = \sin(20\pi t)\tanh(5t)$ with $f = 0$, the solution at each point of the domain is periodic in time for 1D fractional order KdV equation.

Problem 2. In this last example, we consider the following 2D KdV equation defined in (3)–(5) with the following value of the function f

$$f(x, y, t) = t^6 \operatorname{sech}(x) \operatorname{sech}(y) \left[\frac{720}{\Gamma(7-\tau)} t^{-\tau(t)} + \tanh(x) \left(-6(t^6 \operatorname{sech}(x) \operatorname{sech}(y))^2 - \tanh^2(x) + 5 \operatorname{sech}(x)^2 - \tanh^2(y) + \operatorname{sech}(y)^2 \right) \right], \quad (42)$$

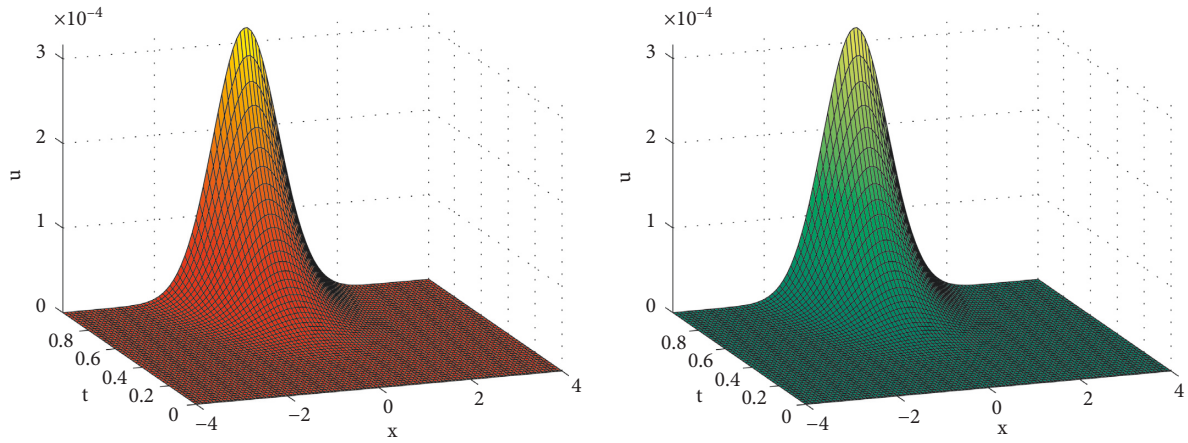


FIGURE 1: Approximate solution of RBF-based method (red) and exact solution (green) to Problem 1 at time $t \in [0, 1]$, $x \in [-4, 4]$, $\alpha = 0.5$, and $\delta t = 0.01$, with CS-RBF, $\varepsilon = 0.5$.

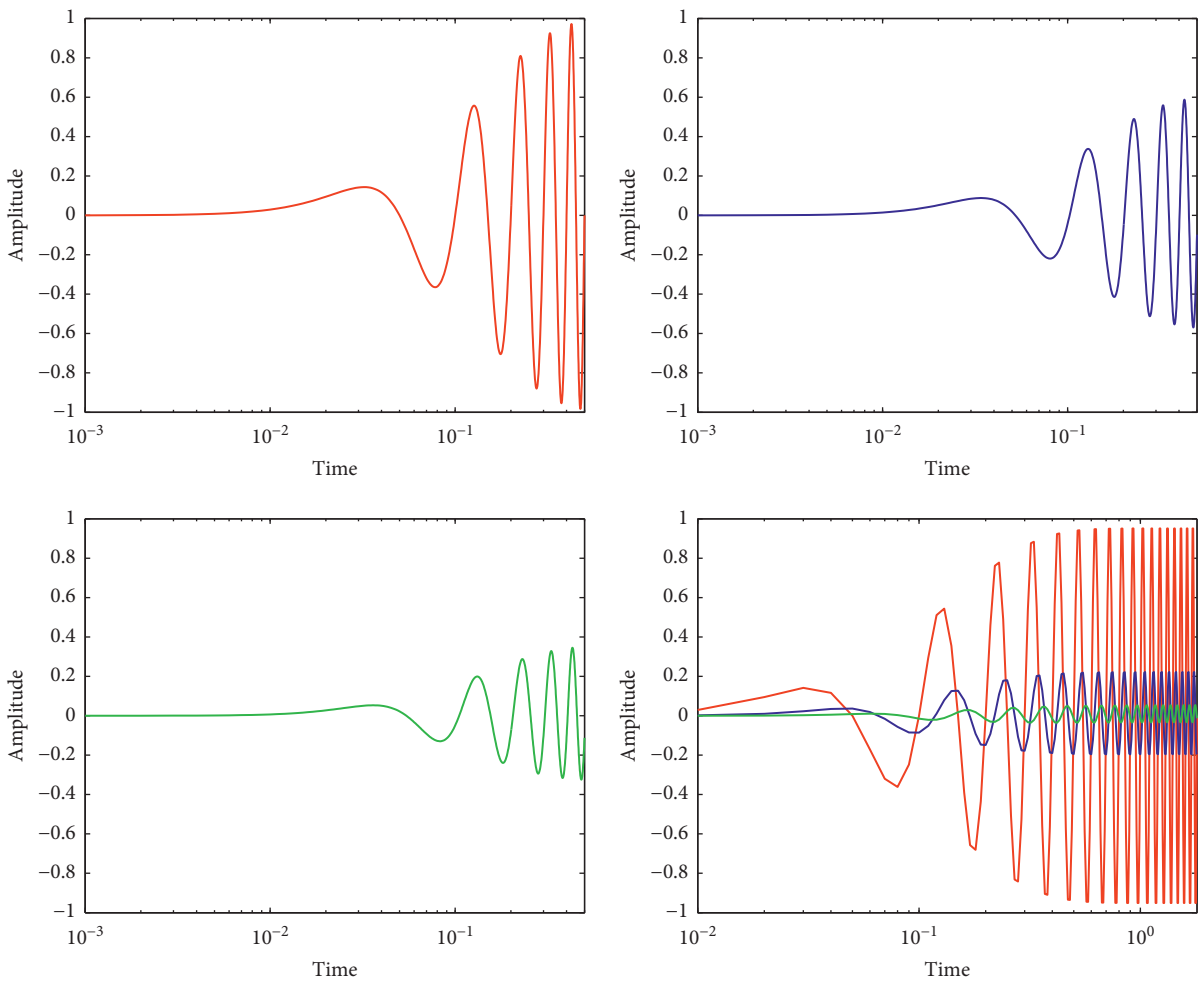


FIGURE 2: Approximate solution: periodicity of solution at $x = -1$ (red), $x = -0.7588$ (blue), and at $x = -0.5075$ (green) at time $t \in [0, 0.5]$, $x \in [-1, 1]$, $\tau = 0.2$, and $\delta t = 0.001$, with CS-RBF, $\varepsilon = 0.5$, corresponding to Problem 1.

TABLE 1: An approximate solution to Problem 1 based on RBF, when $t = 1$, error = $\max(|w_{ap} - w_{ex}|)$.

(τ, N)	$\delta t = 0.1$	$\delta t = 0.01$	$\delta t = 0.001$
$(0.1, 10^2)$	1.3572e-006	3.6674e-008	1.8149e-008
$(0.2, 10^2)$	3.2295e-006	7.7781e-008	1.6031e-008
$(0.3, 10^2)$	5.7785e-006	1.5589e-007	1.6168e-008
$(0.5, 10^2)$	1.3801e-005	5.2623e-007	2.4744e-008

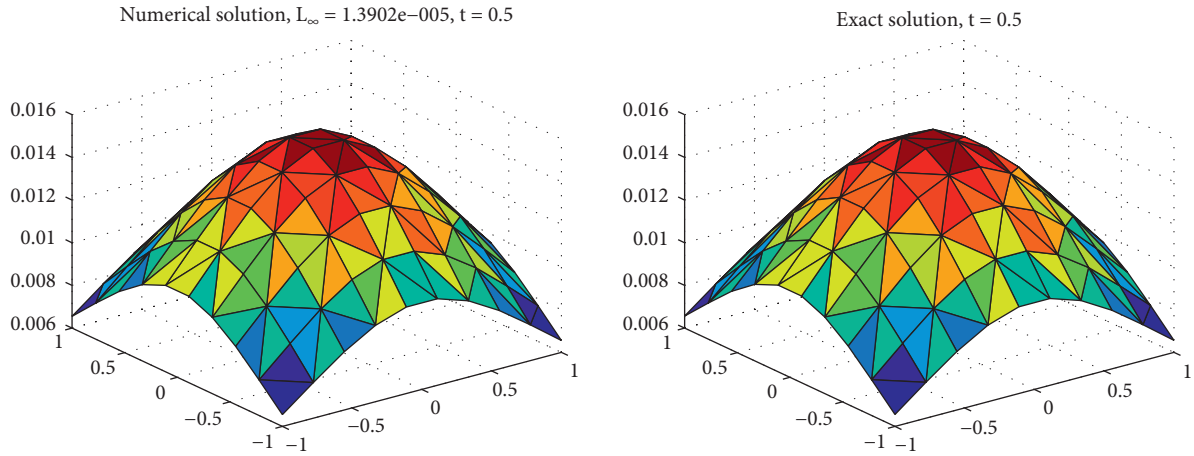


FIGURE 3: A comparison of RBF-based numerical method and exact solution of Problem 2, for $N = 10^2$, $t = 0.5$, $\tau(t) = 0.4 + 0.2 \sin(0.5\pi t/T)$.

TABLE 2: An approximate solution to Problem 2 based on RBF, when $t = 0.5$, error = $\max(|w_{ap} - w_{ex}|)$.

(ϵ, N)	$\delta t = 0.1$	$\delta t = 0.01$	$\delta t = 0.001$	$\delta t = 0.0001$
$(1, 5^2)$	0.0104	0.0016	1.7022e-004	1.8747e-005
$(1, 6^2)$	0.0111	0.0017	1.7335e-004	2.2170e-005
$(1, 7^2)$	0.0102	0.0016	1.7993e-004	1.8235e-005
$(1, 10^2)$	0.0114	0.0017	1.2957e-004	4.3734e-005

with the following initial:

$$w(x, y, 0) = 0, \quad -1 \leq x, y \leq 1, \quad (43)$$

and the boundary conditions can be taken from the following exact solution:

$$w(x, y, t) = t^6 \operatorname{sech}(x) \operatorname{sech}(y), \quad t > 0, (x, y) \in \partial\Omega, \quad (44)$$

$0 < \tau(t) < 1$, $\tau(t) = 0.4 + 0.2 \sin(0.5\pi t/T)$. The current RBF-based solution solves this problem, and the results are displayed in Figure 3 and Table 2, respectively. The current numerical technique appears to be convergent and stability attained when $\delta t \rightarrow 0$. This backs up the prior sections'

convergence and stability analysis of the current numerical system is achieved.

Problem 3. In the last example, we consider the irregular domain within the regular domain $[-1, 1]^2$. The variable order which is used in this computation is defined by the function $\alpha(t) = 0.4 + 0.2 \sin(0.5\pi t/T)$, $T = 1$. We used different number of nodes $N = 56, 196, 400, 676$ in the irregular domain. The radial basis function defined by $\kappa(r, \epsilon) = \sqrt{r^2 + \epsilon}$ is implemented in this problem and its corresponding shape parameter value changes solution accuracy, which is calculated using the formula $\epsilon = (1/\log(N))$ [55]. The results are shown in graphical form and can be seen in Figure 4.

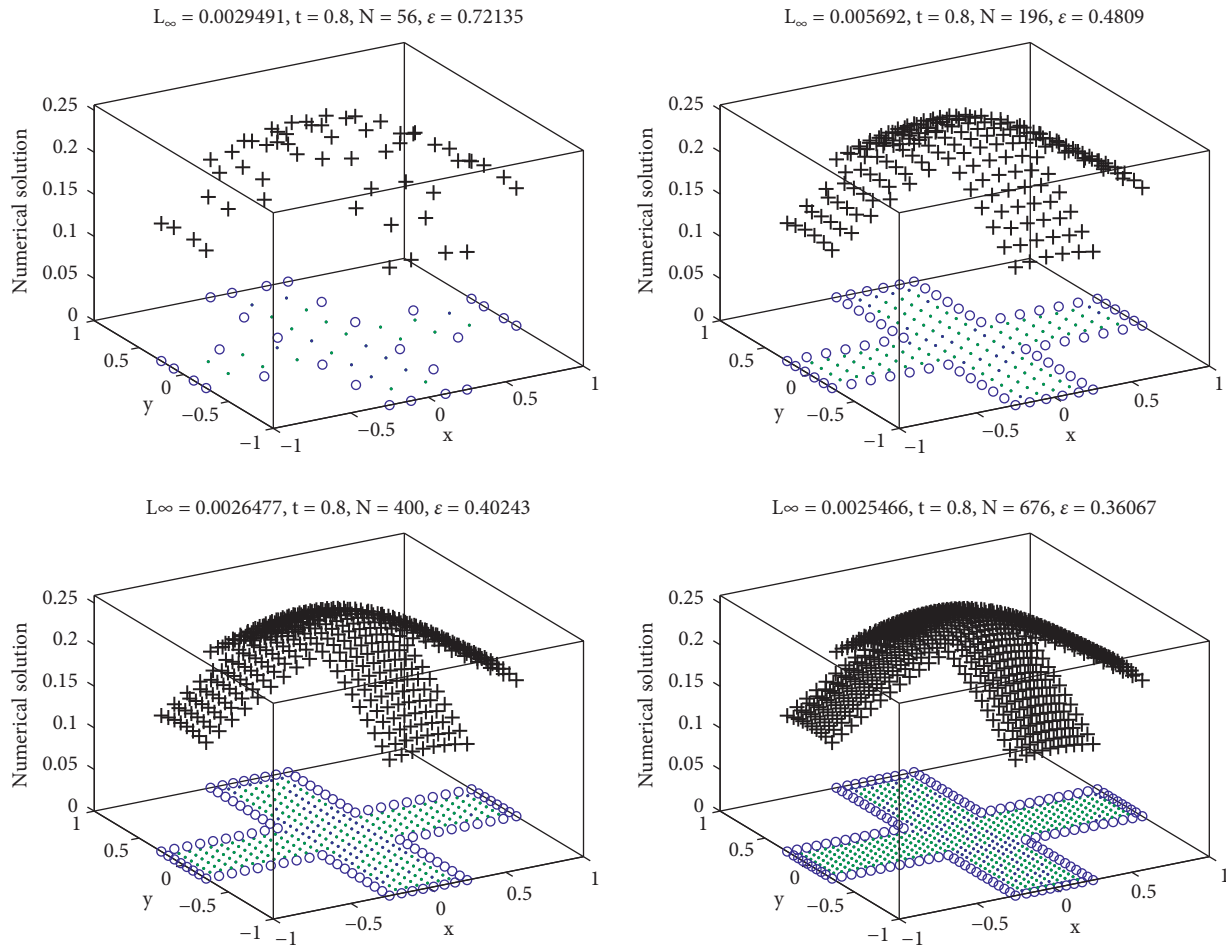


FIGURE 4: RBF-based numerical simulations of Problem 3, in irregular domain, $\tau(t) = 0.4 + 0.2 \sin(0.5\pi t/T)$.

7. Conclusion

The numerical solution of the variable order KdV models in 1D and 2D is achieved using an RBF-based numerical approach. The RBF is used to approximate the spatial derivative, whereas the Coimbra derivative is used to approximate the variable order time differential operator. The numerical scheme's stability and convergence are established. The current numerical technique is found to have a sensitivity in temporal integration. The periodicity of the KdV equation in 1D is explored, and it is demonstrated that the solution is periodic in time at each point of the domain for the fractional order KdV in 1D. The suggested numerical system provides the capacity to numerically approximate numerous complex mechanical problems with ease and precision. The Coimbra variable order operator can be used to examine and analyze the dynamics of a variety of physical models, such as fractional forces, which cannot be accurately modelled with a constant order fractional operator.

Data Availability

The data used to support this study are included in the article.

Conflicts of Interest

The authors declare that they have no conflicts of interest.

References

- [1] G. de Vries and D. J. Korteweg, "On the change of form of long waves advancing in a rectangular canal, and on a new type of long stationary waves," *Philosophical Magazine*, vol. 39, no. 5, pp. 422–443, 1895.
- [2] J. A. Pava, "Nonlinear dispersive equations: existence and stability of solitary and periodic travelling wave solutions," *Number 156*, American Mathematical Soc, Providence, RI, USA, 2009.
- [3] P. Brenner and W. von Wahl, "Global classical solutions of nonlinear wave equations," *Mathematische Zeitschrift*, vol. 176, no. 1, pp. 87–121, 1981.
- [4] T. Tao, "Nonlinear dispersive equations: local and global analysis," *Number 106*, American Mathematical Soc, Washington, DC, USA, 2006.
- [5] M. Uddin, H. U. Jan, A. Ali, and I. A. Shah, "Soliton kernels for solving pdes," *International Journal of Computational Methods*, vol. 13, no. 02, p. 1640009, 2016.
- [6] F. Linares and G. Ponce, *Introduction to Nonlinear Dispersive Equations*, IMPA, Rio de Janeiro, Brazil, 2014.

- [7] J. L. Bona, W. G. Pritchard, and L. R. Scott, "An evaluation of a model equation for water waves," *Philosophical Transactions of the Royal Society of London - Series A: Mathematical and Physical Sciences*, vol. 302, pp. 457–510, 1981.
- [8] J. Bona, J. Wu, and J. Wu, "Temporal growth and eventual periodicity for dispersive wave equations in a quarter plane," *Discrete & Continuous Dynamical Systems - A*, vol. 23, no. 4, pp. 1141–1168, 2009.
- [9] M. Usman, *Forced Oscillations of the Korteweg-De Vries Equation and Their Stability*, PhD Thesis, University of Cincinnati, Cincinnati, OH, USA, 2007.
- [10] J. Shen, J. Wu, and J.-M. Yuan, "Eventual periodicity for the KdV equation on a half-line," *Physica D: Nonlinear Phenomena*, vol. 227, no. 2, pp. 105–119, 2007.
- [11] M. Usman, B. Zhang, and B.-Y. Zhang, "Forced oscillations of the Korteweg-de Vries equation on a bounded domain and their stability," *Discrete & Continuous Dynamical Systems - A*, vol. 26, no. 4, pp. 1509–1523, 2010.
- [12] K. Al-Khaled, N. Haynes, W. Schiesser, and M. Usman, "Eventual periodicity of the forced oscillations for a Korteweg-de Vries type equation on a bounded domain using a sinc collocation method," *Journal of Computational and Applied Mathematics*, vol. 330, pp. 417–428, 2018.
- [13] S. Siraj-ul-Islam, A. Khattak, and I. A. Tirmizi, "A meshfree method for numerical solution of kdv equation," *Engineering Analysis with Boundary Elements*, vol. 32, no. 10, pp. 849–855, 2008.
- [14] M. Uddin, H. Ullah Jan, and M. Usman, "Rbf-fd method for some dispersive wave equations and their eventual periodicity," *Computer Modeling in Engineering and Sciences*, vol. 123, no. 2, pp. 797–819, 2020.
- [15] J. L. Bona and R. Winther, "The Korteweg-de Vries equation in a quarter plane, continuous dependence results," *Differential and Integral Equations*, vol. 2, no. 2, pp. 228–250, 1989.
- [16] B. Fornberg and G. B. Whitham, "A numerical and theoretical study of certain nonlinear wave phenomena," *Philosophical Transactions of the Royal Society of London - Series A: Mathematical and Physical Sciences*, vol. 289, no. 1361, pp. 373–404, 1978.
- [17] A. A. Elsadany, A. Elsonbaty, and H. N. Agiza, "Qualitative dynamical analysis of chaotic plasma perturbations model," *Communications in Nonlinear Science and Numerical Simulation*, vol. 59, pp. 409–423, 2018.
- [18] R. E. Tolba, W. M. Moslem, A. A. Elsadany, N. A. El-Bedwehy, and S. K. El-Labany, "Development of cnoidal waves in positively charged dusty plasmas," *IEEE Transactions on Plasma Science*, vol. 45, no. 9, pp. 2552–2560, 2017.
- [19] Q. Wang, "Numerical solutions for fractional KdV-Burgers equation by Adomian decomposition method," *Applied Mathematics and Computation*, vol. 182, no. 2, pp. 1048–1055, 2006.
- [20] F. C. Meral, T. J. Royston, and R. Magin, "Fractional calculus in viscoelasticity: an experimental study," *Communications in Nonlinear Science and Numerical Simulation*, vol. 15, no. 4, pp. 939–945, 2010.
- [21] F. Höfling and T. Franosch, "Anomalous transport in the crowded world of biological cells," *Reports on Progress in Physics*, vol. 76, no. 4, Article ID 046602, 2013.
- [22] D. A. Benson, R. Schumer, M. M. Meerschaert, and S. W. Wheatcraft, "Fractional dispersion, lévy motion, and the MADE tracer tests," *Dispersion in Heterogeneous Geological Formations*, vol. 42, no. 1-2, pp. 211–240, 2001.
- [23] J.-H. He, "Approximate analytical solution for seepage flow with fractional derivatives in porous media," *Computer Methods in Applied Mechanics and Engineering*, vol. 167, no. 1-2, pp. 57–68, 1998.
- [24] T. A. M. Langlands and B. I. Henry, "Fractional chemotaxis diffusion equations," *Physical Review A*, vol. 81, no. 5, Article ID 051102, 2010.
- [25] Q. Zhang, J. Zhang, S. Jiang, and Z. Zhang, "Numerical solution to a linearized time fractional kdv equation on unbounded domains," *Mathematics of Computation*, vol. 87, no. 310, pp. 693–719, 2017.
- [26] A. Atangana, E. Bonyah, and A. A. Elsadany, "A fractional order optimal 4d chaotic financial model with mittag-leffler law," *Chinese Journal of Physics*, vol. 65, no. 38–53, pp. 38–53, 2020.
- [27] H. Zhang, F. Liu, M. S. Phanikumar, and M. M. Meerschaert, "A novel numerical method for the time variable fractional order mobile-immobile advection-dispersion model," *Computers & Mathematics with Applications*, vol. 66, no. 5, pp. 693–701, 2013.
- [28] H. Sun, W. Chen, and Y. Chen, "Variable-order fractional differential operators in anomalous diffusion modeling," *Physica A: Statistical Mechanics and Its Applications*, vol. 388, no. 21, pp. 4586–4592, 2009.
- [29] X. Zhao, Z.-z. Sun, and G. E. Karniadakis, "Second-order approximations for variable order fractional derivatives: algorithms and applications," *Journal of Computational Physics*, vol. 293, pp. 184–200, 2015.
- [30] A. D. Obembe, M. E. Hossain, and S. A. Abu-Khamsin, "Variable-order derivative time fractional diffusion model for heterogeneous porous media," *Journal of Petroleum Science and Engineering*, vol. 152, pp. 391–405, 2017.
- [31] S. B. Yuste and L. Acedo, "An explicit finite difference method and a new von neumann-type stability analysis for fractional diffusion equations," *SIAM Journal on Numerical Analysis*, vol. 42, no. 5, pp. 1862–1874, 2005.
- [32] Y. L. Kobelev, L. Y. Kobelev, and Y. L. Klimontovich, "Anomalous diffusion with time- and coordinate-dependent memory," in *Doklady Physics*, vol. 48, no. 6, pp. 264–268, Springer, 2003.
- [33] C. F. M. Coimbra, "Mechanics with variable-order differential operators," *Annalen der Physik*, vol. 12, no. 1112, pp. 692–703, 2003.
- [34] N. H. Sweilam and S. M. Al, "Numerical study for multi-strain tuberculosis (tb) model of variable-order fractional derivatives," *Journal of Advanced Research*, vol. 7, no. 2, pp. 271–283, 2016.
- [35] S. Shen, F. Liu, J. Chen, I. Turner, and V. Anh, "Numerical techniques for the variable order time fractional diffusion equation," *Applied Mathematics and Computation*, vol. 218, no. 22, pp. 10861–10870, 2012.
- [36] R. Lin, F. Liu, V. Anh, and I. Turner, "Stability and convergence of a new explicit finite-difference approximation for the variable-order nonlinear fractional diffusion equation," *Applied Mathematics and Computation*, vol. 212, no. 2, pp. 435–445, 2009.
- [37] A. Razminia, A. F. Dizaji, and V. J. Majd, "Solution existence for non-autonomous variable-order fractional differential equations," *Mathematical and Computer Modelling*, vol. 55, no. 3-4, pp. 1106–1117, 2012.
- [38] M. Zayernouri and G. E. Karniadakis, "Fractional spectral collocation methods for linear and nonlinear variable order fpdes," *Journal of Computational Physics*, vol. 293, pp. 312–338, 2015.

- [39] S. G. Samko and B. Ross, "Integration and differentiation to a variable fractional order," *Integral Transforms and Special Functions*, vol. 1, no. 4, pp. 277–300, 1993.
- [40] L. E. S. Ramirez and C. F. M. Coimbra, "On the selection and meaning of variable order operators for dynamic modeling," *International Journal of Differential Equations*, vol. 2010, Article ID 846107, 16 pages, 2010.
- [41] C. M. Soon, C. F. M. Coimbra, and M. H. Kobayashi, "The variable viscoelasticity oscillator," *Annalen der Physik*, vol. 14, no. 6, pp. 378–389, 2005.
- [42] B. Sepehrian and Z. Shamohammadi, "A high order method for numerical solution of time-fractional kdv equation by radial basis functions," *Arabian Journal of Mathematics*, vol. 7, no. 4, pp. 303–315, 2018.
- [43] R. L. Hardy, "Multiquadric equations of topography and other irregular surfaces," *Journal of Geophysical Research*, vol. 76, no. 8, pp. 1905–1915, 1971.
- [44] R. L. Hardy, "Theory and applications of the multiquadric-biharmonic method 20 years of discovery 1968–1988," *Computers & Mathematics with Applications*, vol. 19, no. 8-9, pp. 163–208, 1990.
- [45] R. Franke, *A Critical Comparison of Some Methods for Interpolation of Scattered Data*, NAVAL POSTGRADUATE SCHOOL, Monterey, CA, USA, 1979.
- [46] C. A. Micchelli, "Algebraic aspects of interpolation," *Approximation Theory*, vol. 36, pp. 81–102, 1986.
- [47] I. J. Schoenberg, "Metric spaces and completely monotone functions," *Annals of Mathematics*, vol. 39, no. 4, pp. 811–841, 1938.
- [48] S. A. Sarra and E. J. Kansa, "Multiquadric radial basis function approximation methods for the numerical solution of partial differential equations," *Advances in Computational Mechanics*, vol. 2, no. 2, p. 220, de Madrid, Spain, 2009.
- [49] F. M. Bernal Martínez, *Meshless Methods for Elliptic and Free-Boundary Problems*, Universidad Carlos III de Madrid, PhD Thesis, 2008.
- [50] M. D. Buhmann, "Radial basis functions," *Acta Numerica*, vol. 9, pp. 1–38, 2000.
- [51] G. E. Fasshauer, "Meshfree approximation methods with MATLAB," *World Scientific*, vol. 6, 2007.
- [52] W. R. Madych, "Miscellaneous error bounds for multiquadric and related interpolators," *Computers & Mathematics with Applications*, vol. 24, no. 12, pp. 121–138, 1992.
- [53] T. Belytschko, Y. Krongauz, D. Organ, M. Fleming, and P. Krysl, "Meshless methods: an overview and recent developments," *Computer Methods in Applied Mechanics and Engineering*, vol. 139, no. 1-4, pp. 3–47, 1996.
- [54] D. Ingman and J. Suzdalnitsky, "Control of damping oscillations by fractional differential operator with time-dependent order," *Computer Methods in Applied Mechanics and Engineering*, vol. 193, no. 52, pp. 5585–5595, 2004.
- [55] M. Uddin, "On the selection of a good value of shape parameter in solving time-dependent partial differential equations using rbf approximation method," *Applied Mathematical Modelling*, vol. 38, no. 1, pp. 135–144, 2014.

Research Article

On Discrete Fractional Complex Gaussian Map: Fractal Analysis, Julia Sets Control, and Encryption Application

Amr Elsonbaty ^{1,2}, A. Elsadany,^{1,3} and Fatma Kamal ²

¹Department of Mathematics, College of Science and Humanities in Al-Kharj, Prince Sattam Bin Abdulaziz University, Al-Kharj 11942, Saudi Arabia

²Mathematics and Engineering Physics Department, Faculty of Engineering, Mansoura University, P.O. 35516, Mansoura, Egypt

³Department of Basic Science, Faculty of Computers and Informatics, Suez Canal University, Ismailia, Egypt

Correspondence should be addressed to Amr Elsonbaty; sonbaty2010@gmail.com

Received 16 December 2021; Revised 17 February 2022; Accepted 7 March 2022; Published 19 April 2022

Academic Editor: Amin Jajarmi

Copyright © 2022 Amr Elsonbaty et al. This is an open access article distributed under the Creative Commons Attribution License, which permits unrestricted use, distribution, and reproduction in any medium, provided the original work is properly cited.

This work is devoted to present a generalized complex discrete fractional Gaussian map. Analytical and numerical analyses of the proposed map are conducted. The dynamical behaviors and stability of fixed points of the map are explored. The existence of fractal Mandelbrot and Julia sets is examined along with the corresponding fractal characteristics. The influences of the key parameters of the map and fractional order are examined. Moreover, nonlinear controllers are designed in the complex domain to control Julia sets generated by the map or to achieve synchronization between two Julia sets in master/slave configuration. Numerical simulations are provided to attain a deep understanding of nonlinear behaviors of the proposed map. Then, a suggested efficient chaos-based encryption technique is introduced by integrating the complicated dynamical behavior and fractal sets of the proposed map with the pseudo-chaos generated from the modified lemniscate hyperchaotic map.

1. Introduction

Mathematical models are used to describe and understand the interesting behaviors of nonlinear systems, which arise in different disciplines of science. There are a plethora of mathematical tools, which have proved their efficacy in mathematical modeling of biological, physical, engineering, economic, and natural systems. Among these tools, the differential equations, difference equations, and statistical methods have attracted a considerable interest [1–5].

However, when dealing with systems with memory, that is, the associated rate of changes depends on the past values of state variables in addition to the present values, the conventional continuous-time differential equation and discrete-time maps cannot describe these systems properly. To address this issue, mathematicians and engineers employ fractional calculus to formulate nonlocal

differential operators, which are necessary to study systems with memory. Firstly, they focused on the fractional-order differential equations (FDEs) for the past two decades. The electric circuits, fluid mechanics, electromagnetics, immune systems, nanofluids, epidemics, and biological and financial systems are only examples of the fields, where FDEs are of great importance [6–13]. There are a few definitions for fractional-order derivatives and integrals, which have been developed so far such as Riemann–Liouville, Caputo Grunwald–Letnikov, and Wyl–Riesz fractional operators. More details are provided in references [14–18]. In reference [19], a fractional-order model based on Atangana–Baleanu–Caputo fractional derivative was proposed to understand the dynamics of differentiation of stem cells. The state-of-the-art developments in special functions and mathematical analysis tools associated with fractional-order differential equations are provided in reference [20].

The numerical solutions of FDEs are usually carried out with high computational cost and induce several types of numerical errors.

Therefore, while searching for an efficient and reasonable alternative, it is recognized that the fractional difference operators can be applied in a straightforward way to the mathematical modeling of different nonlinear systems. More recently, attention has been turned to the discrete fractional difference equations [21–25], where they have been successfully applied in different fields.

On the other side, complex maps are found to exhibit very interesting and fascinating geometrical structures known as Julia and Mandelbrot fractal sets [26–28]. These sets are known to have fractal dimensions and have many interesting applications. The nonlinear dynamics and chaotic behavior of discrete fractional Gauss maps are investigated in the literature. It has been observed that the fractional Gauss map is more stable compared with the associated integer map. The width of period-3 windows is found to increase with the decrement in the value of fractional order [29]. Also, the synchronization for standard integer-order Gauss maps and discrete fractional Gauss maps has been studied using a parameter estimation scheme [30]. The emerging nonlinear dynamics and synchronization in coupled integer-order and fractional-order Gauss maps with different topologies have been explored in reference [31, 32]. The motivation of this study is based on the observation that the nonlinear characteristics and dynamics of the fractional complex maps are still almost an unexplored point in literature. Indeed, there are very few works that begin to investigate only the case of fractional-order complex differential equations [33, 34]. The present work extends the aforementioned works to the more general and unexplored case, where the state variable of the map has complex values, and it also investigates the emerging Julia and Mandelbrot fractal sets along with synchronization methodology of discrete fractional Gaussian map in complex domain for the first time, to the best of authors' knowledge. Moreover, the present work combines the induced fractal sets into a proposed efficient chaos-based encryption technique.

The very complicated behaviors of chaotic systems along with noise-like dynamics, very broadband spectrum, and ability to attain synchronization between distant systems have been utilized efficiently in a plethora of schemes for chaos-based communications [35–52]. In the last two decades, the chaos-based cryptography has become a focus research point of great interest. The critical evaluation of chaos-based encryption systems reveals that it is essential to keep high complexity and dimensionality of chaotic dynamics in encryption schemes along with effectively preventing any information leakage by possible eavesdroppers attacks [40–42]. The chaotic maps, in particular, are easily implementable on digital hardware, which can be straightforwardly integrated with modern communication systems. However, several works have highlighted the problem of degradation and suppression of chaotic behavior in simple structure and low-dimensional chaotic maps. These problems result from hardware finite precision of floating numbers [43–45]. Also, the small key space in these

chaotic maps is another drawback. The employment of multiple chaos systems and switching between their outputs is offered along with sufficient long finite precision computations to improve the performance of chaotic maps [46]. The pseudo-chaotic orbits can be employed as another solution to the aforementioned chaos degradation issue [47, 48]. More specifically, pseudo-chaotic time series can be attained by subtracting the output sequences of two mathematically equivalent chaotic maps, which are non-equivalent in computations when machine finite precision is considered [47, 48]. The application of discrete fractional complex maps in the field of chaos-based encryption systems is also an unexplored research point, to the best of our knowledge. So, this article aims also at investigating this challenging task and providing a reliable encryption machine based on the complicated dynamics of a proposed fractional complex map.

This study is organized as follows: the mathematical model of the proposed discrete fractional complex Gaussian map is presented in Section 2. The control and synchronization of Julia sets generated by the proposed map are examined in Section 3. The proposed hybrid chaos-fractal encryption scheme is presented in Section 4, while the associated security analysis is addressed in Section 5. Section 6 contains conclusion and final discussion.

2. Discrete Fractional Complex Gaussian Map

The discrete fractional complex Gaussian map is proposed in the following form:

$${}^C\Delta_0^\alpha z(t) = e^{-az^2(t+\alpha-1)} + b, \quad (1)$$

where z , $a \neq 0$, and $b \neq 0$ take complex values, whereas the fractional order $\alpha \in (0, 1]$. The complex discrete fractional map (1) has infinite number of fixed points, which can be evaluated from the following equation:

$$e^{-az^{*2}} = -b, \quad (2)$$

or

$$z^* = \left[\frac{\ln|b| + i\{\theta_0 + (2k+1)\pi\}}{a} \right]^{1/2}, \quad (3)$$

$$k = 0, \pm 1, \pm 2, \dots,$$

where θ_0 denotes the principal argument of complex-valued constant b . This means that the equilibrium points of the proposed map are determined according to the assigned values for a , b , and k .

The asymptotic stability analysis of fixed points in the complex fractional Gaussian map (1) is conducted in the following subsection:

2.1. Stability Analysis of Fixed Points

Theorem 1. *The fixed point z^* of the fractional complex Gaussian map (1) is locally asymptotically stable if*

$$|-2az^* e^{-az^{*2}}| < \left(2 \cos \frac{\text{Arg}(-2az^* e^{-az^{*2}}) - \pi}{2 - \alpha} \right)^\alpha,$$

$$\left| \text{Arg}(-2az^* e^{-az^{*2}}) \right| > \frac{\alpha\pi}{2}. \tag{4}$$

Proof. Assume that $\varepsilon(t) = z(t) - z^*$, then the next linearized map is derived from equation (1):

$$\begin{aligned} {}^C\Delta_0^\alpha \varepsilon(t) &= -2az^* e^{-az^{*2}} \varepsilon(t + \alpha - 1) \\ &= \gamma \varepsilon(t + \alpha - 1). \end{aligned} \tag{5}$$

Expressing the above equation in terms of its real and imaginary parts, it follows that

$$\begin{aligned} \Delta_0^\alpha \varepsilon_r(t) + i {}^C\Delta_0^\alpha \varepsilon_i(t) &= (\gamma_r + i\gamma_i) \\ &\cdot (\varepsilon_r(t + \alpha - 1) + i\varepsilon_i(t + \alpha - 1)), \end{aligned} \tag{6}$$

and therefore the next equivalent 2D discrete fractional system is attained:

$$\begin{aligned} \Delta_0^\alpha \varepsilon_r(t) &= \gamma_r \varepsilon_r(t + \alpha - 1) - \gamma_i \varepsilon_i(t + \alpha - 1), \\ \Delta_0^\alpha \varepsilon_i(t) &= \gamma_i \varepsilon_r(t + \alpha - 1) + \gamma_r \varepsilon_i(t + \alpha - 1). \end{aligned} \tag{7}$$

Now, the above two equations can be expressed as follows:

$$\begin{pmatrix} \Delta_0^\alpha \varepsilon_r(t) \\ \Delta_0^\alpha \varepsilon_i(t) \end{pmatrix} = \begin{pmatrix} \gamma_r & -\gamma_i \\ \gamma_i & \gamma_r \end{pmatrix} \begin{pmatrix} \varepsilon_r(t + \alpha - 1) \\ \varepsilon_i(t + \alpha - 1) \end{pmatrix}, \tag{8}$$

where it can be verified that the eigenvalues of the matrix of coefficients are given by $\gamma_r \pm i\gamma_i$.

Define Λ by

$$\Lambda = \begin{pmatrix} \gamma_r & -\gamma_i \\ \gamma_i & \gamma_r \end{pmatrix}, \tag{9}$$

such that $\text{tr}(\Lambda) = 2\gamma_r$, and $\det(\Lambda) = \gamma_r^2 + \gamma_i^2 > 0$. The zero equilibrium point of equation (8) is asymptotically stable if its associated eigenvalues satisfy

$$\sqrt{\gamma_r^2 + \gamma_i^2} < \left(2 \cos \frac{|\tan^{-1}(\gamma_i/\gamma_r)| - \pi}{2 - \alpha} \right)^\alpha, \left| \tan^{-1} \left(\frac{\gamma_i}{\gamma_r} \right) \right| > \frac{\alpha\pi}{2}. \tag{10}$$

For $z^* = [\ln|b| + i\{\theta_0 + (2k + 1)\pi\}/a]^{1/2}$, $k = 0, \pm 1, \pm 2, \dots$, the stability conditions reduce to

$$\begin{aligned} |-2az^* e^{-az^{*2}}| &< \left(2 \cos \frac{|\text{Arg}(-2az^* e^{-az^{*2}})| - \pi}{2 - \alpha} \right)^\alpha \\ &\cdot \left| \text{Arg}(-2az^* e^{-az^{*2}}) \right| > \frac{\alpha\pi}{2}. \end{aligned} \tag{11}$$

In this case, the trajectories which start from small initial perturbations $\varepsilon_r(0)$, and $\varepsilon_i(0)$, around the origin will algebraically decay to the equilibrium point such that $\|\varepsilon(n)\| = O(n^{-\alpha})$, as $n \rightarrow \infty$.

For the special case, where principal argument of b is considered, that is, $k = 0$, we get

$$\begin{aligned} z_{1,2}^* &= \left[\frac{1/2 \ln(b_r^2 + b_i^2) + i(\theta_0 + \pi)}{a_r + ia_i} \right]^{1/2} \\ &= \left[\frac{(1/2 a_r \ln(b_r^2 + b_i^2) - a_i(\theta_0 + \pi)) + i(a_r(\theta_0 + \pi) + 1/2 a_i \ln(b_r^2 + b_i^2))}{a_r^2 + a_i^2} \right]^{1/2} \\ &= \frac{1}{\sqrt{a_r^2 + a_i^2}} r^{*1/2} \left[\cos\left(\frac{\phi_0}{2}\right) + i \sin\left(\frac{\phi_0}{2}\right) \right], \frac{1}{\sqrt{a_r^2 + a_i^2}} r^{*1/2} \left[\cos\left(\frac{\phi_0 + \pi}{2}\right) + i \sin\left(\frac{\phi_0 + \pi}{2}\right) \right], \end{aligned} \tag{12}$$

where $a = a_r + ia_i$ and $b = b_r + ib_i$,

$$\begin{aligned} r^* &= \sqrt{\left(\frac{1}{2} a_r \ln(b_r^2 + b_i^2) - a_i(\theta_0 + \pi) \right)^2 + \left(a_r(\theta_0 + \pi) + \frac{1}{2} a_i \ln(b_r^2 + b_i^2) \right)^2}, \\ \phi_0 &= \tan^{-1} \left(\frac{a_r(\theta_0 + \pi) + 1/2 a_i \ln(b_r^2 + b_i^2)}{1/2 a_r \ln(b_r^2 + b_i^2) - a_i(\theta_0 + \pi)} \right). \end{aligned} \tag{13}$$

The specific forms of $z_{1,2}^*$ can be substituted in above-mentioned stability conditions to investigate their stability.

By the aid of numerical simulations, previous results regarding stability conditions of fixed points are validated for different values of α, k, a , and b (Figure 1). The obtained solution orbits indicate that the stability conditions are satisfied for selected parameter sets employed in Figure 1.

2.2. Fractal Sets Induced by Discrete Fractional Complex Gaussian Map. The notions of Julia fractal set and Mandelbrot fractal set in integer-order complex-valued maps can be extended to the general case of discrete fractional-order complex maps. Given the next discrete fractional map of order α

$$\Delta_0^\alpha z(t) = \Psi(z(t + \alpha - 1), \mu), \quad (14)$$

where $\Psi: \mathbb{C} \rightarrow \mathbb{C}$ and $\mu \in \mathbb{C}$. The Julia set generated by map (5) is described in the following definition [26–28, 33, 34]:

Definition 2. The filled-in Julia set of complex-valued discrete fractional map (5) is defined as the set Ω of initial points $z \in \mathbb{C}$, whose solution orbits are bounded. The boundary of Ω set is referred to as $\partial\Omega$ and it is known as the Julia set Y_Ψ^α of the map (5).

The main characteristics of Julia set Y_Ψ^α are summarized as follows [27, 28, 33, 34]:

- (1) $Y_\Psi^\alpha \neq \emptyset$ (Julia set is nonempty).
- (2) Y_Ψ^α is invariant with respect to associated map (5) in the forward and backward directions of time.
- (3) Assuming that an attractive fixed point \hat{z} of the discrete fractional map (5) has period p and exists at $\bar{\alpha}$, then Y_Ψ^α includes the basin of attraction of \hat{z} .

The well-known Mandelbrot set has been investigated by Benoit Mandelbrot in 1979 [27, 28]. Its concept can also be generalized to the discrete fractional case. More specifically, fixing the value of fractional order α , the Mandelbrot set χ_Ψ^α consists of the set of values of parameter $\mu \in \mathbb{C}$ at which the values of $|z(t)|$, $t > 0$ are bounded for $z(0) = 0$.

The space-filling dimension can be employed to quantify the fractal properties of Julia and Mandelbrot sets. In particular, the box-counting measure for dimension is one of the most accessible measures in fractal analysis and it is defined as follows:

Definition 3. Consider the nonempty bounded subset Ξ of \mathbb{R}^n and suppose that there are N_ρ boxes with side length ρ , which are required to cover the set Ξ . Then, the box-counting dimension (Minkowski–Bouligand dimension) is determined by the following equation:

$$\dim_\Xi = \lim_{\rho \rightarrow 0} \frac{\log(N_\rho)}{\log(1/\rho)}, \quad (15)$$

where N_ρ is the number of boxes to cover Ξ . In addition, the upper box dimension (entropy dimension) and the lower

box dimension (lower Minkowski dimension) of Ξ are also defined, respectively, by the following equations:

$$\overline{\dim}_\Xi = \overline{\lim}_{\rho \rightarrow 0} \frac{\log(N_\rho)}{\log(1/\rho)}, \quad (16)$$

$$\underline{\dim}_\Xi = \underline{\lim}_{\rho \rightarrow 0} \frac{\log(N_\rho)}{\log(1/\rho)}.$$

The generation of Mandelbrot and Julia sets is explored through numerical simulations at different values of parameters. The following table summarizes the obtained results at different values of fractional order α , constant q , and exponent p . In addition, the box-counting dimensions for the different cases considered in simulations are also presented in Table 1. The corresponding Mandelbrot and Julia sets are depicted in Figures 2 to 4.

3. Control and Synchronization of Julia Sets

The problem of achieving control and synchronization of Julia sets generated by the discrete fractional complex Gaussian map is discussed in this section.

For two discrete fractional-order complex Gaussian maps, the first map is known as the master map and it produces the output $z_1(t)$, while the second map, with the output $z_2(t)$, will be referred to as the slave one.

Definition 4. The synchronization between the master and slave maps is achieved, if $z_2(t) \rightarrow z_1(t)$ as $t \rightarrow \infty$. In other words, it can be expressed as follows [33, 34]:

$$\lim_{t \rightarrow \infty} |z_2(t) - z_1(t)| = 0. \quad (17)$$

When the synchronization is attained between two trajectories, it implies that the corresponding characteristics of convergence and divergence are identical. Assume that Y_1^α and Y_2^α denote the Julia sets induced by fractional-order master and fractional-order slave Gaussian maps, respectively, at fractional order α . Therefore, the synchronization between the mentioned two Julia sets can be defined as follows [29,30]:

Definition 5. The asymptotic synchronization of the two Julia sets Y_1^α and Y_2^α is satisfied if

$$\lim_{t \rightarrow \infty} (Y_1^\alpha \cup Y_2^\alpha - Y_1^\alpha \cap Y_2^\alpha) = \emptyset. \quad (18)$$

3.1. Control of Julia Sets of Discrete Fractional Complex Gaussian Map. In this section, the appropriate controller is designed in order to change the characteristics and geometry of Julia sets generated by the proposed fractional map via varying the type of stability of one of the fixed points of the present map. More specifically, we consider the feedback controller in the following form:

$$q(t) = -\zeta(z(t) - \tilde{z}) - e^{-az^2(t)} - b, \quad (19)$$

where \tilde{z} is the selected unstable fixed point intended to be stabilized under the influence of controller and $\zeta = \zeta_r + i\zeta_i$

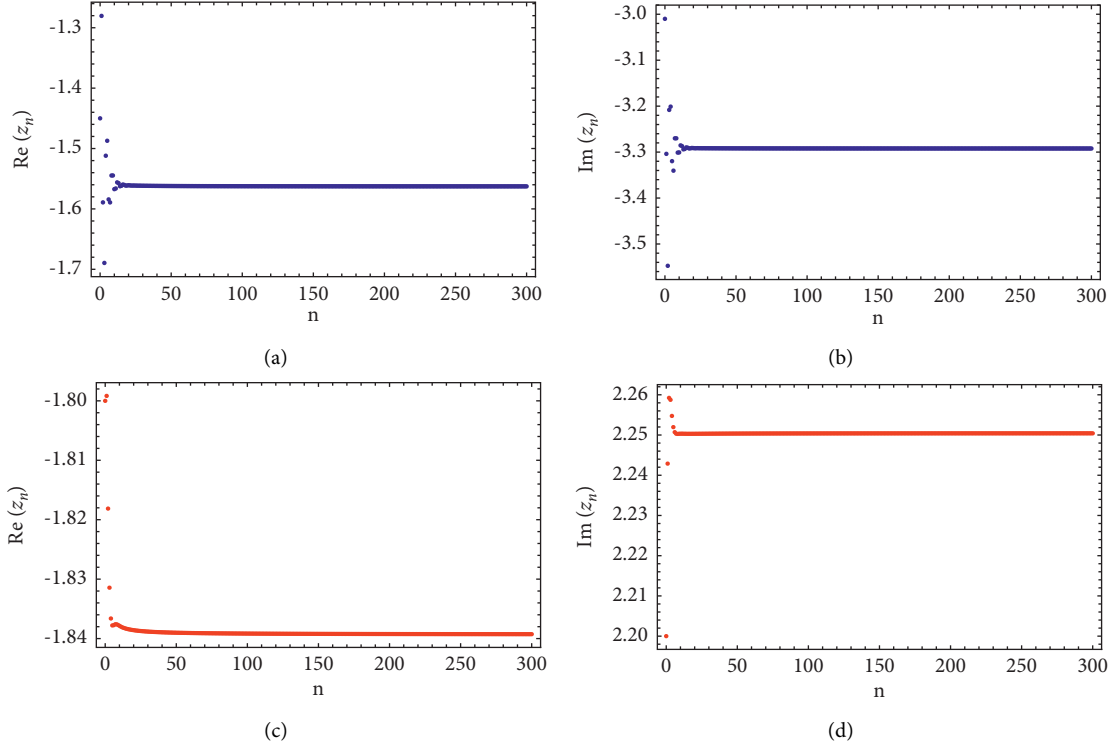


FIGURE 1: Time series solution of fractional Gaussian map depicting stable fixed points at (a, b) $a = 0.15 - 0.15i, \alpha = 0.9, b = 0.71 + 0.25i$ and (c, d) $a = 0.3 + 0.2i, \alpha = 0.85, b = 0.3 - 0.1i$.

TABLE 1: Summary of fractal sets generated from complex fractional Gaussian map and their fractal dimensions.

Graph	Fractal set	Parameters	Dimension
Figure 2(a)	Mandelbrot set	$\alpha = 1,$ $a = 0.5 + 0.3i$	1.544
Figure 2(b)	Julia set	$\alpha = 1,$ $a = 0.5 + 0.3i, b = 0.3 + 0.3i$	1.838
Figure 2(c)	Julia set	$\alpha = 1,$ $a = 0.5 + 0.3i, b = -0.15 - 0.4i$	1.6438
Figure 2(d)	Mandelbrot set	$\alpha = 1,$ $a = 0.19 - 0.5i$	1.429
Figure 2(e)	Julia set	$\alpha = 1, a = 0.19 - 0.5i, b = 0.5 - 0.5i$	1.8321
Figure 3(a)	Mandelbrot set	$\alpha = 0.8, a = 0.19 - 0.5i$	1.753
Figure 3(b)	Mandelbrot set	$\alpha = 0.5, a = 0.19 - 0.5i$	1.4775
Figure 3(c)	Mandelbrot set	$\alpha = 0.3, a = 0.19 - 0.5i$	1.512
Figure 3(d)	Julia set	$\alpha = 0.8, a = 0.19 - 0.5i, b = 0.5 - 0.5i$	1.781
Figure 3(e)	Julia set	$\alpha = 0.5, a = 0.19 - 0.5i, b = 0.5 - 0.5i$	1.6574
Figure 3(f)	Julia set	$\alpha = 0.3, a = 0.19 - 0.5i, b = 0.5 - 0.5i$	1.932
Figure 4(a)	Mandelbrot set	$\alpha = 0.9, a = -0.59 + 0.93i$	1.5016
Figure 4(b)	Julia set	$\alpha = 0.9, a = -0.59 + 0.93i, b = -0.75 - 0.05i$	1.753
Figure 4(c)	Mandelbrot set	$\alpha = 0.5, a = 1.15 - 0.7i$	1.483
Figure 4(d)	Julia set	$\alpha = 0.5, a = 1.15 - 0.7i, b = 0.5 - 0.5i$	1.4485

represents the complex-valued gain of the controller, which can be evaluated as follows:

Theorem 6. Assume that the gain ζ of controller $\varrho(t)$ of the controlled fractional-order complex Gaussian map

$$\Delta_0^\alpha z(t) = e^{-az^2(t+\alpha-1)} + b + \varrho(t + \alpha - 1), \quad (20)$$

fulfills the two inequalities

$$\zeta_r > 0, \quad \sqrt{\zeta_r^2 + \zeta_i^2} < 2^\alpha, \quad (21)$$

then the fixed point \tilde{z} become stable, such that the associated Julia set in its neighborhood is changed.

Proof. By applying the control signal (6), we get the following controlled fractional-order complex map:

$$\Delta_0^\alpha z(t) = -\zeta(z(t + \alpha - 1) - \tilde{z}). \quad (22)$$

Defining $\delta(t) = z(t) - \tilde{z} \in \mathbb{C}$, equation (22) takes the following form:

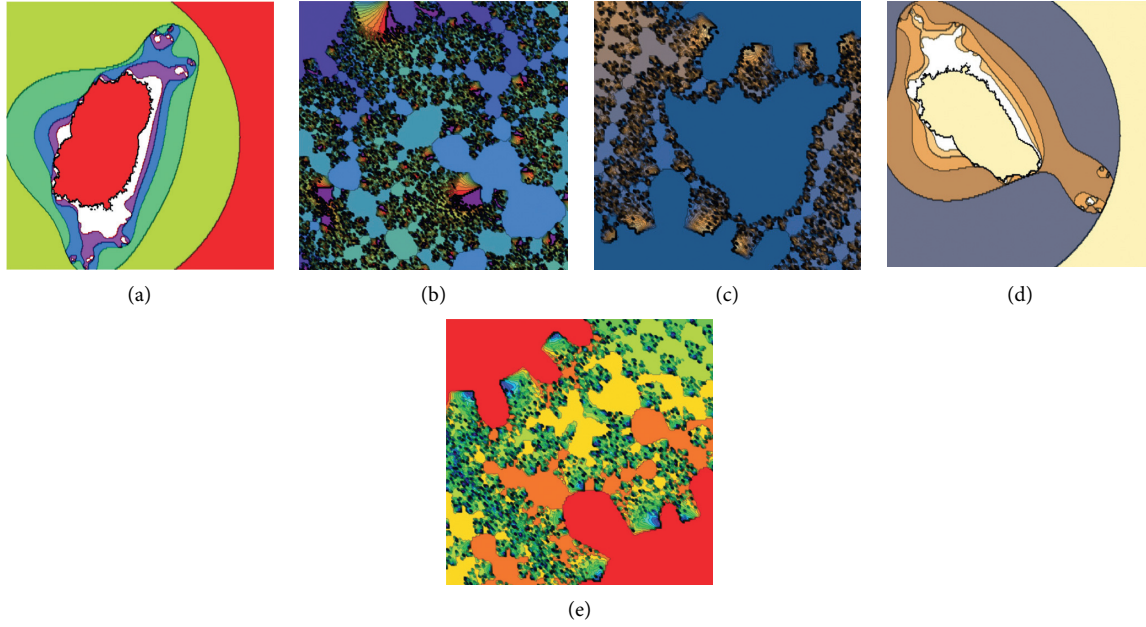


FIGURE 2: The Mandelbrot and Julia sets of generalized fractional Gaussian map obtained at specified values in Table 1.

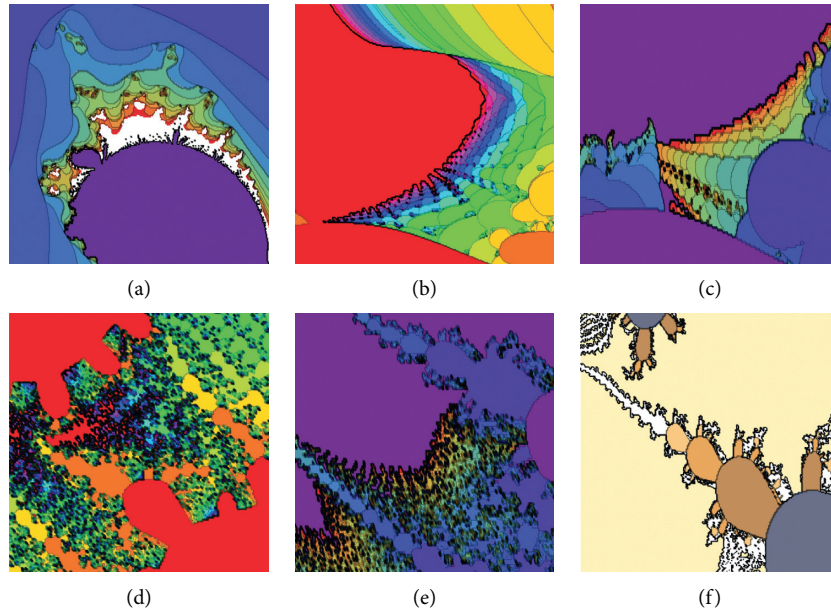


FIGURE 3: The Mandelbrot and Julia sets of generalized fractional Gaussian map obtained at specified values in Table 1.

$$\Delta_0^\alpha \delta(t) = -\zeta_r \delta(t + \alpha - 1). \quad (23)$$

The corresponding two-dimensional real-valued fractional map can be expressed as follows:

$$\begin{aligned} \Delta_0^\alpha \delta_r(t) &= -\zeta_r \delta_r(t + \alpha - 1) + \zeta_i \delta_i(t + \alpha - 1), \\ \Delta_0^\alpha \delta_i(t) &= -\zeta_i \delta_r(t + \alpha - 1) - \zeta_r \delta_i(t + \alpha - 1). \end{aligned} \quad (24)$$

Then, the coefficients of the above system can be put in the following matrix:

$$\Lambda = \begin{pmatrix} -\zeta_r & \zeta_i \\ -\zeta_i & -\zeta_r \end{pmatrix}, \quad (25)$$

and the associated eigenvalues are computed as $-\zeta_r \pm i\zeta_i$. Hence, the sufficient conditions required for local asymptotic stability of \bar{z} can be formulated as $\zeta_r > 0$ and $\sqrt{\zeta_r^2 + \zeta_i^2} < 2^\alpha$. \square

3.2. Synchronization of Julia Sets. The discrete fractional master system is defined in the following form:

$$\Delta_0^\alpha z_1(t) = e^{-az_1^2(t+\alpha-1)} + b, \quad (26)$$

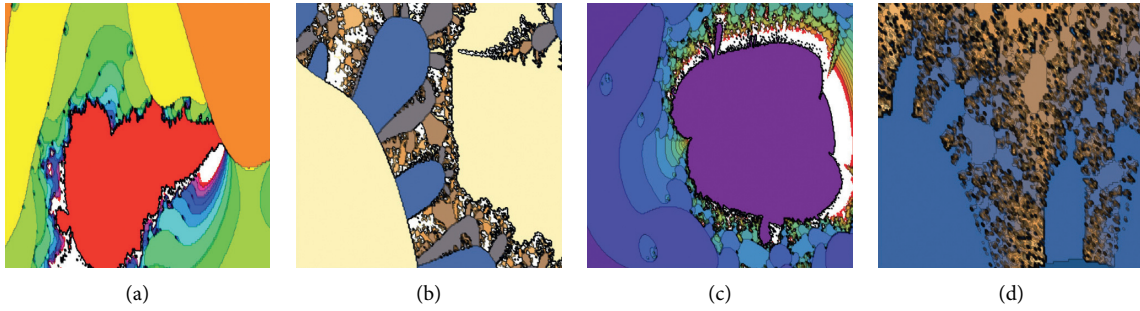


FIGURE 4: The Mandelbrot and Julia sets of generalized fractional Gaussian map obtained at specified values in Table 1.

whereas the corresponding slave system is formulated as follows:

$$\Delta_0^\alpha z_2(t) = e^{-az_2^2(t+\alpha-1)} + b + \phi(z_1, z_2, t + \alpha - 1), \quad (27)$$

where $\phi(z_1, z_2, t + \alpha - 1)$ is the adequate controller to be designed. Note that the initial values of two systems are assumed to be different and since the present map has infinite number of fixed points, the solutions z_1 and z_2 may converge to different fixed points in the way that they induce distinct filled Julia sets. When the synchronization is achieved between the two maps, it is achieved for the associated Julia sets.

Theorem 7. *The two fractional maps (8) and (9) are synchronized under the influence of the following controller:*

$$\begin{aligned} \phi(z_1, z_2, t + \alpha - 1) = & e^{-az_1^2(t+\alpha-1)} - e^{-az_2^2(t+\alpha-1)} \\ & - \kappa(z_2(t + \alpha - 1) - z_1(t + \alpha - 1)), \end{aligned} \quad (28)$$

where the gain $\kappa = \kappa_r + i\kappa_i$, satisfying $|\kappa| < 2^\alpha$ and $\kappa_r > 0$.

Proof. The discrete fractional error map is obtained by subtracting equation (8) from equation (9) as follows:

$$\begin{aligned} \Delta_0^\alpha e(t) = & e^{-az_2^2(t+\alpha-1)} - e^{-az_1^2(t+\alpha-1)} + \phi(z_1, z_2, t + \alpha - 1), \\ e(t) = & z_2(t) - z_1(t). \end{aligned} \quad (29)$$

Using the proposed controller (10) into the above fractional error system, it results in

$$\Delta_0^\alpha e(t) = -\kappa e(t + \alpha - 1), \quad (30)$$

or

$$\begin{aligned} \Delta_0^\alpha (e_r(t) + ie_i(t)) = & (-\kappa_r - i\kappa_i) \\ & \cdot (e_r(t + \alpha - 1) + ie_i(t + \alpha - 1)), \end{aligned} \quad (31)$$

which can be expressed in the following two dimensional system:

$$\begin{aligned} \Delta_0^\alpha e_r(t) = & -\kappa_r e_r(t + \alpha - 1) + \kappa_i e_i(t + \alpha - 1), \\ {}^C \Delta e_i(t) = & -\kappa_i e_r(t + \alpha - 1) - \kappa_r e_i(t + \alpha - 1). \end{aligned} \quad (32)$$

It is obvious that the eigenvalues of error system are $-\kappa_r \pm i\kappa_i$, so that the asymptotic stability to zero fixed point of error system is attained provided that $|\kappa| < 2^\alpha$ and $\kappa_r > 0$.

Numerical simulations are now employed to validate the theoretical results acquired in this section. The synchronization between orbits of two fractional-order complex Gaussian maps initiated from different initial conditions is shown in Figure 5. \square

4. Proposed Encryption Algorithm

The objective of this section is to introduce an efficient chaos-based encryption technique, which utilizes the idea of pseudo-chaotic dynamics along with complicated fractal patterns to boost its security performance.

Consider the following two modified chaotic lemniscate maps [47]:

$$\begin{aligned} x_1(n+1) = & \frac{\cos[2^{3/2+r} \cos[2^r x_1(n)] \sin[2^r x_1(n)] / 1 + \sin^2[2^r x_1(n)]]}{1 + \sin^2[2^{3/2+r} \cos[2^r x_1(n)] \sin[2^r x_1(n)] / 1 + \sin^2[2^r x_1(n)]]}, \\ y_1(n+1) = & \frac{2\sqrt{2} \cos[2^r \cos[2^r y_1(n)] / 1 + \sin^2[2^r y_1(n)]] \sin[2^r \cos[2^r y_1(n)] / 1 + \sin^2[2^r y_1(n)]]}{1 + \sin^2[2^r \cos[2^r y_1(n)] / 1 + \sin^2[2^r y_1(n)]]}, \end{aligned} \quad (33)$$

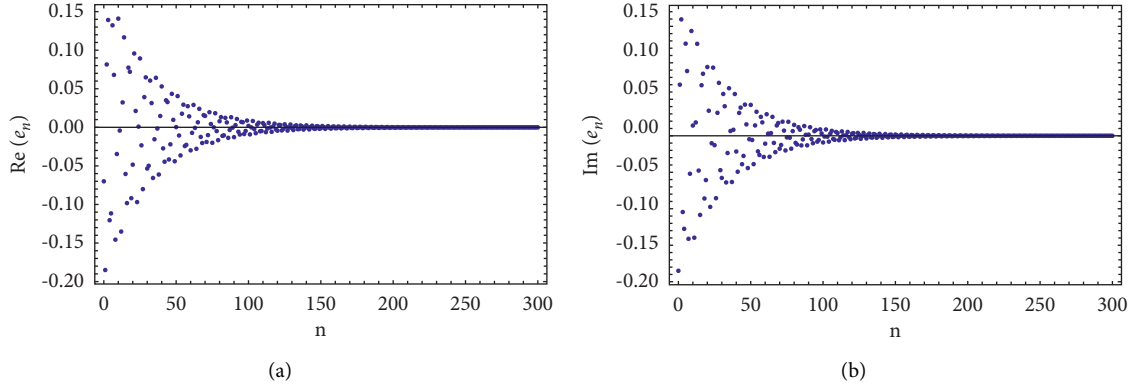


FIGURE 5: Synchronization errors between master and slave systems at $a = 0.15 - 0.15i$, $\alpha = 0.9$, $b = 0.71 + 0.25i$, where initial value for master system is $(-1.43 - 3i)$ and that for slave system is $(-1.4 - 2.8i)$, whereas $\kappa = 1 + i$.

$$\begin{aligned}
 x_2(n) &= \frac{\cos\left[2^{3/2} \cos(2^r x_2(n))/\sqrt{1 + \sin^2(2^r x_2(n))} \times 2^r \sin(2^r x_2(n))/\sqrt{1 + \sin^2(2^r x_2(n))}\right]}{1 + \sin^2\left[2^{3/2} \cos(2^r x_2(n))/\sqrt{1 + \sin^2(2^r x_2(n))} \times 2^r \sin(2^r x_2(n))/\sqrt{1 + \sin^2(2^r x_2(n))}\right]}, \\
 y_2(n) &= \frac{2 \cos\left[2^r/\sqrt{1 + \sin^2(2^r y_2(n))} \times \cos(2^r y_2(n))/\sqrt{1 + \sin^2(2^r y_2(n))}\right]}{1 + \sin^2\left[2^r \cos(2^r y_2(n))/1 + \sin^2(2^r y_2(n))\right]} \times \frac{\sin\left[2^r \sin(2^r x_2(n))/1 + \sin^2(2^r x_2(n))\right]}{1/\sqrt{2}}.
 \end{aligned} \tag{34}$$

It is obvious that these two maps are mathematically equivalent, yet the finite floating-point representation renders the corresponding orbits diverge exponentially from each other even in the case where identical initial conditions are used. Now, a set of q random perturbation values, $\{b_1, b_2, \dots, b_q\}$, is chosen and used to update the generated sequences from the above two systems as follows:

For $n = 1: 1000$

$$\begin{aligned}
 X_i(n) &= x_i(n) + b_1, \\
 Y_i(n) &= y_i(n) + b_1, \\
 i &= 1, 2.
 \end{aligned} \tag{35}$$

For $n = 1001: 2000$

$$\begin{aligned}
 X_i(n) &= x_i(n) + b_2, \\
 Y_i(n) &= y_i(n) + b_2, \\
 i &= 1, 2.
 \end{aligned} \tag{36}$$

...

For $n = (q - 1)(1000) + 1: q \times 1000$,

$$\begin{aligned}
 X_i(n) &= x_i(n) + b_q, \\
 Y_i(n) &= y_i(n) + b_q, \\
 i &= 1, 2.
 \end{aligned} \tag{37}$$

The modular one operations are employed to get

$$\begin{aligned}
 \hat{X}_i(n) &= \text{mod}(X_i(n), 1), \\
 \hat{Y}_i(n) &= \text{mod}(Y_i(n), 1),
 \end{aligned} \tag{38}$$

and hence, the associated lower bound errors can be obtained by setting

$$\begin{aligned}
 e_X(n) &= \frac{\hat{X}_1(n) - \hat{X}_2(n)}{2}, \\
 e_Y(n) &= \frac{\hat{Y}_1(n) - \hat{Y}_2(n)}{2}.
 \end{aligned} \tag{39}$$

Fractal images are used in the proposed encryption technique to boost the security performance of the technique via incorporating additional layers of encryption. More specifically, the color components of each pixel in randomly selected two fractal images are used to confuse the values of each color component in the way that the first fractal image is used with the plain image and the second one is concerned with the shuffled plain image. In order to control and reduce the computation cost, a catalog of secretly pregenerated fractal images can be saved and then employed as one of the secret keys in the scheme. The advantages of using discrete fractional complex maps in the generation of fractal images are that they significantly increase key space. In particular, the two complex-valued parameters a and b in addition to the real-valued parameters α , r , $x(0)$, and $y(0)$ are the key parameters in the system in addition to the random perturbing values for pseudo-chaotic signals. This implies that using IEEE 754 double-precision floating-point format, the established key space is approximately 2^{3922} for 256×256 plain images and increases considerably for larger plain images. The pseudo-chaotic time series represented by the obtained lower bound errors are utilized in the encryption process as illustrated in the next section.

4.1. Steps of the Proposed Algorithm

Step 1. The original color image is separated into R-channel P_r , G-channel P_g , and B-channel P_b , which are arranged into three matrices of size $M \times N$.

Step 2. Establish three time-varying and plain-image dependent perturbation values $\xi_{r,g,b}$ by evaluating

$$\xi_{r,g,b} = \nu\tau(t) + \frac{1}{3(M \times N)^2} \sum_{i=1}^M \sum_{j=1}^N P_{r,g,b}(i, j), \quad (40)$$

where the value of $\tau(t)$ refers to a scaled value of time difference between the moment when the plain image was supplied to encryption machine and another secretly specified moment in the past, for example, 10:45:12:73 Jan 1, 2000. The difference can be taken in units of milliseconds. Also, the scaling factor ν is used to render $\nu\tau(t)$ spans the required range of time range. Moreover, i and j are pixel positions of the R-channel, G-channel, and B-channel matrices of plain images, that is, P_r, P_g, P_b , respectively. We use $\xi_{r,g,b}$ as perturbation values for chaotic map parameter r , such that

$$r_{1,2,3} = r_0 + \xi_{r,g,b}, \quad (41)$$

where r_0 is a base-value for r . Therefore, three pseudo-chaotic sequences are generated and utilized in permutation and diffusion processes of the aforementioned three plain image channels.

Step 3. The chaotic lemniscate map is used to generate two pseudo-chaotic sequences $e_x(i), e_y(i)$ and used in creating the following sequences:

$$\begin{aligned} rowCol_i &= \text{mod}(\text{floor}(e_x(i) \times 10^{15}), 450) + 1, \\ ks_i &= \text{mod}(\text{floor}(e_y(i) \times 10^{15}), 256). \end{aligned} \quad (42)$$

We use mod operation between variables x_i and $M = N$ to get a sequence to build a new position for pixels value image matrices IR, IG, IB as shuffling process. Also, we use mod operation between the variable y_i and 256 to get a random sequence that we used it in encryption process as a secret key.

Step 4. We get $row(j)$ and $column(j)$ as a new position of image pixels, where $j = 1, 2, \dots, M$, from $rowCol_i$ sequence.

Step 5. Rearrange the pixel position as shuffle process as follows:

$$\begin{aligned} IR_{sh}(i, j) &= IR(row(i), column(j)), \\ IG_{sh}(i, j) &= IG(row(i), column(j)), \\ IB_{sh}(i, j) &= IB(row(i), column(j)), \end{aligned} \quad (43)$$

where IR_{sh} and IR are the matrix for shuffled and plain images, respectively, where $i = 1, 2, \dots, M$ and $j = 1, 2, \dots, N$ are the image matrix dimensions.

Step 6. We use two randomly selected fractal images from previously constructed catalog, for example, Figures 6(a) and 6(b), as secret keys Key_{f1} and Key_{f2} for each red, green, and blue color images by separating each color image from each fractal image and using it as secret keys with corresponding color in the plain image. Therefore, we have six secret keys based on the two fractal images.

In addition, to enhance the confusion of the secret key, we do a shuffle process as in step 4 to R-channel, G-channel, and B-channel of fractal image (Figure 6(a)) before using them as a secret key.

Step 7. We divide the sequence ks to three sequences ksr, ksg, ksb for each color in the plain image. To set the secret keys in matrix form, the *reshape* function is used as follows:

$$\begin{aligned} ksR &= \text{reshape}(ksr, M, N), \\ ksG &= \text{reshape}(ksg, M, N), \\ ksB &= \text{reshape}(ksb, M, N), \end{aligned} \quad (44)$$

to be used as secret keys ksR, ksG, ksB for red, green, and blue channels in the plain images, respectively.

Step 8. Apply two bitwise XOR operation between Key_f, ks, I_{sh} to establish the encrypted image I_{en} as follows:

$$\begin{aligned} IR_{en}(i, j) &= ((IR_{sh}(i, j) \oplus Key_{fR1}(i, j)) \oplus Key_{fR2}(i, j)) \oplus ksR(i, j), \\ IG_{en}(i, j) &= ((IG_{sh}(i, j) \oplus Key_{fG1}(i, j)) \oplus Key_{fG2}(i, j)) \oplus ksG(i, j), \\ IB_{en}(i, j) &= ((IB_{sh}(i, j) \oplus Key_{fB1}(i, j)) \oplus Key_{fB2}(i, j)) \oplus ksB(i, j), \end{aligned} \quad (45)$$

where IR_{en}, IG_{en} , and IB_{en} are the encrypted images for each color component in plain image.

The process of decryption is carried out using the reverse approach. The proposed encryption scheme is applied to three colored images. The three perturbation constants that are used in the proposed scheme are 3.9724×10^{-4} ,

3.7782×10^{-4} , and 4.0288×10^{-4} for baboon, pepper, and house images, respectively. The values of $r_0, x(0), y(0)$ are taken as 35, 0.5, 0.5, respectively. Figure 7 depicts the original, shuffled, and encrypted images for the three images with size $M = N = 450$ after applying the presented algorithm.

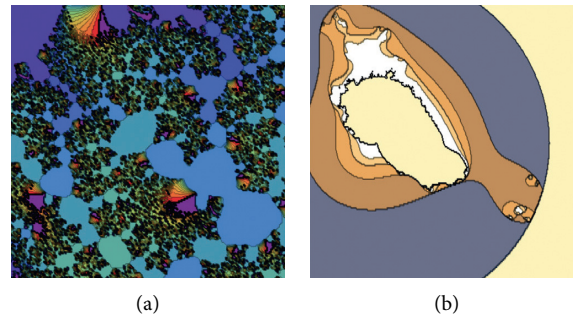


FIGURE 6: Example of fractal images that are generated by the proposed fractional complex map (1).



FIGURE 7: The plain, shuffled, and encrypted images in (a), (b), and (c), respectively, for baboon, pepper, and house images.

5. Security Analysis

The proper encryption scheme must be evaluated to investigate its efficacy in resisting several types of attacks. These involve brute force, statistical, differential, known-plaintext, chosen-plaintext, and chosen-ciphertext attacks. In this section, a thorough security analysis is carried out considering these types of attacks.

5.1. Histogram. The histogram analysis is used to visualize the distribution of pixels in an image before and after the encryption process. Uniformity of pixels distribution in encrypted data implies that statistical features of input data are efficiently hidden by encryption operation. Histograms for red, green, and blue plain, shuffled, and encrypted images for baboon image are shown in Figure 8 whereas histograms for red, green, and blue plain, shuffled, and encrypted images

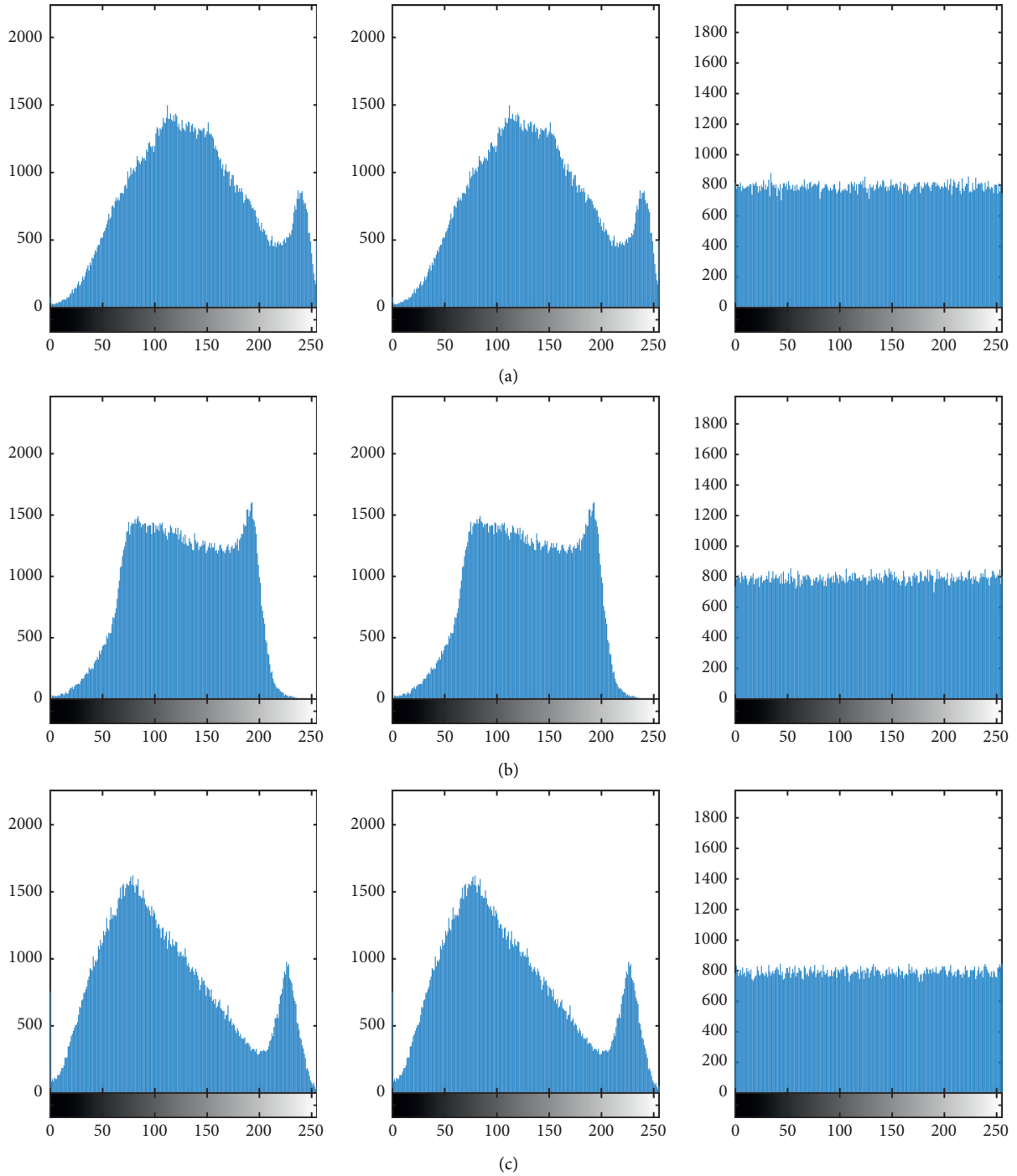


FIGURE 8: Histograms for (a) red, (b) green, and (c) blue baboon image for plain, shuffled, and encrypted image, respectively.

for pepper image are shown in Figure 9. Finally, histograms for red, green, and blue plain, shuffled, and encrypted images for house image are shown in Figure 10.

In order to quantify the uniformity of histograms, the variance of histogram is utilized as a useful measure. The variance of histogram is calculated as follows [51]:

$$\text{Var}(h) = \frac{1}{256^2} \sum_{i=1}^{256} \sum_{j=1}^{256} \frac{1}{2} (h_i - h_j)^2, \quad (46)$$

where h represents the histogram values arranged in vector form and h_i and h_j denote the numbers of pixels having values of i and j , respectively. The variance of histogram for original and ciphered images is depicted in Table 2 with the percentage of reduction between the plain and encrypted images. Noting that the percentage of reduction is greater than 99.6% in the red, green, blue baboon images and greater than 99.8% in three separated colors for pepper and house images. These results confirm the efficiency of the proposed technique.

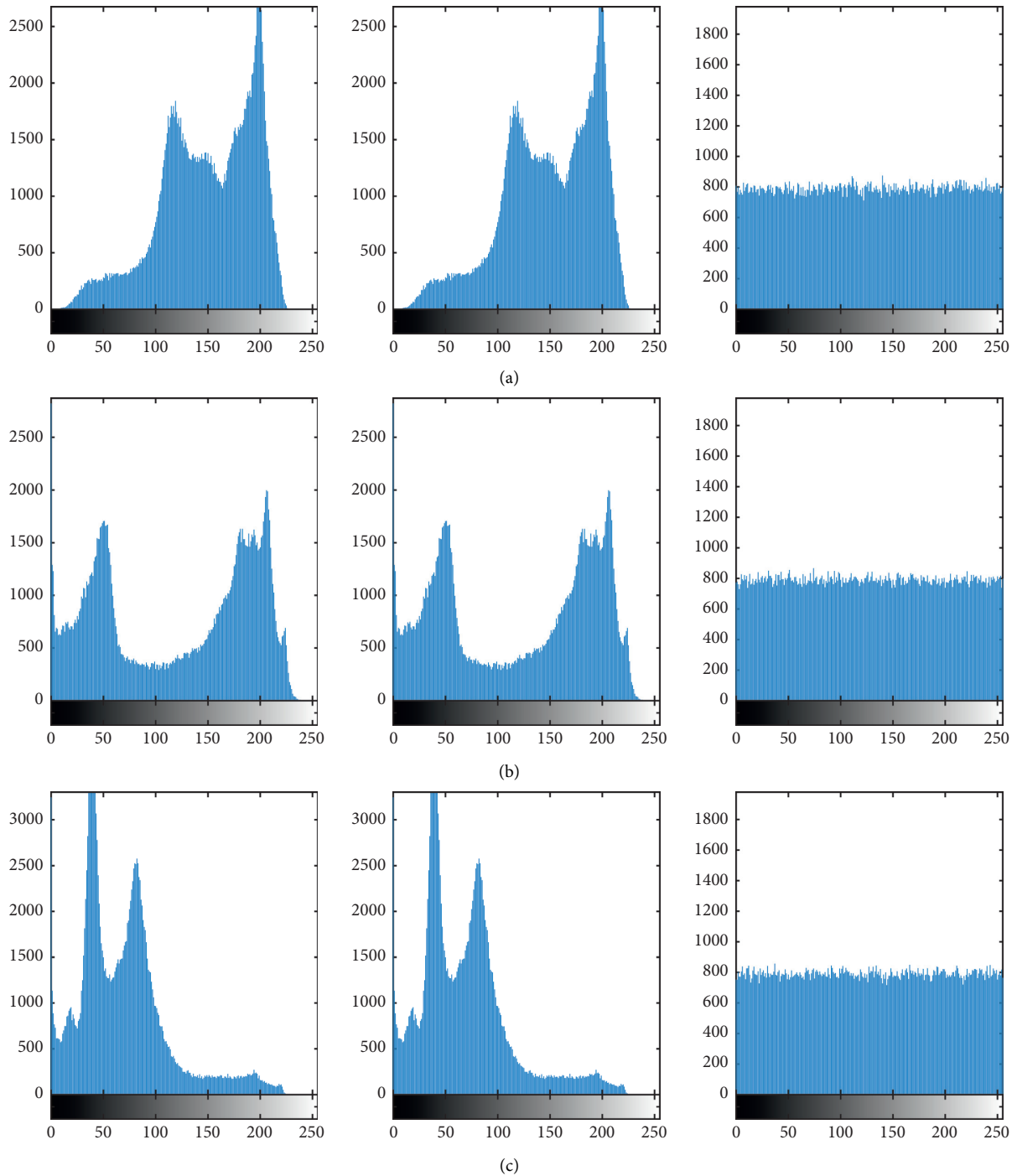


FIGURE 9: Histograms for (a) red, (b) green, and (c) blue pepper image for plain, shuffled, and encrypted image, respectively.

5.2. Key Space Analysis. Evaluating the size of secret key space in a specific encryption technique is a crucial step to evaluate its performance against brute force attacks. When the capabilities and characteristics of the state-of-the-art computer are taken into account, it is found that a threshold value for a minimum sufficient key space is a size of 2^{100} to ensure that the brute-force attacks are unfeasible [47, 51]. In our suggested scheme, the two complex-valued parameters a and b in addition to the real-valued parameters α , r , $x(0)$, and $y(0)$ are the key parameters in the system in addition to the random perturbing

values for pseudo-chaotic signals. This implies that using IEEE 754 double-precision floating-point format, the attained key space is approximately 2^{3922} for 256×256 plain images and increases considerably for larger plain images. Accordingly, the presented scheme has key space that is much greater than the minimum value of 2^{100} .

5.3. Correlation Analysis. The correlation analysis utilized to measure and quantify the similarity among adjacent pixels throughout the image under consideration, which can be the

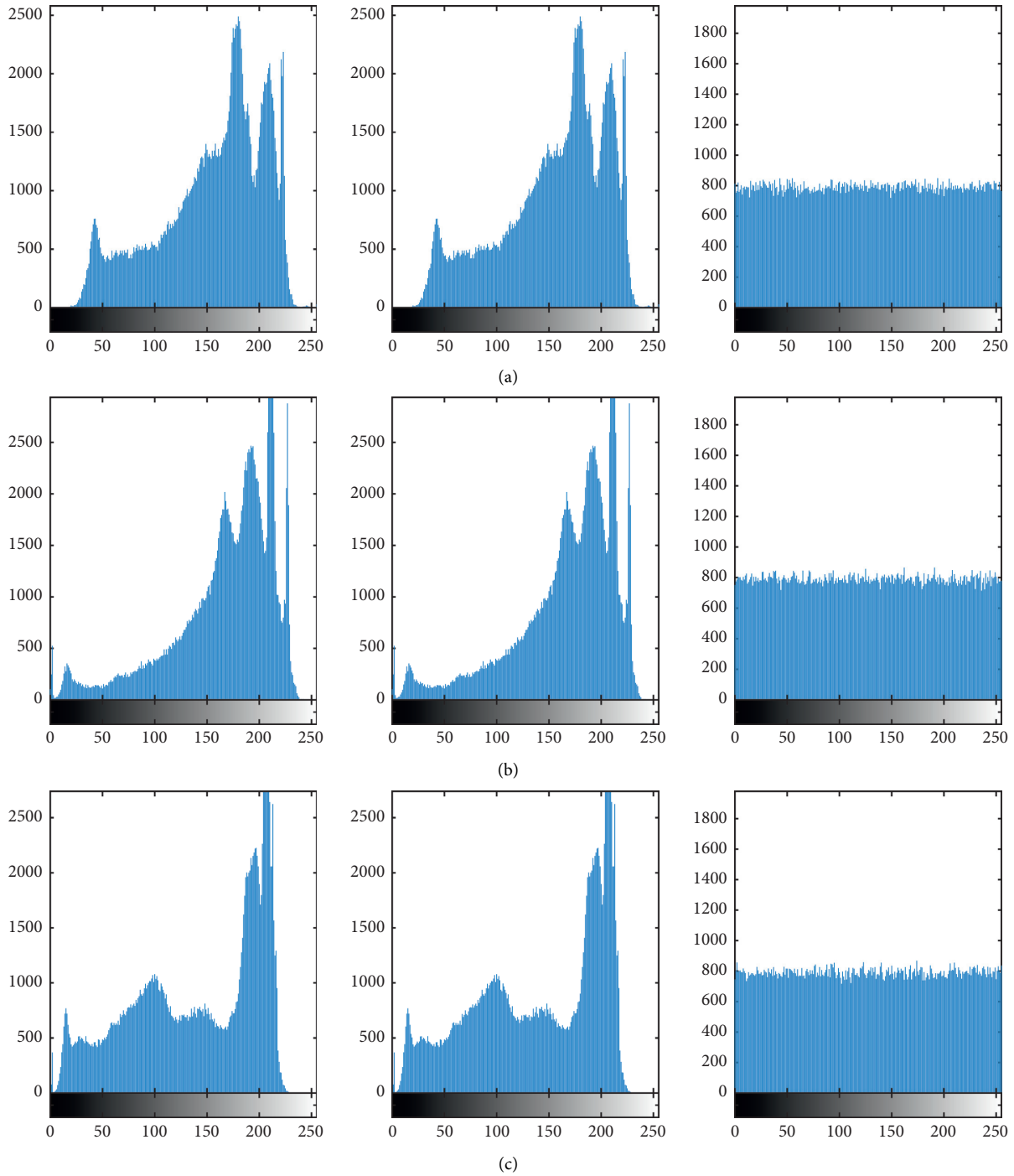


FIGURE 10: Histograms for (a) red, (b) green, and (c) blue house image for plain, shuffled, and encrypted image, respectively.

plain image or the encrypted image. The efficient encryption scheme should make the correlation coefficient as small as possible to boost the security against conventional statistical attacks. The correlation coefficient can be defined as follows:

$$r = \frac{\text{cov}(x, y)}{\sigma_x \sigma_y}, \quad (47)$$

where $\sigma_\phi = \sqrt{\text{var}(\phi)}$, $\sigma_\psi = \sqrt{\text{var}(\psi)}$.

$$\text{var}(\phi) = \frac{1}{N} \sum_{i=1}^N (\phi_i - E(\phi))^2, \quad (48)$$

$$\text{cov}(\phi, \psi) = \frac{1}{N} \sum_{i=1}^N (\phi_i - E(\phi))((\psi_i) - E(\psi)),$$

where the values of pixels of plain and encrypted images are denoted by ϕ and ψ , respectively. The correlation values between adjacent pixels in horizontal, vertical, and diagonal

TABLE 2: The histogram variance and its reduction for the original and cipher images for baboon, pepper, and house images.

		Variance		
	Plain	Encrypted	Reduction (%)	
Baboon	Red	176920	701.4429	99.6035
	Green	348200	755.0115	99.7832
	Blue	188610	650.039	99.6553
Pepper	Red	520530	818.9017	99.8427
	Green	695920	672.1017	99.9034
	Blue	1122000	694.6978	99.9381
House	Red	440620	710.8939	99.8387
	Green	756780	764.3449	99.899
	Blue	577050	800.1174	99.8613

directions are acquired for baboon, pepper, and house images and listed in Table 3. It is obvious that the proposed algorithm is immune to statistical attacks because it is successfully minimized the values of correlation coefficients in the encrypted images to about zero.

5.4. Information Entropy. The information entropy is another powerful analysis tool used to find the unpredictability and randomness in the proposed scheme. It is reported that the optimum value is 8. The information entropy of a given image is outlined as follows:

$$H(m) = \sum_{i=1}^{2^N-1} p_i \log_2 \frac{1}{p_i}, \quad (49)$$

where $H(m)$ denotes the entropy in bits, m is an input parameter, and finally the value of probability for parameter m is referred to as p_i .

The entropy values for red, green, and blue images have been evaluated for baboon, pepper, and house encrypted images and summarized in Table 4. It is cleared that the entropy values for the three images are very close to 8; therefore, the proposed scheme is less feasible to expose information of the plain image.

5.5. Differential Attack Analysis. To evaluate the immunity of the proposed cryptosystem against the powerful differential, two useful quantities reevaluated, namely, the number of pixels changing rate (NPCR) and unified average changing intensity (UACI). These measures identify the sensitivity of the encryption scheme to change a single-pixel value of supplied plain image or sensitivity to small changes in the secret key. The equations to evaluate NPCR and UACI are expressed as follows [47]:

$$\text{NPCR}(\%) = \frac{1}{M \times N} \sum_{i=1}^M \sum_{j=1}^N |\text{sign}(C_1(i, j) - C_2(i, j))| \times 100,$$

$$\text{UACI}(\%) = \frac{1}{M \times N} \sum_{i=1}^M \sum_{j=1}^N \frac{|C_1(i, j) - C_2(i, j)|}{255} \times 100, \quad (50)$$

TABLE 3: The correlation values between adjacent pixels, in all directions, were obtained for red, green, and blue color components in baboon, pepper, and house images, respectively.

			Correlation coefficients		
			Horizontal	Vertical	Diagonal
Baboon	Red	Plain	0.9193	0.864	0.8403
		Cipher	-0.0005	-0.0039	0.001
	Green	Plain	0.8795	0.7997	0.7628
		Cipher	0.0032	-0.001	-0.0028
	Blue	Plain	0.9285	0.8827	0.8597
		Cipher	-0.0021	-0.0013	0.0027
Pepper	Red	Plain	0.9681	0.9703	0.9519
		Cipher	0.0001	-0.0000	-0.0007
	Green	Plain	0.9786	0.979	0.9616
		Cipher	0.0000	-0.0036	-0.0003
	Blue	Plain	0.9654	0.9643	0.9414
		Cipher	-0.0048	-0.0044	-0.0029
House	Red	Plain	0.9484	0.9467	0.9087
		Cipher	-0.0001	0.0024	0.0005
	Green	Plain	0.9286	0.9481	0.8893
		Cipher	-0.0005	-0.0003	-0.0004
	Blue	Plain	0.9704	0.9718	0.9472
		Cipher	-0.0005	0.0013	-0.0008

TABLE 4: The entropy for encrypted image for red, green, and blue images for baboon, pepper, and house image, respectively.

Plain	Red (%)	Green (%)	Blue (%)
Baboon	7.9992	7.9991	7.9993
Pepper	7.9991	7.9992	7.9992
House	7.9992	7.9991	7.9991

where the well-known sign function is referred to as $\text{sign}()$, while C_i s refer to the cipher image. In Table 5, the evaluated values of UACI and NPCR are given for the three submitted plain images. It is observed that the values of NPCR are generally greater than 99.5, while those of UACI are greater than 33.4, which indicates the sensitivity to a pixel change in the proposed encryption algorithm.

5.6. Cropping Attack. In order to detect the robustness of the proposed technique, some blocks of size 450×100 of a cipher house image are converted into black. The restored image after is depicted in Figure 11. Although there is a loss of significant information, the encrypted image after the decryption process is still recognizable.

Finally, the aforementioned results are summarized. The proposed encryption technique combines the pseudo-chaos of modified chaotic lemniscate map [47], which has a distinct complicated dynamics and large value of positive Lyapunov exponent with the fractal images generated by complex discrete fractional Gauss map. When compared with different state-of-the-art chaos-based encryption techniques, the main advantages of the present encryption technique are as follows: (a) it deploys superior positive values of maximum Lyapunov exponents. For example, the maximum value of Lyapunov exponent of chaos employed in the image encryption system [48] and bit-level

TABLE 5: NPCR and UACI results for red, green, and blue images for baboon, pepper, and house images, respectively.

Image		NPCR (%)	UACI (%)
Baboon	Red	99.601	33.559
	Green	99.6015	33.4034
	Blue	99.6133	33.534
Pepper	Red	99.6281	33.5021
	Green	99.597	33.4069
	Blue	99.5901	33.5242
House	Red	99.598	33.4591
	Green	99.5817	33.4822
	Blue	99.5936	33.542

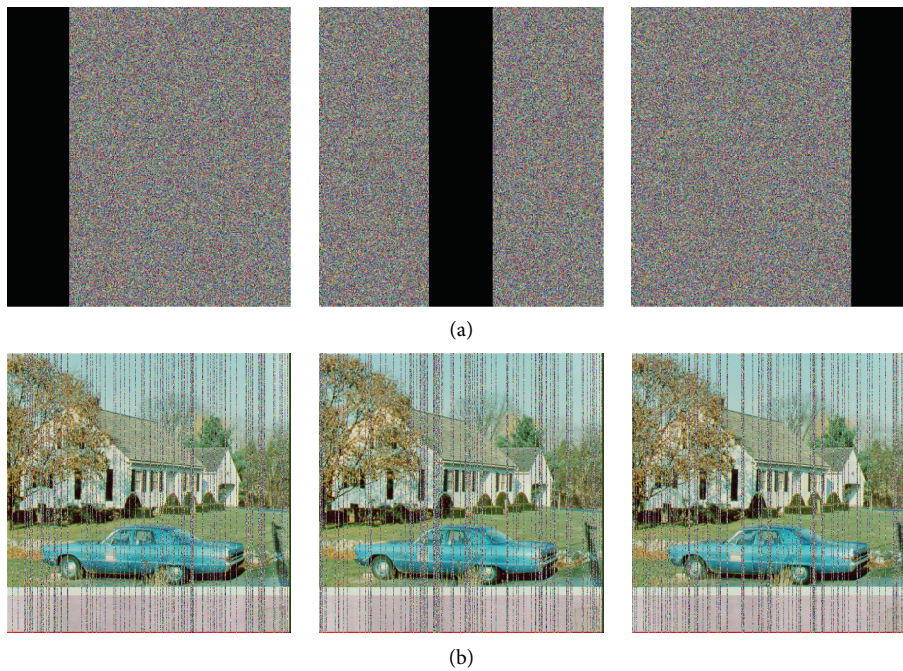


FIGURE 11: The encrypted house image after converting the left, middle, and right blocks, respectively, of the house image into black color (a) and the corresponding recognizable decrypted images (b).

permutation spatial system [48] is less than three, while it is greater than 30 in the present scheme. (b) The pseudo-chaotic time series tame the possible degradation of statistical features of chaos signals in the cases, where they are applied immediately [46]. (c) The assigned keys for the suggested encryption technique are set in a way that renders them controlled by plain data features as well as the time moment of their processing. This means that if identical plain images are encrypted at different instants, different secret keys will be used for the encryption process inducing different cipher images. Moreover, the pseudo-chaos or lower bound errors between the outputs of two interval extensions are employed in the presented scheme instead of applying chaotic signals directly in permutation and diffusion stages. This adds another layer of security and hides the internal characteristics of chaos generators maps. More details about the lower bound errors and analysis of interval extensions can be found in references [49, 50]. Now, the critical scenario of known-plaintext attack (KPA) is considered, where the opponent successfully attains the specific

plain image and corresponding cipher image, and then he cannot proceed further to obtain any extra useful information about secret keys' values, which will be used for upcoming plain images as the scheme utilizes time-varying secret keys. The proposed encryption technique can resist KPA even in special cases when uniform plain images with zero values of pixels are deployed, which may lead to a degenerate performance in other encryption techniques [52–54]. The adoption of fractal images in the scheme boosts complexity, key space range, and security performance. Moreover, if the opponent employs chosen-ciphertext attack (CCA) to supply some specially selected cipher images to decryption part of the scheme, he would not fulfill his target too.

The running time of the proposed encryption scheme on personal computer with 16 GB RAM and Intel Core i7-8550U CPU 1.8 GHz is approximately 0.582 s for 450×450 colored images. The comparison aspects with some recent chaos-based encryption techniques are summarized in Table 6. The MCC and AVR abbreviations are used to denote

TABLE 6: Some comparisons with recent chaos-based encryption techniques.

Work	UACI	NPCR	MLE	Entropy	Key space	MCC	AVR (sec)
Proposed work	33.532	99.814	Up to 60	7.999	2^{3922}	0.0031	0.582
Reference [55] (2 rounds)	33.484	99.809	2	7.903	2^{318}	0.0191	0.385
Reference [56]	33.421	99.611	2	7.997	2^{312}	0.0131	1.860
Reference [57]	33.452	99.607	0.82	7.991	2^{187}	0.0082	0.478
Reference [58]	33.411	99.610	6.756	7.998	2^{399}	0.0143	0.8342

the maximum correlation coefficients attained in all directions of encrypted color baboon/pepper images and average running time, respectively.

6. Conclusion

This study establishes a framework to study dynamical and fractal characteristics, in addition to potential applications, of generalized complex-valued discrete fractional Gaussian map. The occurrence of Mandelbrot and Julia sets of the proposed map is scrutinized at different scenarios for values of parameters. The control and synchronization problems of Julia sets in the complex domain are addressed. A combined pseudo-chaos-fractal image encryption technique is introduced as an efficient tool to resist several kinds of attacks. A thorough security analysis is carried out to validate its robustness and efficiency against statistical, differential, and cropping attacks. Indeed, there is a trade-off between increasing chaoticity and security strength from one side and computational speed from the other side. The present application in this work is the first step and subsequent work will focus on realization aspects on a suitable digital hardware platform, that is, DSP or FPGA, further reduce its running time, and discuss all possible issues that need separate work and cannot be treated here. Future work can also involve extending this study to the case of higher dimensional complex fractional maps [31, 32].

Data Availability

No data were used to support this study.

Conflicts of Interest

The authors declare that they have no conflicts of interest.

Acknowledgments

This research work was funded through the project number (IF-PSAU-2021/01/17817) by the Deputyship for Research and Innovation, Ministry of Education in Saudi Arabia. The authors extend their appreciation to the Deputyship for Research and Innovation, Ministry of Education in Saudi Arabia for funding this research work through the project number (IF-PSAU-2021/01/17817).

References

- [1] S. H. Strogatz, *Nonlinear Dynamics and Chaos with Applications to Physics, Biology, Chemistry, and Engineering*, CRC Press, Boca Raton, Florida, 2018.
- [2] Y. A. Kuznetsov, *Elements of Applied Bifurcation Theory*, Springer Science & Business Media, Berlin/Heidelberg, Germany, 2013.
- [3] J. Guckenheimer and P. Holmes, *Nonlinear Oscillations, Dynamical Systems, and Bifurcations of Vector fields*, Springer Science & Business Media, Berlin/Heidelberg, Germany, 2013.
- [4] E. M. Izhikevich, *Dynamical Systems in Neuroscience: The Geometry of Excitability and Bursting*, MIT Press, Cambridge, MA, 2007.
- [5] P. N. V. Tu, *Dynamical Systems- an Introduction with Applications in Economics and Biology*, Springer-Verlag, Berlin/Heidelberg, Germany, 1995.
- [6] D. Baleanu and A. M. Lopes, *Applications in engineering, life and social sciences, part b, in Handbook of Fractional Calculus with Applications*, De Gruyter, Germany, 2019.
- [7] Y. Sun and W. Sumelka, "Fractional viscoplastic model for soils under compression," *Acta Mechanica*, vol. 230, no. 9, pp. 3365–3377, 2019.
- [8] M. A. Matlob and Y. Jamali, "The concepts and applications of fractional order differential calculus in modeling of visco-elastic systems: a Primer," *Critical Reviews in Biomedical Engineering*, vol. 47, no. 4, pp. 249–276, 2019.
- [9] S. Aman, I. Khan, Z. Ismail, and M. Zuki Salleh, "Applications of fractional derivatives to nanoids: exact and numerical solutions," *Mathematical Modelling of Natural Phenomena*, vol. 13, pp. 1–12, 2018.
- [10] Y. Zhang, H. Sun, H. H. Stowell, M. Zayernouri, and S. E. Hansen, "A review of applications of fractional calculus in Earth system dynamics," *Chaos, Solitons & Fractals*, vol. 102, pp. 29–46, 2017.
- [11] A. M. A. El-Sayed, H. M. Nour, A. Elsaid, A. E. Matouk, and A. Elsonbaty, "Dynamical behaviors, circuit realization, chaos control, and synchronization of a new fractional order hyperchaotic system," *Applied Mathematical Modelling*, vol. 40, no. 5–6, pp. 3516–3534, 2016.
- [12] R. Hilfer, *Applications of Fractional Calculus in Physics*, World Scientific, New Jersey, 2000.
- [13] N. Engheia, "On the role of fractional calculus in electromagnetic theory," *IEEE Antennas and Propagation Magazine*, vol. 39, no. 4, pp. 35–46, 1997.
- [14] F. Jarad, E. Uurlu, T. Abdeljawad, and D. Baleanu, "On a new class of fractional operators," *Advances in Difference Equations*, vol. 2017, pp. 1–16, 2017.
- [15] F. Jarad, T. Abdeljawad, and D. Baleanu, "Caputo type modification of the Hadamard fractional derivatives," *Advances in Difference Equations*, vol. 2012, pp. 1–8, 2012.
- [16] T. Abdeljawad, "On Riemann and Caputo fractional differences," *Computers & Mathematics with Applications*, vol. 62, no. 3, pp. 1602–1611, 2011.
- [17] S. Momani and R. W. Ibrahim, "On a fractional integral equation of periodic functions involving Weyl-Riesz operator in Banach algebras," *Journal of Mathematical Analysis and Applications*, vol. 339, no. 2, pp. 1210–1219, 2008.

- [18] K. Diethelm and N. J. Ford, "Analysis of fractional differential equations," *Journal of Mathematical Analysis and Applications*, vol. 265, no. 2, pp. 229–248, 2002.
- [19] R. Singh, A. U. Rehman, A. U. Rehman et al., "Fractional order modeling and analysis of dynamics of stem cell differentiation in complex network," *AIMS Mathematics*, vol. 7, no. 4, pp. 5175–5198, 2022.
- [20] P. Agarwal, R. P. Agarwal, and M. Ruzhansky, *Special Functions and Analysis of Differential Equations*, CRC Press, Boca Raton, Florida, 2020.
- [21] L.-L. Huang, G.-C. Wu, D. Baleanu, and H. Y. Wang, "Discrete fractional calculus for interval-valued systems," *Fuzzy Sets and Systems*, vol. 404, pp. 141–158, 2021.
- [22] A. Elsonbaty and A. A. Elsadany, "On discrete fractional-order Lotka-Volterra model based on the Caputo difference discrete operator," *Mathematical Sciences*, pp. 1–13, 2021.
- [23] G. C. Wu, M. Luo, L. L. Huang, and S. Banerjee, "Short memory fractional differential equations for new memristor and neural network design," *Nonlinear Dynamics*, vol. 100, no. 4, pp. 3611–3623, 2020.
- [24] Y. Wang, S. Liu, and H. Li, "On fractional difference logistic maps: dynamic analysis and synchronous control," *Nonlinear Dynamics*, vol. 102, no. 1, pp. 579–588, 2020.
- [25] C. Goodrich and A. C. Peterson, *Discrete Fractional Calculus*, Springer International Publishing, Germany, 2015.
- [26] K. Falconer, *Fractal Geometry: Mathematical Foundations and Applications*, John Wiley & Sons, Chichester, 2014.
- [27] B. B. Mandelbrot, C. J. Evertsz, and M. C. Gutzwiller, *Fractals and Chaos: The Mandelbrot Set and beyond*, Springer, Salmon Tower Building New York City, 2004.
- [28] H. Peitgen, H. Jurgens, and D. Saupe, *Chaos and Fractals: New Frontiers in Science*, Springer-Verlag, Berlin/Heidelberg, Germany, 1992.
- [29] A. Deshpande and V. D. Gejji, "Chaos in discrete fractional difference equations," *Pramana - Journal of Physics*, vol. 87, no. 4, pp. 1–10, 2016.
- [30] Y. Peng, K. Sun, and S. He, "Synchronization for the integer-order and fractional-order chaotic maps based on parameter estimation with JAYA-IPSO algorithm," *The European Physical Journal Plus*, vol. 135, no. 3, pp. 1–12, 2020.
- [31] S. S. Pakhare, S. Bhalekar, and P. M. Gade, "Synchronization in coupled integer and fractional-order maps," *Chaos, Solitons & Fractals*, vol. 156, Article ID 111795, 2022.
- [32] S. S. Pakhare, V. D. Gejji, D. S. Badwaik, A. Deshpande, and P. M. Gade, "Emergence of order in dynamical phases in coupled fractional gauss map," *Chaos, Solitons & Fractals*, vol. 135, Article ID 109770, 2020.
- [33] Y. Wang, S. Liu, and H. Li, "Adaptive synchronization of Julia sets generated by Mittag-Leffler function," *Communications in Nonlinear Science and Numerical Simulation*, vol. 83, Article ID 105115, 2020.
- [34] Y. Wang, S. Liu, and W. Wang, "Fractal dimension analysis and control of Julia set generated by fractional Lotka-Volterra models," *Communications in Nonlinear Science and Numerical Simulation*, vol. 72, pp. 417–431, 2019.
- [35] S. Askar, A. Al-Khedhairi, A. Elsonbaty, and A. Elsadany, "Chaotic discrete fractional-order food chain model and hybrid image encryption scheme Application," *Symmetry Plus*, vol. 13, no. 2, p. 161, 2021.
- [36] A. E. Elfiqui, H. S. Khallaf, S. F. Hegazy, A. Elsonbaty, H. M. H. Shalaby, and S. S. A. Obayya, "Chaotic polarization-assisted $\{L\}$ DPSK-MPPM modulation for free-space optical communications," *IEEE Transactions on Wireless Communications*, vol. 18, no. 9, pp. 4225–4237, 2019.
- [37] L. Kocarev and S. Lian, *Chaos-Based Cryptography*, Springer, Salmon Tower Building New York City, 2011.
- [38] P. Stavroulakis, *Chaos Applications in Telecommunications*, CRC Press, Boca Raton Florida, 2006.
- [39] G. Chen and X. Yu, *Chaos Control- Theory and Applications*, Springer, Salmon Tower Building New York City, 2003.
- [40] Z. Lin, G. Wang, X. Wang, S. Yu, and J. Lü, "Security performance analysis of a chaotic stream cipher," *Nonlinear Dynamics*, vol. 94, no. 2, pp. 1003–1017, 2018.
- [41] A. Sonbaty, S. F. Hegazy, and S. S. Obayya, "Simultaneous concealment of time delay signature in chaotic nanolaser with hybrid feedback," *Optics and Lasers in Engineering*, vol. 107, pp. 342–351, 2018.
- [42] G. Ye, C. Pan, X. Huang, and Q. Mei, "An efficient pixel-level chaotic image encryption algorithm," *Nonlinear Dynamics*, vol. 94, no. 1, pp. 745–756, 2018.
- [43] S. Li, G. Chen, and X. Mou, "On the dynamical degradation of digital piecewise linear chaotic maps," *International Journal of Bifurcation and Chaos*, vol. 15, no. 10, pp. 3119–3151, 2005.
- [44] L.-C. Cao, Y.-L. Luo, S.-H. Qiu, and J.-X. Liu, "A perturbation method to the tent map based on Lyapunov exponent and its application," *Chinese Physics B*, vol. 24, no. 10, p. 100501, 2015.
- [45] C. Li, T. Xie, Q. Liu, and G. Cheng, "Cryptanalyzing image encryption using chaotic logistic map," *Nonlinear Dynamics*, vol. 78, no. 2, pp. 1545–1551, 2014.
- [46] E. G. Nepomuceno, L. G. Nardo, J. Arias-Garcia, D. N. Butusov, and A. Tutueva, "Image encryption based on the pseudo-orbits from 1D chaotic map," *Chaos: An Interdisciplinary Journal of Nonlinear Science*, vol. 29, no. 6, Article ID 061101, 2019.
- [47] A. Al-Khedhairi, A. Elsonbaty, A. A. Elsadany, and E. A. A. Hagra, "Hybrid cryptosystem based on pseudo chaos of novel fractional order map and elliptic curves," *IEEE Access*, vol. 8, pp. 57733–57748, 2020.
- [48] L. Hongjuna and W. Xingyuan, "Color image encryption based on one-time keys and robust chaotic maps," *Computers & Mathematics with Applications*, vol. 59, pp. 3320–3327, 2010.
- [49] E. G. Nepomuceno, S. A. M. Martins, G. F. V. Amaral, and R. Riveret, "On the lower bound error for discrete maps using associative property," *Systems Science & Control Engineering*, vol. 5, no. 1, pp. 462–473, 2017.
- [50] R. E. Moore and R. B. Kearfott, *Introduction to Interval Analysis*, SIAM, Thailand, 2009.
- [51] Z. Y. Qian, W. X. Yuan, "A symmetric image encryption algorithm based on mixed linear–nonlinear coupled map lattice," *Information Scientist*, vol. 273, pp. 329–351, 2014.
- [52] Z. Lin, S. Yu, X. Feng, and J. Lü, "Cryptanalysis of a chaotic stream cipher and its improved scheme," *International Journal of Bifurcation and Chaos*, vol. 28, no. 7, pp. 1850086–1850112, 2018.
- [53] D. Xiao, X. Liao, and P. Wei, "Analysis and improvement of a chaos-based image encryption algorithm," *Chaos, Solitons & Fractals*, vol. 40, no. 5, pp. 2191–2199, 2009.
- [54] C. Li, D. Lin, B. Feng, J. Lü, and F. Hao, "Cryptanalysis of a chaotic image encryption algorithm based on information entropy," *IEEE Access*, vol. 6, pp. 75834–75842, 2018.
- [55] M. Alawida, J. S. Teh, A. Samsudin, and W. H. Alshoura, "An image encryption scheme based on hybridizing digital chaos and finite state machine," *Signal Processing*, vol. 164, pp. 249–266, 2019.
- [56] M. Alawida, A. Samsudin, J. S. Teh, and R. S. Alkhaldeh, "A new hybrid digital chaotic system with applications in image encryption," *Signal Processing*, vol. 160, pp. 45–58, 2019.

- [57] Y.-Q. Zhang, Y. He, P. Li, and X.-Y. Wang, "A new color image encryption scheme based on 2DNLCML system and genetic operations," *Optics and Lasers in Engineering*, vol. 128, Article ID 106040, 2020.
- [58] M. Zhou and C. Wang, "A novel image encryption scheme based on conservative hyperchaotic system and closed-loop diffusion between blocks," *Signal Processing*, vol. 171, Article ID 107484, 2020.

Research Article

Qualitative Behavior of Solutions of Tenth-Order Recursive Sequence Equation

E. M. Elsayed ^{1,2}, B. S. Alofi ¹ and Abdul Qadeer Khan ³

¹King Abdulaziz University, Faculty of Science, Mathematics Department, P.O. Box 80203, Jeddah 21589, Saudi Arabia

²Department of Mathematics, Faculty of Science, Mansoura University, Mansoura, Egypt

³Department of Mathematics, University of Azad Jammu and Kashmir, Muzaaffarabad 13100, Pakistan

Correspondence should be addressed to Abdul Qadeer Khan; abdulqadeerkhan1@gmail.com

Received 17 September 2021; Revised 14 November 2021; Accepted 31 December 2021; Published 14 February 2022

Academic Editor: Baogui Xin

Copyright © 2022 E. M. Elsayed et al. This is an open access article distributed under the Creative Commons Attribution License, which permits unrestricted use, distribution, and reproduction in any medium, provided the original work is properly cited.

Most nonlinear difference equations have exact solutions that are not always possible to obtain theoretically. As a result, a large number of researchers investigate several qualitative aspects of difference equations in order to predict their lengthy behavior. The goal of our research is to obtain the solutions of a tenth-order difference equation $U_{n+1} = U_{n-9}U_{n-5}U_{n-1}/U_{n-7}U_{n-3} (\pm 1 \pm U_{n-9}U_{n-5}U_{n-1})$, $n \geq 0$, where the initial values are positive real numbers. Stability and periodicity are also investigated.

1. Introduction

Solving the difference equation is one of the problems that is difficult to determine the solvability. The aim of this study is to solve difference equation of the tenth order and solve four specific cases of the following difference equation:

$$U_{n+1} = \frac{U_{n-9}U_{n-5}U_{n-1}}{U_{n-7}U_{n-3} (\pm 1 \pm U_{n-9}U_{n-5}U_{n-1})}, \quad n \geq 0, \quad (1)$$

where the initial conditions $U_{-9}, U_{-8}, U_{-7}, U_{-6}, U_{-5}, U_{-4}, U_{-3}, U_{-2}, U_{-1}, U_0$ are the arbitrary positive real numbers. We also provide some properties of solutions such as periodicity in two cases and stability in the other two cases. Difference equations are used in a variety of probability problems such as hypergeometric, binomial, and poisson distribution. Difference equations are related to difference equations in the same way that discrete mathematics and continuous mathematician are related. Difference equations are of importance to computer scientists for a variety of reasons. For example, when estimating the cost of an algorithm in big-O notation, converting a difficult differential problem to

a nearly equivalent difference equation is the first step in solving. The study of asymptotic stability of nonlinear rational difference equations of high order is a difficult but rewarding task. It is particularly beneficial for analyzing the characteristics of mathematical models using different applications such as biological systems. The main topic in study is that the difference equations theory has been the asymptotic behavior of rational form of difference equation.

In addition, various nonlinear trends in science and engineering can be modeled by this type of equation, and the solution of this type of equation provides a prototype for the development of theory [1]. In the literature, many applications theories' differences equations have been investigated. El-Dessoky [2] investigated the behavior properties of the solutions of the rational difference equation:

$$U_{n+1} = aU_n + \frac{bU_nU_{n-3}}{cU_{n-4} + dU_{n-3}}. \quad (2)$$

Ghazela et al. [3] researched the analytic qualities of sixth-order difference equations:

$$U_{n+1} = \frac{bU_{n-5}}{cU_{n-2}U_{n-5} + d} \tag{3}$$

Al-Matrafi and Al-Zubaidi [4] achieved global and local stability and forms of positive periodic solutions for two types of recursive equations:

$$U_{n+1} = aU_{n-1} \pm \frac{bU_{n-1}U_{n-4}}{cU_{n-4} - dU_{n-6}} \tag{4}$$

Exploring some properties of the behavior of solutions appropriate to the class of recursive equation:

$$U_{n+1} = aU_{n-1} \pm \frac{bU_{n-1}U_{n-3}}{cU_{n-3} - dU_{n-5}} \tag{5}$$

was the prime objective for Alayachi et al. in [5]. Sadiq and Kalim [6] studied solutions, equilibrium points, and periodicity of four types of difference equations:

$$U_{n+1} = \frac{U_{n-20}}{\pm 1 \pm U_{n-6}U_{n-13}U_{n-20}} \tag{6}$$

Elsayed in [7] was able to get the solutions to this difference questions:

$$U_{n+1} = \frac{U_n U_{n-2} U_{n-4}}{U_{n-1} U_{n-3} (\pm 1 \pm U_n U_{n-2} U_{n-4})} \tag{7}$$

For more articles in this direction, we refer the reader to [8–14] and references cited therein.

2. The First Case:

$$U_{n+1} = U_{n-9}U_{n-5}U_{n-1}/U_{n-7}U_{n-3} (1 + U_{n-9} U_{n-5} U_{n-1})$$

The aim of this section is studying the solutions form of the particular case:

$$U_{n+1} = \frac{U_{n-9}U_{n-5}U_{n-1}}{U_{n-7}U_{n-3}(1 + U_{n-9}U_{n-5}U_{n-1})}, \quad n = 0, 1, \dots \tag{8}$$

Theorem 1. Assume that $(U_n)_{n=-9}^{\infty}$ are solutions of difference equations. Then, for $n = 0, 1, 2, \dots$, we see that all solutions of equation (8) are given by the following formulas:

$$U_{12n-9} = \frac{A \prod_{k=0}^{n-1} (1 + 6kAEI)}{\prod_{k=0}^{n-1} (1 + (6k + 2)AEI)},$$

$$U_{12n-3} = \frac{G \prod_{k=0}^{n-1} (1 + (6k + 3)AEI)}{\prod_{k=0}^{n-1} (1 + (6k + 5)AEI)},$$

$$U_{12n-8} = \frac{B \prod_{k=0}^{n-1} (1 + 6kBFJ)}{\prod_{k=0}^{n-1} (1 + (6k + 2)BFJ)},$$

$$U_{12n-2} = \frac{H \prod_{k=0}^{n-1} (1 + (6k + 3)BFJ)}{\prod_{k=0}^{n-1} (1 + (6k + 5)BFJ)},$$

$$U_{12n-7} = \frac{C \prod_{k=0}^{n-1} (1 + (6k + 1)AEI)}{\prod_{k=0}^{n-1} (1 + (6k + 3)AEI)},$$

$$U_{12n-1} = \frac{I \prod_{k=0}^{n-1} (1 + (6k + 4)AEI)}{\prod_{k=0}^{n-1} (1 + (6k + 6)AEI)},$$

$$U_{12n-6} = \frac{D \prod_{k=0}^{n-1} (1 + (6k + 1)BFJ)}{\prod_{k=0}^{n-1} (1 + (6k + 3)BFJ)},$$

$$U_{12n} = \frac{J \prod_{k=0}^{n-1} (1 + (6k + 4)BFJ)}{\prod_{k=0}^{n-1} (1 + (6k + 6)BFJ)},$$

$$U_{12n-5} = \frac{E \prod_{k=0}^{n-1} (1 + (6k + 2)AEI)}{\prod_{k=0}^{n-1} (1 + (6k + 4)AEI)},$$

$$U_{12n+1} = \frac{AEI \prod_{k=0}^{n-1} (1 + (6k + 5)AEI)}{CG (1 + AEI) \prod_{k=0}^{n-1} (1 + (6k + 7)AEI)}$$

$$U_{12n-4} = \frac{F \prod_{k=0}^{n-1} (1 + (6k + 2)BFJ)}{\prod_{k=0}^{n-1} (1 + (6k + 4)BFJ)},$$

$$U_{12n+2} = \frac{BFJ \prod_{k=0}^{n-1} (1 + (6k + 5)BFJ)}{DH (1 + BFJ) \prod_{k=0}^{n-1} (1 + (6k + 7)BFJ)}, \tag{9}$$

where $U_{-9} = A, U_{-8} = B, U_{-7} = C, U_{-6} = D, U_{-5} = E, U_{-4} = F, U_{-3} = G, U_{-2} = H, U_{-1} = I, \text{ and } U_0 = J.$

Proof. For $n = 1$, the result holds. Now suppose that $n > 0$ and that our assumption holds for $n - 1$, that is,

$$U_{12n-21} = \frac{A \prod_{k=0}^{n-2} (1 + 6kAEI)}{\prod_{k=0}^{n-2} (1 + (6k + 2)AEI)},$$

$$U_{12n-15} = \frac{G \prod_{k=0}^{n-2} (1 + (6k + 3)AEI)}{\prod_{k=0}^{n-2} (1 + (6k + 5)AEI)},$$

$$U_{12n-20} = \frac{B \prod_{k=0}^{n-2} (1 + 6kBFJ)}{\prod_{k=0}^{n-2} (1 + (6k + 2)BFJ)},$$

$$U_{12n-14} = \frac{H \prod_{k=0}^{n-2} (1 + (6k + 3)BFJ)}{\prod_{k=0}^{n-2} (1 + (6k + 5)BFJ)},$$

$$U_{12n-19} = \frac{C \prod_{k=0}^{n-2} (1 + (6k + 1)AEI)}{\prod_{k=0}^{n-2} (1 + (6k + 3)AEI)},$$

$$U_{12n-13} = \frac{I \prod_{k=0}^{n-2} (1 + (6k + 4)AEI)}{\prod_{k=0}^{n-2} (1 + (6k + 6)AEI)},$$

Now, we find from equation (8) that

$$\begin{aligned}
 U_{12n-18} &= \frac{D \prod_{k=0}^{n-2} (1 + (6k + 1)BFJ)}{\prod_{k=0}^{n-2} (1 + (6k + 3)BFJ)}, \\
 U_{12n-12} &= \frac{J \prod_{k=0}^{n-2} (1 + (6k + 4)BFJ)}{\prod_{k=0}^{n-2} (1 + (6k + 6)BFJ)}, \\
 U_{12n-17} &= \frac{E \prod_{k=0}^{n-2} (1 + (6k + 2)AEI)}{\prod_{k=0}^{n-2} (1 + (6k + 4)AEI)}, \\
 U_{12n-11} &= \frac{AEI \prod_{k=0}^{n-2} (1 + (6k + 5)AEI)}{CG (1 + AEI) \prod_{k=0}^{n-2} (1 + (6k + 7)AEI)}, \\
 U_{12n-16} &= \frac{F \prod_{k=0}^{n-2} (1 + (6k + 2)BFJ)}{\prod_{k=0}^{n-2} (1 + (6k + 4)BFJ)}, \\
 U_{12n-10} &= \frac{BFJ \prod_{k=0}^{n-2} (1 + (6k + 5)BFJ)}{DH (1 + BFJ) \prod_{k=0}^{n-2} (1 + (6k + 7)BFJ)}. \quad (10)
 \end{aligned}$$

$$\begin{aligned}
 U_{12n-9} &= \frac{U_{12n-19} U_{12n-15} U_{12n-11}}{U_{12n-17} U_{12n-13} (1 + U_{12n-19} U_{12n-15} U_{12n-11})} \\
 &= \frac{C \prod_{k=0}^{n-2} (1 + (6k + 1)AEI) / \prod_{k=0}^{n-2} (1 + (6k + 3)AEI) G \prod_{k=0}^{n-2} (1 + (6k + 3)AEI) / C \prod_{k=0}^{n-2} (1 + (6k + 5)AEI) AEI \prod_{k=0}^{n-2} (1 + (6k + 5)AEI) / GC (1 + AEI) \prod_{k=0}^{n-2} (1 + (6k + 7)AEI)}{E \prod_{k=0}^{n-2} (1 + (6k + 2)AEI) / \prod_{k=0}^{n-2} (1 + (6k + 4)AEI) / \prod_{k=0}^{n-2} (1 + (6k + 4)AEI) / \prod_{k=0}^{n-2} (1 + (6k + 6)AEI)} \\
 &\quad \times \frac{1}{(1 + C \prod_{k=0}^{n-2} (1 + (6k + 1)AEI) / \prod_{k=0}^{n-2} (1 + (6k + 3)AEI) G \prod_{k=0}^{n-2} (1 + (6k + 3)AEI) / \prod_{k=0}^{n-2} (1 + (6k + 5)AEI) AEI \prod_{k=0}^{n-2} (1 + (6k + 5)AEI) / GC (1 + AEI) \prod_{k=0}^{n-2} (1 + (6k + 7)AEI))}, \\
 U_{12n-9} &= \frac{AGCEI \prod_{k=0}^{n-2} (1 + (6k + 1)AEI) / GC (1 + AEI) \prod_{k=0}^{n-2} (1 + (6k + 7)AEI)}{EI \prod_{k=0}^{n-2} (1 + (6k + 2)AEI) / \prod_{k=0}^{n-2} (1 + (6k + 6)AEI) (1 + AGCEI \prod_{k=0}^{n-2} (1 + (6k + 1)AEI) / GC (1 + AEI) \prod_{k=0}^{n-2} (1 + (6k + 7)AEI))} \\
 &= \frac{A \prod_{k=0}^{n-2} (1 + (6k + 1)AEI) / (1 + AEI) \prod_{k=0}^{n-2} (1 + (6k + 7)AEI)}{\prod_{k=0}^{n-2} (1 + (6k + 2)AEI) / \prod_{k=0}^{n-2} (1 + (6k + 6)AEI) (1 + AEI \prod_{k=0}^{n-2} (1 + (6k + 1)AEI) / (1 + AEI) \prod_{k=0}^{n-2} (1 + (6k + 7)AEI))} \\
 &= \frac{A / (1 + (6n - 5)AEI)}{\prod_{k=0}^{n-2} (1 + (6k + 2)AEI) / \prod_{k=0}^{n-2} (1 + (6k + 6)AEI) (1 + AEI / (1 + (6n - 5)AEI))}, \\
 U_{12n-9} &= \frac{A}{\prod_{k=0}^{n-2} (1 + (6k + 2)AEI) / \prod_{k=0}^{n-2} (1 + (6k + 6)AEI) (1 + (6n - 5)AEI + AEI)} \\
 &= \frac{A}{\prod_{k=0}^{n-2} (1 + (6k + 2)AEI) / \prod_{k=0}^{n-2} (1 + (6k + 6)AEI) (1 + (6n - 5)AEI + AEI)} \\
 &= \frac{A \prod_{k=0}^{n-1} (1 + 6kAEI)}{\prod_{k=0}^{n-1} (1 + (6k + 2)AEI)}, \\
 U_{12n-8} &= \frac{U_{12n-18} U_{12n-14} U_{12n-10}}{U_{12n-16} U_{12n-12} (1 + U_{12n-18} U_{12n-14} U_{12n-10})} \\
 &= \frac{D \prod_{k=0}^{n-2} (1 + (6k + 1)BFJ) / \prod_{k=0}^{n-2} (1 + (6k + 3)BFJ) H \prod_{k=0}^{n-2} (1 + (6k + 3)BFJ) / \prod_{k=0}^{n-2} (1 + (6k + 5)BFJ) BFJ \prod_{k=0}^{n-2} (1 + (6k + 5)BFJ) / DH (1 + BFJ) \prod_{k=0}^{n-2} (1 + (6k + 7)BFJ)}{F \prod_{k=0}^{n-2} (1 + (6k + 2)BFJ) / \prod_{k=0}^{n-2} (1 + (6k + 4)BFJ) / \prod_{k=0}^{n-2} (1 + (6k + 4)BFJ) / \prod_{k=0}^{n-2} (1 + (6k + 6)BFJ)} \\
 &\quad \times \frac{1}{(1 + D \prod_{k=0}^{n-2} (1 + (6k + 1)BFJ) / \prod_{k=0}^{n-2} (1 + (6k + 3)BFJ) H \prod_{k=0}^{n-2} (1 + (6k + 3)BFJ) / \prod_{k=0}^{n-2} (1 + (6k + 5)BFJ) BFJ \prod_{k=0}^{n-2} (1 + (6k + 5)BFJ) / DH (1 + BFJ) \prod_{k=0}^{n-2} (1 + (6k + 7)BFJ))}, \\
 &= \frac{DH BFJ \prod_{k=0}^{n-2} (1 + (6k + 1)BFJ) / DH (1 + BFJ) \prod_{k=0}^{n-2} (1 + (6k + 7)BFJ)}{FJ \prod_{k=0}^{n-2} (1 + (6k + 2)BFJ) / \prod_{k=0}^{n-2} (1 + (6k + 6)BFJ) (1 + BFJ \prod_{k=0}^{n-2} (1 + (6k + 1)BFJ) / (1 + BFJ) \prod_{k=0}^{n-2} (1 + (6k + 7)BFJ))} \\
 &= \frac{B \prod_{k=0}^{n-2} (1 + (6k + 1)BFJ) / (1 + BFJ) \prod_{k=0}^{n-2} (1 + (6k + 7)BFJ)}{\prod_{k=0}^{n-2} (1 + (6k + 2)BFJ) / \prod_{k=0}^{n-2} (1 + (6k + 6)BFJ) (1 + BFJ \prod_{k=0}^{n-2} (1 + (6k + 1)BFJ) / (1 + BFJ) \prod_{k=0}^{n-2} (1 + (6k + 7)BFJ))} \\
 &= \frac{B / (1 + (6n - 5)BFJ)}{\prod_{k=0}^{n-2} (1 + (6k + 2)BFJ) / \prod_{k=0}^{n-2} (1 + (6k + 6)BFJ) (1 + BFJ / (1 + (6n - 5)BFJ))}, \\
 U_{12n-8} &= \frac{B}{\prod_{k=0}^{n-2} (1 + (6k + 2)BFJ) / \prod_{k=0}^{n-2} (1 + (6k + 6)BFJ) (1 + (6n - 5)BFJ + BFJ)} \\
 &= \frac{B}{\prod_{k=0}^{n-2} (1 + (6k + 2)BFJ) / \prod_{k=0}^{n-2} (1 + (6k + 6)BFJ) (1 + (6n - 5)BFJ + BFJ)} \\
 &= \frac{B \prod_{k=0}^{n-1} (1 + 6kBFJ)}{\prod_{k=0}^{n-1} (1 + (6k + 2)BFJ)},
 \end{aligned}$$

$$\begin{aligned}
 U_{12n-7} &= \frac{U_{12n-17}U_{12n-13}U_{12n-9}}{U_{12n-15}U_{12n-11}(1+U_{12n-17}U_{12n-13}U_{12n-9})} \\
 &= \frac{E\prod_{k=0}^{n-2}(1+(6k+2)AEI)/\prod_{k=0}^{n-2}(1+(6k+4)AEI)I\prod_{k=0}^{n-2}(1+(6k+4)AEI)/\prod_{k=0}^{n-2}(1+(6k+6)AEI)A\prod_{k=0}^{n-1}(1+6kAEI)/\prod_{k=0}^{n-1}(1+(6k+2)AEI)}{G\prod_{k=0}^{n-2}(1+(6k+3)AEI)/\prod_{k=0}^{n-2}(1+(6k+5)AEI)AEI\prod_{k=0}^{n-2}(1+(6k+5)AEI)/CG(1+AEI)\prod_{k=0}^{n-2}(1+(6k+7)AEI)} \\
 &\quad \times \frac{1}{(1+E\prod_{k=0}^{n-2}(1+(6k+2)AEI)/\prod_{k=0}^{n-2}(1+(6k+4)AEI)I\prod_{k=0}^{n-2}(1+(6k+4)AEI)/\prod_{k=0}^{n-2}(1+(6k+6)AEI)A\prod_{k=0}^{n-1}(1+6kAEI)/\prod_{k=0}^{n-1}(1+(6k+2)AEI))} \\
 &= \frac{\prod_{k=0}^{n-1}(1+6kAEI)/(1+(6n-4)AEI)\prod_{k=0}^{n-2}(1+(6k+6)AEI)}{\prod_{k=0}^{n-2}(1+(6k+3)AEI)/C(1+AEI)\prod_{k=0}^{n-2}(1+(6k+7)AEI)(1+AEI\prod_{k=0}^{n-1}(1+6kAEI)/(1+(6n-4)AEI)\prod_{k=0}^{n-2}(1+(6k+6)AEI))} \\
 &= \frac{1/(1+(6n-4)AEI)}{\prod_{k=0}^{n-2}(1+(6k+3)AEI)/C(1+AEI)\prod_{k=0}^{n-2}(1+(6k+7)AEI)(1+AEI/(1+(6n-4)AEI))} \\
 &= \frac{C(1+AEI)}{\prod_{k=0}^{n-2}(1+(6k+3)AEI)/\prod_{k=0}^{n-2}(1+(6k+7)AEI)((1+(6n-4)AEI)+AEI)} \\
 &= \frac{C\prod_{k=0}^{n-1}(1+(6k+1)AEI)}{\prod_{k=0}^{n-1}(1+(6k+3)AEI)}, \\
 U_{12n-6} &= \frac{U_{12n-16}U_{12n-12}U_{12n-8}}{U_{12n-14}U_{12n-10}(1+U_{12n-16}U_{12n-12}U_{12n-8})} \\
 &= \frac{F\prod_{k=0}^{n-2}(1+(6k+2)BFJ)/\prod_{k=0}^{n-2}(1+(6k+4)BFJ)I\prod_{k=0}^{n-2}(1+(6k+4)BFJ)/\prod_{k=0}^{n-2}(1+(6k+6)BFJ)B\prod_{k=0}^{n-1}(1+6kBFJ)/\prod_{k=0}^{n-1}(1+(6k+2)BFJ)}{H\prod_{k=0}^{n-2}(1+(6k+3)BFJ)/\prod_{k=0}^{n-2}(1+(6k+5)BFJ)BFJ\prod_{k=0}^{n-2}(1+(6k+5)BFJ)/DH(1+BFJ)\prod_{k=0}^{n-2}(1+(6k+7)BFJ)} \\
 &\quad \times \frac{1}{\left(1+\frac{F\prod_{k=0}^{n-2}(1+(6k+2)BFJ)I\prod_{k=0}^{n-2}(1+(6k+4)BFJ)}{\prod_{k=0}^{n-2}(1+(6k+4)BFJ)}\frac{B\prod_{k=0}^{n-1}(1+6kBFJ)}{\prod_{k=0}^{n-1}(1+(6k+2)BFJ)}\right)} \\
 &= \frac{\prod_{k=0}^{n-1}(1+6kBFJ)/(1+(6n-4)BFJ)\prod_{k=0}^{n-2}(1+(6k+6)BFJ)}{\prod_{k=0}^{n-2}(1+(6k+3)BFJ)/D(1+BFJ)\prod_{k=0}^{n-2}(1+(6k+7)BFJ)(1+BFJ\prod_{k=0}^{n-1}(1+6kBFJ)/(1+(6n-4)BFJ)\prod_{k=0}^{n-2}(1+(6k+6)BFJ))} \\
 &= \frac{1/(1+(6n-4)BFJ)}{\prod_{k=0}^{n-2}(1+(6k+3)BFJ)/D(1+BFJ)\prod_{k=0}^{n-2}(1+(6k+7)BFJ)(1+BFJ/(1+(6n-4)BFJ))} \\
 &= \frac{C\prod_{k=0}^{n-1}(1+(6k+1)BFJ)}{\prod_{k=0}^{n-1}(1+(6k+3)BFJ)},
 \end{aligned} \tag{11}$$

Also, we can prove the other relations. The proof is complete.

Theorem 2. Equation (8) has a unique equilibrium point $\bar{U} = 0$, which is nonhyperbolic.

Proof. To obtain equilibrium points of (8),

$$\bar{U} = \frac{\bar{U}^3}{\bar{U}^2(1+\bar{U}^3)}. \tag{12}$$

Thus,

$$\begin{aligned}
 \bar{U}^3(1+\bar{U}^3) &= \bar{U}^3, \\
 \bar{U}^3(1+\bar{U}^3-1) &= 0, \\
 \bar{U}^6 &= 0.
 \end{aligned} \tag{13}$$

Hence, $\bar{U} = 0$ is the equilibrium point of equation (8). Define a function $h: (0, \infty)^5 \rightarrow (0, \infty)$, such that

$$h(r, s, t, u, v) = \frac{rst}{uv(1+rst)}. \tag{14}$$

Then,

$$\begin{aligned}
 h_r(r, s, t, u, v) &= \frac{st}{uv(1+rst)^2}, \\
 h_s(r, s, t, u, v) &= \frac{rt}{uv(1+rst)^2}, \\
 h_t(r, s, t, u, v) &= \frac{rs}{uv(1+rst)^2}, \\
 h_u(r, s, t, u, v) &= -\frac{rst}{u^2v(1+rst)}, \\
 h_v(r, s, t, u, v) &= -\frac{rst}{uv^2(1+rst)}.
 \end{aligned} \tag{15}$$

Therefore,

$$\begin{aligned}
 h_r(\bar{U}, \bar{U}, \bar{U}, \bar{U}, \bar{U}) &= 1, \\
 h_s(\bar{U}, \bar{U}, \bar{U}, \bar{U}, \bar{U}) &= 1, \\
 h_t(\bar{U}, \bar{U}, \bar{U}, \bar{U}, \bar{U}) &= 1, \\
 h_u(\bar{U}, \bar{U}, \bar{U}, \bar{U}, \bar{U}) &= -1, \\
 h_v(\bar{U}, \bar{U}, \bar{U}, \bar{U}, \bar{U}) &= -1.
 \end{aligned} \tag{16}$$

It follows the characteristic equation given by

$$\lambda^{10} - \lambda^9 + \lambda^8 - \lambda^6 + \lambda^4 - \lambda^2 = 0. \quad (17)$$

Hence,

$$\lambda^8 - \lambda^7 + \lambda^6 - \lambda^4 + \lambda^2 - 1 = 0. \quad (18)$$

Clearly, $\lambda = 1$ is one root of equation (17). Therefore, the equilibrium point is nonhyperbolic.

We provide numerical examples for equation (8) in order to confirm the results of this section.

Example 1. Assume the initial conditions are $U_{-9} = 7$, $U_{-8} = 15$, $U_{-7} = 9$, $U_{-6} = 5$, $U_{-5} = 10$, $U_{-4} = 8$, $U_{-3} = 16$, $U_{-2} = 10$, $U_{-1} = 6$, and $U_0 = 11$ (Figure 1).

Example 2. Suppose that $U_{-9} = 0.1$, $U_{-8} = 0.2$, $U_{-7} = 0.3$, $U_{-6} = 0.4$, $U_{-5} = 0.5$, $U_{-4} = 0.1$, $U_{-3} = 0.2$, $U_{-2} = 0.3$, $U_{-1} = 0.4$, and $U_0 = 0.5$ (Figure 2).

3. Second Case:

$$U_{n+1} = \frac{U_{n-9}U_{n-5}U_{n-1}}{(1 - U_{n-9}U_{n-5}U_{n-1})} U_{n-7}U_{n-3}$$

The solutions to difference equations

$$U_{n+1} = \frac{U_{n-9}U_{n-5}U_{n-1}}{U_{n-7}U_{n-3}(1 - U_{n-9}U_{n-5}U_{n-1})}, \quad n = 0, 1, \dots, \quad (19)$$

are investigated in this section.

Theorem 3. Assume that $\{U_n\}_{n=-9}^{\infty}$ are solutions of difference equations. Then, for $n = 0, 1, 2, \dots$, we see that all solutions of equation (19) are given by the following formulas:

$$U_{12n-9} = \frac{A \prod_{k=0}^{n-1} (1 - 6kAEI)}{\prod_{k=0}^{n-1} (1 - (6k + 2)AEI)},$$

$$U_{12n-3} = \frac{G \prod_{k=0}^{n-1} (1 - (6k + 3)AEI)}{\prod_{k=0}^{n-1} (1 - (6k + 5)AEI)},$$

$$U_{12n-8} = \frac{B \prod_{k=0}^{n-1} (1 - 6kBFJ)}{\prod_{k=0}^{n-1} (1 - (6k + 2)BFJ)},$$

$$U_{12n-2} = \frac{H \prod_{k=0}^{n-1} (1 - (6k + 3)BFJ)}{\prod_{k=0}^{n-1} (1 - (6k + 5)BFJ)},$$

$$U_{12n-7} = \frac{C \prod_{k=0}^{n-1} (1 - (6k + 1)AEI)}{\prod_{k=0}^{n-1} (1 - (6k + 3)AEI)},$$

$$U_{12n-1} = \frac{I \prod_{k=0}^{n-1} (1 - (6k + 4)AEI)}{\prod_{k=0}^{n-1} (1 - (6k + 6)AEI)},$$

$$U_{12n-6} = \frac{D \prod_{k=0}^{n-1} (1 - (6k + 3)BFJ)}{\prod_{k=0}^{n-1} (1 - (6k + 1)BFJ)},$$

$$U_{12n} = \frac{J \prod_{k=0}^{n-1} (1 - (6k + 4)BFJ)}{\prod_{k=0}^{n-1} (1 - (6k + 4)BFJ)},$$

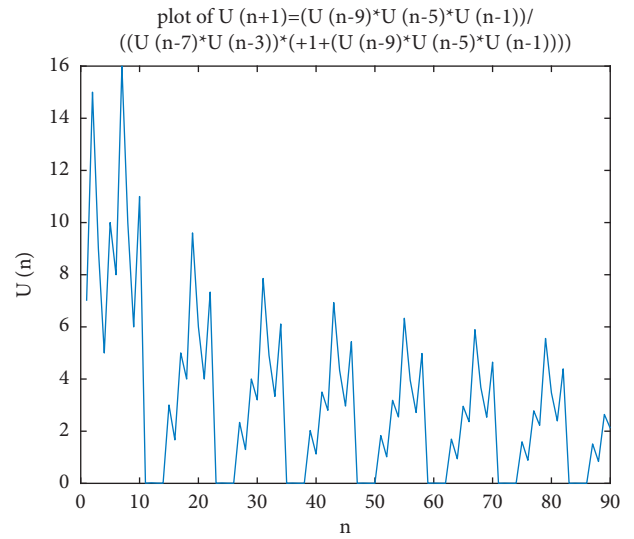


FIGURE 1: The solution of equation (8) when $U_{-9} = 7$, $U_{-8} = 15$, $U_{-7} = 9$, $U_{-6} = 5$, $U_{-5} = 10$, $U_{-4} = 8$, $U_{-3} = 16$, $U_{-2} = 10$, $U_{-1} = 6$, and $U_0 = 11$.

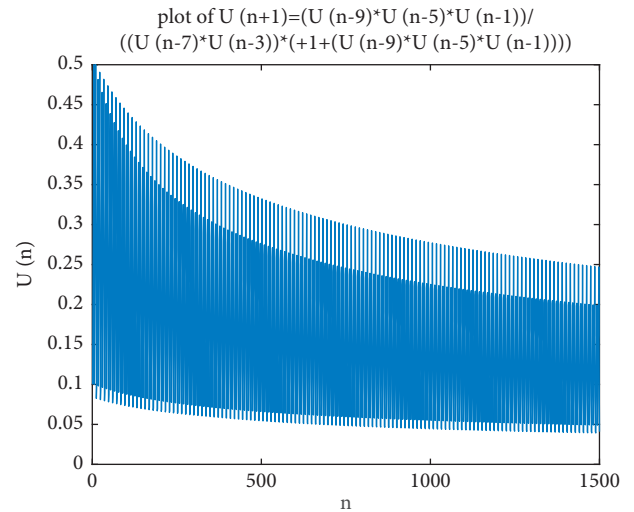


FIGURE 2: The local stability of equilibrium point of equation (8) when $U_{-9} = 0.1$, $U_{-8} = 0.2$, $U_{-7} = 0.3$, $U_{-6} = 0.4$, $U_{-5} = 0.5$, $U_{-4} = 0.1$, $U_{-3} = 0.2$, $U_{-2} = 0.3$, $U_{-1} = 0.4$, and $U_0 = 0.5$.

$$U_{12n-5} = \frac{E \prod_{k=0}^{n-1} (1 - (6k + 2)AEI)}{\prod_{k=0}^{n-1} (1 - (6k + 4)AEI)},$$

$$U_{12n+1} = \frac{AEI \prod_{k=0}^{n-1} (1 - (6k + 5)AEI)}{(1 - AEI) \prod_{k=0}^{n-1} (1 - (6k + 7)AEI)},$$

$$U_{12n-4} = \frac{F \prod_{k=0}^{n-1} (1 - (6k + 2)BFJ)}{\prod_{k=0}^{n-1} (1 - (6k + 4)BFJ)},$$

$$U_{12n+2} = \frac{BFJ \prod_{k=0}^{n-1} (1 - (6k + 5)BFJ)}{(1 - BFJ) \prod_{k=0}^{n-1} (1 - (6k + 7)BFJ)}, \quad (20)$$

where $U_{-9} = A, U_{-8} = B, U_{-7} = C, U_{-6} = D, U_{-5} = E, U_{-4} = F, U_{-3} = G, U_{-2} = H, U_{-1} = I,$ and $U_0 = J.$

Proof. The proof is identical to the method to prove Theorem 1.

Theorem 4. Equation (19) has a unique equilibrium point $\bar{U} = 0,$ which is nonhyperbolic.

Proof. To obtain equilibrium points of equation (19),

$$\bar{U} = \frac{\bar{U}^3}{\bar{U}^2(1 - \bar{U}^3)}. \tag{21}$$

Thus,

$$\begin{aligned} \bar{U}^3(1 - \bar{U}^3) &= \bar{U}^3, \\ \bar{U}^3(1 - \bar{U}^3 - 1) &= 0, \\ \bar{U}^6 &= 0. \end{aligned} \tag{22}$$

Hence, $\bar{U} = 0$ is the equilibrium point of equation (19). Define a function $h: (0, \infty)^5 \rightarrow (0, \infty),$ such that

$$h(r, s, t, u, v) = \frac{rst}{uv(1 - rst)}. \tag{23}$$

Then,

$$\begin{aligned} h_r(r, s, t, u, v) &= \frac{st}{uv(1 - rst)^2}, \\ h_s(r, s, t, u, v) &= \frac{rt}{uv(1 - rst)^2}, \\ h_t(r, s, t, u, v) &= \frac{rs}{uv(1 - rst)^2}, \\ h_u(r, s, t, u, v) &= -\frac{rst}{u^2v(1 - rst)}, \\ h_v(r, s, t, u, v) &= -\frac{rst}{uv^2(1 - rst)}. \end{aligned} \tag{24}$$

Therefore,

$$\begin{aligned} h_r(\bar{U}, \bar{U}, \bar{U}, \bar{U}, \bar{U}) &= 1, \\ h_s(r, s, t, u, v) &= 1, \\ h_t(\bar{U}, \bar{U}, \bar{U}, \bar{U}, \bar{U}) &= 1, \\ h_u(r, s, t, u, v) &= -1, \\ h_v(\bar{U}, \bar{U}, \bar{U}, \bar{U}, \bar{U}) &= -1. \end{aligned} \tag{25}$$

It follows the characteristic equation given by

$$\lambda^{10} - \lambda^9 + \lambda^8 - \lambda^6 + \lambda^4 - \lambda^2 = 0. \tag{26}$$

Hence,

$$\lambda^8 - \lambda^7 + \lambda^6 - \lambda^4 + \lambda^2 - 1 = 0. \tag{27}$$

Clearly, $\lambda = 1$ is one root of equation (26). Therefore, the equilibrium point is nonhyperbolic.

Example 3. We consider the present numerical example for equation (19) for confirming the results of this section where the initial conditions are $U_{-9} = 4, U_{-8} = 12, U_{-7} = 6, U_{-6} = 2, U_{-5} = 8, U_{-4} = 3, U_{-3} = 11, U_{-2} = 5, U_{-1} = 2,$ and $U_0 = 7$ (Figure 3).

Example 4. We provide another numerical example for equation (19) with initial values $U_{-9} = 0.1, U_{-8} = 0.2, U_{-7} = 0.3, U_{-6} = 0.4, U_{-5} = 0.5, U_{-4} = 0.1, U_{-3} = 0.2, U_{-2} = 0.3, U_{-1} = 0.4,$ and $U_0 = 0.5$ (Figure 4).

4. Third Case:

$$U_{n+1} = U_{n-9}U_{n-5}U_{n-1}/U_{n-7}U_{n-3}(-1 - U_{n-9}U_{n-5}U_{n-1})$$

The goal of this section is to obtain the solutions form of the particular case:

$$U_{n+1} = \frac{U_{n-9}U_{n-5}U_{n-1}}{U_{n-7}U_{n-3}(-1 - U_{n-9}U_{n-5}U_{n-1})}, \quad n = 0, 1, \dots \tag{28}$$

Theorem 5. Every solution $\{U_n\}_{n=-9}^\infty$ of equation (28) is periodic with period twelve, and it is in the form

$$\left\{ A, B, C, D, E, F, G, H, I, J, -\frac{AEI}{CG(AEI + 1)}, -\frac{BFJ}{DH(BFJ + 1)}, \dots \right\} \tag{29}$$

or

$$\begin{aligned} U_{12n-9} &= A, \\ U_{12n-8} &= B, \\ U_{12n-7} &= C, \\ U_{12n-6} &= D, \\ U_{12n-5} &= E, \\ U_{12n-4} &= F, \\ U_{12n-3} &= G, \\ U_{12n-2} &= H, \\ U_{12n-1} &= I, \\ U_{12n} &= J, \end{aligned} \tag{30}$$

$$U_{12n+1} = -\frac{AEI}{CG(AEI + 1)},$$

$$U_{12n+2} = -\frac{BFJ}{DH(BFJ + 1)},$$

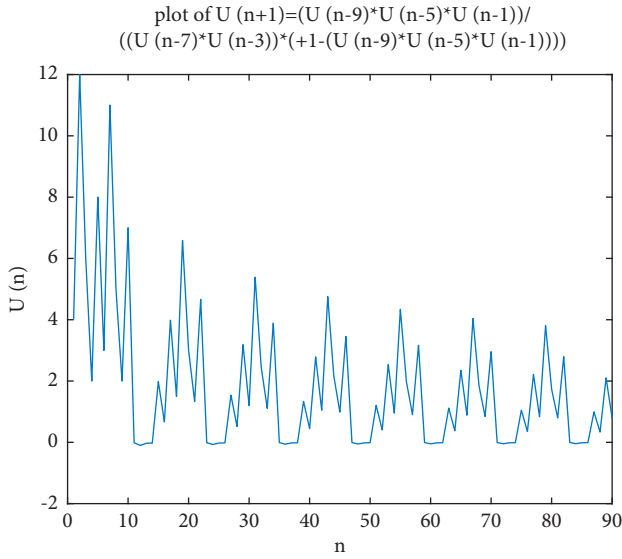


FIGURE 3: The solution of equation (19) when $U_{-9} = 4$, $U_{-8} = 12$, $U_{-7} = 6$, $U_{-6} = 2$, $U_{-5} = 8$, $U_{-4} = 3$, $U_{-3} = 11$, $U_{-2} = 5$, $U_{-1} = 2$, and $U_0 = 7$.

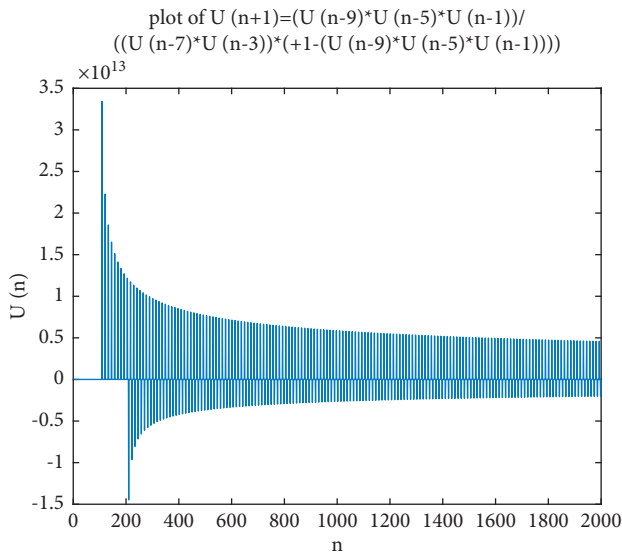


FIGURE 4: The local stability of equilibrium point of equation (19) with $U_{-9} = 0.1$, $U_{-8} = 0.2$, $U_{-7} = 0.3$, $U_{-6} = 0.4$, $U_{-5} = 0.5$, $U_{-4} = 0.1$, $U_{-3} = 0.2$, $U_{-2} = 0.3$, $U_{-1} = 0.4$, and $U_0 = 0.5$.

where $U_{-9} = A$, $U_{-8} = B$, $U_{-7} = C$, $U_{-6} = D$, $U_{-5} = E$, $U_{-4} = F$, $U_{-3} = G$, $U_{-2} = H$, $U_{-1} = I$, and $U_0 = J$.

Proof. From $n = 1$,

$$\begin{aligned} U_{12n-21} &= A, \\ U_{12n-20} &= B, \\ U_{12n-19} &= C, \\ U_{12n-18} &= D, \end{aligned}$$

$$\begin{aligned} U_{12n-17} &= E, \\ U_{12n-16} &= F, \\ U_{12n-15} &= G, \\ U_{12n-14} &= H, \\ U_{12n-13} &= I, \\ U_{12n-12} &= J, \\ U_{12n-11} &= \frac{AEI}{CG(AEI + 1)}, \\ U_{12n-10} &= \frac{BFJ}{DH(BFJ + 1)}. \end{aligned} \tag{31}$$

From equation (28), we see that

$$\begin{aligned} U_{12n-9} &= \frac{U_{12n-19}U_{12n-15}U_{12n-11}}{U_{12n-17}U_{12n-13}(-1 - U_{12n-19}U_{12n-15}U_{12n-11})} \\ &= \frac{CG(-AEI/CG(AEI + 1))}{EI(-1 - CG(-AEI/CG(AEI + 1)))} \\ &= A, \end{aligned}$$

$$\begin{aligned} U_{12n-8} &= \frac{U_{12n-18}U_{12n-14}U_{12n-10}}{U_{12n-16}U_{12n-12}(-1 - U_{12n-18}U_{12n-14}U_{12n-10})} \\ &= \frac{DH(-BFJ/DH(BFJ + 1))}{FJ(-1 - DH(-BFJ/DH(BFJ + 1)))} \\ &= B, \end{aligned}$$

$$\begin{aligned} U_{12n-7} &= \frac{U_{12n-17}U_{12n-13}U_{12n-9}}{U_{12n-15}U_{12n-11}(-1 - U_{12n-17}U_{12n-13}U_{12n-9})} \\ &= \frac{AEI}{G(-AEI/CG(AEI + 1))(-1 - AEI)} \\ &= C, \end{aligned}$$

$$\begin{aligned} U_{12n-6} &= \frac{U_{12n-16}U_{12n-12}U_{12n-8}}{U_{12n-14}U_{12n-10}(-1 - U_{12n-16}U_{12n-12}U_{12n-8})} \\ &= \frac{BFJ}{H(-BFJ/DH(BFJ + 1))(-1 - BFJ)} \\ &= D, \end{aligned}$$

$$\begin{aligned} U_{12n-5} &= \frac{U_{12n-15}U_{12n-11}U_{12n-7}}{U_{12n-13}U_{12n-9}(-1 - U_{12n-15}U_{12n-11}U_{12n-7})} \\ &= \frac{G(-AEI/CG(AEI + 1))C}{IA(-1 - G(-AEI/CG(AEI + 1))C)} \\ &= E, \end{aligned}$$

$$\begin{aligned} U_{12n-4} &= \frac{U_{12n-14}U_{12n-10}U_{12n-6}}{U_{12n-12}U_{12n-8}(-1 - U_{12n-14}U_{12n-10}U_{12n-6})} \\ &= \frac{H(-BFJ/DH(BFJ + 1))D}{JB(-1 - H(-BFJ/DH(BFJ + 1))D)} \\ &= F, \end{aligned}$$

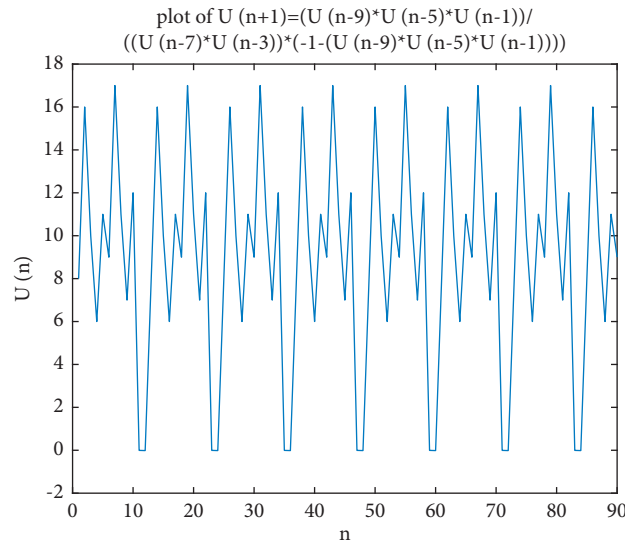


FIGURE 5: The solution of equation (28) with period twelve when $U_{-9} = 8, U_{-8} = 16, U_{-7} = 10, U_{-6} = 6, U_{-5} = 11, U_{-4} = 9, U_{-3} = 17, U_{-2} = 11, U_{-1} = 7,$ and $U_0 = 12.$

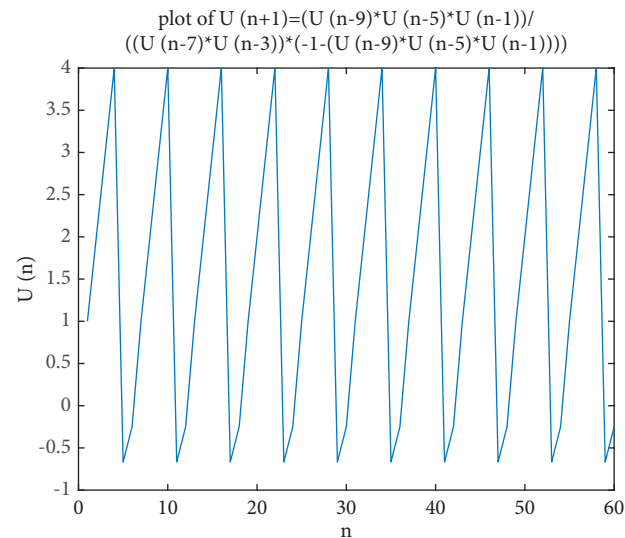


FIGURE 6: The solution of equation (28) with period six when initial values satisfies the conditions in Theorem 6, that are $U_{-9} = 1, U_{-8} = 2, U_{-7} = 3, U_{-6} = 4, U_{-5} = -0.6667, U_{-4} = -0.25, U_{-3} = 1, U_{-2} = 2, U_{-1} = 3,$ and $U_0 = 4.$

$$\begin{aligned}
 U_{12n-3} &= \frac{U_{12n-13}U_{12n-9}U_{12n-5}}{U_{12n-11}U_{12n-7}(-1 - U_{12n-13}U_{12n-9}U_{12n-5})} \\
 &= \frac{IAE}{(-AEI/CG(AEI + 1))C(-1 - IAE)} \\
 &= G, \\
 U_{12n-2} &= \frac{U_{12n-12}U_{12n-8}U_{12n-4}}{U_{12n-10}U_{12n-6}(-1 - U_{12n-12}U_{12n-8}U_{12n-4})} \\
 &= \frac{JBF}{(-BFJ/DH(BFJ + 1))D(-1 - JBF)} \\
 &= H.
 \end{aligned}
 \tag{32}$$

Theorem 6. Every solution $\{U_n\}_{n=-9}^{\infty}$ of equation (28) is periodic with period six, and it is of the form

$$\{A, B, C, D, E, F, A, \dots\}, \tag{33}$$

iff

$$\begin{aligned}
 A &= G, \\
 B &= H, \\
 C &= I, \\
 D &= J, \\
 AEI &= -2, \\
 BFJ &= -2.
 \end{aligned}
 \tag{34}$$

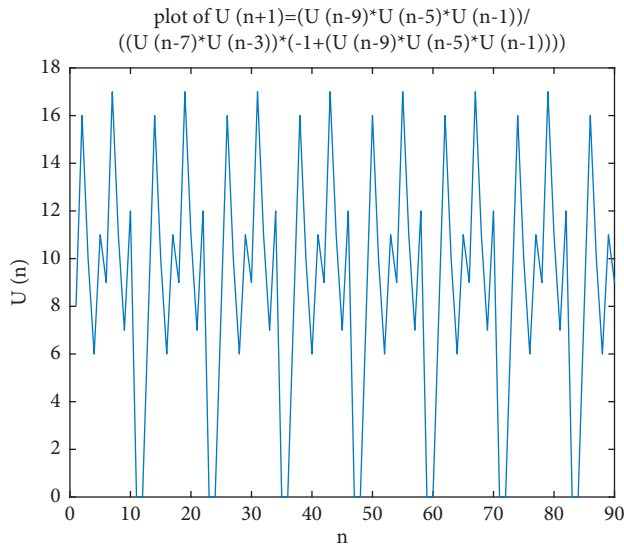


FIGURE 7: The solution of equation (35) with period twelve when $U_{-9} = 8, U_{-8} = 16, U_{-7} = 10, U_{-6} = 6, U_{-5} = 11, U_{-4} = 9, U_{-3} = 17, U_{-2} = 11, U_{-1} = 7,$ and $U_0 = 12.$

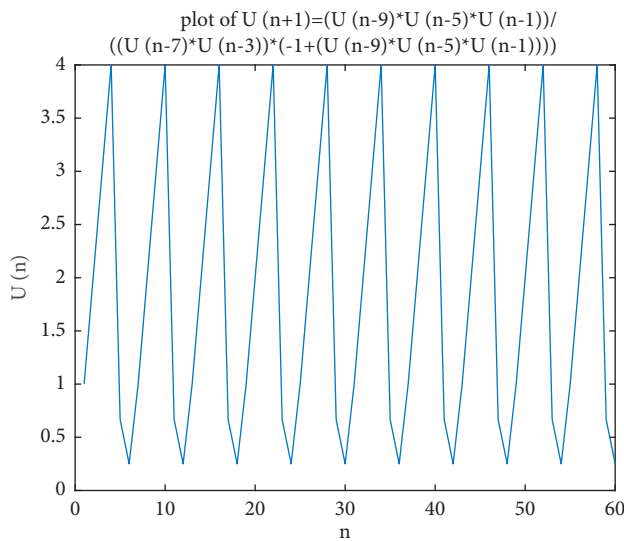


FIGURE 8: The solution of equation (35) with period six when initial values satisfies the conditions in Theorem 8, that are $U_{-9} = 1, U_{-8} = 2, U_{-7} = 3, U_{-6} = 4, U_{-5} = 0.6667, U_{-4} = 0.25, U_{-3} = 1, U_{-2} = 2, U_{-1} = 3,$ and $U_0 = 4.$

Example 5. We present numerical example for equation (28) for illustrating the results of this section where the initial conditions are $U_{-9} = 8, U_{-8} = 16, U_{-7} = 10, U_{-6} = 6, U_{-5} = 11, U_{-4} = 9, U_{-3} = 17, U_{-2} = 11, U_{-1} = 7,$ and $U_0 = 12$ (Figure 5).

Example 6. For confirming the results of this section, we consider numerical example for equation (28) where the initial conditions are $U_{-9} = 1, U_{-8} = 2, U_{-7} = 3, U_{-6} = 4, U_{-5} = -0.6667, U_{-4} = -0.25, U_{-3} = 1, U_{-2} = 2, U_{-1} = 3,$ and $U_0 = 4$ (Figure 6).

5. Fourth Case:

$$U_{n+1} = \frac{U_{n-9}U_{n-5}U_{n-1}}{U_{n-7}U_{n-3}(-1 + U_{n-9}U_{n-5}U_{n-1})}$$

The solutions to difference equations

$$U_{n+1} = \frac{U_{n-9}U_{n-5}U_{n-1}}{U_{n-7}U_{n-3}(-1 + U_{n-9}U_{n-5}U_{n-1})}, \quad n = 0, 1, \dots, \tag{35}$$

are studied in this section.

Theorem 7. Every solution $\{U_n\}_{n=-9}^\infty$ of equation (35) is periodic with period twelve, and it is in the form

$$\left\{ A, B, C, D, E, F, G, H, I, J, +\frac{AEI}{CG(AEI - 1)}, +\frac{BFJ}{DH(BFJ - 1)}, A, B, \dots \right\}, \tag{36}$$

where $U_{-9} = A, U_{-8} = B, U_{-7} = C, U_{-6} = D, U_{-5} = E, U_{-4} = F, U_{-3} = G, U_{-2} = H, U_{-1} = I,$ and $U_0 = J.$

Proof. The proof is identical to the method to prove Theorem 5.

Theorem 8. Every solution $\{U_n\}_{n=-9}^\infty$ of equation (35) is periodic with period six, and it is in the form

$$\{A, B, C, D, E, F, A, \dots\}. \tag{37}$$

iff

$$\begin{aligned} A &= G, \\ B &= H, \\ C &= I, \\ D &= J, \\ AEI &= 2, \\ BFJ &= 2. \end{aligned} \tag{38}$$

We provide numerical examples of equation (35) for confirming our results.

Example 7. Assume that the starting conditions are as follows: $U_{-9} = 8, U_{-8} = 16, U_{-7} = 10, U_{-6} = 6, U_{-5} = 11, U_{-4} = 9, U_{-3} = 17, U_{-2} = 11, U_{-1} = 7,$ and $U_0 = 12$ (Figure 7).

Example 8. Let the initial conditions be given by $U_{-9} = 1, U_{-8} = 2, U_{-7} = 3, U_{-6} = 4, U_{-5} = 0.6667, U_{-4} = 0.25, U_{-3} = 1, U_{-2} = 2, U_{-1} = 3,$ and $U_0 = 4$ (Figure 8).

6. Conclusion

This research discussed the structure and behavior of solutions for four special cases of equation (1). In the second and third sections, we proved the stability of the equilibrium point. In the fourth and fifth sections, we obtained the periodic solutions to the equations with periodicity twelve.

In addition, we studied the conditions of existence of the periodic solutions with period six.

Data Availability

The data used to support the findings of this study are included within the article.

Conflicts of Interest

The authors declare that they have no conflicts of interest.

References

- [1] A. Khaliq, S. K. S. Hassan, M. Saqib, and D. S. Mashat, "Behavior of a seventh order rational difference equations," *Dynamic Systems and Applications*, vol. 28, no. 4, pp. 1056–2176, 2019.
- [2] M. M. El-Dessoky, E. M. Elabbasy, and A. Asiri, "Dynamics and solutions of a fifth-order nonlinear difference equation," *Discrete Dynamics in Nature and Society*, vol. 2018, Article ID 9129354, 21 pages, 2018.
- [3] M. Ghazel, E. M. Elsayed, A. E. Matouk, and A. M. Mousallam, "Investigating dynamical behaviors of the difference equation $x_{n+1} = Cx_n - 5/A + Bx_n - 2x_n - 5$," *The Journal of Nonlinear Science and Applications*, vol. 10, no. 9, pp. 4662–4679, 2017.
- [4] M. B. Almatrafi and M. M. Alzubaidi, "Qualitative analysis for two fractional difference equations," *Nonlinear Engineering*, vol. 9, no. 1, pp. 265–272, 2020.
- [5] H. S. Alayachi, M. S. M. Noorani, A. Q. Khan, and M. B. Almatraf, "Analytic solutions and stability of sixth order difference equations," *Mathematical Problems in Engineering*, vol. 2020, Article ID 1230979, 12 pages, 2020.
- [6] S. Sadiq, M. Kalim, and M. Kalim, "Dynamics of some higher order rational difference equations," *International Journal of Advanced and Applied Sciences*, vol. 5, no. 7, pp. 64–70, 2018.
- [7] E. M. Elsayed and T. F. Ibrahim, "Solutions and periodicity of a rational recursive sequences of order five," *Bulletin of the Malaysian Mathematical Sciences Society*, vol. 38, no. 1, pp. 95–112, 2015.
- [8] M. B. Almatrafi, "Solutions structures for some systems of fractional difference equations," *Open Journal of Mathematical Analysis*, vol. 3, no. 1, pp. 51–61, 2019.
- [9] A. M. Alotaibi, M. S. M. Noorani, and M. A. El-Moneam, "On the asymptotic behavior of some nonlinear difference equations," *Journal of Computational Analysis and Applications*, vol. 26, pp. 604–627, 2019.
- [10] E. Chatterjee, E. A. Grove, Y. Kostrov, and G. Ladas, "On the trichotomy character of," *Journal of Difference Equations and Applications*, vol. 9, no. 12, pp. 1113–1128, 2003.
- [11] X. Yan and W. Li, "Global attractivity for a class of nonlinear difference equations," *Soochow J. Math.* vol. 29, no. 3, pp. 327–338, 2003.
- [12] X. Yang, W. Su, B. Chen, G. M. Megson, and D. J. Evans, "On the recursive sequence," *Applied Mathematics and Computation*, vol. 162, no. 3, pp. 1485–1497, 2005.
- [13] Y. Yazlik and M. Kara, "On a solvable system of difference equations of higher-order with period two coefficients," *Communications Faculty of Science University of Ankara Series A1-Mathematics and Statistics*, vol. 68, no. 2, pp. 1675–1693, 2019.
- [14] L. Zhang, G. Zhang, and H. Liu, "Periodicity and attractivity for a rational recursive sequence," *Journal of Applied Mathematics and Computing*, vol. 19, no. 1-2, pp. 191–201, 2005.

Research Article

On the Dynamics of a Discrete Fractional-Order Cournot–Bertrand Competition Duopoly Game

Abdulrahman Al-Khedhairi ¹, Abdelalim A. Elsadany ^{2,3} and Amr Elsonbaty ^{2,4}

¹Department of Statistics and Operations Research, College of Science, King Saud University, Riyadh, Saudi Arabia

²Mathematics Department, College of Science and Humanities Studies in Al-Kharj, Prince Sattam Bin Abdulaziz University, Al-Kharj 11942, Saudi Arabia

³Department of Basic Science, Faculty of Computers and Informatics, Suez Canal University, Ismailia 41522, Egypt

⁴Department of Engineering Mathematics and Physics, Faculty of Engineering, Mansoura University, Mansoura 35516, Egypt

Correspondence should be addressed to Abdelalim A. Elsadany; aelsadany1@yahoo.com

Received 7 July 2021; Accepted 13 November 2021; Published 7 February 2022

Academic Editor: Ali Ahmadian

Copyright © 2022 Abdulrahman Al-Khedhairi et al. This is an open access article distributed under the Creative Commons Attribution License, which permits unrestricted use, distribution, and reproduction in any medium, provided the original work is properly cited.

A discrete fractional-order Cournot–Bertrand competition duopoly game is introduced based on the fractional-order difference calculus of the Caputo operator. The model is designed when players can make long memory decisions. The local stability of equilibrium points is discussed for the proposed model. Some numerical simulations explore the model's bifurcation and chaos by employing bifurcation diagrams, phase portraits, maximal Lyapunov exponents, and time series. According to our findings, the fractional-order parameter has an effect on the game's stability and dynamics.

1. Introduction

Game theory is one of the most interesting and complex topics that many researchers are interested in understanding. Game theory is concerned with predicting results for strategic games in which participants, for example, two or more firms competing on the market, have incomplete information on the intentions of others. It is known that the game theory is relevant to the study of corporate behavior in oligopolistic markets, for example, the decisions that companies must make in terms of production and pricing levels, as well as the amount of money invested in research and development. The decision-making mechanism has an important role to play in the process of adjusting the production and profits of firms. Firms typically use one of the following to change their market growth: naïve learning expectation, adaptive learning expectation, limited learning rationality, and local learning approximation. Discrete oligopoly dynamics based on company profit maximizations have been considered [1–7]. Furthermore, these models have been utilized to examine the dynamic characteristics of

competitive markets, which has been classified as steady state, periodic, and chaotic [8–14].

Fractional calculus, particularly discrete fractional calculus, has attracted substantial interest in recent decades due to its extensive significance in a wide range of scientific disciplines, including complex systems with memory and heredity. Researchers turned their attention to a discrete fractional calculus and tried to develop a complete theoretical framework for this subject. This is due to the importance of this field in many real issues, such as discrete adaptive systems, biological growth systems, and digital engineering systems, all of which contain memory [15–20]. The discrete difference analogues of classical Caputo and Riemann derivatives have been introduced in [21]. In addition, advances have been made in the study of fractional finite difference equations and the inclusion of fractional difference equations [22–26]. Recently, the stability of fractional time systems in a variety of real-world problems has been investigated. These studies have shown that discrete fractional systems are more realistic to process real systems and have a rich dynamic compared to discrete systems with

integer-order. Many studies have studied continuous fractional differentiation representing the effects of economic memory that have been presented [27–30] and the references that exist in them as well. The fractional-order difference equation, which is a natural extension of the integer-order difference equation, has long-term memory effects that have been explored in a few studies [25, 31–36]. Recently, the fractional difference calculus was used in the Cournot duopoly game [37] and the Bertrand duopoly game [38]. This reflects the long-term memory effects of Cournot–Bertrand dynamic games in the fractional-order form for the game. Xin et al. [37, 38] investigated the dynamics of the Cournot and Bertrand games, which indicated the market evolution of the two enterprises.

This work is especially interested in the novel discrete fractional-order Cournot–Bertrand duopoly game, which is a modification of the Cournot–Bertrand duopoly game with integer-order [39]. We aim to extend this game to a fractional case and to study the dynamics of the game. As we know, fractional-order calculus is a general form of integer-order calculus, so it has a higher representation for phenomena with a long memory. It can be shown that the fractional differentiation parameter is a vital indicator of the bifurcation path and the chaos that is created and disappeared. We will investigate the dynamics of the discrete fractional-order Cournot–Bertrand duopoly game such as the stability, bifurcation, and chaos of the proposed game. To analyze complexity of the game, explicit stability criteria [40, 41], asymptotic stability criteria [42] and the local stability regions of the boundary and Nash equilibrium points are provided through numerical simulation. The dynamic behavior of the proposed game is illustrated through an exploratory investigation of equilibrium point stability and numerical simulation. In this work, we are analyzing a Cournot–Bertrand duopoly game similar to Wang and Ma [39], but using a discrete fractional calculus. The equilibrium point structure dynamic reflects economic

explanations for the proposed game’s market of two enterprises.

The work is organized as seen follows. Section 2 describes the market dynamics of two enterprises using a discrete fractional-order Cournot–Bertrand duopoly game. The Nash equilibrium local stability conditions are established in Section 3. Using numerical simulations, we investigate local bifurcations, maximal Lyapunov exponents, and phase portraits of complex dynamics in Section 4. Section 5 contains a summary of the findings as well as a few observations.

2. Preliminaries

In this section, some preliminaries about fractional-order difference calculus are introduced. On an arbitrary time scale, dynamic behaviors and applications of fractional difference models were investigated in the last decade where delta difference equation was used [40–43].

Assume that a sequence $u(n)$ is given, and the isolated time scale \aleph_a is represented in terms of real valued constant τ , i.e., $\{\tau, \tau + 1, \tau + 2, \dots\}$, such that $u: \aleph_\tau \rightarrow \mathbb{R}$. Also, the difference operator is denoted by Δ , where $\Delta u(n) = u(n + 1) - u(n)$. Then, we summarize some of the basic definitions related to discrete fractional calculus as follows.

Definition 1. For $\alpha > 0$, the fractional sum of order α is given by [21]

$$\Delta_\tau^{-\alpha} u(t) = \frac{1}{\Gamma(\alpha)} \sum_{m=\tau}^{t-\alpha} \frac{\Gamma(t-m)}{\Gamma(t-m-\alpha+1)} u(m), \quad t \in \aleph_{\tau+\alpha}. \tag{1}$$

Definition 2. The Caputo-like delta difference of order α is defined by [21, 42]

$${}^C \Delta_\tau^\alpha u(t) = \Delta_\tau^{-(n-\alpha)} \Delta^n u(t) = \frac{1}{\Gamma(n-\alpha)} \sum_{m=\tau}^{t-(n-\alpha)} \frac{\Gamma(t-m)}{\Gamma(t-m-n+\alpha+1)} \Delta^n u(m), \tag{2}$$

$$t \in \aleph_{\tau+\alpha}, n = [\alpha] + 1.$$

Theorem 1 (See [21, 40–43]). *In order to solve the delta fractional difference equation,*

$$\begin{cases} {}^C \Delta_\tau^\alpha u(t) = f(t + \alpha - 1, u(t + \alpha - 1)), \\ \Delta^k u(t) = u_k, n = [\alpha] + 1, \quad k = 0, 1, \dots, n - 1. \end{cases} \tag{3}$$

As a result, the corresponding discrete integral equation is

$$u(t) = u_0(t) + \frac{1}{\Gamma(\alpha)} \sum_{m=\tau+n-\alpha}^{t-\alpha} (t - \sigma(m))^{\alpha-1} f(m + \alpha - 1, u(m + \alpha - 1)), \quad t \in \aleph_{\tau+n}, \tag{4}$$

where

$$u_0(t) = \sum_{k=0}^{n-1} \frac{\Gamma(t - \tau + 1)}{k! \Gamma(t - \tau - k + 1)} \Delta^k u(t). \quad (5)$$

Remark 1. If $\tau = 0$, we rewrite discrete integral equation in the following numerical form:

$$u(n) = u_0(t) + \frac{1}{\Gamma(\alpha)} \sum_{m=1}^n \frac{\Gamma(n - m + \alpha)}{\Gamma(n - m + 1)} f(u(m - 1)). \quad (6)$$

Theorem 2 (See [40–42]). *The linear discrete-time fractional-order system is*

$${}^C \Delta_t^\alpha U(t) = GU(t + \alpha - 1), \quad (7)$$

where $U(t) = (u_1(t), u_2(t), \dots, u_n(t))^T$, $0 < \alpha \leq 1$, $G \in \mathbb{R}^{n \times n}$, and $\forall t \in \mathbb{N}_{\tau+1-\alpha}$. *The zero equilibrium of system (10) is asymptotically stable if*

$$\lambda \in \left\{ z \in \mathbb{C}: |z| < \left(2 \cos \frac{|\arg z| - \pi}{2 - \alpha} \right)^\alpha, |\arg z| > \frac{\alpha\pi}{2} \right\}, \quad (8)$$

for all the eigenvalues λ of matrix G .

3. Discrete Fractional-Order Cournot–Bertrand Duopoly Game

According to traditional oligopoly models [1, 6], firms compete in the same strategic variable, such as output (Cournot) or price (Bertrand). A hybrid model, commonly known as the Cournot–Bertrand model [6, 39], permits certain enterprises to compete in output, while others compete in pricing. Real-world market observations that match Cournot–Bertrand behavior have bolstered the model’s validity and rapidly growing literature on advancements and applications. Long-term memory effects in dynamic oligopoly games are economically significant [34, 37, 38]. Therefore, we introduce the novel discrete fractional-order Cournot–Bertrand duopoly game, which is a modification of the Cournot–Bertrand duopoly game with integer order. As a consequence, it has a better representation of phenomena with a long memory in oligopoly game. The main goal is to establish out how the fractal parameter affects game dynamics including stability, bifurcation, and chaos.

We suggest a simple Cournot–Bertrand duopoly common oligopoly game [39]. Two enterprises, denoted by the letters $i = 1, 2$, produced differentiated goods with perfect replacements and set their product pricing based on the same market rule. Assume that $p_i(t)$ and $q_i(t)$ denote the goods price and quantity output of firm i for the period $t \in \mathbb{Z}^+$. The inverse demand functions for a variety of products 1 and 2 originate from the representative consumer maximization of the following utility function [39]:

$$U(q_1, q_2) = q_1 + q_2 - \frac{1}{2}(q_1^2 + 2dq_1q_2 + q_2^2), \quad (9)$$

subjected to restrictions on the budget $p_1q_1 + p_2q_2 = M$. Then, the inverse demand functions is defined as follows:

$$\begin{cases} p_1 = 1 - q_1 - dq_2, \\ p_2 = 1 - q_2 - dq_1, \end{cases} \quad (10)$$

where p_1 and p_2 represent the pricing of firm 1’s and firm 2’s items, respectively, and q_1 and q_2 are the quantities of products of company 1 and company 2. The parameter $d \in [0, 1]$ is the product differentiation between two firms. Products are homogeneous goods when $d = 1$, and each firm has a monopoly case when $d = 0$. The demand system can be written in two strategic variables q_1 and p_2 .

$$\begin{cases} p_1 = 1 - d - (1 - d^2)q_1 + dp_2, \\ q_2 = 1 - p_2 - dq_1. \end{cases} \quad (11)$$

Consider that the two companies have the same unit cost $c > 0$ and that the cost function has the same linear form:

$$C_i(q_i) = cq_i, i = 1, 2. \quad (12)$$

Thus, the profit functions for firms are given by

$$\begin{cases} \pi_1 = (1 - d - (1 - d^2)q_1 + dp_2 - c)q_1, \\ \pi_2 = (p_2 - c)(1 - p_2 - dq_1). \end{cases} \quad (13)$$

In the classical dynamical Cournot–Bertrand duopoly game, to decide the corresponding profit-maximizing, every player erroneously believes that its rival’s pricing in period $(t + 1)$ is the same as in period (t) . Therefore, this type of game does not have a long memory effect. The traditional game will be introduced using discrete fractional-order calculus, and the two players will make decisions using a new dynamic adjustment mechanism with long memory and local marginal profit expectation. Thus, the marginal profit of two players is as follows [39]:

$$\begin{cases} \frac{\partial \pi_1}{\partial q_1} = ((1 - d - 2(1 - d^2)q_1 + dp_2) - c), \\ \frac{\partial \pi_2}{\partial p_2} = (1 + c - 2p_2 - dq_1). \end{cases} \quad (14)$$

Assume that the two businesses have limited information about the market demand function and also their price decision is based on a dynamic adjustment process with limited rationality and a long-term memory effect of marginal profit. In the next step, the firm decides to raise (reduce) the price of its product based on if the long-term marginal profit is greater (less) than zero. As a result, we utilize the dynamic adjustment process for the Cournot–Bertrand game as follows:

$$\begin{cases} \Delta^\alpha q_1 = \nu_1 q_1 (t + \alpha - 1) \frac{\partial \pi_1}{\partial q_1}, \\ \Delta^\alpha p_2 = \nu_2 p_2 (t + \alpha - 1) \frac{\partial \pi_2}{\partial p_2}, \end{cases} \quad (15)$$

where ν_i is the speed of adjustment of firm $i, i = 1, 2$ and $\alpha \in (0, 1)$ denotes a fractional-order number, indicating the

long-term memory effect. Thus, the discrete fractional-order Cournot–Bertrand duopoly game is as follows:

$$\begin{cases} \Delta^\alpha q_1 = \nu_1 q_1 (t + \alpha - 1) (1 - c - d + d p_2 (t + \alpha - 1) - 2 q_1 (t + \alpha - 1) + 2 d^2 q_1 (t + \alpha - 1)), \\ \Delta^\alpha p_2 = \nu_2 p_2 (t + \alpha - 1) (1 + c - 2 p_2 (t + \alpha - 1) - d q_1 (t + \alpha - 1)). \end{cases} \quad (16)$$

Remark 2. When $\alpha = 1$, the model (16) devolves to the Wang-Ma model [39]:

$$\begin{cases} q_1 (t + 1) = q_1 (t) + \nu_1 q_1 (t) (1 - c - d + d p_2 (t) - 2 q_1 (t) + 2 d^2 q_1 (t)), \\ p_2 (t + 1) = p_2 (t) + \nu_2 p_2 (t) (1 + c - 2 p_2 (t) - d q_1 (t)). \end{cases} \quad (17)$$

We will show that the model game parameters, especially the long-term memory effect, have an effect on the long-term dynamic response of our novel game when compared to the Wang-Ma game [39].

In the next sections, several theoretical features corresponding to game (16) are investigated.

4. The Equilibrium Points and Their Local Stability

We solve the following equation to find the equilibrium points of game system (16):

$$\begin{cases} (1 - c - d + d p_2 (t) - 2 q_1 (t) + 2 d^2 q_1 (t)) = 0, \\ (1 + c - 2 p_2 (t) - d q_1 (t)) = 0. \end{cases} \quad (18)$$

Their four equilibria are $E_0 = (0, 0)$, $E_1 = (0, 1 + c/2)$, $E_2 = (1 - c - d/2(1 - d^2), 0)$, and $E_* = (2 - 2c - d + c d/4 - 3d^2, 2 + 2c - d + c d - d^2 - 2cd^2/4 - 3d^2)$. In economics, its equilibria mean

- (i) The equilibrium E_0 is trivial equilibrium point
- (ii) The equilibrium point E_1 implies that the best quantity of the first player is $q_1^* = 0$ if the second

player sets its optimal product price $p_2^* = 1 + c/2$. Likewise, the second player's best price is $p_2^* = 1 + c/2$ if the player uses a zero-price approach. Clearly, E_1 is a border equilibrium point that corresponds to the pure monopoly.

- (iii) The E_2 equilibria indicates that the best quantity of the first player is $q_1^* = 1 - c - d/2(1 - d^2)$ if the second company determines the best good price $p_2^* = 0$. Likewise, the first company's best pricing is $q_1^* = 1 - c - d/2(1 - d^2)$ if the company uses a zero-price approach. Clearly, E_2 is a border equilibrium point.
- (iv) The equilibrium E_* indicates two enterprises will preserve their equilibrium quantity and pricing jointly since no enterprise can gain an advantage by deviating unilaterally from its own equilibrium. Clearly, the point E_* is a Nash equilibrium. The complexity of system (16) will be explored. First, the Jacobian matrix of system (16) is computed at a given equilibrium point $\bar{E} = (q_1^*, p_2^*)$, and it can be expressed as

$$J(q_1, p_2) = \begin{pmatrix} \nu_1(1 - c - d + d p_2^* + 4(d^2 - 1)q_1^*) & \nu_1 d q_1^* \\ -\nu_2 d p_2^* & \nu_2(1 + c - 4p_2^* - d q_1^*) \end{pmatrix}. \quad (19)$$

Then, the following theorems are presented to clarify linear stability for each equilibrium point in the model.

The trivial equilibrium point E_0 is unstable.

Proof. The Jacobian matrix's eigenvalues at E_0 can be demonstrated to be $(\nu_2(1 + c), \nu_1(1 - c - d))$, which indicate that one of them is always positive, and thus, the conditions of asymptotic stability in Theorem 2 are not satisfied. \square

The equilibrium point E_1 is asymptotically stable if

$$\begin{aligned} \nu_1(cd + 2 - 2c - d) < 0, \nu_2(1 + c) \\ < 2^\alpha, |\nu_1(cd + 2 - 2c - d)| < 2^{\alpha+1}. \end{aligned} \quad (20)$$

Proof. The eigenvalues of Jacobian matrix at E_1 are $(-\nu_2(1 + c), 1/2\nu_1(c d + 2 - 2c - d))$, which means that the conditions of asymptotic stability in Theorem 2 are satisfied

if the second eigenvalue has a negative sign, and also, the modulus of the two eigenvalues is bounded by 2^α and $2^{\alpha+1}$, respectively. Figure 1 shows stability regions in some three and two-dimensional spaces of model's parameters, whereas

$$\begin{aligned} \nu_1(c+d-1) < 0, \nu_2(2cd^2 - cd - 2c + d^2 + d - 2) > 0, \quad 0 < d < 1, \\ |\nu_2(c+d-1)| < 2^\alpha, \\ \nu_2(2cd^2 - cd - 2c + d^2 + d - 2) < 2^{\alpha+1}(1-d^2). \end{aligned} \tag{21}$$

Proof. The eigenvalues of Jacobian matrix at E_2 are $(\nu_1(c+d-1), \nu_2(2cd^2 - cd - 2c + d^2 + d - 2)/2(d^2 - 1))$, which means that the conditions of asymptotic stability in Theorem 2 are satisfied if the two eigenvalues have negative signs, and also, the modulus of the two eigenvalues is bounded by 2^α and $2^{\alpha+1}(1-d^2)$, respectively. \square

However, detailed numerical examinations in space of promoters show that the aforementioned conditions cannot be simultaneously achieved at feasible values of parameters, and therefore, due to the impossibility of numerically satisfying the above conditions, the equilibrium point E_2 is unstable.

Finally, the Nash equilibrium point E_* has long complicated expressions for its associated eigenvalues which

Figure 2 shows the resulting time series when the values of parameters are selected in stable regions of E_1 .

The equilibrium E_2 is asymptotically stable if and only if

\square renders numerical investigations of regions of stability inevitable. Figure 3 shows stability regions in some three and two-dimensional spaces of model's parameters, whereas Figure 4 illustrates the resulting time series when the values of parameters are selected in stable regions of E_* .

5. Numerical Simulations

In this section, the complex dynamic features of the discrete fractional Cournot–Bertrand model (16) are investigated using various methods such as bifurcation diagrams, phase portraits, and MLE. The effects of major model parameters are investigated. For the present fractional discrete model (16) using theorem (4), the system (16) can be numerically rewritten as follows:

$$\begin{cases} q_1(n) = q_1(0) + \frac{1}{\Gamma(\alpha)} \sum_{i=1}^n \frac{\Gamma(n-i+\alpha)}{\Gamma(n-i+1)} \nu_1 q_1(i-1) ((1-c-d+dp_2(i-1) - 2q_1(i-1) + 2d^2 q_1(i-1))), \\ p_2(n) = p_2(0) + \frac{1}{\Gamma(\alpha)} \sum_{i=1}^n \frac{\Gamma(n-i+\alpha)}{\Gamma(n-i+1)} \nu_2 p_2(i-1) (1+c-2p_2(i-1) - dq_1(i-1)). \end{cases} \tag{22}$$

The initial point $(q_1(0), p_2(0)) = (0.2, 0.1)$ is used in the following simulations. In particular, the complicated dynamics exhibited by the model are examined via using the bifurcation diagram, phase portraits, and maximal Lyapunov exponent (MLE). The Lyapunov exponent for a one-dimensional map can be calculated by calculating the average value for perturbations from the trajectory over a time interval. The Lyapunov exponents for an n -dimensional mapping can be obtained using the eigenvalues of the product of Jacobian matrices for integer-order systems. In order to approximate the values of Lyapunov exponents of the discrete fractional model (16), the Jacobian matrix method which has been introduced by Wu and Baleanu [44] can be employed [45, 46]. In the following part, the numerical analysis will look at the effects of the model's main parameters, as well as the effects of long-term memory and adjustment speeds.

First, the influences of parameter ν_1 in integer-order and fractional-order cases are explored. Figure 5 shows bifurcation diagrams and MLE plots versus parameter ν_1 along with examples of phase portraits at some selected values of parameters.

Second, the influences of parameter ν_2 in integer-order and fractional-order cases are explored. Figure 6 shows bifurcation diagrams and MLE plots versus parameter ν_2 , along with examples of phase portraits at some selected values of parameters.

Third, the influences of parameter d in integer-order and fractional-order cases are explored. Figure 7 shows bifurcation diagrams and MLE plots versus parameter d along with examples of phase portraits at some selected values of parameters.

Finally, the effects of fractional-order α are explored. Figure 8 shows bifurcation diagrams and MLE plots versus parameter α along with examples of phase portraits at some selected values of parameters.

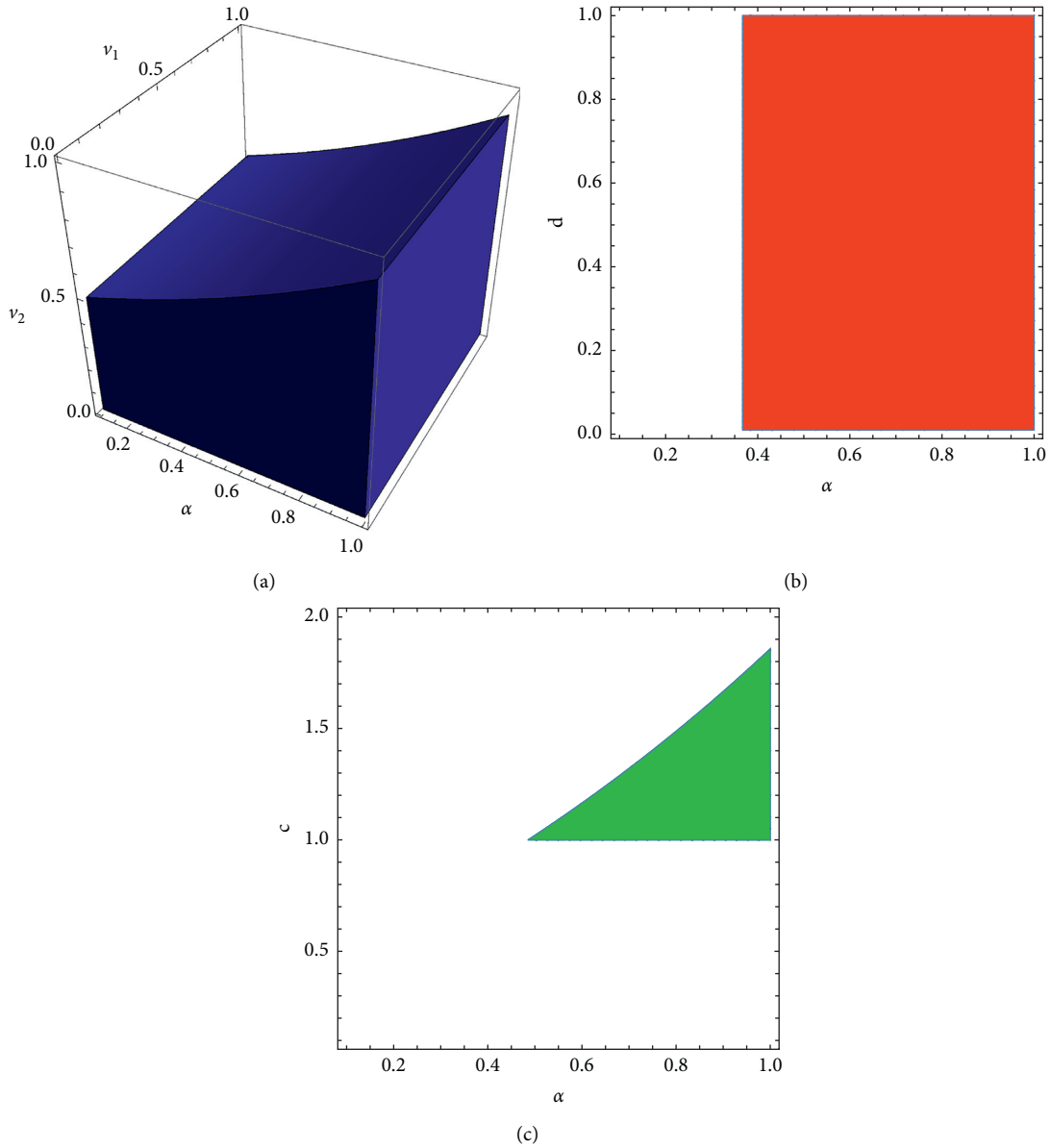


FIGURE 1: Stability regions of equilibrium point E_1 in some three and two-dimensional spaces of model's parameters when (a) $c = 1.15; d = 0.6$, (b) $c = 1.15; v_1 = 0.5; v_2 = 0.6$, and (c) $d = 0.5; v_1 = 0.7; v_2 = 0.7$.

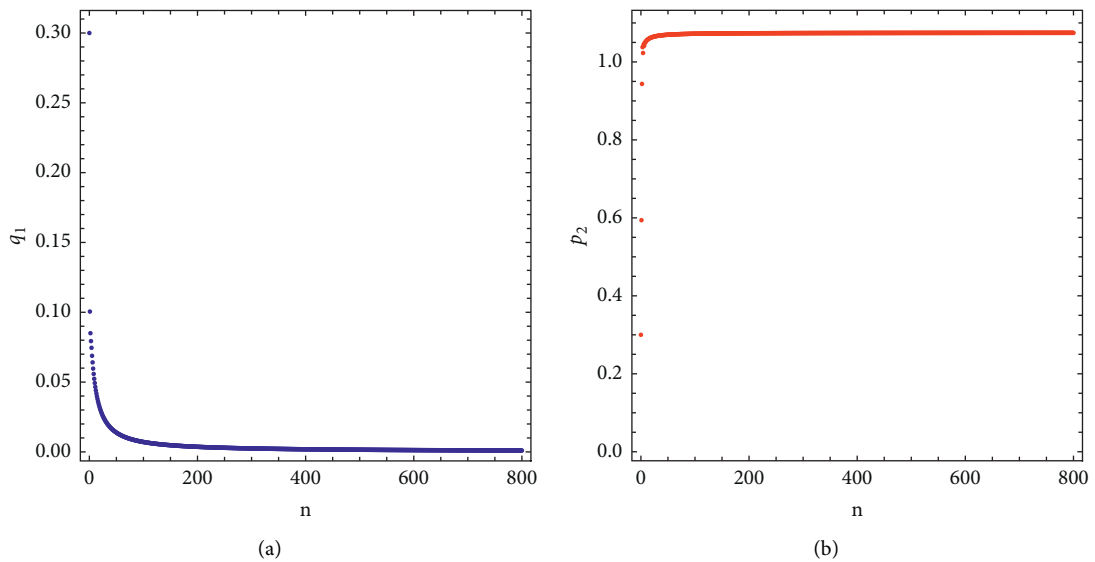


FIGURE 2: Time series of model (16) at $c = 1.15, d = 0.5, v_1 = 0.7, v_2 = 0.7$, and $\alpha = 0.9$.

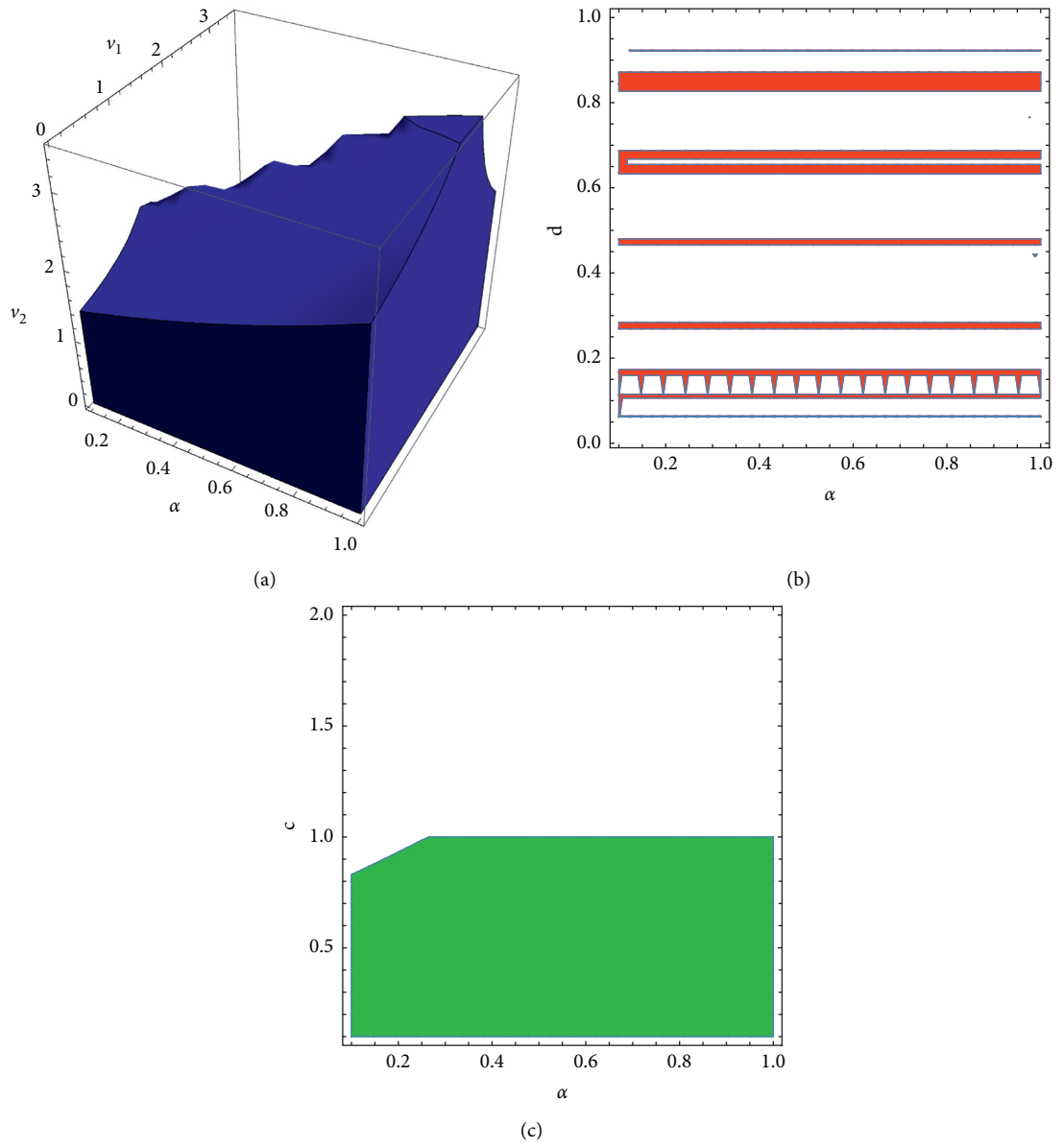


FIGURE 3: Stability regions of equilibrium point E_* in some three and two-dimensional spaces of model's parameters when (a) $c = 0.15; d = 0.8$, (b) $c = 1; v_1 = 0.4; v_2 = 0.7$, and (c) $d = 0.5; v_1 = 0.3; v_2 = 0.6$.

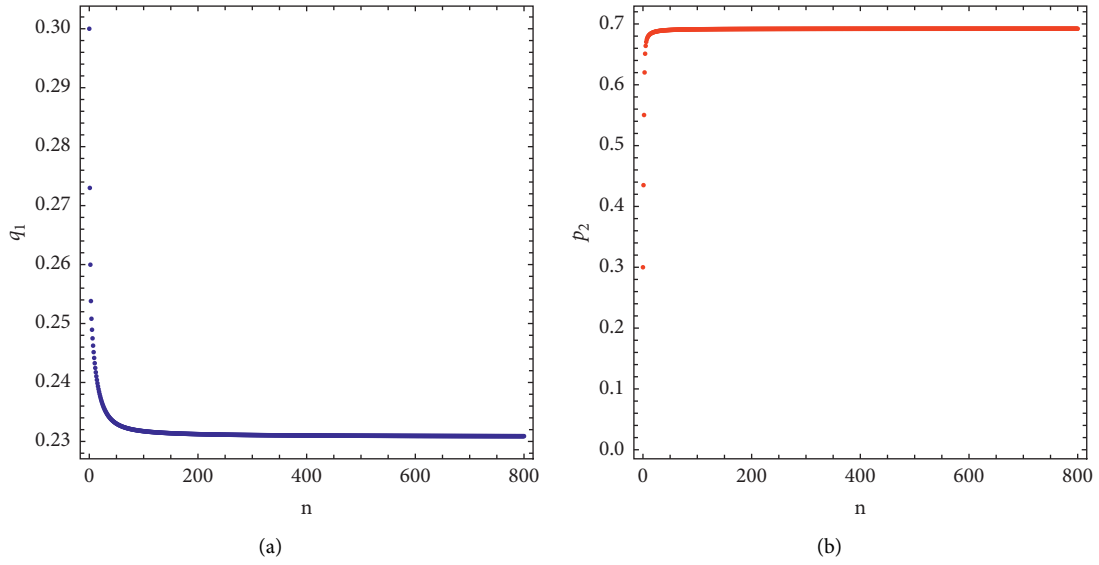


FIGURE 4: Time series of model (16) at $c = 0.5, d = 0.5, \nu_1 = 0.3, \nu_2 = 0.6,$ and $\alpha = 0.9$.

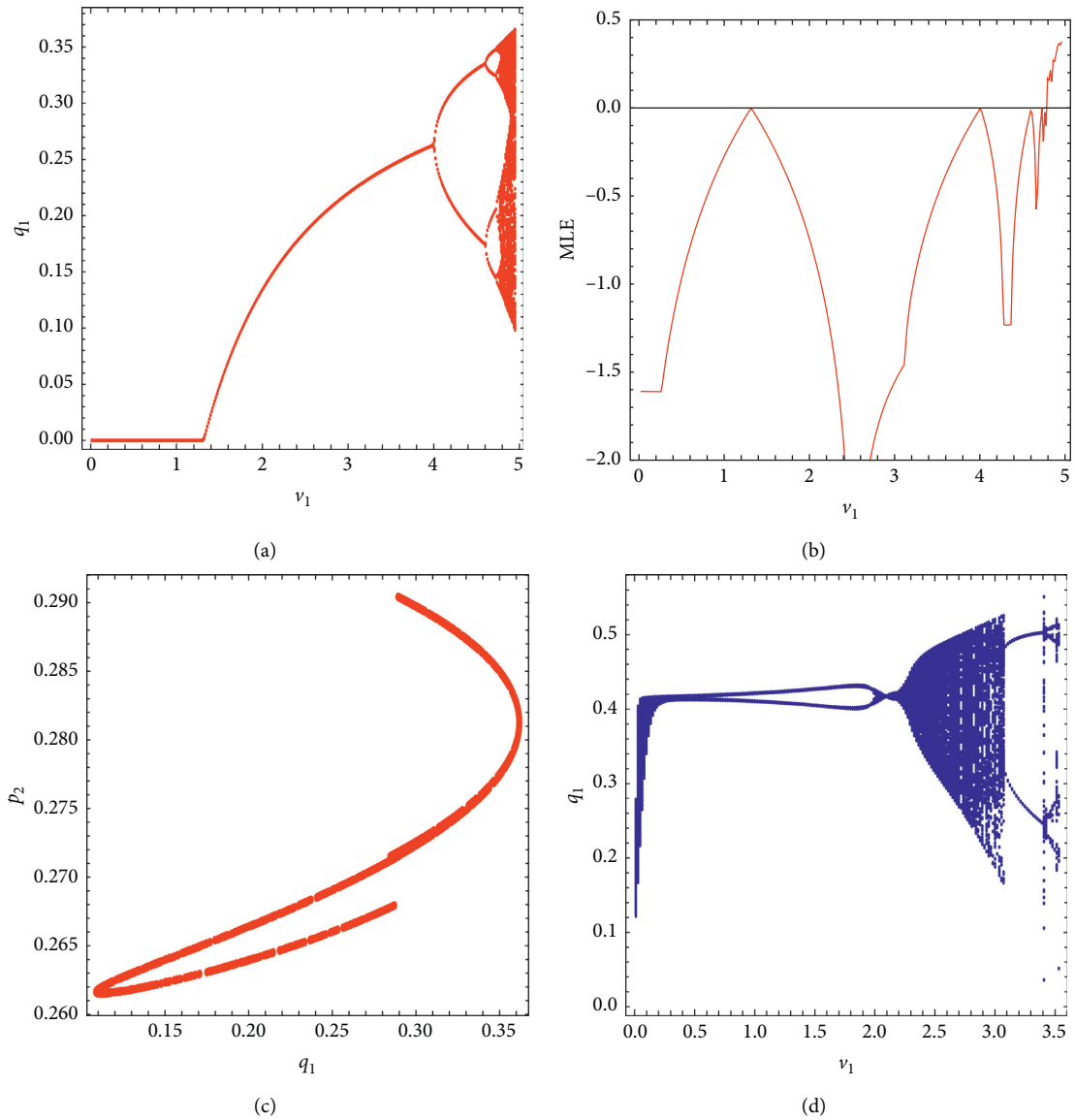


FIGURE 5: Continued.

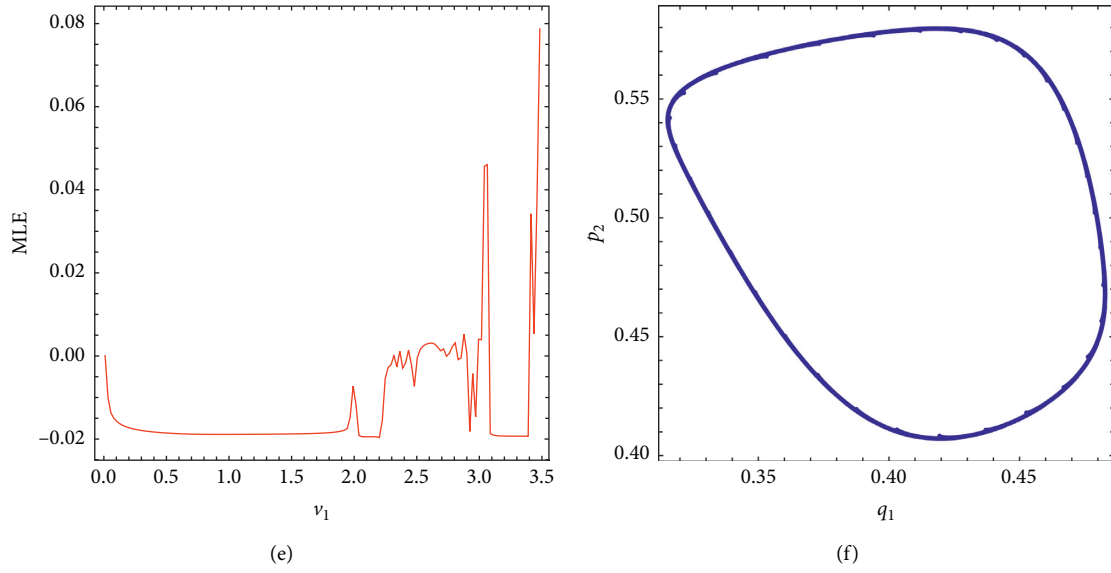


FIGURE 5: (a) Bifurcation diagram of system (16) vs. ν_1 at $c = 0.1; d = 0.2; \nu_2 = 2; \alpha = 1$. (b) MLE plot of system (16) vs. ν_1 at $c = 0.1; d = 0.2; \nu_2 = 2; \alpha = 1$. (c) Phase portrait of system (16) at $c = 0.1; d = 0.2; \nu_1 = 4.9; \nu_2 = 2; \alpha = 1$. (d)–(f) similar to (a)–(c) but for $\alpha = 0.95$.

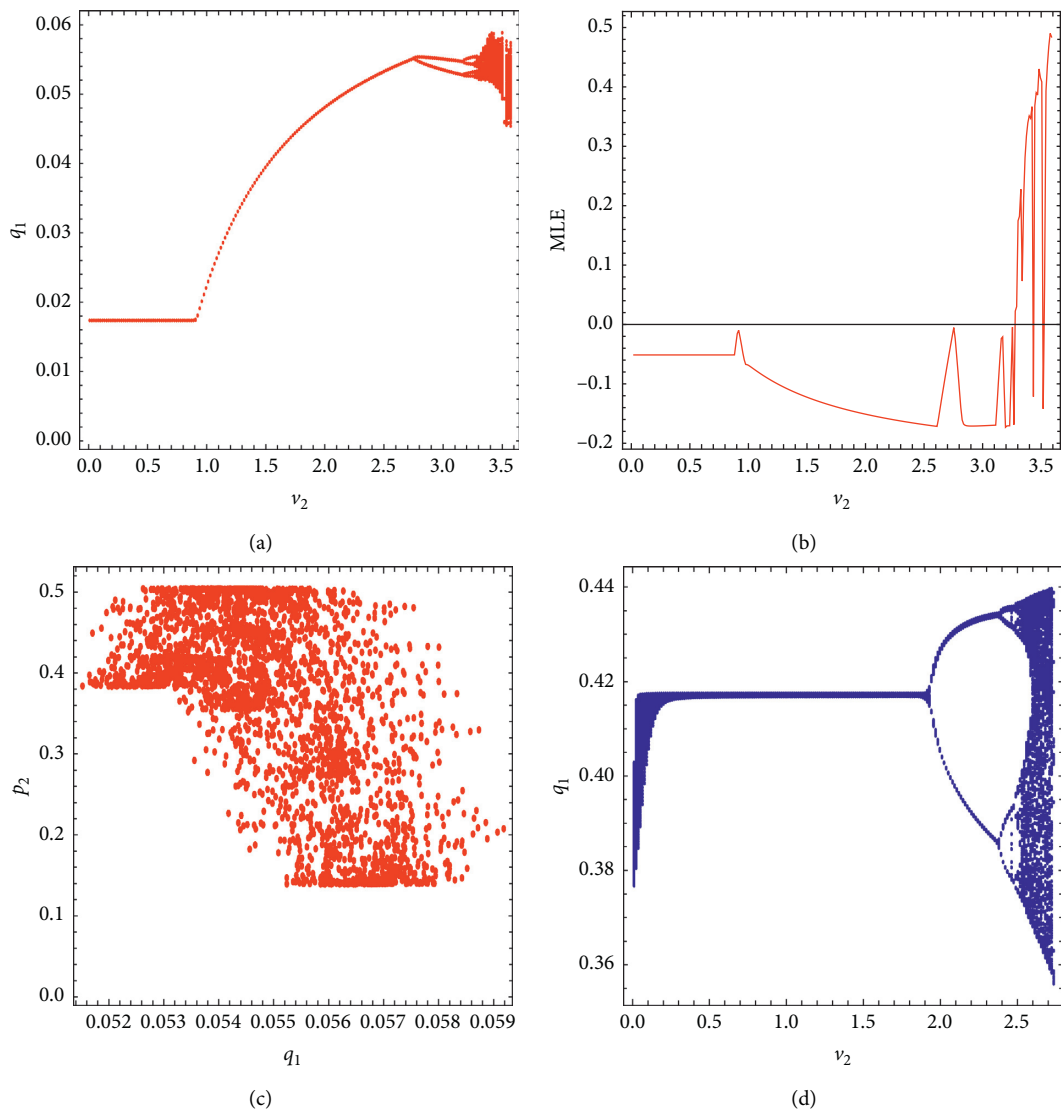


FIGURE 6: Continued.

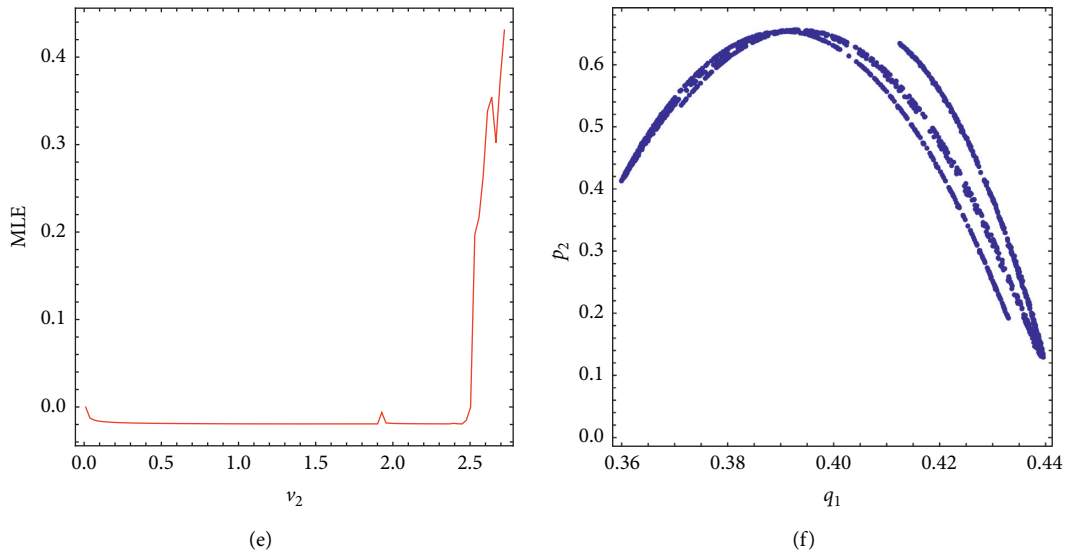


FIGURE 6: (a) Bifurcation diagram of system (16) vs. ν_2 at $c = 0.1; d = 0.2; \nu_1 = 1.5; \alpha = 1$. (b) MLE plot of system (16) vs. ν_2 at $c = 0.1; d = 0.2; \nu_1 = 1.5; \alpha = 1$. (c) Phase portrait of system (16) at $c = 0.1; d = 0.2; \nu_1 = 1.5; \nu_2 = 3.4; \alpha = 1$. (d)–(f) similar to (a)–(c) but for $\alpha = 0.95$.

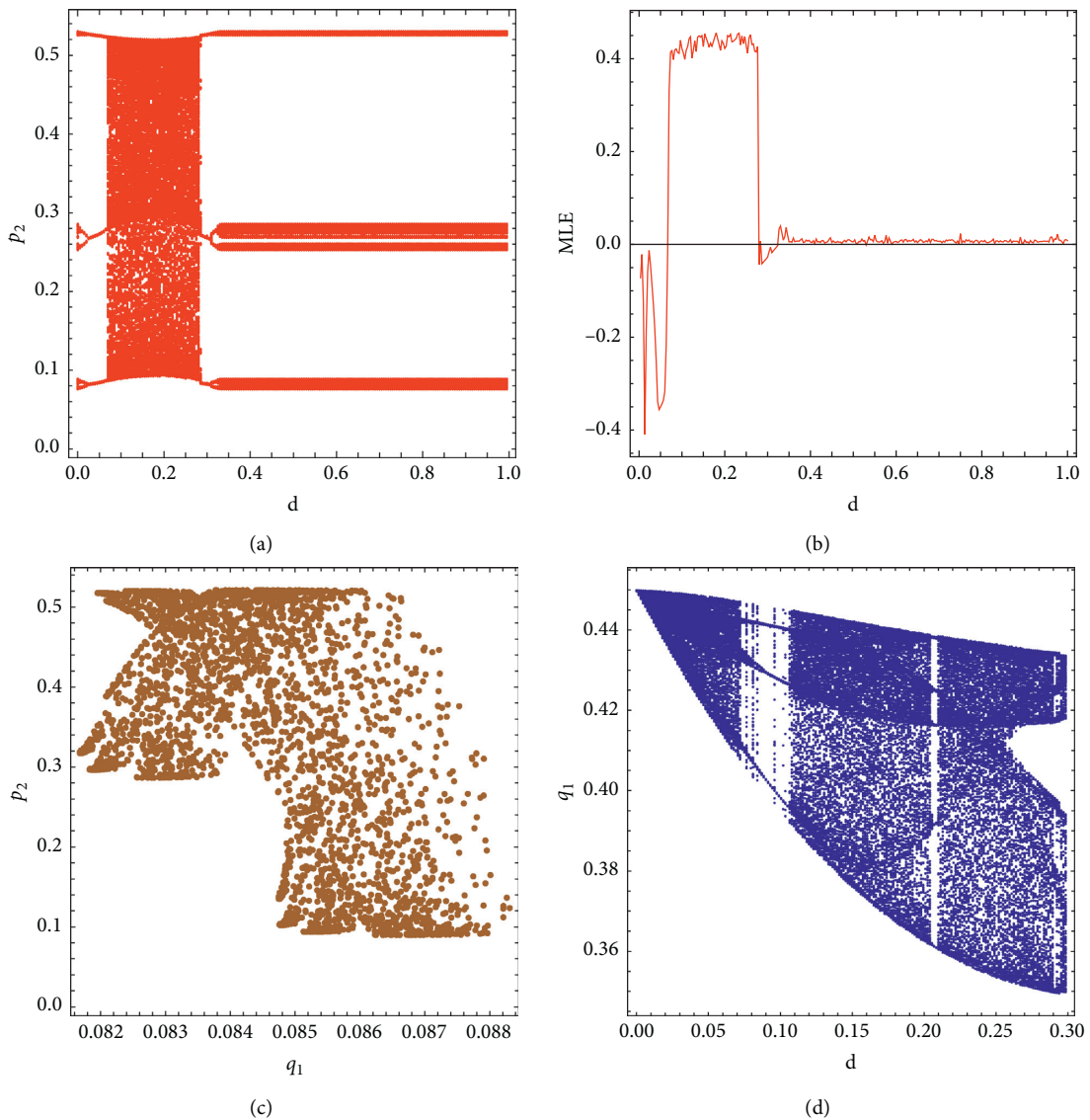


FIGURE 7: Continued.

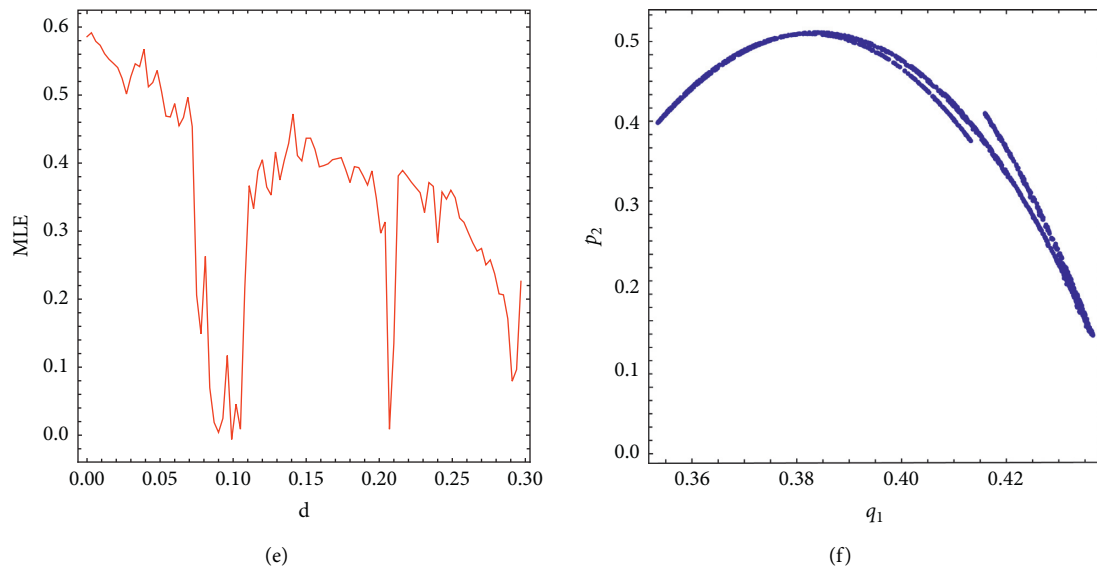


FIGURE 7: (a) Bifurcation diagram of system (16) vs. d at $c = 0.1; \nu_1 = 1.5; \nu_2 = 3.5; \alpha = 1$. (b) MLE plot of system (16) vs. d at $c = 0.1; \nu_1 = 1.5; \nu_2 = 3.5; \alpha = 1$. (c) Phase portrait of system (16) at $c = 0.1; d = 0.1; \nu_1 = 1.5; \nu_2 = 3.5; \alpha = 1$. (d)–(f) similar to (a)–(c) but for $\alpha = 0.95$.

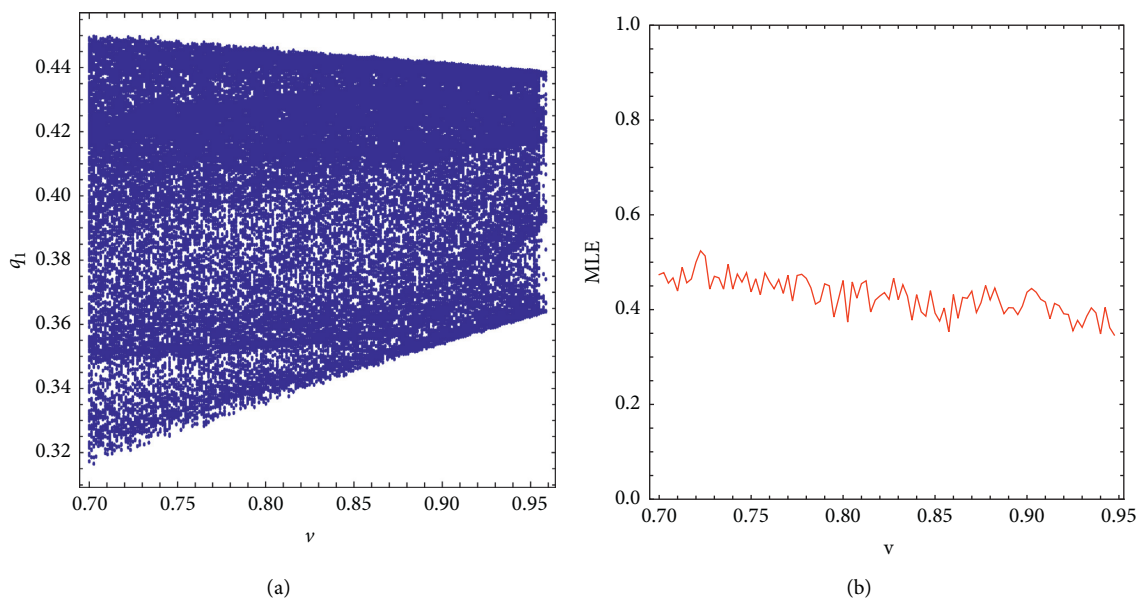


FIGURE 8: Continued.

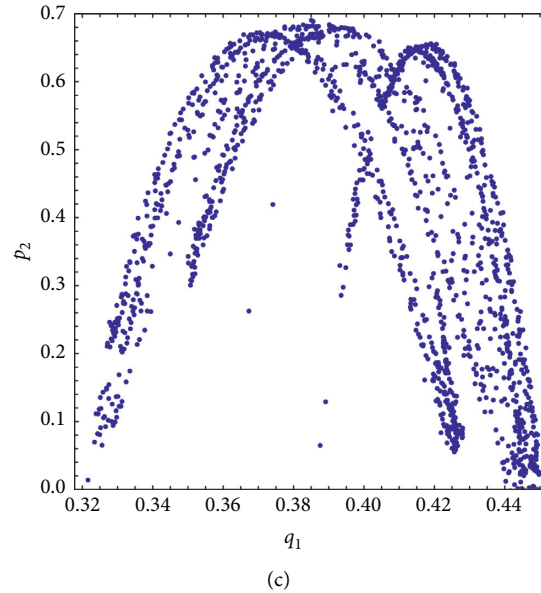


FIGURE 8: (a) Bifurcation diagram of system (16) vs. α at $c = 0.1; d = 0.2; \nu_1 = 1.5; \nu_2 = 2.67$. (b) MLE plot of system (16) vs. α at $c = 0.1; d = 0.2; \nu_1 = 1.5; \nu_2 = 2.67$. (c) Phase portrait of system (16) at $c = 0.1; d = 0.2; \nu_1 = 1.5; \nu_2 = 2.67; \alpha = 0.7$.

6. Conclusion

The new fractional-order Cournot–Bertrand game based on a long memory effect is proposed. The stability of the game’s equilibrium points, including the Nash equilibria, has been explored both qualitatively and numerically. Bifurcation, phase portraiture, time series, and maximal Lyapunov exponents’ diagrams have been used to analyze the complex dynamic characteristics of the proposed game. When we compared our new model to the Wang–Ma model [39], we found that the game parameters, especially the long-term memory influence, had an effect on the long-term dynamic response of our novel model. This is important for understanding the performance of the duopoly game with the long-term memory effect. According to our findings, the Cournot–Bertrand duopoly game with the long-term memory effect is more efficient than the duopoly game without long-term memory impact from economic viewpoint. As a consequence, we advise researchers to investigate the competitive games of long-term memory impact further.

Data Availability

No data were used to support this study.

Conflicts of Interest

The authors declare that they have no conflicts of interest.

Acknowledgments

The authors would like to express sincere gratitude to all referees and editors for their valuable comments and constructive suggestion to the earlier version of this study. They

would also like to thank the Deanship of Scientific Research at Prince Sattam bin Abdulaziz University, Al-Kharj, Saudi Arabia.

References

- [1] T. Puu, “Chaos in duopoly pricing,” *Chaos, Solitons & Fractals*, vol. 1, no. 6, pp. 573–581, 1991.
- [2] G. I. Bischi and A. Naimzada, “Global analysis of a dynamic duopoly game with bounded rationality,” in *Advances in Dynamic Games and Applications*, J. A. Filar, V. Gaitsgory, and K. Mizukami, Eds., vol. 5, Basel, Switzerland, Birkhauser, 2000.
- [3] G. I. Bischi and M. Kopel, “Equilibrium selection in a nonlinear duopoly game with adaptive expectations,” *Journal of Economic Behavior & Organization*, vol. 46, no. 1, pp. 73–100, 2001.
- [4] A. Agliari, L. Gardini, and T. Puu, “Global bifurcations of basins in a triopoly game,” *International Journal of Bifurcation and Chaos*, vol. 12, no. 10, pp. 2175–2207, 2002.
- [5] H. N. Agiza and A. A. Elsadany, “Nonlinear dynamics in the cournot duopoly game with heterogeneous players,” *Physica A: Statistical Mechanics and Its Applications*, vol. 320, pp. 512–524, 2003.
- [6] G. I. Bischi, C. Chiarella, M. Kopel, and F. Szidarovszky, *Nonlinear Oligopolies: Stability and Bifurcations*, Springer Science & Business Media, Berlin, Germany, 2009.
- [7] H. N. Agiza and A. A. Elsadany, “Chaotic dynamics in nonlinear duopoly game with heterogeneous players,” *Applied Mathematics and Computation*, vol. 149, no. 3, pp. 843–860, 2004.
- [8] S. Askar, “The rise of complex phenomena in Cournot duopoly games due to demand functions without inflection points,” *Communications in Nonlinear Science and Numerical Simulation*, vol. 19, no. 6, pp. 1918–1925, 2014.
- [9] E. Ahmed, G. A. Ashry, and S. S. Askar, “On multi-objective optimization and game theory in production management,”

- International Journal of Nonlinear Science*, vol. 24, pp. 29–33, 2017.
- [10] L. Cerboni Baiardi and A. K. Naimzada, “An oligopoly model with rational and imitation rules,” *Mathematics and Computers in Simulation*, vol. 156, pp. 254–278, 2019.
- [11] A. Ibrahim, “Local stability condition of the equilibrium of a constraint profit maximization duopoly model,” *AIP Conference Proceedings*, vol. 2138, Article ID 030020, 2019.
- [12] J. Andaluz, A. A. Elsadany, and G. Jarne, “Dynamic Cournot oligopoly game based on general isoelastic demand,” *Nonlinear Dynamics*, vol. 99, no. 2, pp. 1053–1063, 2020.
- [13] S. S. Askar and A. Al-Khedhairi, “Dynamic investigations in a duopoly game with price competition based on relative profit and profit maximization,” *Journal of Computational and Applied Mathematics*, vol. 367, Article ID 112464, 2020.
- [14] W. Zhou, Y. Cao, A. Elsonbaty, A. A. Elsadany, and T. Chu, “Bifurcation analysis of a bounded rational duopoly game with consumer surplus,” *International Journal of Bifurcation and Chaos*, vol. 31, no. 7, Article ID 2150097, 2021.
- [15] I. Podlubny, *Fractional Differential Equations: An Introduction to Fractional Derivatives, Fractional Differential Equations, to Methods of Their Solution and Some of Their Applications*, Elsevier, Amsterdam, Netherlands, 1999.
- [16] A. A. Kilbas, H. M. Srivastava, and J. J. Trujillo, *Theory and Applications of Fractional Differential Equations*, Elsevier, Amsterdam, Netherlands, 2006.
- [17] I. Petras, *Fractional-order Nonlinear Systems: Modeling, Analysis and Simulation*, Springer Science Business Media, Berlin, Germany, 2011.
- [18] C. Goodrich and A. C. Peterson, *Discrete Fractional Calculus*, Springer, Berlin, Germany, 2015.
- [19] P. Ostalczyk, *Discrete Fractional Calculus: Applications in Control and Image Processing*, World Scientific, Singapore, 2015.
- [20] H. Sun, Y. Zhang, D. Baleanu, W. Chen, and Y. Chen, “A new collection of real world applications of fractional calculus in science and engineering,” *Communications in Nonlinear Science and Numerical Simulation*, vol. 64, pp. 213–231, 2018.
- [21] T. Abdeljawad, “On Riemann and caputo fractional differences,” *Computers & Mathematics with Applications*, vol. 62, no. 3, pp. 1602–1611, 2011.
- [22] A. E. M. El-Misiery and E. Ahmed, “On a fractional model for earthquakes,” *Applied Mathematics and Computation*, vol. 178, no. 2, pp. 207–211, 2006.
- [23] K. Diethelm, “A fractional calculus based model for the simulation of an outbreak of dengue fever,” *Nonlinear Dynamics*, vol. 71, no. 4, pp. 613–619, 2013.
- [24] T. Abdeljawad, S. Banerjee, and G. C. Wu, “Discrete tempered fractional calculus for new chaotic systems with short memory and image encryption,” *Optik*, vol. 218, Article ID 163698, 2020.
- [25] L.-L. Huang, J. H. Park, G.-C. Wu, and Z.-W. Mo, “Variable-order fractional discrete-time recurrent neural networks,” *Journal of Computational and Applied Mathematics*, vol. 370, Article ID 112633, 2020.
- [26] Y. Li, C. Sun, H. Ling, A. Lu, and Y. Liu, “Oligopolies price game in fractional order system,” *Chaos, Solitons & Fractals*, vol. 132, Article ID 109583, 2020.
- [27] W.-C. Chen, “Nonlinear dynamics and chaos in a fractional-order financial system,” *Chaos, Solitons & Fractals*, vol. 36, no. 5, pp. 1305–1314, 2008.
- [28] Z. Wang, X. Huang, and G. Shi, “Analysis of nonlinear dynamics and chaos in a fractional order financial system with time delay,” *Computers & Mathematics with Applications*, vol. 62, no. 3, pp. 1531–1539, 2011.
- [29] V. E. Tarasov, “No nonlocality. no fractional derivative,” *Communications in Nonlinear Science and Numerical Simulation*, vol. 62, pp. 157–163, 2018.
- [30] A. Yousefpour, H. Jahanshahi, J. M. Munoz-Pacheco, S. Bekiros, and Z. Wei, “A fractional-order hyper-chaotic economic system with transient chaos,” *Chaos, Solitons & Fractals*, vol. 130, Article ID 109400, 2020.
- [31] G. C. Wu and D. Baleanu, “Discrete fractional logistic map and its chaos,” *Nonlinear Dynamics*, vol. 75, no. 1–2, pp. 283–287, 2014.
- [32] S. He, S. Banerjee, and B. Yan, “Chaos and symbol complexity in a conformable fractional-order memcapacitor system,” *Complexity*, vol. 2018, pp. 1–15, Article ID 4140762, 2018.
- [33] L. Yuan, S. Zheng, and Z. Alam, “Dynamics analysis and cryptographic application of fractional logistic map,” *Nonlinear Dynamics*, vol. 96, no. 1, pp. 615–636, 2019.
- [34] A. Al-Khedhairi, “Differentiated Cournot duopoly game with fractional-order and its discretization,” *Engineering Computations*, vol. 36, no. 3, pp. 781–806, 2019.
- [35] A.-A. Khennaoui, A. Ouannas, S. Bendoukha, G. Grassi, R. P. Lozi, and V.-T. Pham, “On fractional-order discrete-time systems: chaos, stabilization and synchronization,” *Chaos, Solitons & Fractals*, vol. 119, pp. 150–162, 2019.
- [36] L.-L. Huang, G.-C. Wu, D. Baleanu, and H.-Y. Wang, “Discrete fractional calculus for interval-valued systems,” *Fuzzy Sets and Systems*, vol. 404, pp. 141–158, 2021.
- [37] B. Xin, W. Peng, and Y. Kwon, “A discrete fractional-order Cournot duopoly game,” *Physica A: Statistical Mechanics and Its Applications*, vol. 558, Article ID 124993, 2020.
- [38] B. Xin, F. Cao, W. Peng, and A. A. Elsadany, “A Bertrand duopoly game with long-memory effects,” *Complexity*, vol. 2020, Article ID 2924169, 7 pages, 2020.
- [39] H. Wang and J. Ma, “Complexity analysis of a Cournot-Bertrand duopoly game model with limited information,” *Discrete Dynamics in Nature and Society*, vol. 2013, Article ID 287371, 6 pages, 2013.
- [40] J. Čermák, I. Györi, and L. Nechvátal, “On explicit stability conditions for a linear fractional difference system,” *Fractional Calculus and Applied Analysis*, vol. 18, p. 651, 2015.
- [41] D. Mozyrska and M. Wyrwas, “Explicit criteria for stability of fractional h -difference two-dimensional systems,” *International Journal of Dynamics and Control*, vol. 5, no. 1, pp. 4–9, 2017.
- [42] R. Abu-Saris and Q. Al-Mdallal, “On the asymptotic stability of linear system of fractional-order difference equations,” *Fractional Calculus and Applied Analysis*, vol. 16, no. 3, pp. 613–629, 2013.
- [43] F. Chen, X. Luo, and Y. Zhou, “Existence results for nonlinear fractional difference equation,” *Advances in Difference Equations*, vol. 2011, Article ID 713201, 2010.
- [44] G. C. Wu and D. Baleanu, “Jacobian matrix algorithm for Lyapunov exponents of the discrete fractional maps,” *Communications in Nonlinear Science and Numerical Simulation*, vol. 22, no. 1–3, pp. 95–100, 2015.
- [45] A. Ouannas, A.-A. Khennaoui, S. Momani, and V.-T. Pham, “The discrete fractional duffing system: chaos, 0-1 test, C0 complexity, entropy, and control,” *Chaos: An Interdisciplinary Journal of Nonlinear Science*, vol. 30, no. 8, Article ID 083131, 2020.
- [46] A. Elsonbaty and A. A. Elsadany, “On discrete fractional-order Lotka-Volterra model based on the Caputo difference discrete operator,” *The Mathematical Scientist*, 2021.

Research Article

Bifurcation Analysis of a Discrete Food Chain Model with Harvesting

Abdul Qadeer Khan  and Shahid Mehmood Qureshi

Department of Mathematics, University of Azad Jammu and Kashmir, Muzaffarabad 13100, Pakistan

Correspondence should be addressed to Abdul Qadeer Khan; abdulqadeerkhan1@gmail.com

Received 17 May 2021; Revised 10 August 2021; Accepted 20 August 2021; Published 14 October 2021

Academic Editor: Baogui Xin

Copyright © 2021 Abdul Qadeer Khan and Shahid Mehmood Qureshi. This is an open access article distributed under the Creative Commons Attribution License, which permits unrestricted use, distribution, and reproduction in any medium, provided the original work is properly cited.

We explore existence of fixed points, topological classifications around fixed points, existence of periodic points and prime period, and bifurcation analysis of a three-species discrete food chain model with harvesting. Finally, theoretical results are numerically verified.

1. Introduction

Many different types of interactions exist in nature between various species of organisms on this planet Earth and are studied under the discipline of ecology. Ecological interactions are most fundamental part in biology which determines community structure and development. Not all interactions are positive, some are negative also. One of the examples of negative correlation is ammensalism. Ammensalism is a type of ecological interactions between the members of two different species in which one is harmed, destroyed, or inhabited by the member of another species, while the other remains unaffected, neither harmed nor benefitted. It is a type of competitive behavior among different species and is frequently used to refer to asymmetrical competitive association. Research in the field of ecology draws the attention of several mathematicians such as Lotka [1] and Volterra [2]. Nowadays, ecologist and mathematician jointly contributed to the growth of this area of knowledge. Recently, many researchers have investigated the dynamical properties of discrete-time ecological models such as prey-predation, competitions, neutralism, and mutualism by studying fixed points, local and global attractivity, bounded, existence of bifurcation, and many more. For instance, Beddington et al. [3] have explored the behavior of following predator-prey model:

$$\begin{aligned}x_{n+1} &= x_n e^{r(1-(x_n/K)) - ay_n}, \\y_{n+1} &= \alpha x_n (1 - e^{-ay_n}).\end{aligned}\quad (1)$$

Chen [4] has explored global attractivity and permanence of the following discrete multispecies system:

$$\begin{aligned}x_{i_{n+1}} &= x_{i_n} e^{b_{i_n} - \sum_{l=1}^k a_{il_n} x_{l_n} - \sum_{l=1}^k c_{il_n} y_{l_n}}, \\y_{j_{n+1}} &= y_{j_n} e^{-r_{j_n} + \sum_{l=1}^k d_{jl_n} x_{l_n} - \sum_{l=1}^k e_{jl_n} y_{l_n}}.\end{aligned}\quad (2)$$

Fang and Chen [5] have explored the permanence of multispecies Lotka–Volterra competition predator-prey system with delays. Furthermore, Fang et al. [6] have explored the dynamics of the following system:

$$\begin{aligned}x_{n+1} &= x_n e^{a_n - b_n x_n - (c_n y_n / (m_{1n} + m_{2n} x_n + m_{3n} y_n))}, \\y_{n+1} &= y_n e^{-d_n - e_n y_n + (f_n x_n / (m_{1n} + m_{2n} x_n + m_{3n} y_n))}.\end{aligned}\quad (3)$$

Agiza et al. [7] have explored chaotic dynamics of the following discrete model with Holling type II:

$$\begin{aligned}x_{n+1} &= ax_n (1 - x_n) - \frac{bx_n y_n}{1 + \epsilon x_n}, \\y_{n+1} &= \frac{dx_n y_n}{1 + \epsilon x_n}.\end{aligned}\quad (4)$$

Huo and Li [8] have explored stable periodic solution of the following discrete model:

$$\begin{aligned}x_{n+1} &= x_n e^{r_{1n} - b_{1n} x_n - a_{1n} y_n}, \\y_{n+1} &= y_n e^{r_{2n} - a_{2n} (y_n/x_n)}.\end{aligned}\quad (5)$$

Lu and Zhang [9] have studied the permanence and global attractivity of the following discrete system:

$$\begin{aligned}x_{n+1} &= x_n e^{a_n - b_n x_n - (m_n y_n / (A_n + x_n))}, \\y_{n+1} &= y_n e^{d_n - e_n (y_n/x_n)}.\end{aligned}\quad (6)$$

Zhao and Zhang [10] explored the chaos and permanence of the following discrete model:

$$\begin{aligned}x_{n+1} &= (1-d)x_n e^{r(1-(x_n/k) - a y_n)} + d\sigma x_{n-1} e^{r(1-(x_{n-1}/k))}, \\y_{n+1} &= (1-d)x_n (1 - e^{-a y_n}).\end{aligned}\quad (7)$$

Zhao et al. [11] have investigated the dynamics of the following discrete model:

$$\begin{aligned}x_{n+1} &= x_n e^{r(1-(x_n/k))} f(y_n, y_{n-1}), \\y_{n+1} &= x_n (1 - f(y_n, y_{n-1})),\end{aligned}\quad (8)$$

where $f(y_n, y_{n-1}) = e^{-a((1-d)y_n + d\sigma y_{n-1})}$.

On the contrary, in recent years, many papers have been published to investigate the bifurcation analysis of certain discrete models by choosing step size as a bifurcation parameter. For example, Salman et al. [12] have explored bifurcation analysis of the following discrete system:

$$x_{n+1} = x_n + \frac{\delta}{2} (x_n (1 - x_n^2) - y_n), \quad (9)$$

$$y_{n+1} = y_n + \delta y_n (-s + c x_n),$$

by choosing step size δ as a bifurcation parameter. Liu and Xiao [13] have explored bifurcation analysis of the following discrete system:

$$\begin{aligned}x_{n+1} &= x_n + \delta (r x_n (1 - x_n) - b x_n y_n), \\y_{n+1} &= y_n + \delta (-d + b x_n) y_n,\end{aligned}\quad (10)$$

by choosing step size δ as a bifurcation parameter. Hasan and Hama [14] have explored bifurcation analysis of the following discrete system:

$$\begin{aligned}x_{n+1} &= x_n + d x_n \left(1 - x_n - \frac{y_n}{1 + a x_n + b y_n} \right), \\y_{n+1} &= y_n + d y_n \left(\frac{c x_n}{1 + a x_n + b y_n} - e \right),\end{aligned}\quad (11)$$

by choosing step size d as a bifurcation parameter. Wu and Zhang [15] have explored bifurcation analysis of the following discrete system:

$$\begin{aligned}x_{n+1} &= x_n + \delta x_n (K_1 - \alpha_1 x_n - \beta_{12} y_n - \gamma_1 x_n y_n), \\y_{n+1} &= y_n + \delta y_n (K_2 - \alpha_2 y_n - \beta_{21} x_n - \gamma_2 x_n y_n),\end{aligned}\quad (12)$$

by choosing step size δ as a bifurcation parameter. Rana [16] has explored bifurcation analysis of the following discrete system:

$$\begin{aligned}x_{n+1} &= x_n + \delta \left(x_n (1 - x_n) - \frac{a x_n y_n}{x_n + y_n} \right), \\y_{n+1} &= x_n + \delta \left(-d y_n + \frac{b x_n y_n}{x_n + y_n} \right),\end{aligned}\quad (13)$$

by choosing step size δ as a bifurcation parameter. Rana and Kulsum [17] have explored bifurcation analysis of the following discrete system:

$$\begin{aligned}x_{n+1} &= x_n + \delta x_n \left(1 - x_n - \frac{y_n}{x_n^2 + a} \right), \\y_{n+1} &= y_n + \delta y_n \left(\alpha - \frac{\beta y_n}{x_n} \right),\end{aligned}\quad (14)$$

by choosing step size δ as a bifurcation parameter. Motivated from the aforementioned studies, in this work, we explore existence of fixed points, topological classifications around fixed points, periodic points, and bifurcation analysis, by choosing step size h as a bifurcation parameter, of the following three species discrete food chain model with harvesting:

$$\begin{aligned}x_{n+1} &= x_n + h (a_1 (1 - k_1) x_n - \alpha_{11} x_n^2), \\y_{n+1} &= y_n + h (a_2 (1 - k_2) y_n - \alpha_{22} y_n^2 - \alpha_{21} x_n y_n), \\z_{n+1} &= z_n + h (a_3 z_n - \alpha_{33} z_n^2 - \alpha_{32} y_n z_n),\end{aligned}\quad (15)$$

which is a discrete form of the following model:

$$\begin{aligned}\frac{dx}{dt} &= a_1 (1 - k_1) x - \alpha_{11} x^2, \\ \frac{dy}{dt} &= a_2 (1 - k_2) y - \alpha_{22} y^2 - \alpha_{21} x y, \\ \frac{dz}{dt} &= a_3 z - \alpha_{33} z^2 - \alpha_{32} y z,\end{aligned}\quad (16)$$

by Euler forward formula, where h is step size and t is customary denoted by n . It is noted that, in model (16), $x(t)$, $y(t)$, and $z(t)$, respectively, denote populations of first, second, and third species. Moreover $z(t)$ denotes growth rate of first, second, and third species; α_{ii} ($i = 1, 2, 3$) denotes the rate of decrease of first, second, and third species due to internal competitions; α_{21} denotes rate of decrease of second species due to attack of first species; α_{32} denotes the rate of decrease of third species due to attack of second species; k_1 and k_2 , respectively, denote the harvesting rate of first and second species. It is also important to note that all parameters $h, a_1, a_2, a_3, k_1, k_2, \alpha_{11}, \alpha_{22}, \alpha_{21}, \alpha_{32}$, and α_{33} are positive. In addition, it is important here to mention that we

will explore dynamical properties of the discrete-time model (15) instead of the continuous-time model, which is depicted in (16), because discrete-time models governed by difference equations are more realistic and appropriate than the continuous ones in the case where populations have non-overlapping generations, and moreover, discrete models can also provide efficient computational results for numerical simulations [12, 13].

This paper is structured as follows. In Section 2, we study the existence of fixed points of model (15) algebraically. The linearized form of model (15) is presented in Section 3. In Section 4, we explored topological classification around fixed points of the model. Existence of periodic points of model (15) is explored in Section 5. In Section 6, we explored detailed analysis of bifurcation around fixed points of model (15). Theoretical results are verified numerically in Section 7. Brief summary of the paper is presented in Section 8.

2. Study of Equilibrium Points

Here, we will study the boundary and interior equilibrium points of model (15) as follows.

Lemma 1. *Model (15) has atmost eight equilibrium points in \mathbb{R}_+^3 . Precisely,*

- (i) $\forall h, a_1, a_2, a_3, k_1, k_2, \alpha_{11}, \alpha_{22}, \alpha_{21}, \alpha_{32}, \alpha_{33} > 0$; model (15) has a trivial equilibrium point: $P_1 = (0, 0, 0)$.
- (ii) $\forall a_3, \alpha_{33} > 0$; model (15) has boundary equilibrium point: $P_2 = (0, 0, a_3/\alpha_{33})$.
- (iii) $P_3 = (0, (1 - k_2)a_2/\alpha_{22}, 0)$ is a boundary equilibrium point of (15) if $k_2 < 1$.
- (iv) $P_4 = ((1 - k_1)a_1/\alpha_{11}, 0, 0)$ is a boundary equilibrium point of (15) if $k_1 < 1$.
- (v) $P_5 = (0, (1 - k_2)a_2/\alpha_{22}, (a_3\alpha_{22} - \alpha_{32}(1 - k_2)a_2)/\alpha_{22}\alpha_{33})$ is a boundary equilibrium point of (15) if $a_3 > \alpha_{32}(1 - k_2)a_2/\alpha_{22}$ with $k_2 < 1$.
- (vi) $P_6 = ((1 - k_1)a_1/\alpha_{11}, 0, a_3/\alpha_{33})$ is a boundary equilibrium point of (15) if $k_1 < 1$.
- (vii) $P_7 = ((1 - k_1)a_1/\alpha_{11}, (a_2(1 - k_2)\alpha_{11} - a_1(1 - k_1)\alpha_{21})/\alpha_{11}\alpha_{22}, 0)$ is a boundary equilibrium point of (15) if $a_2 > a_1(1 - k_1)\alpha_{21}/(1 - k_2)\alpha_{11}$ with $k_1, k_2 < 1$.
- (viii) $P_8 = ((1 - k_1)a_1/\alpha_{11}, (a_2(1 - k_2)\alpha_{11} - a_1(1 - k_1)\alpha_{21})/\alpha_{11}\alpha_{22}, (a_3\alpha_{11}\alpha_{22} - a_2(1 - k_2)\alpha_{11}\alpha_{32} + a_1(1 - k_1)\alpha_{21}\alpha_{32})/\alpha_{11}\alpha_{22}\alpha_{33})$ is an interior equilibrium point of (15) if $k_1 < 1, a_2 > a_1(1 - k_1)\alpha_{21}/(1 - k_2)\alpha_{11}$ and $a_3 > (a_2(1 - k_2)\alpha_{11}\alpha_{32} - a_1(1 - k_1)\alpha_{21}\alpha_{32})/\alpha_{11}\alpha_{22}$.

Proof. If model (15) has an equilibrium point, $P = (x, y, z)$, then

$$\begin{aligned} x &= x + h(a_1(1 - k_1)x - \alpha_{11}x^2), \\ y &= y + h(a_2(1 - k_2)y - \alpha_{22}y^2 - \alpha_{21}xy), \\ z &= z_n + h(a_3z - \alpha_{33}z^2 - \alpha_{32}yz). \end{aligned} \tag{17}$$

The simple computation yields that, for the values of $P_i (i = 1, \dots, 7)$, (17) satisfied identically. So, one can conclude that model (15) has seven boundary points: $P_i (i = 1, \dots, 7)$. In order to find interior point, from (17), one obtains

$$\begin{aligned} a_1(1 - k_1) - \alpha_{11}x &= 0, \\ a_2(1 - k_2) - \alpha_{22}y - \alpha_{21}x &= 0, \\ a_3 - \alpha_{33}z - \alpha_{32}y &= 0. \end{aligned} \tag{18}$$

From 1st of (18), one obtains

$$x = \frac{(1 - k_1)a_1}{\alpha_{11}}. \tag{19}$$

From 2nd equation of (18) and (19), one obtains

$$y = \frac{a_2(1 - k_2)\alpha_{11} - a_1(1 - k_1)\alpha_{21}}{\alpha_{11}\alpha_{22}}. \tag{20}$$

From 3rd equation of (18) and (20), one obtains

$$z = \frac{a_3\alpha_{11}\alpha_{22} - a_2(1 - k_2)\alpha_{11}\alpha_{32} + a_1(1 - k_1)\alpha_{21}\alpha_{32}}{\alpha_{11}\alpha_{22}\alpha_{33}}. \tag{21}$$

From (19)–(21), one can conclude that P_8 is an interior equilibrium point of (15) if $k_1 < 1, a_2 > (a_1(1 - k_1)\alpha_{21}/(1 - k_2)\alpha_{11})$, and $a_3 > (a_2(1 - k_2)\alpha_{11}\alpha_{32} - a_1(1 - k_1)\alpha_{21}\alpha_{32})/\alpha_{11}\alpha_{22}$. \square

3. Linearized Form of Model (15)

The variational matrix $J|_P$ about P under the map:

$$(f_1, f_2, f_3) \mapsto (x_{n+1}, y_{n+1}, z_{n+1}), \tag{22}$$

where

$$\begin{aligned} f_1 &= x + h(a_1(1 - k_1)x - \alpha_{11}x^2), \\ f_2 &= y + h(a_2(1 - k_2)y - \alpha_{22}y^2 - \alpha_{21}xy), \\ f_3 &= z + h(a_3z - \alpha_{33}z^2 - \alpha_{32}yz), \end{aligned} \tag{23}$$

is

$$J|_P = \begin{pmatrix} 1 + h(a_1(1 - k_1) - 2\alpha_{11}x) & 0 & 0 \\ -h\alpha_{21}y & 1 + h(a_2(1 - k_2) - 2\alpha_{22}y - \alpha_{21}x) & 0 \\ 0 & -h\alpha_{32}z & 1 + h(a_3 - 2\alpha_{33}z - \alpha_{32}y) \end{pmatrix}, \tag{24}$$

with

$$\begin{aligned}\lambda_1 &= 1 + h(a_1(1 - k_1) - 2\alpha_{11}x), \\ \lambda_2 &= 1 + h(a_2(1 - k_2) - 2\alpha_{22}y - \alpha_{21}x), \\ \lambda_3 &= 1 + h(a_3 - 2\alpha_{33}z - \alpha_{32}y).\end{aligned}\quad (25)$$

4. Dynamical Behavior: Topological Properties of Equilibrium Points

The dynamical behavior about fixed points P_i ($i = 1, \dots, 8$) of model (15) is explored in this section.

4.1. *Dynamical Behavior about P_1 .* From (25), eigenvalues of $J|_{P_1}$ about P_1 are

$$\begin{aligned}\lambda_1 &= 1 + ha_1(1 - k_1), \\ \lambda_2 &= 1 + ha_2(1 - k_2), \\ \lambda_3 &= 1 + ha_3.\end{aligned}\quad (26)$$

The dynamical behavior about P_1 of model (15) is concluded as follows.

Lemma 2.

- (i) For all allowed parametric values, $h, a_1, a_2, a_3, k_1, k_2, \alpha_{11}, \alpha_{22}, \alpha_{21}, \alpha_{32}, \alpha_{33} > 0$, P_1 is not sink.
(ii) P_1 is a source if

$$0 < h < \min\left\{\frac{2}{a_1(k_1 - 1)}, \frac{2}{a_2(k_2 - 1)}\right\}.\quad (27)$$

- (iii) P_1 is a saddle if

$$h > \max\left\{\frac{2}{a_1(k_1 - 1)}, \frac{2}{a_2(k_2 - 1)}\right\}.\quad (28)$$

- (iv) P_1 is nonhyperbolic if

$$h = \frac{2}{a_1(k_1 - 1)},\quad (29)$$

or

$$h = \frac{2}{a_2(k_2 - 1)}.\quad (30)$$

4.2. *Dynamical Behavior about P_2 .* From (25), eigenvalues of $J|_{P_2}$ about P_2 are

$$\begin{aligned}\lambda_1 &= 1 + ha_1(1 - k_1), \\ \lambda_2 &= 1 + ha_2(1 - k_2), \\ \lambda_3 &= 1 - ha_3.\end{aligned}\quad (31)$$

The dynamical behavior about P_2 is concluded as follows:

Lemma 3. (i) P_2 is a sink if

$$h > \max\left\{\frac{2}{a_1(k_1 - 1)}, \frac{2}{a_2(k_2 - 1)}\right\}, \quad 0 < h < \frac{2}{a_3}.\quad (32)$$

- (ii) P_2 is a source if

$$0 < h < \min\left\{\frac{2}{a_1(k_1 - 1)}, \frac{2}{a_2(k_2 - 1)}\right\}, \quad h > \frac{2}{a_3}.\quad (33)$$

- (iii) P_2 is a saddle if

$$h < \min\left\{\frac{2}{a_1(k_1 - 1)}, \frac{2}{a_2(k_2 - 1)}\right\}, \quad 0 < h < \frac{2}{a_3}.\quad (34)$$

- (iv) P_2 is nonhyperbolic if

$$h = \frac{2}{a_3},\quad (35)$$

or

$$h = \frac{2}{a_1(k_1 - 1)},\quad (36)$$

or

$$h = \frac{2}{a_2(k_2 - 1)}.\quad (37)$$

4.3. *Dynamical Behavior about P_3 .* From (25), eigenvalues of $J|_{P_3}$ about P_3 are

$$\begin{aligned}\lambda_1 &= 1 + ha_1(1 - k_1), \\ \lambda_2 &= 1 - ha_2(1 - k_2),\end{aligned}\quad (38)$$

$$\lambda_3 = 1 + h\left(\frac{a_3\alpha_{22} - a_2\alpha_{32}(1 - k_2)}{\alpha_{22}}\right).$$

The dynamical behavior about P_3 is concluded as follows.

Lemma 4.

- (i) P_3 is a sink if

$$h > \max\left\{\frac{2}{a_1(k_1 - 1)}, \frac{2\alpha_{22}}{a_2\alpha_{32}(1 - k_2) - a_3\alpha_{22}}\right\},\quad (39)$$

$$0 < h < \frac{2}{a_2(1 - k_2)}.$$

- (ii) P_3 is a source if

$$0 < h < \min\left\{\frac{2}{a_1(k_1 - 1)}, \frac{2\alpha_{22}}{a_2\alpha_{32}(1 - k_2) - a_3\alpha_{22}}\right\},$$

$$h > \frac{2}{a_2(1 - k_2)}.$$

(40)

(iii) P_3 is a saddle if

$$h > \max \left\{ \frac{2}{a_1(k_1 - 1)}, \frac{2}{a_2(1 - k_2)} \right\}, \quad (41)$$

$$0 < h < \frac{2\alpha_{22}}{a_2\alpha_{32}(1 - k_2) - a_3\alpha_{22}}.$$

(iv) P_3 is nonhyperbolic if

$$h = \frac{2}{a_2(1 - k_2)}, \quad (42)$$

or

$$h = \frac{2}{a_1(k_1 - 1)}, \quad (43)$$

or

$$h = \frac{2\alpha_{22}}{a_2\alpha_{32}(1 - k_2) - a_3\alpha_{22}}. \quad (44)$$

4.4. *Dynamical Behavior about P_4 .* From (25), eigenvalues of $J|_{P_4}$ about P_4 are

$$\begin{aligned} \lambda_1 &= 1 - ha_1(1 - k_1), \\ \lambda_2 &= 1 + ha_2(1 - k_2), \\ \lambda_3 &= 1 + ha_3. \end{aligned} \quad (45)$$

The dynamical behavior about P_4 is concluded as follows.

Lemma 5.

(i) For all allowed parametric values, $h, a_1, a_2, a_3, k_1, k_2, \alpha_{11}, \alpha_{22}, \alpha_{21}, \alpha_{32}, \alpha_{33} > 0$, P_4 is not sink.

(ii) P_4 is a source if

$$h > \max \left\{ \frac{2}{a_1(1 - k_1)}, \frac{2}{a_2(k_2 - 1)} \right\}. \quad (46)$$

(iii) P_4 is a saddle if

$$0 < h < \min \left\{ \frac{2}{a_1(1 - k_1)}, \frac{2}{a_2(k_2 - 1)} \right\}. \quad (47)$$

(iv) P_4 is nonhyperbolic if

$$h = \frac{2}{a_1(1 - k_1)}, \quad (48)$$

or

$$h = \frac{2}{a_2(k_2 - 1)}. \quad (49)$$

4.5. *Dynamical Behavior about P_5 .* From (25), eigenvalues of $J|_{P_5}$ about P_5 are

$$\begin{aligned} \lambda_1 &= 1 + ha_1(1 - k_1), \\ \lambda_2 &= 1 - ha_2(1 - k_2), \\ \lambda_3 &= 1 + h \left(-a_3 + \frac{\alpha_{32}(1 - k_2)a_2}{\alpha_{22}} \right). \end{aligned} \quad (50)$$

The dynamical behavior about P_5 is concluded as follows.

Lemma 6. (i) P_5 is a sink if

$$h > \max \left\{ \frac{2}{a_1(k_1 - 1)}, \frac{2\alpha_{22}}{a_3\alpha_{22} - a_2\alpha_{32}(1 - k_2)} \right\}, \quad (51)$$

$$0 < h < \frac{2}{a_2(1 - k_2)}.$$

(ii) P_5 is a source if

$$0 < h < \min \left\{ \frac{2}{a_1(k_1 - 1)}, \frac{2\alpha_{22}}{a_3\alpha_{22} - a_2\alpha_{32}(1 - k_2)} \right\},$$

$$h > \frac{2}{a_2(1 - k_2)}. \quad (52)$$

(iii) P_5 is a saddle if

$$h > \max \left\{ \frac{2}{a_1(k_1 - 1)}, \frac{2\alpha_{22}}{a_3\alpha_{22} - a_2\alpha_{32}(1 - k_2)} \right\}, \quad (53)$$

$$h > \frac{2}{a_2(1 - k_2)}.$$

(iv) P_5 is nonhyperbolic if

$$h = \frac{2}{a_1(k_1 - 1)}, \quad (54)$$

or

$$h = \frac{a_3\alpha_{22} - 2\alpha_{22}}{a_2\alpha_{32}(1 - k_2)}, \quad (55)$$

or

$$h = \frac{2}{a_2(1 - k_2)}. \quad (56)$$

4.6. *Dynamical Behavior about P_6 .* From (25), eigenvalues of $J|_{P_6}$ about P_6 are

$$\begin{aligned} \lambda_1 &= 1 - ha_1(1 - k_1), \\ \lambda_2 &= 1 + h \left(a_2(1 - k_2) - \frac{a_1\alpha_{21}(1 - k_1)}{\alpha_{11}} \right), \\ \lambda_3 &= 1 - ha_3. \end{aligned} \quad (57)$$

The dynamical behavior about P_6 is concluded as follows.

Lemma 7.

(i) P_6 is a sink if

$$0 < h < \min \left\{ \frac{2}{a_1(1-k_1)}, \frac{2}{a_3} \right\}$$

$$h > \frac{2\alpha_{11}}{a_1\alpha_{21}(1-k_1) - a_2\alpha_{11}(1-k_2)}. \quad (58)$$

(ii) P_6 is a source if

$$h > \max \left\{ \frac{2}{a_1(1-k_1)}, \frac{2}{a_3} \right\},$$

$$0 < h < \frac{2\alpha_{11}}{a_1\alpha_{21}(1-k_1) - a_2\alpha_{11}(1-k_2)}. \quad (59)$$

(iii) P_6 is a saddle if

$$0 < h < \min \left\{ \frac{2}{a_1(1-k_1)}, \frac{2}{a_3} \right\},$$

$$0 < h < \frac{2\alpha_{11}}{a_1\alpha_{21}(1-k_1) - a_2\alpha_{11}(1-k_2)}. \quad (60)$$

(iv) P_6 is nonhyperbolic if

$$h = \frac{2}{a_1(1-k_1)}, \quad (61)$$

or

$$h = \frac{2}{a_3}, \quad (62)$$

or

$$h = \frac{2\alpha_{11}}{a_1\alpha_{21}(1-k_1) - a_2\alpha_{11}(1-k_2)}. \quad (63)$$

4.7. Dynamical Behavior about P_7 . From (25), eigenvalues of $J|_{P_7}$ about P_7 are

$$\lambda_1 = 1 - ha_1(1-k_1),$$

$$\lambda_2 = 1 - h \left(a_2(1-k_2) - \frac{2a_1\alpha_{21}(1-k_1)}{\alpha_{11}} \right),$$

$$\lambda_3 = 1 + h \left(a_3 - \frac{a_2(1-k_2)\alpha_{32}}{\alpha_{22}} + \frac{a_1\alpha_{21}\alpha_{32}(1-k_1)}{\alpha_{11}\alpha_{22}} \right). \quad (64)$$

The dynamical behavior about P_7 is concluded as follows:

Lemma 8.

(i) P_7 is a sink if

$$0 < h < \min \left\{ \frac{2}{a_1(1-k_1)}, \frac{2\alpha_{11}}{a_2\alpha_{11}(1-k_2) - 2a_1\alpha_{21}(1-k_1)} \right\},$$

$$h > \frac{2\alpha_{11}\alpha_{22}}{a_3\alpha_{11}\alpha_{22} - a_2\alpha_{11}\alpha_{32}(1-k_2) + a_1\alpha_{21}\alpha_{32}(1-k_1)}. \quad (65)$$

(ii) P_7 is a source if

$$h > \max \left\{ \frac{2}{a_1(1-k_1)}, \frac{2\alpha_{11}}{a_2\alpha_{11}(1-k_2) - 2a_1\alpha_{21}(1-k_1)} \right\},$$

$$0 < h < \frac{2\alpha_{11}\alpha_{22}}{a_3\alpha_{11}\alpha_{22} - a_2\alpha_{11}\alpha_{32}(1-k_2) + a_1\alpha_{21}\alpha_{32}(1-k_1)}. \quad (66)$$

(iii) P_7 is a saddle if

$$0 < h < \min \left\{ \frac{2}{a_1(1-k_1)}, \frac{2\alpha_{11}}{a_2\alpha_{11}(1-k_2) - 2a_1\alpha_{21}(1-k_1)} \right\},$$

$$0 < h < \frac{2\alpha_{11}\alpha_{22}}{a_3\alpha_{11}\alpha_{22} - a_2\alpha_{11}\alpha_{32}(1-k_2) + a_1\alpha_{21}\alpha_{32}(1-k_1)}. \quad (67)$$

(iv) P_7 is nonhyperbolic if

$$h = \frac{2}{a_1(1-k_1)}, \quad (68)$$

or

$$h = \frac{2\alpha_{11}}{a_2\alpha_{11}(1-k_2) - 2a_1\alpha_{21}(1-k_1)}, \quad (69)$$

or

$$h = \frac{2\alpha_{11}\alpha_{22}}{a_3\alpha_{11}\alpha_{22} - a_2\alpha_{11}\alpha_{32}(1-k_2) + a_1\alpha_{21}\alpha_{32}(1-k_1)}. \quad (70)$$

4.8. Dynamical Behavior about P_8 . From (25), eigenvalues of $J|_{P_8}$ about P_8 are

$$\lambda_1 = 1 - ha_1(1-k_1),$$

$$\lambda_2 = 1 - h \left(a_2(1-k_2) - \frac{2a_1\alpha_{21}(1-k_1)}{\alpha_{11}} \right),$$

$$\lambda_3 = 1 - h \left(a_3 - \frac{a_2(1-k_2)\alpha_{32}}{\alpha_{22}} + \frac{a_1\alpha_{21}\alpha_{32}(1-k_1)}{\alpha_{11}\alpha_{22}} \right). \quad (71)$$

The dynamical behavior about P_8 is concluded as follows.

Lemma 9.

(i) P_8 is a sink if

$$0 < h < \min \left\{ \frac{2}{a_1(1-k_1)}, \frac{2\alpha_{11}}{a_2\alpha_{11}(1-k_2) - 2a_1\alpha_{21}(1-k_1)}, \frac{2\alpha_{11}\alpha_{22}}{a_3\alpha_{11}\alpha_{22} - a_2\alpha_{11}\alpha_{32}(1-k_2) + a_1\alpha_{21}\alpha_{32}(1-k_1)} \right\}. \quad (72)$$

(ii) P_8 is a source if

$$h > \max \left\{ \frac{2}{a_1(1-k_1)}, \frac{2\alpha_{11}}{a_2\alpha_{11}(1-k_2) - 2a_1\alpha_{21}(1-k_1)}, \frac{2\alpha_{11}\alpha_{22}}{a_3\alpha_{11}\alpha_{22} - a_2\alpha_{11}\alpha_{32}(1-k_2) + a_1\alpha_{21}\alpha_{32}(1-k_1)} \right\}. \quad (73)$$

(iii) P_8 is a saddle if

$$0 < h < \min \left\{ \frac{2}{a_1(1-k_1)}, \frac{2\alpha_{11}}{a_2\alpha_{11}(1-k_2) - 2a_1\alpha_{21}(1-k_1)} \right\},$$

$$h > \frac{2\alpha_{11}\alpha_{22}}{a_3\alpha_{11}\alpha_{22} - a_2\alpha_{11}\alpha_{32}(1-k_2) + a_1\alpha_{21}\alpha_{32}(1-k_1)}. \quad (74)$$

(iv) P_8 is nonhyperbolic if

$$h = \frac{2}{a_1(1-k_1)}, \quad (75)$$

or

$$h = \frac{2\alpha_{11}}{a_2\alpha_{11}(1-k_2) - 2a_1\alpha_{21}(1-k_1)}, \quad (76)$$

or

$$h = \frac{2\alpha_{11}\alpha_{22}}{a_3\alpha_{11}\alpha_{22} - a_2\alpha_{11}\alpha_{32}(1-k_2) + a_1\alpha_{21}\alpha_{32}(1-k_1)}. \quad (77)$$

5. Periodic Points

We will prove that P_i ($i = 1, \dots, 8$) of model (15) are periodic points of period n .

Theorem 1. *Equilibrium points P_i ($i = 1, \dots, 8$) of model (15) are periodic points of prime period 1.*

Proof. From (15), define

$$F(x, y, z) := (f_1, f_2, f_3), \quad (78)$$

where f_1, f_2 , and f_3 are represented in (23). From (78), the computation yields

$$\begin{aligned} F|_{P_1=(0,0,0)} &= P_1, \\ F|_{P_2=(0,0,(a_3/\alpha_{33}))} &= P_2, \\ F|_{P_3=(0,(1-k_2)a_2/\alpha_{22},0)} &= P_3, \\ F|_{P_4=((1-k_1)a_1/\alpha_{11},0,0)} &= P_4, \\ F|_{P_5=(0,(1-k_2)a_2/\alpha_{22},(a_3\alpha_{22}-\alpha_{32}(1-k_2)a_2)/\alpha_{22}\alpha_{33})} &= P_5, \\ F|_{P_6=((1-k_1)a_1/\alpha_{11},0,a_3/\alpha_{33})} &= P_6, \\ F|_{P_7=((1-k_1)a_1/\alpha_{11},(a_2(1-k_2)\alpha_{11}-a_1(1-k_1)\alpha_{21})/\alpha_{11}\alpha_{22},0)} &= P_7, \\ F|_{P_8=((1-k_1)a_1/\alpha_{11},(a_2(1-k_2)\alpha_{11}-a_1(1-k_1)\alpha_{21})/\alpha_{11}\alpha_{22},(a_3\alpha_{11}\alpha_{22}-a_2(1-k_2)\alpha_{11}\alpha_{32}+a_1(1-k_1)\alpha_{21}\alpha_{32})/\alpha_{11}\alpha_{22}\alpha_{33})} &= P_8. \end{aligned} \quad (79)$$

Hence, from (79), we can say that equilibrium points $P_i (i = 1, \dots, 8)$ of three species model (15) are periodic points of prime period 1. \square

Now, it is proved that equilibrium points $P_i (i = 1, \dots, 8)$ are period points of period n .

Theorem 2. P_1 of model (15) is a periodic point of period n .

Proof. From (78), the following computation yields the required statement:

$$\begin{aligned} F^2 &= (f_1 + h[a_1(1-k_1)f_1 - \alpha_{11}(f_1)^2], \\ & f_2 + h[a_2(1-k_2)f_2 - \alpha_{22}(f_2)^2 - \alpha_{21}f_1f_2], \\ & f_3 + h[a_3f_3 - \alpha_{33}(f_2)^2 - \alpha_{32}f_2f_3]) \Rightarrow F^2|_{P_1} = P_1, \\ F^3 &= (f_1^2 + h[a_1(1-k_1)f_1^2 - \alpha_{11}(f_1^2)^2], \\ & f_2^2 + h[a_2(1-k_2)f_2^2 - \alpha_{22}(f_2^2)^2 - \alpha_{21}f_1^2f_2^2(x, y, z)], \\ & f_3^2 + h[a_3f_3^2 - \alpha_{33}(f_2^2)^2 - \alpha_{32}f_2^2f_3^2]) \Rightarrow F^3|_{P_1} = P_1, \\ & \vdots \\ F^n &= (f_1^n + h[a_1(1-k_1)f_1^n - \alpha_{11}(f_1^n)^2], \\ & f_2^n + h[a_2(1-k_2)f_2^n - \alpha_{22}(f_2^n)^2 - \alpha_{21}f_1^n f_2^n], \\ & f_3^n + h[a_3f_3^n - \alpha_{33}(f_2^n)^2 - \alpha_{32}f_2^n f_3^n]) \Rightarrow F^n|_{P_1} = P_1. \end{aligned} \quad (80) \quad \square$$

Theorem 3. P_2 of model (15) is a periodic point of period n .

Proof. Utilizing the computation as we have done in (80), one gets the following required statement:

$$\begin{aligned} F^2|_{P_2=(0,0,a_3/\alpha_{33})} &= P_2, \\ F^3|_{P_2=(0,0,a_3/\alpha_{33})} &= P_2, \\ & \vdots \\ F^n|_{P_2=(0,0,a_3/\alpha_{33})} &= P_2. \end{aligned} \quad (81) \quad \square$$

Theorem 4. P_3 of model (15) is a periodic point of period n .

Proof. In view of (80), one gets the following required statement:

$$\begin{aligned} F^2|_{P_3=(0,(1-k_2)a_2/\alpha_{22},0)} &= P_3, \\ F^3|_{P_3=(0,(1-k_2)a_2/\alpha_{22},0)} &= P_3, \\ & \vdots \\ F^n|_{P_3=(0,(1-k_2)a_2/\alpha_{22},0)} &= P_3. \end{aligned} \quad (82) \quad \square$$

Theorem 5. P_4 of model (15) is a periodic point of period n .

Proof. In view of (80), one gets the following required statement:

$$\begin{aligned} F^2|_{P_4=((1-k_1)a_1/\alpha_{11},0,0)} &= P_4, \\ F^3|_{P_4=((1-k_1)a_1/\alpha_{11},0,0)} &= P_4, \\ & \vdots \\ F^n|_{P_4=((1-k_1)a_1/\alpha_{11},0,0)} &= P_4. \end{aligned} \quad (83) \quad \square$$

Theorem 6. P_5 of model (15) is a periodic point of period n .

Proof. From (80), one obtains

$$\begin{aligned} F^2|_{P_5=(0,(1-k_2)a_2/\alpha_{22},(a_3\alpha_{22}-\alpha_{32}(1-k_2)a_2)/\alpha_{22}\alpha_{33})} &= P_5, \\ F^3|_{P_5=(0,(1-k_2)a_2/\alpha_{22},(a_3\alpha_{22}-\alpha_{32}(1-k_2)a_2)/\alpha_{22}\alpha_{33})} &= P_5, \\ & \vdots \\ F^n|_{P_5=(0,(1-k_2)a_2/\alpha_{22},(a_3\alpha_{22}-\alpha_{32}(1-k_2)a_2)/\alpha_{22}\alpha_{33})} &= P_5. \end{aligned} \quad (84) \quad \square$$

Theorem 7. P_6 of model (15) is a periodic point of period n .

Proof. From (80), one obtains

$$\begin{aligned} F^2|_{P_6=((1-k_1)a_1/\alpha_{11},0,a_3/\alpha_{33})} &= P_6, \\ F^3|_{P_6=((1-k_1)a_1/\alpha_{11},0,a_3/\alpha_{33})} &= P_6, \\ & \vdots \\ F^n|_{P_6=((1-k_1)a_1/\alpha_{11},0,a_3/\alpha_{33})} &= P_6. \end{aligned} \quad (85) \quad \square$$

Theorem 8. P_7 of model (15) is a periodic point of period n .

Proof. From (80), one obtains

$$\begin{aligned} F^2|_{P_7=((1-k_1)a_1/\alpha_{11},(a_2(1-k_2)\alpha_{11}-a_1(1-k_1)\alpha_{21})/\alpha_{11}\alpha_{22},0)} &= P_7, \\ F^3|_{P_7=((1-k_1)a_1/\alpha_{11},(a_2(1-k_2)\alpha_{11}-a_1(1-k_1)\alpha_{21})/\alpha_{11}\alpha_{22},0)} &= P_7, \\ & \vdots \\ F^n|_{P_7=((1-k_1)a_1/\alpha_{11},(a_2(1-k_2)\alpha_{11}-a_1(1-k_1)\alpha_{21})/\alpha_{11}\alpha_{22},0)} &= P_7. \end{aligned} \quad (86) \quad \square$$

Theorem 9. P_8 of model (15) is a periodic point of period n .

Proof. From (80), one obtains

$$\begin{aligned}
 F^2|_{P_8} &= ((1-k_1)a_1/\alpha_{11}, (a_2(1-k_2)\alpha_{11}-a_1(1-k_1)\alpha_{21})/\alpha_{11}\alpha_{22}, (a_3\alpha_{11}\alpha_{22}-a_2(1-k_2)\alpha_{11}\alpha_{32}+a_1(1-k_1)\alpha_{21}\alpha_{32})/\alpha_{11}\alpha_{22}\alpha_{33}) = P_8, \\
 F^3|_{P_8} &= ((1-k_1)a_1/\alpha_{11}, (a_2(1-k_2)\alpha_{11}-a_1(1-k_1)\alpha_{21})/\alpha_{11}\alpha_{22}, (a_3\alpha_{11}\alpha_{22}-a_2(1-k_2)\alpha_{11}\alpha_{32}+a_1(1-k_1)\alpha_{21}\alpha_{32})/\alpha_{11}\alpha_{22}\alpha_{33}) = P_8, \\
 &\vdots \\
 F^n|_{P_8} &= ((1-k_1)a_1/\alpha_{11}, (a_2(1-k_2)\alpha_{11}-a_1(1-k_1)\alpha_{21})/\alpha_{11}\alpha_{22}, (a_3\alpha_{11}\alpha_{22}-a_2(1-k_2)\alpha_{11}\alpha_{32}+a_1(1-k_1)\alpha_{21}\alpha_{32})/\alpha_{11}\alpha_{22}\alpha_{33}) = P_8.
 \end{aligned} \tag{87}$$

6. Analysis of Bifurcation

In this section, we give analysis of bifurcation about fixed points P_i ($i = 1, \dots, 8$) of model (15) by bifurcation theory [18, 19].

6.1. Analysis of Bifurcation at P_1 . Here, we will study analysis of bifurcation at P_1 of model (15). From (26), the simple computation yields $\lambda_1|_{(29)} = -1$, but $\lambda_{2,3}|_{(29)} = 1 - (2a_2(1 - k_2)/a_1(1 - k_1)), 1 - (2a_3/a_1(1 - k_1)) \neq 1$ or -1 . This suggests that model (15) could undergo a flip bifurcation around P_1 if $\Omega = (h, a_1, a_2, a_3, k_1, k_2, \alpha_{11}, \alpha_{22}, \alpha_{21}, \alpha_{32}, \alpha_{33})$ passes the curve:

$$\mathcal{F}|_{P_1} = \left\{ \Omega: h = \frac{2}{a_1(k_1 - 1)} \right\}. \tag{88}$$

However, flip bifurcation cannot occur by computation, so P_1 is degenerated with high co-dimension as $\Omega \in \mathcal{F}|_{P_1}$.

6.2. Analysis of Bifurcation at P_2 . We will study analysis of bifurcation at P_2 of model (15). From (26), the simple computation yields $\lambda_3|_{(35)} = -1$, but $\lambda_{1,2}|_{(35)} = 1 + (2a_1(1 - k_1)/a_3), 1 + (2a_2(1 - k_2)/a_3) \neq 1$ or -1 . This suggests that model (15) could undergo a flip bifurcation around P_2 if Ω passes the curve:

$$\mathcal{F}|_{P_2} = \left\{ \Omega: h = \frac{2}{a_3} \right\}. \tag{89}$$

The proof of following theorem shows that model (15) undergoes flip bifurcation around P_2 if $\Omega \in \mathcal{F}|_{P_2}$.

Theorem 10. *Model (15) undergo flip bifurcation around P_2 if $\Omega \in \mathcal{F}|_{P_2}$.*

Proof. It is noticed that three-species model (15) is invariant with respect to $x = y = 0$. Thus, we restrict (15) on $x = y = 0$, to determine the bifurcation, where it takes the form

$$z_{n+1} = z_n + h(a_3z_n - \alpha_{33}z_n^2). \tag{90}$$

From (90), define

$$f(z) := z + h(a_3z - \alpha_{33}z^2). \tag{91}$$

Now, one denotes $h = h^* = (2/a_3)$ and $z = z^* = (a_3/\alpha_{33})$. The computation yields

$$f_z|_{h=h^*, z=z^*} = -1, \tag{92}$$

$$f_{zz}|_{h=h^*, z=z^*} = -\frac{4\alpha_{33}}{a_3} \neq 0, \tag{93}$$

$$f_h|_{h=h^*, z=z^*} = -\frac{a_3^2}{\alpha_{33}} \neq 0. \tag{94}$$

From (92)–(94), it can be concluded that the model undergoes flip bifurcation around P_2 if $\Omega \in \mathcal{F}|_{P_2}$. \square

6.3. Analysis of Bifurcation at P_3 . From (38), the computation yields $\lambda_2|_{(42)} = -1$, but $\lambda_{1,3}|_{(42)} = 1 + (2a_1(1 - k_1)/a_2(1 - k_2)), 1 + (2/a_2(1 - k_2))[a_3\alpha_{22} - a_2\alpha_{32}(1 - k_2)] \neq 1$ or -1 . This suggests that model (15) could undergo a flip bifurcation around P_3 if Ω passes the curve:

$$\mathcal{F}|_{P_3} = \left\{ \Omega: h = \frac{2}{a_2(1 - k_2)} \right\}. \tag{95}$$

The proof of following theorem shows that model (15) undergoes flip bifurcation around P_3 if $\Omega \in \mathcal{F}|_{P_3}$.

Theorem 11. *Model (15) undergoes flip bifurcation around P_3 if $\Omega \in \mathcal{F}|_{P_3}$.*

Proof. It is noticed that, w.r.t $x = z = 0$, model (15) is invariant. So, one restricts model (15) on $x = z = 0$, where it becomes

$$y_{n+1} = y_n + h(a_2(1 - k_2)y_n - \alpha_{22}y_n^2). \tag{96}$$

From (96), define

$$f(y) := y + ha_2(1 - k_2)y - h\alpha_{22}y^2. \tag{97}$$

Denote $h = h^* = (2/a_2(1 - k_2))$ and $y = y^* = (a_2(1 - k_2)/\alpha_{22})$. By computation, one obtains

$$f_y|_{h=h^*=(2/a_2(1-k_2)), y=y^*=(a_2(1-k_2)/\alpha_{22})} = -1, \quad (98)$$

$$f_{yy}|_{h=h^*=(2/a_2(1-k_2)), y=y^*=(a_2(1-k_2)/\alpha_{22})} = -\frac{4\alpha_{22}}{a_2(1-k_2)} \neq 0, \quad (99)$$

$$f_h|_{h=h^*=(2/a_2(1-k_2)), y=y^*=(a_2(1-k_2)/\alpha_{22})} = \frac{a_2(1-k_2)}{\alpha_{22}} \neq 0. \quad (100)$$

So, model (15) undergoes flip bifurcation by (98)–(100) if $\Omega \in \mathcal{F}|_{P_3}$. \square

6.4. Analysis of Bifurcation at P_4 . From (45), the computation yields $\lambda_1|_{(48)} = -1$, but $\lambda_{2,3}|_{(48)} = 1 + (2a_2(1-k_2)/a_1(1-k_1)), 1 + (2a_3/a_1(1-k_1)) \neq 1$ or -1 . This suggests that model (15) could undergo a flip bifurcation around P_4 if Ω passes the curve:

$$\mathcal{F}|_{P_3} = \left\{ \Omega: h = \frac{2}{a_1(1-k_1)} \right\}. \quad (101)$$

The proof of the following theorem shows that model (15) undergoes flip bifurcation around P_4 if $\Omega \in \mathcal{F}|_{P_4}$.

Theorem 12. *Model (15) undergoes flip bifurcation around P_4 if $\Omega \in \mathcal{F}|_{P_4}$.*

Proof. It is noticed that, w.r.t $y = z = 0$, model (15) is invariant. So, one restricts model (15) on $y = z = 0$, where it becomes

$$x_{n+1} = x_n + h(a_1(1-k_1)x_n - \alpha_{11}x_n^2). \quad (102)$$

From (102), define

$$f(x) := x + ha_1(1-k_1)x - h\alpha_{11}x^2. \quad (103)$$

Denote $h = h^* = (2/a_1(1-k_1)), x = x^* = (a_1(1-k_1)/\alpha_{11})$. By computation, one obtains

$$f_x|_{h=h^*=(2/a_1(1-k_1)), x=x^*=(a_1(1-k_1)/\alpha_{11})} = -1, \quad (104)$$

$$f_{xx}|_{h=h^*=(2/a_1(1-k_1)), x=x^*=(a_1(1-k_1)/\alpha_{11})} = -\frac{4\alpha_{11}}{a_1(1-k_1)} \neq 0, \quad (105)$$

$$f_h|_{h=h^*=(2/a_1(1-k_1)), x=x^*=(a_1(1-k_1)/\alpha_{11})} = \frac{a_1(1-k_1)}{\alpha_{11}} \neq 0. \quad (106)$$

So, model (15) undergoes flip bifurcation by (104)–(106) if $\Omega \in \mathcal{F}|_{P_4}$. \square

6.5. Analysis of Bifurcation at P_5 . From (50), the computation yields $\lambda_1|_{(54)} = -1$, but $\lambda_{2,3}|_{(54)} = 1 + (2a_2(1-k_2)/a_1(1-k_1)), 1 - (2/a_1(1-k_1))[-a_3 + (\alpha_{32}(1-k_2)a_2/\alpha_{22})] \neq 1$ or -1 . This suggests that model (15) could undergo flip bifurcation around P_5 if Ω passes the curve:

$$\mathcal{F}|_{P_5} = \left\{ \Omega: h = \frac{2}{a_1(k_1-1)} \right\}. \quad (107)$$

The proof of the following theorem shows that model (15) undergoes flip bifurcation around P_5 if $\Omega \in \mathcal{F}|_{P_5}$.

Theorem 13. *Model (15) undergoes flip bifurcation around P_5 if $\Omega \in \mathcal{F}|_{P_5}$.*

Proof. Recall that if $\Omega \in \mathcal{F}|_{P_5}$, then $\lambda_1|_{(54)} = -1$, but $\lambda_{2,3}|_{(54)} = 1 + (2a_2(1-k_2)/a_1(1-k_1)), 1 - (2/a_1(1-k_1))[-a_3 + (\alpha_{32}(1-k_2)a_2/\alpha_{22})] \neq 1$ or -1 . So, hereafter, detailed flip bifurcation is explored if Ω varies in the nbhd of h , i.e., $h = h + \varepsilon$, by assuming $h \neq (2\alpha_{22}/(a_3\alpha_{22} - a_2\alpha_{32}(1-k_2))), 2/a_2(1-k_2)$. Let

$$u_n = x_n,$$

$$v_n = y_n - \frac{(1-k_2)a_2}{\alpha_{22}}, \quad (108)$$

$$w_n = z_n - \frac{a_3\alpha_{22} - \alpha_{32}(1-k_2)a_2}{\alpha_{22}\alpha_{33}}.$$

Then, (15) gives

$$\begin{pmatrix} u_{n+1} \\ v_{n+1} \\ w_{n+1} \end{pmatrix} = \begin{pmatrix} 1 + ha_1(1 - k_1) & 0 & 0 \\ -h\alpha_{21}\frac{(1 - k_2)a_2}{\alpha_{22}} & 1 - ha_2(1 - k_2) & 0 \\ 0 & -h\alpha_{32}\left(\frac{a_3\alpha_{32} - \alpha_{32}(1 - k_2)a_2}{\alpha_{22}\alpha_{33}}\right) & 1 + h\left(-a_3 + \frac{\alpha_{32}(1 - k_2)a_2}{\alpha_{22}}\right) \end{pmatrix} \begin{pmatrix} u_n \\ v_n \\ w_n \end{pmatrix} + \begin{pmatrix} h\alpha_{11}u_n^2 + a_1(1 - k_1)\epsilon u_n - \alpha_{11}\epsilon u_n^2 \\ h\left[\frac{(a_2(1 - k_2))^2}{\alpha_{22}} - \alpha_{22}\left(v_n + \frac{(1 - k_2)a_2}{\alpha_{22}}\right)^2 + \alpha_{21}u_nv_n\right] \\ \epsilon\left[a_2(1 - k_2)\left(v_n + \frac{a_2(1 - k_2)}{\alpha_{22}}\right) - \alpha_{22}\left(v_n + \frac{(1 - k_2)a_2}{\alpha_{22}}\right)^2 - \alpha_{21}u_n\left(v_n + \frac{a_2(1 - k_2)}{\alpha_{22}}\right)\right] \\ h\left[a_3\left(\frac{a_3\alpha_{32} - \alpha_{32}(1 - k_2)a_2}{\alpha_{22}\alpha_{33}}\right) - \alpha_{33}\left(w_n + \frac{a_3\alpha_{22} - \alpha_{32}(1 - k_2)a_2}{\alpha_{22}\alpha_{33}}\right)^2 - \alpha_{32}v_nw_n - \frac{(1 - k_2)a_2}{\alpha_{22}}\left(\frac{a_3\alpha_{32} - \alpha_{32}(1 - k_2)a_2}{\alpha_{22}\alpha_{33}}\right)\right] + \epsilon\left[a_3\left(w_n + \frac{a_3\alpha_{32} - \alpha_{32}(1 - k_2)a_2}{\alpha_{22}\alpha_{33}}\right) - \alpha_{33}\left(w_n + \frac{a_3\alpha_{22} - \alpha_{32}(1 - k_2)a_2}{\alpha_{22}\alpha_{33}}\right)^2 - \alpha_{32}\left(v_n + \frac{(1 - k_2)a_2}{\alpha_{22}}\right)\left(w_n + \frac{a_3\alpha_{22} - \alpha_{32}(1 - k_2)a_2}{\alpha_{22}\alpha_{33}}\right)\right] \end{pmatrix}. \tag{109}$$

By using transformation,

$$\begin{pmatrix} u_n \\ v_n \\ w_n \end{pmatrix} = \begin{pmatrix} a_{11} & 0 & 0 \\ a_{21} & a_{22} & 0 \\ 1 & 1 & 1 \end{pmatrix} \begin{pmatrix} x_n \\ y_n \\ z_n \end{pmatrix}. \tag{110}$$

(109) takes the form

$$\begin{pmatrix} x_{n+1} \\ y_{n+1} \\ z_{n+1} \end{pmatrix} = \begin{pmatrix} -1 & 0 & 0 \\ 0 & \lambda_2 & 0 \\ 0 & 0 & \lambda_3 \end{pmatrix} \begin{pmatrix} x_n \\ y_n \\ z_n \end{pmatrix} + \begin{pmatrix} F(x_n, y_n, z_n, \epsilon) \\ G(x_n, y_n, z_n, \epsilon) \\ H(x_n, y_n, z_n, \epsilon) \end{pmatrix}, \tag{111}$$

where

$$\begin{aligned}
 a_{11} &= \frac{(-a_1 - a_2 + a_1 k_1 + a_2 k_2) \alpha_{22} (a_1 \alpha_{22} + a_3 \alpha_{22} - a_1 k_1 \alpha_{22} - a_2 \alpha_{32} + a_2 k_2 \alpha_{32}) \alpha_{33}}{a_2 (-1 + k_2) (-a_2 + a_3 + a_2 k_2) \alpha_{21} \alpha_{32}^2}, \\
 a_{21} &= -\frac{(a_1 \alpha_{22} + a_3 \alpha_{22} - a_1 k_1 \alpha_{22} - a_2 \alpha_{32} + a_2 k_2 \alpha_{32}) \alpha_{33}}{(-a_2 + a_3 + a_2 k_2) \alpha_{32}^2}, \\
 a_{22} &= -\frac{(-a_2 \alpha_{22} + a_3 \alpha_{22} + a_2 k_2 \alpha_{22} - a_2 \alpha_{32} + a_2 k_2 \alpha_{32}) \alpha_{33}}{(-a_2 + a_3 + a_2 k_2) \alpha_{32}^2}, \\
 F &= x_n a_1 (1 - k_1) \varepsilon - x_n^2 a_{11} \alpha_{11} + h x_n^2 a_{11} \alpha_{11} - x_n^2 a_{11} \alpha_{11} \varepsilon, \\
 G &= -\frac{a_1 a_{11} (1 - k_1) \varepsilon - x_n^2 a_{11}^2 \alpha_{11} + h x_n^2 a_{11}^2 \alpha_{11} - x_n^2 \varepsilon a_{11}^2 \alpha_{11}}{a_{11}} \\
 &\quad + \frac{h \left(\frac{a_2^2 (1 - k_2)^2}{\alpha_{22}} \right) + x_n a_{11} \alpha_{21} (x_n a_{21} + y_n \alpha_{22}) - \alpha_{22} (x_n a_{21} + y_n \alpha_{22} (1 - k_2 / \alpha_{22}))^2}{a_{21}} \\
 &\quad + \frac{\varepsilon a_2 (1 - k_2) (x_n a_{21} + y_n \alpha_{22} + (a_2 (1 - k_2) / \alpha_{22})) - x_n \varepsilon a_{11} \alpha_{21} (x_n a_{21} + y_n \alpha_{22} + (a_2 (1 - k_2) / \alpha_{22}))}{a_{21}} \\
 &\quad - \frac{\varepsilon \alpha_{22} (x_n a_{21} + y_n \alpha_{22} + (a_2 (1 - k_2) / \alpha_{11}))^2}{a_{21}}, \\
 H &= h \left[-x_n (x_n + y_n + z_n) a_{11} \alpha_{32} - \frac{a_2 (1 - k_2) a_3 \alpha_{32} - a_2 \alpha_{32} (1 - k_2)}{\alpha_{22}^2 \alpha_{33}} \right. \\
 &\quad \left. + \frac{a_3 (a_3 \alpha_{32} - a_2 \alpha_{32} (1 - k_2))}{\alpha_{22} \alpha_{33}} - \left(x_n + y_n + z_n + \frac{a_3 \alpha_{32} - a_2 \alpha_{32} (1 - k_2)}{\alpha_{22} \alpha_{33}} \right)^2 \alpha_{33} \right] \\
 &\quad - \frac{h \left(\frac{a_2^2 (1 - k_2)^2}{\alpha_{22}} \right) + x_n a_{11} \alpha_{21} (x_n a_{21} + y_n \alpha_{22}) - \alpha_{22} (x_n a_{21} + y_n \alpha_{22} ((1 - k_2) / \alpha_{22}))^2}{a_{21}} \\
 &\quad + \frac{\varepsilon a_2 (1 - k_2) (x_n a_{21} + y_n \alpha_{22} + (a_2 (1 - k_2) / \alpha_{22})) - x_n \varepsilon a_{11} \alpha_{21} (x_n a_{21} + y_n \alpha_{22} + (a_2 (1 - k_2) / \alpha_{22}))}{a_{21}} \\
 &\quad - \frac{\varepsilon \alpha_{22} (x_n a_{21} + y_n \alpha_{22} + (a_2 (1 - k_2) / \alpha_{11}))^2}{a_{21}} \\
 &\quad \varepsilon a_3 \left(x_n + y_n + z_n + \frac{a_3 \alpha_{32} - a_2 \alpha_{32} (1 - k_2)}{\alpha_{22} \alpha_{33}} \right) \\
 &\quad - \varepsilon \left(x_n a_{21} + y_n \alpha_{22} + \frac{a_2 (1 - k_2)}{\alpha_{22}} \right) \alpha_{32} \left(x_n + y_n + z_n + \frac{a_3 \alpha_{32} - a_2 (1 - k_2) \alpha_{32}}{\alpha_{22} \alpha_{33}} \right) \\
 &\quad - \left(x_n + y_n + z_n + \frac{a_3 \alpha_{32} - a_2 \alpha_{32} (1 - k_2)}{\alpha_{22} \alpha_{33}} \right)^2 \alpha_{33}.
 \end{aligned} \tag{112}$$

Now, consider (111) on the center manifold, i.e.,

$$W^c(0) = \{(x_n, y_n, z_n) | (y_n, z_n) = (\chi_1(x_n), \chi_2(x_n)), \chi_i(0) = 0, D\chi_i(0) = 0, i = 1, 2\}, \quad (113)$$

where

$$\chi_i(x_n) = a_i x^2 + b_i x^3 + O(x)^4, \quad \text{for } i = 1, 2. \quad (114)$$

From (111) and (113), one obtains

$$\begin{aligned} \chi_1(-x_n + F(x_n, \chi_1, \chi_2)) &= \lambda_2 \chi_1(x_n) + G(x_n, \chi_1, \chi_2), \\ \chi_2(-x_n + F(x_n, \chi_1, \chi_2)) &= \lambda_3 \chi_2(x_n) + H(x_n, \chi_1, \chi_2). \end{aligned} \quad (115)$$

From (115), computation yields $a_1 = b_1 = a_2 = b_2 = 0$. Finally, map (111); restrict to $W^c(0)$ as

$$f(x_n) = -x_n + x_n a_1 (1 - k_1) \varepsilon - x_n^2 a_{11} \alpha_{11} + h x_n^2 a_{11} \alpha_{11} - x_n^2 a_{11} \alpha_{11} \varepsilon + O(|x_n| + |\varepsilon|)^3. \quad (116)$$

For the model to undergo flip bifurcation, the following should be nonzero:

$$\begin{aligned} \Omega_1 &= \left(\frac{\partial^2 f}{\partial x_n \partial \varepsilon} + \frac{1}{2} \frac{\partial f}{\partial \varepsilon} \frac{\partial^2 f}{\partial x_n^2} \right) \Big|_O = a_1 (1 - k_1) \neq 0, \\ \Omega_2 &= \left(\frac{1}{6} \frac{\partial^3 f}{\partial x_n^3} + \left(\frac{1}{2} \frac{\partial^2 f}{\partial x_n^2} \right)^2 \right) \Big|_O = (a_{11} \alpha_{11} - h a_{11} \alpha_{11})^2 > 0. \end{aligned} \quad (117)$$

From (117), one can say that about P_5 model (15) undergoes flip bifurcation if $\Omega \in \mathcal{F}|_{P_5}$. Moreover, period-2 points bifurcating from P_5 are stable since $\Omega_2 = (a_{11} \alpha_{11} - h a_{11} \alpha_{11})^2 > 0$. \square

6.6. Analysis of Bifurcation at P_6 . From (57), the computation yields $\lambda_1|_{(61)} = -1$, but $\lambda_{2,3}|_{(61)} = 1 + (2/a_1(1 - k_1)) [a_2(1 - k_2) - (a_1 \alpha_{21}(1 - k_1)/\alpha_{11})]$, $1 - (2a_3/a_1(1 - k_1)) \neq 1$ or -1 . This suggests that model (15) could undergo flip bifurcation around P_6 if Ω passes the curve:

$$\mathcal{F}|_{P_6} = \left\{ \Omega: h = \frac{2}{a_1(1 - k_1)} \right\}. \quad (118)$$

The proof of the following theorem shows that model (15) undergoes flip bifurcation around P_6 if $\Omega \in \mathcal{F}|_{P_6}$.

Theorem 14. *Model (15) undergoes flip bifurcation around P_6 if $\Omega \in \mathcal{F}|_{P_6}$.*

Proof. Recall that if $\Omega \in \mathcal{F}|_{P_6}$, then $\lambda_1|_{(61)} = -1$, but $\lambda_{2,3}|_{(61)} = 1 + (2/a_1(1 - k_1)) [a_2(1 - k_2) - (a_1 \alpha_{21}(1 - k_1)/\alpha_{11})]$, $1 - (2a_3/a_1(1 - k_1)) \neq 1$ or -1 . So, hereafter, detailed flip bifurcation is explored if Ω varies in the nbhd of h , i.e., $h = h + \varepsilon$, by assuming $h \neq (2/a_3), 2\alpha_{11}/(a_1 \alpha_{21}(1 - k_1) - a_2 \alpha_{11}(1 - k_2))$. Let

$$\begin{aligned} u_n &= x_n - \frac{(1 - k_1)a_1}{\alpha_{11}}, \\ v_n &= y_n, \\ w_n &= z_n - \frac{a_3}{\alpha_{33}}. \end{aligned} \quad (119)$$

Then, (15) gives

$$\begin{aligned}
\begin{pmatrix} u_{n+1} \\ v_{n+1} \\ w_{n+1} \end{pmatrix} &= \begin{pmatrix} 1 - ha_1(1 - k_1) & 0 & 0 \\ 0 & 1 + h\left(a_2(1 - k_2) - \frac{a_1\alpha_{21}(1 - k_1)}{\alpha_{11}}\right) & 0 \\ 0 & -h\alpha_{32}\frac{a_3}{\alpha_{32}} & 1 - ha_3 \end{pmatrix} \begin{pmatrix} u_n \\ v_n \\ w_n \end{pmatrix} \\
&+ \left(h\frac{(a_1(1 - k_1))^2}{\alpha_{11}} - h\alpha_{11}\left(u_n + \frac{a_1(1 - k_1)}{\alpha_{11}}\right)^2 + \varepsilon a_1(1 - k_1)\left(u_n + \frac{a_1(1 - k_1)}{\alpha_{11}}\right) - \varepsilon\alpha_{11}\left(u_n + \frac{a_1(1 - k_1)}{\alpha_{11}}\right)^2 \right. \\
&- h\alpha_{22}v_n^2 - h\alpha_{22}u_nv_n + \varepsilon a_2(1 - k_2)v_n - \varepsilon\alpha_{22}v_n^2 - \varepsilon\alpha_{21}v_n\left(u_n + \frac{a_1(1 - k_1)}{\alpha_{11}}\right) \\
&h\left(\frac{a_3^2}{\alpha_{33}} - \alpha_{33}\left(w_n + \frac{a_3}{\alpha_{33}}\right)^2 - \alpha_{32}v_nw_n \right) \\
&\left. + \varepsilon a_3\left(w_n + \frac{a_3}{\alpha_{33}}\right) - \varepsilon\alpha_{33}\left(w_n + \frac{a_3}{\alpha_{33}}\right)^2 - \varepsilon\alpha_{32}v_n\left(w_n + \frac{a_3}{\alpha_{33}}\right) \right). \tag{120}
\end{aligned}$$

Using transformation,

$$\begin{pmatrix} u_n \\ v_n \\ w_n \end{pmatrix} = \begin{pmatrix} 0 & 1 & 0 \\ 0 & 0 & b_{23} \\ 1 & 0 & 1 \end{pmatrix} \begin{pmatrix} x_n \\ y_n \\ z_n \end{pmatrix}. \tag{121}$$

$$\begin{pmatrix} x_{n+1} \\ y_{n+1} \\ z_{n+1} \end{pmatrix} = \begin{pmatrix} -1 & 0 & 0 \\ 0 & \lambda_2 & 0 \\ 0 & 0 & \lambda_3 \end{pmatrix} \begin{pmatrix} x_n \\ y_n \\ z_n \end{pmatrix} + \begin{pmatrix} F_1(x_n, y_n, z_n, \varepsilon) \\ G_1(x_n, y_n, z_n, \varepsilon) \\ H_1(x_n, y_n, z_n, \varepsilon) \end{pmatrix}, \tag{122}$$

where

(120) becomes

$$\begin{aligned}
b_{23} &= \frac{\alpha_{33}(-a_2\alpha_{11} - a_3\alpha_{11} + a_2k_2\alpha_{11} + a_1\alpha_{21} - a_1k_1\alpha_{21})}{a_3\alpha_{11}\alpha_{32}}, \\
F_1 &= -z_n a_2(1 - k_2)\varepsilon + z_n\left(y_n + \frac{a_1(1 - k_1)}{\alpha_{11}}\right)\alpha_{21}\varepsilon + hz_n\alpha_{22} + hy_nz_n\alpha_{22} + z_n^2b_{23}\alpha_{22}\varepsilon \\
&+ a_3\left(x_n + y_n + \frac{a_3}{\alpha_{33}}\right)\varepsilon - z_nb_{23}\alpha_{32}\left(x_n + y_n + \frac{a_3}{\alpha_{33}}\right)\varepsilon - \left(x_n + y_n + \frac{a_3}{\alpha_{33}}\right)^2\alpha_{33}\varepsilon \\
&+ h\left(- (x_n + y_n)z_nb_{23}\alpha_{32} + \frac{a_3^2}{\alpha_{33}} - \left(x_n + y_n + \frac{a_3}{\alpha_{33}}\right)^2\alpha_{33}\right), \tag{123} \\
G_1 &= a_1(1 - k_1)\left(y_n + \frac{a_1(1 - k_1)}{\alpha_{11}}\right)\varepsilon - h\left(y_n + \frac{a_1(1 - k_1)}{\alpha_{11}}\right)^2 \\
&+ \frac{ha_1^2(1 - k_1)^2}{\alpha_{11}} - \left(y_n + \frac{a_1(1 - k_1)}{\alpha_{11}}\right)^2\alpha_{11}\varepsilon, \\
H_1 &= -z_n a_2(1 - k_2)\varepsilon + z_n\left(y_n + \frac{a_1(1 - k_1)}{\alpha_{11}}\right)\alpha_{21}\varepsilon + hz_n\alpha_{22} + hy_nz_n\alpha_{22} + z_n^2b_{23}\alpha_{22}\varepsilon.
\end{aligned}$$

Now, from model (122) on the center manifold,

$$W^c(0) = \{(x_n, y_n, z_n) | (y_n, z_n) = (\chi_3(x_n), \chi_4(x_n)), \chi_i(0) = 0, D\chi_i(0) = 0, i = 3, 4\}, \quad (124)$$

where

$$\chi_i(x_n) = a_i x^2 + b_i x^3 + O(x)^4, \quad \text{for } i = 3, 4. \quad (125)$$

From (122) and (124), one has

$$\begin{aligned} \chi_3(-x_n + F_1(x_n, \chi_3, \chi_4)) &= \lambda_2 \chi_3(x_n) + G_1(x_n, \chi_3, \chi_4), \\ \chi_4(-x_n + F_1(x_n, \chi_3, \chi_4)) &= \lambda_3 \chi_4(x_n) + H_1(x_n, \chi_3, \chi_4). \end{aligned} \quad (126)$$

From (126), the calculation yields: $a_3 = b_3 = a_4 = b_4 = 0$. Thus, map (122); restrict to $W^c(0)$ as

$$f(x_n) = -x_n + a_3 \left(x_n + \frac{a_3}{\alpha_{33}}\right) \varepsilon - \left(x_n + \frac{a_3}{\alpha_{33}}\right)^2 \alpha_{33} \varepsilon + h \left(\frac{a_3^2}{\alpha_{33}} - \left(x_n + \frac{a_3}{\alpha_{33}}\right)^2 \alpha_{33}\right). \quad (127)$$

From (117) and (127), the computation yields: $\Omega_1 = 3a_3 - (ha_3^2/\alpha_{33}) \neq 0$ and $\Omega_2 = h^2 \alpha_{33}^2 > 0$. This implies that about P_6 model (15) undergoes flip bifurcation if $\Omega \in \mathcal{F}|_{P_6}$. Moreover, period-2 points bifurcating from P_6 are stable since $\Omega_2 = h^2 \alpha_{33}^2 > 0$. \square

6.7. Analysis of Bifurcation at P_7 . From (64), the computation yields $\lambda_1|_{(68)} = -1$, but $\lambda_{2,3}|_{(68)} = 1 - (2/a_1(1 - k_1)) [a_2(1 - k_2) - (2a_1\alpha_{21}(1 - k_1)/\alpha_{11})]$, $1 + (2/a_1(1 - k_1)) [a_3 - (a_2(1 - k_2)\alpha_{32}/\alpha_{22}) + (a_1\alpha_{21}\alpha_{32}(1 - k_1)/\alpha_{11}\alpha_{22})] \neq 1$ or -1 . This suggests that model (15) could undergo flip bifurcation around P_7 if Ω passes the curve:

$$\mathcal{F}|_{P_7} = \left\{ \Omega: h = \frac{2}{a_1(1 - k_1)} \right\}. \quad (128)$$

The proof of the following theorem shows that model (15) undergoes flip bifurcation around P_7 if $\Omega \in \mathcal{F}|_{P_7}$.

Theorem 15. *Model (15) undergoes flip bifurcation around P_7 if $\Omega \in \mathcal{F}|_{P_7}$.*

Proof. Recall that if $\Omega \in \mathcal{F}|_{P_7}$, then $\lambda_1|_{(68)} = -1$, but $\lambda_{2,3}|_{(68)} = 1 - (2/a_1(1 - k_1)) [a_2(1 - k_2) - (2a_1\alpha_{21}(1 - k_1)/\alpha_{11})]$, $1 + (2/a_1(1 - k_1)) [a_3 - (a_2(1 - k_2)\alpha_{32}/\alpha_{22}) + (a_1\alpha_{21}\alpha_{32}(1 - k_1)/\alpha_{11}\alpha_{22})] \neq 1$ or -1 . So, in the following, flip bifurcation is explored by assuming $h \neq (2\alpha_{11}/(a_2\alpha_{11}(1 - k_2) - 2a_1\alpha_{21}(1 - k_1)))$, $(2\alpha_{11}\alpha_{22}/a_3\alpha_{11}\alpha_{22} - a_2\alpha_{11}\alpha_{32}(1 - k_2) + a_1\alpha_{21}\alpha_{32}(1 - k_1))$. Let

$$\begin{aligned} u_n &= x_n - \frac{(1 - k_1)a_1}{\alpha_{11}}, \\ v_n &= y_n - \frac{a_2(1 - k_2)\alpha_{11} - a_1(1 - k_1)\alpha_{21}}{\alpha_{11}\alpha_{22}}, \end{aligned} \quad (129)$$

$$w_n = z_n.$$

Then, (15) gives

$$\begin{aligned}
\begin{pmatrix} u_{n+1} \\ v_{n+1} \\ w_{n+1} \end{pmatrix} &= \begin{pmatrix} 1 - ha_1(1 - k_1) & 0 & 0 \\ -h\alpha_{21}\left(\frac{a_2(1 - k_2)\alpha_{11} - a_1(1 - k_1)\alpha_{21}}{\alpha_{11}\alpha_{22}}\right) & 1 - h\left(a_2(1 - k_2) - \frac{2a_1\alpha_{21}(1 - k_1)}{\alpha_{11}}\right) & 0 \\ 0 & 0 & 1 + h\left(a_3 - \frac{a_2(1 - k_2)\alpha_{32}}{\alpha_{22}} + \frac{a_1\alpha_{21}\alpha_{32}(1 - k_1)}{\alpha_{11}\alpha_{22}}\right) \end{pmatrix} \\
&\cdot \begin{pmatrix} u_n \\ v_n \\ w_n \end{pmatrix} \\
&+ \left(h\left(\frac{(a_1(1 - k_1))^2}{\alpha_{11}} - \alpha_{11}\left(u_n + \frac{a_1(1 - k_1)}{\alpha_{11}}\right)^2\right) \right. \\
&+ \varepsilon\left(a_1(1 - k_1)\left(u_n + \frac{a_1(1 - k_1)}{\alpha_{11}}\right) - \alpha_{11}\left(u_n + \frac{a_1(1 - k_1)}{\alpha_{11}}\right)^2\right) \\
&\cdot h\left[a_2(1 - k_2)\left(\frac{a_2(1 - k_2)\alpha_{11} - a_1(1 - k_1)\alpha_{21}}{\alpha_{11}\alpha_{22}}\right) + \alpha_{22}\left(v_n + \frac{a_2(1 - k_2)\alpha_{11} - a_1(1 - k_1)\alpha_{21}}{\alpha_{11}\alpha_{22}}\right)^2 \right. \\
&- \left. \alpha_{21}\frac{a_1(1 - k_1)}{\alpha_{11}}\left(\frac{a_2(1 - k_2)\alpha_{11} - a_1(1 - k_1)\alpha_{21}}{\alpha_{11}\alpha_{22}}\right)\right] + \varepsilon\left[a_2(1 - k_2)\left(v_n + \frac{a_2(1 - k_2)\alpha_{11} - a_1(1 - k_1)\alpha_{21}}{\alpha_{11}\alpha_{22}}\right) \right. \\
&- \left. \alpha_{22}\left(v_n + \frac{a_2(1 - k_2)\alpha_{11} - a_1(1 - k_1)\alpha_{21}}{\alpha_{11}\alpha_{22}}\right)^2 \right. \\
&- \left. \alpha_{21}\left(u_n + \frac{a_1(1 - k_1)}{\alpha_{11}}\right)\left(v_n + \frac{a_2(1 - k_2)\alpha_{11} - a_1(1 - k_1)\alpha_{21}}{\alpha_{11}\alpha_{22}}\right)\right] h(-\alpha_{33}w_n^2 - \alpha_{32}v_n w_n) + \varepsilon(a_3 w_n - \alpha_{33}w_n^2 \\
&- \alpha_{32}w_n\left(v_n + \frac{a_2(1 - k_2)\alpha_{11} - a_1(1 - k_1)\alpha_{21}}{\alpha_{11}\alpha_{22}}\right)). \tag{130}
\end{aligned}$$

Using transformation,

$$\begin{pmatrix} u_n \\ v_n \\ w_n \end{pmatrix} = \begin{pmatrix} c_{11} & 0 & 0 \\ 1 & 1 & 0 \\ 0 & 0 & 1 \end{pmatrix} \begin{pmatrix} x_n \\ y_n \\ z_n \end{pmatrix}. \tag{131}$$

(130) gives

$$\begin{pmatrix} x_{n+1} \\ y_{n+1} \\ z_{n+1} \end{pmatrix} = \begin{pmatrix} -1 & 0 & 0 \\ 0 & \lambda_2 & 0 \\ 0 & 0 & \lambda_3 \end{pmatrix} \begin{pmatrix} x_n \\ y_n \\ z_n \end{pmatrix} + \begin{pmatrix} F_2(x_n, y_n, z_n, \varepsilon) \\ G_2(x_n, y_n, z_n, \varepsilon) \\ H_2(x_n, y_n, z_n, \varepsilon) \end{pmatrix}, \tag{132}$$

where

$$\begin{aligned}
 c_{11} &= \frac{\alpha_{11}\alpha_{22}(ha_1(1-k_1) - ha_2(1-k_2) - (2ha_1(1-k_1)\alpha_{21}/\alpha_{11}))}{h\alpha_{21}(a_2(1-k_2)\alpha_{11} - a_1(1-k_1)\alpha_{21})}, \\
 F_2 &= \frac{h[(a_1(1-k_1))^2/\alpha_{11}] - (x_n c_{11} + (a_1(1-k_1)/\alpha_{11}))^2 \alpha_{11}] + \varepsilon[a_1(1-k_1)(x_n c_{11} + (a_1(1-k_1)/\alpha_{11})) - (x_n c_{11} + (a_1(1-k_1)/\alpha_{11}))^2 \alpha_{11}]}{c_{11}}, \\
 G_2 &= h \left[\frac{a_2(1-k_2)(a_2 a_{11}(1-k_2) - a_1(1-k_1)\alpha_{21})}{\alpha_{11}\alpha_{22}} - \frac{a_1(1-k_1)\alpha_{21}(a_2 a_{11}(1-k_2) - a_1(1-k_1)\alpha_{21})}{\alpha_{11}^2 \alpha_{22}} \right. \\
 &\quad \left. + \left(x_n + y_n + \frac{a_2 a_{11}(1-k_2) - a_1(1-k_1)\alpha_{21}}{\alpha_{11}\alpha_{22}} \right)^2 \alpha_{22} \right] \\
 &\quad \cdot \frac{h[(a_1(1-k_1))^2/\alpha_{11}] - (x_n c_{11} + (a_1(1-k_1)/\alpha_{11}))^2 \alpha_{11}] + \varepsilon[a_1(1-k_1)(x_n c_{11} + (a_1(1-k_1)/\alpha_{11})) - (x_n c_{11} + (a_1(1-k_1)/\alpha_{11}))^2 \alpha_{11}]}{c_{11}} \\
 &\quad + \varepsilon \left[a_2(1-k_2) \left(x_n + y_n + \frac{a_2 a_{11}(1-k_2) - a_1(1-k_1)\alpha_{21}}{\alpha_{11}\alpha_{22}} \right) \right. \\
 &\quad \left. + \frac{a_1(1-k_1)\alpha_{21}(x_n + y_n + ((a_2 a_{11}(1-k_2) - a_1(1-k_1)\alpha_{21})/\alpha_{11}\alpha_{22}))^3 (x_n c_{11} ((a_2 a_{11}(1-k_2) - a_1(1-k_1)\alpha_{21})/\alpha_{11}\alpha_{22})) \alpha_{22}}{a_{11}} \right], \\
 H_2 &= h(-x_n + y_n)z_n \alpha_{32} - z^2 \alpha_{33} + \varepsilon \left[z_n a_3 - z_n \left(x_n + y_n + \frac{a_2 a_{11}(1-k_2) - a_1(1-k_1)\alpha_{21}}{\alpha_{11}\alpha_{22}} \right) \alpha_{32} - z_n^2 \alpha_{33} \right].
 \end{aligned}
 \tag{133}$$

Now, using system (132) on the center manifold,

$$W^c(0) = \{ (x_n, y_n, z_n) \mid (y_n, z_n) = (\chi_5(x_n), \chi_6(x_n)), \chi_i(0) = 0, D\chi_i(0) = 0, i = 5, 6 \},
 \tag{134}$$

where

$$\chi_i(x_n) = a_i x^2 + b_i x^3 + O(x)^4, \quad \text{for } i = 5, 6.
 \tag{135}$$

In view of (132) and (134), we obtain

$$\begin{aligned}
 \chi_5(-x_n + F_2(x_n, \chi_5, \chi_6)) &= \lambda_2 \chi_5(x_n) + G_2(x_n, \chi_5, \chi_6), \\
 \chi_6(-x_n + F_2(x_n, \chi_5, \chi_6)) &= \lambda_3 \chi_6(x_n) + H_2(x_n, \chi_5, \chi_6).
 \end{aligned}
 \tag{136}$$

From (136), one gets: $a_5 = b_5 = a_6 = b_6 = 0$. Finally, map (132); restrict to $W^c(0)$ as

$$f(x_n) = -x_n + \frac{h[(a_1(1-k_1))^2/\alpha_{11}] - (x_n c_{11} + (a_1(1-k_1)/\alpha_{11}))^2 \alpha_{11}] + \varepsilon[a_1(1-k_1)(x_n c_{11} + (a_1(1-k_1)/\alpha_{11})) - (x_n c_{11} + (a_1(1-k_1)/\alpha_{11}))^2 \alpha_{11}]}{c_{11}} \tag{137}$$

From (117) and (137), the computation yields: $\Omega_1 = a_1(1 - k_1)(1 - 2c_{11}) \neq 0$. Moreover, $\Omega_2 = (h\alpha_{11}c_{11} + 2\alpha_{11}c_{11}\varepsilon)^2 > 0$. This implies that about P_7 model (15) undergoes flip bifurcation if $\Omega \in \mathcal{F}|_{P_7}$. Moreover, period-2 points bifurcating from P_7 are stable since $\Omega_2 = (h\alpha_{11}c_{11} + 2\alpha_{11}c_{11}\varepsilon)^2 > 0$. \square

6.8. Analysis of Bifurcation at P_8 . From (71), the computation yields $\lambda_1|_{(75)} = -1$, but $\lambda_{2,3}|_{(75)} = 1 - (2/a_1(1 - k_1)) [a_2(1 - k_2) - (2a_1\alpha_{21}(1 - k_1)/\alpha_{11})]$, $1 - (2/a_1(1 - k_1)) [a_3 - (a_2(1 - k_2)\alpha_{32}/\alpha_{22}) + (a_1\alpha_{21}\alpha_{32}(1 - k_1)/\alpha_{11}\alpha_{22})] \neq 1$ or -1 . This suggests that model (15) could undergo flip bifurcation around P_8 if Ω passes the curve:

$$\mathcal{F}|_{P_8} = \left\{ \Omega: h = \frac{2}{a_1(1 - k_1)} \right\}. \tag{138}$$

The proof of the following theorem shows that model (15) undergoes flip bifurcation around P_8 if $\Omega \in \mathcal{F}|_{P_8}$.

Theorem 16. Model (15) undergoes flip bifurcation around P_8 if $\Omega \in \mathcal{F}|_{P_8}$.

Proof. Recall that if $\Omega \in \mathcal{F}|_{P_8}$, then $\lambda_1|_{(75)} = -1$, but $\lambda_{2,3}|_{(75)} = 1 - (2/a_1(1 - k_1)) [a_2(1 - k_2) - (2a_1\alpha_{21}(1 - k_1)/\alpha_{11})]$, $1 - (2/a_1(1 - k_1)) [a_3 - (a_2(1 - k_2)\alpha_{32}/\alpha_{22}) + (a_1\alpha_{21}\alpha_{32}(1 - k_1)/\alpha_{11}\alpha_{22})] \neq 1$ or -1 . So, in the following, flip bifurcation is explored by assuming $h \neq (2\alpha_{11}/(a_2\alpha_{11}(1 - k_2) - 2a_1\alpha_{21}(1 - k_1)))$, $(2\alpha_{11}\alpha_{22}/(a_3\alpha_{11}\alpha_{22} - a_2\alpha_{11}\alpha_{32}(1 - k_2) + a_1\alpha_{21}\alpha_{32}(1 - k_1)))$. Let

$$\begin{aligned} u_n &= x_n - \frac{(1 - k_1)a_1}{\alpha_{11}}, \\ v_n &= y_n - \frac{a_2(1 - k_2)\alpha_{11} - a_1(1 - k_1)\alpha_{21}}{\alpha_{11}\alpha_{22}}, \\ w_n &= z_n - \frac{a_3\alpha_{11}\alpha_{22} - a_2(1 - k_2)\alpha_{11}\alpha_{32} + a_1(1 - k_1)\alpha_{21}\alpha_{32}}{\alpha_{11}\alpha_{22}\alpha_{33}}. \end{aligned} \tag{139}$$

Then, (15) becomes

$$\begin{pmatrix} u_{n+1} \\ v_{n+1} \\ w_{n+1} \end{pmatrix} = \begin{pmatrix} 1 - ha_1(1 - k_1) & 0 & 0 \\ -h\alpha_{21}\left(\frac{a_2(1 - k_2)\alpha_{11} - a_1(1 - k_1)\alpha_{21}}{\alpha_{11}\alpha_{22}}\right) & 1 - h\left(a_2(1 - k_2) - \frac{2a_1\alpha_{21}(1 - k_1)}{\alpha_{11}}\right) & 0 \\ 0 & -h\alpha_{32}\left(\frac{a_3\alpha_{11}\alpha_{22} - a_2(1 - k_2)\alpha_{11}\alpha_{32} + a_1(1 - k_1)\alpha_{21}\alpha_{32}}{\alpha_{11}\alpha_{22}\alpha_{33}}\right) & 1 - h\left(a_3 - \frac{a_2(1 - k_2)\alpha_{32}}{\alpha_{22}} + \frac{a_1\alpha_{21}\alpha_{32}(1 - k_1)}{\alpha_{11}\alpha_{22}}\right) \end{pmatrix} \begin{pmatrix} u_n \\ v_n \\ w_n \end{pmatrix} + \begin{pmatrix} F_3(x_n, y_n, z_n, \varepsilon) \\ G_3(x_n, y_n, z_n, \varepsilon) \\ H_3(x_n, y_n, z_n, \varepsilon) \end{pmatrix}, \tag{140}$$

where

$$\begin{aligned}
 F_3 &= h \left(\frac{(a_1(1-k_1))^2}{\alpha_{11}} - \alpha_{11} \left(u_n + \frac{a_1(1-k_1)}{\alpha_{11}} \right)^2 \right) + \varepsilon \left(a_1(1-k_1) \left(u_n + \frac{a_1(1-k_1)}{\alpha_{11}} \right) - \alpha_{11} \left(u_n + \frac{a_1(1-k_1)}{\alpha_{11}} \right)^2 \right), \\
 G_3 &= h \left(a_2(1-k_2) \left(\frac{a_2(1-k_2)\alpha_{11} - a_1(1-k_1)\alpha_{21}}{\alpha_{11}\alpha_{22}} \right) \right. \\
 &\quad - \alpha_{21} \left(v_n + \frac{a_2(1-k_2)\alpha_{11} - a_1(1-k_1)\alpha_{21}}{\alpha_{11}\alpha_{22}} \right)^2 - \alpha_{21}u_nv_n \\
 &\quad - \alpha_{21} \frac{a_1(1-k_1)}{\alpha_{11}} \left(\frac{a_2(1-k_2)\alpha_{11} - a_1(1-k_1)\alpha_{21}}{\alpha_{11}\alpha_{22}} \right) \left. \right) \\
 &\quad + \varepsilon \left(a_2(1-k_2) \left(v_n + \frac{a_2(1-k_2)\alpha_{11} - a_1(1-k_1)\alpha_{21}}{\alpha_{11}\alpha_{22}} \right) - \alpha_{22} \left(v_n + \frac{a_2(1-k_2)\alpha_{11} - a_1(1-k_1)\alpha_{21}}{\alpha_{11}\alpha_{22}} \right)^2 \right. \\
 &\quad \left. - \alpha_{21} \left(u_n + \frac{a_1(1-k_1)}{\alpha_{11}} \right) \left(v_n + \frac{a_2(1-k_2)\alpha_{11} - a_1(1-k_1)\alpha_{21}}{\alpha_{11}\alpha_{22}} \right) \right), \\
 H_3 &= h \left(a_3 \left(\frac{a_3\alpha_{11}\alpha_{22} - a_2(1-k_2)\alpha_{11}\alpha_{32} + a_1(1-k_1)\alpha_{21}\alpha_{32}}{\alpha_{11}\alpha_{22}\alpha_{33}} \right) - \alpha_{32}v_nw_n \right. \\
 &\quad - \alpha_{33} \left(w_n + \frac{a_3\alpha_{11}\alpha_{22} - a_2(1-k_2)\alpha_{11}\alpha_{32} + a_1(1-k_1)\alpha_{21}\alpha_{32}}{\alpha_{11}\alpha_{22}\alpha_{33}} \right)^2 \\
 &\quad - \alpha_{32} \frac{a_2(1-k_2)\alpha_{11} - a_1(1-k_1)\alpha_{21}}{\alpha_{11}\alpha_{22}} \left(\frac{a_3\alpha_{11}\alpha_{22} - a_2(1-k_2)\alpha_{11}\alpha_{32} + a_1(1-k_1)\alpha_{21}\alpha_{32}}{\alpha_{11}\alpha_{22}\alpha_{33}} \right) \left. \right) \\
 &\quad + \varepsilon \left(a_3 \left(w_n + \frac{a_3\alpha_{11}\alpha_{22} - a_2(1-k_2)\alpha_{11}\alpha_{32} + a_1(1-k_1)\alpha_{21}\alpha_{32}}{\alpha_{11}\alpha_{22}\alpha_{33}} \right) \right. \\
 &\quad - \alpha_{33} \left(w_n + \frac{a_3\alpha_{11}\alpha_{22} - a_2(1-k_2)\alpha_{11}\alpha_{32} + a_1(1-k_1)\alpha_{21}\alpha_{32}}{\alpha_{11}\alpha_{22}\alpha_{33}} \right)^2 - \alpha_{32} \left(v_n + \frac{a_2(1-k_2)\alpha_{11} - a_1(1-k_1)\alpha_{21}}{\alpha_{11}\alpha_{22}} \right) \\
 &\quad \left. \varepsilon \times \left(w_n + \frac{a_3\alpha_{11}\alpha_{22} - a_2(1-k_2)\alpha_{11}\alpha_{32} + a_1(1-k_1)\alpha_{21}\alpha_{32}}{\alpha_{11}\alpha_{22}\alpha_{33}} \right) \right).
 \end{aligned} \tag{141}$$

Now, by utilizing transformation,

$$\begin{pmatrix} u_n \\ v_n \\ w_n \end{pmatrix} = \begin{pmatrix} d_{11} & 0 & 0 \\ d_{21} & d_{22} & 0 \\ 1 & 1 & 1 \end{pmatrix} \begin{pmatrix} x_n \\ y_n \\ z_n \end{pmatrix}, \tag{142}$$

gives

$$\begin{pmatrix} x_{n+1} \\ y_{n+1} \\ z_{n+1} \end{pmatrix} = \begin{pmatrix} -1 & 0 & 0 \\ 0 & \lambda_2 & 0 \\ 0 & 0 & \lambda_3 \end{pmatrix} \begin{pmatrix} x_n \\ y_n \\ z_n \end{pmatrix} + \begin{pmatrix} F_2^*(x_n, y_n, z_n, \varepsilon) \\ G_2^*(x_n, y_n, z_n, \varepsilon) \\ H_2^*(x_n, y_n, z_n, \varepsilon) \end{pmatrix}, \tag{143}$$

where

$$\begin{aligned}
 d_{11} &= \frac{\alpha_{11}^2 (ha_1 - ha_1 k_1 - ha_2 (1 - k_2) - (2ha_1 (1 - k_1) \alpha_{21} / \alpha_{11})) \alpha_{22}^2 \alpha_{33} (ha_1 - ha_1 k_1 - h(a_3 - (a_2 (1 - k_2) \alpha_{32} / \alpha_{22}) + (a_1 (1 - k_1) \alpha_{21} \alpha_{32} / \alpha_{11} \alpha_{22})))}{h^2 \alpha_{21} (a_2 (1 - k_2) \alpha_{11} - a_1 (1 - k_1) \alpha_{21}) \alpha_{32} (a_3 \alpha_{11} \alpha_{22} - a_2 (1 - k_2) \alpha_{11} \alpha_{32} + a_1 (1 - k_1) \alpha_{21} \alpha_{32})}, \\
 d_{21} &= \frac{\alpha_{11} \alpha_{22} (ha_1 - ha_1 k_1 - h(a_3 - (a_2 (1 - k_2) \alpha_{32} / \alpha_{22}) + (a_1 (1 - k_1) \alpha_{21} \alpha_{32} / \alpha_{11} \alpha_{22}))) \alpha_{33}}{h \alpha_{32} (a_3 \alpha_{11} \alpha_{22} - a_2 (1 - k_2) \alpha_{11} \alpha_{32} + a_1 (1 - k_1) \alpha_{21} \alpha_{32})}, \\
 d_{22} &= \frac{\alpha_{33} (-a_2 \alpha_{11} \alpha_{22} + a_3 \alpha_{11} \alpha_{22} + a_2 k_2 \alpha_{11} \alpha_{22} - 2a_1 \alpha_{21} \alpha_{22} + 2a_1 k_1 \alpha_{21} \alpha_{22} - a_2 \alpha_{11} \alpha_{32} + a_2 k_2 \alpha_{11} \alpha_{32} + a_1 \alpha_{21} \alpha_{32} - a_1 k_1 \alpha_{21} \alpha_{32})}{\alpha_{32} (a_3 \alpha_{11} \alpha_{22} - a_2 \alpha_{11} \alpha_{32} + a_2 k_2 \alpha_{11} \alpha_{32} + a_1 \alpha_{21} \alpha_{32} - a_1 k_1 \alpha_{21} \alpha_{32})}, \\
 F_2^* &= \frac{h(((a_1 (1 - k_1))^2 / \alpha_{11}) - (x_n d_{11} + (a_1 (1 - k_1) / \alpha_{11}))^2 \alpha_{11}) + \varepsilon(a_1 (1 - k_1) (x_n d_{11} + (a_1 (1 - k_1) / \alpha_{11})) - (x_n d_{11} + (a_1 (1 - k_1) / \alpha_{11}))^2 \alpha_{11})}{d_{11}}, \\
 G_2^* &= \frac{d_{21} (h(((a_1 (1 - k_1))^2 / \alpha_{11}) - (x_n d_{11} + (a_1 (1 - k_1) / \alpha_{11}))^2 \alpha_{11}) + \varepsilon(a_1 (1 - k_1) (x_n d_{11} + (a_1 (1 - k_1) / \alpha_{11})) - (x_n d_{11} + (a_1 (1 - k_1) / \alpha_{11}))^2 \alpha_{11}))}{d_{11} d_{22}} \\
 &+ \frac{h}{d_{22}} \left(-x_n d_{11} (d_{21} x_n + d_{22} y_n) \alpha_{21} - \alpha_{21} \left(d_{21} x_n + d_{22} y_n + \frac{a_2 a_{11} (1 - k_2) - a_1 (1 - k_1) \alpha_{21}}{\alpha_{11} \alpha_{22}} \right)^2 \right. \\
 &+ \frac{a_2 (1 - k_2) (a_2 a_{11} (1 - k_2) - a_1 (1 - k_1) \alpha_{21})}{\alpha_{11} \alpha_{22}} - \frac{a_1 (1 - k_1) \alpha_{21} (a_2 a_{11} (1 - k_2) - a_1 (1 - k_1) \alpha_{21})}{\alpha_{11}^2 \alpha_{22}} \left. \right) \\
 &+ \frac{\varepsilon}{d_{22}} \left(a_2 (1 - k_2) \left(d_{21} x_n + d_{22} y_n + \frac{a_2 a_{11} (1 - k_2) - a_1 (1 - k_1) \alpha_{21}}{\alpha_{11} \alpha_{22}} \right) \right. \\
 &- \frac{a_1 (1 - k_1) \alpha_{21} (d_{11} x_n + (a_1 (1 - k_1) / \alpha_{11})) (d_{21} x_n + d_{22} y_n + ((a_2 a_{11} (1 - k_2) - a_1 (1 - k_1) \alpha_{21}) / \alpha_{11} \alpha_{22}))}{\alpha_{11}} \\
 &\left. - \left(d_{21} x_n + d_{22} y_n + \frac{a_2 a_{11} (1 - k_2) - a_1 (1 - k_1) \alpha_{21}}{\alpha_{11} \alpha_{22}} \right)^2 \alpha_{22} \right), \\
 H_2^* &= h \left(-(y_n + 2z_n) (d_{21} x_n + d_{22} y_n) \alpha_{32} - \alpha_{32} \left(x_n + y_n + z_n + \frac{a_3 \alpha_{11} \alpha_{22} - a_2 (1 - k_2) \alpha_{11} \alpha_{32} + a_1 (1 - k_1) \alpha_{21} \alpha_{32}}{\alpha_{11} \alpha_{22} \alpha_{33}} \right)^2 \right. \\
 &+ \frac{a_3 (a_3 \alpha_{11} \alpha_{22} - a_2 (1 - k_2) \alpha_{11} \alpha_{32} + a_1 (1 - k_1) \alpha_{21} \alpha_{32})}{\alpha_{11} \alpha_{22} \alpha_{33}} \\
 &- \frac{(a_2 a_{11} (1 - k_2) - a_1 (1 - k_1) \alpha_{21}) \alpha_{32} (a_3 \alpha_{11} \alpha_{22} - a_2 (1 - k_2) \alpha_{11} \alpha_{32} + a_1 (1 - k_1) \alpha_{21} \alpha_{32})}{\alpha_{11}^2 \alpha_{22}^2 \alpha_{33}} \left. \right) \\
 &+ \frac{(d_{21} - d_{22}) (h(((a_1 (1 - k_1))^2 / \alpha_{11}) - (d_{11} x_n + (a_1 (1 - k_1) / \alpha_{11}))^2 \alpha_{11}) + \varepsilon(a_1 (1 - k_1) (d_{11} x_n + (a_1 (1 - k_1) / \alpha_{11})) - (d_{11} x_n + (a_1 (1 - k_1) / \alpha_{11}))^2 \alpha_{11}))}{d_{11} d_{22}} \\
 &- \frac{h}{d_{22}} \left(-d_{11} x_n (d_{21} x_n + d_{22} y_n) \alpha_{21} - \alpha_{21} \left(d_{21} x_n + d_{22} y_n + \frac{a_2 a_{11} (1 - k_2) - a_1 (1 - k_1) \alpha_{21}}{\alpha_{11} \alpha_{22}} \right)^2 \right. \\
 &+ \frac{a_2 (1 - k_2) (a_2 a_{11} (1 - k_2) - a_1 (1 - k_1) \alpha_{21})}{\alpha_{11} \alpha_{22}} - \frac{a_1 (1 - k_1) \alpha_{21} (a_2 a_{11} (1 - k_2) - a_1 (1 - k_1) \alpha_{21})}{\alpha_{11}^2 \alpha_{22}} \left. \right) \\
 &+ \frac{\varepsilon}{d_{22}} \left(a_2 (1 - k_2) \left(d_{21} x_n + d_{22} y_n + \frac{a_2 a_{11} (1 - k_2) - a_1 (1 - k_1) \alpha_{21}}{\alpha_{11} \alpha_{22}} \right) \right. \\
 &- \frac{a_1 (1 - k_1) \alpha_{21} (d_{11} x_n + (a_1 (1 - k_1) / \alpha_{11})) (d_{21} x_n + d_{22} y_n + ((a_2 a_{11} (1 - k_2) - a_1 (1 - k_1) \alpha_{21}) / \alpha_{11} \alpha_{22}))}{\alpha_{11}} \\
 &\left. - \left(d_{21} x_n + d_{22} y_n + \frac{a_2 a_{11} (1 - k_2) - a_1 (1 - k_1) \alpha_{21}}{\alpha_{11} \alpha_{22}} \right)^2 \alpha_{22} \right) \\
 &+ \varepsilon \left(a_3 \left(x_n + y_n + z_n + \frac{a_3 \alpha_{11} \alpha_{22} - a_2 (1 - k_2) \alpha_{11} \alpha_{32} + a_1 (1 - k_1) \alpha_{21} \alpha_{32}}{\alpha_{11} \alpha_{22} \alpha_{33}} \right) \right. \\
 &- \alpha_{32} \left(d_{21} x_n + d_{22} y_n + \frac{a_2 a_{11} (1 - k_2) - a_1 (1 - k_1) \alpha_{21}}{\alpha_{11} \alpha_{22}} \right) \\
 &\times \left(x_n + y_n + z_n + \frac{a_3 \alpha_{11} \alpha_{22} - a_2 (1 - k_2) \alpha_{11} \alpha_{32} + a_1 (1 - k_1) \alpha_{21} \alpha_{32}}{\alpha_{11} \alpha_{22} \alpha_{33}} \right) \\
 &\left. - \left(x_n + y_n + z_n + \frac{a_3 \alpha_{11} \alpha_{22} - a_2 (1 - k_2) \alpha_{11} \alpha_{32} + a_1 (1 - k_1) \alpha_{21} \alpha_{32}}{\alpha_{11} \alpha_{22} \alpha_{33}} \right)^2 \alpha_{33} \right).
 \end{aligned} \tag{144}$$

Now, from system (143) on the center manifold

$$W^c(0) = \{(x_n, y_n, z_n) | (y_n, z_n) = (\chi_7(x_n), \chi_8(x_n)), \chi_i(0) = 0, D\chi_i(0) = 0, i = 7, 8\}, \tag{145}$$

where

$$\chi_i(x_n) = a_i x^2 + b_i x^3 + O(x)^4, \quad \text{for } i = 7, 8. \tag{146}$$

From (143) and (145), we obtain

$$\begin{aligned} \chi_7(-x_n + F_2^*(x_n, \chi_7, \chi_8)) &= \lambda_2 \chi_7(x_n) + G_2^*(x_n, \chi_7, \chi_8), \\ \chi_8(-x_n + F_2^*(x_n, \chi_7, \chi_8)) &= \lambda_3 \chi_8(x_n) + H_2^*(x_n, \chi_7, \chi_8). \end{aligned} \tag{147}$$

From (147), computation yields: $a_7 = b_7 = a_8 = b_8 = 0$. Finally, map (143); restrict to $W^c(0)$ as

$$f_1^*(x_n) = -x_n + \frac{h[(a_1(1-k_1)/\alpha_{11}) - (x_n d_{11} + (a_1(1-k_1)/\alpha_{11}))^2 \alpha_{11}] + \varepsilon[a_1(1-k_1)(x_n d_{11} + (a_1(1-k_1)/\alpha_{11})) - (x_n d_{11} + (a_1(1-k_1)/\alpha_{11}))^2 \alpha_{11}]}{d_{11}}. \tag{148}$$

From (117) and (148), the computation yields: $\Omega_1 = a_1(1-k_1)(1-2d_{11}) \neq 0$. Moreover, $\Omega_2 = (h\alpha_{11}d_{11} + 2\alpha_{11}d_{11}\varepsilon)^2 > 0$. This implies that about P_8 model (15) undergoes flip bifurcation if $\Omega \in \mathcal{F}|_{P_8}$. Moreover, period-2 points bifurcating from P_8 are stable since $\Omega_2 = (h\alpha_{11}d_{11} + 2\alpha_{11}d_{11}\varepsilon)^2 > 0$. \square

7. Numerical Simulations

Numerical simulations of three-species model (15) are performed in this section to check previous theoretical findings and to show rich dynamical behaviors. In this regard, following eight cases are presented to address the accuracy of theoretical results obtained about fixed points for model (15):

Case I: if $a_1 = 4.1, a_2 = 4.2, a_3 = 0.08, k_1 = 2.2, k_2 = 0.6, \alpha_{11} = 0.04, \alpha_{22} = 0.4, \alpha_{21} = 0.09, \alpha_{32} = 0.09$, and $\alpha_{33} = 0.4$, then, from (29), one gets $h = 0.4065040650406504$. From (27), if $h = 0.01 < \min\{0.4065040650406504, 0.20703933747412007\}$ and starting from (0.9, 0.1, 0.2), then Figure 1(a) indicates that P_1 of (15) is a source. However, if $h = 0.5 > \max\{0.4065040650406504, 0.2070393374741\}$, then Figure 1(b) indicates that P_1 of (15) is a saddle. Hence, theoretical results obtained in Lemma 2 coincide with numerical simulations.

Case II: if $a_1 = 4.1, a_2 = 4.2, a_3 = 2.7, k_1 = 2.2, k_2 = 0.6, \alpha_{11} = 1.2, \alpha_{22} = 1.4, \alpha_{21} = 1.9, \alpha_{32} = 0.9$, and $\alpha_{33} = 0.4$, then, from (35), one gets $h = 0.7407407407407407$. Figure 2(a) indicates if $h = 0.01 < 0.7407407407407407$, then P_2 of (15) is a sink. However, if $h = 0.95 > 0.7407407407407407$, then Figure 2(b) indicates that P_2 is unstable. Moreover, if $h = 0.7407407407407407$, then P_2 exchanges the stability,

and in fact, flip bifurcation takes place by Theorem 10. Therefore, the flip bifurcation diagrams are presented in Figure 3. Finally, maximum Lyapunov exponents corresponding to Figure 3 are drawn in Figure 4.

Case III: if $a_1 = 4.1, a_2 = 4.2, a_3 = 2.7, k_1 = 2.2, k_2 = 1.6, \alpha_{11} = 1.2, \alpha_{22} = 1.4, \alpha_{21} = 1.9, \alpha_{32} = 0.9$, and $\alpha_{33} = 0.4$, then, from (42), one gets $h = 0.7936507936507935$. Hence, P_3 is stable if $h < 0.7936507936507935$, and exchange stability is $h = 0.7407407407407407$, and in fact, flip bifurcation takes place by Theorem 11. Therefore, the flip bifurcation diagrams with initial value (0, 0.3, 0.1) are presented in Figure 5. Finally, maximum Lyapunov exponents corresponding to Figure 5 are drawn in Figure 6.

Case IV: if $a_1 = 5.1, a_2 = 4.2, a_3 = 2.7, k_1 = 0.09, k_2 = 1.6, \alpha_{11} = 1.2, \alpha_{22} = 1.4, \alpha_{21} = 1.9, \alpha_{32} = 0.9$, and $\alpha_{33} = 0.4$, then, from (48), one gets $h = 0.43094160741219567$. Hence, P_4 is stable if $h < 0.43094160741219567$, and exchange stability is $h = 0.43094160741219567$, and in fact, flip bifurcation takes place by Theorem 12. Therefore, the flip bifurcation diagrams with initial value (0.1, 0.2, 0.1) are presented in Figure 7. Finally, maximum Lyapunov exponents corresponding to Figure 7 are drawn in Figure 8.

Case V: if $a_1 = 7.1, a_2 = 4.2, a_3 = 2.7, k_1 = 1.9, k_2 = 1.6, \alpha_{11} = 1.2, \alpha_{22} = 1.4, \alpha_{21} = 1.9, \alpha_{32} = 0.9$, and $\alpha_{33} = 0.4$, then, from (54), one gets $h = 0.31298904538341166$. Hence, P_5 is stable if $h < 0.31298904538341166$, and exchange stability is $h = 0.31298904538341166$, and in fact, flip bifurcation takes place by Theorem 13. Therefore, the flip bifurcation diagrams with initial value (0, 0.1, 0.1) are presented in Figure 9. Finally, maximum Lyapunov exponents corresponding to Figure 9 are drawn in Figure 10.

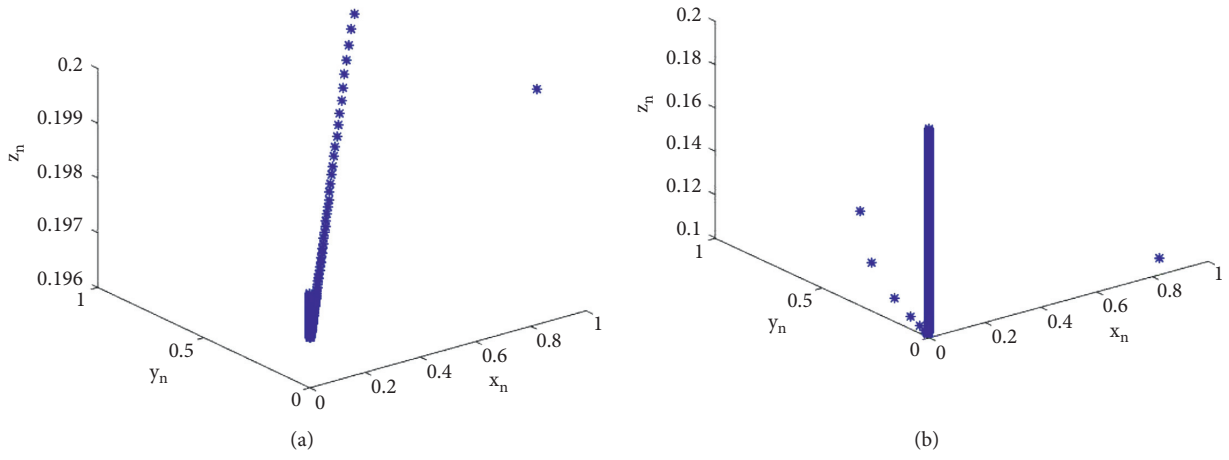


FIGURE 1: Phase portrait about P_1 .

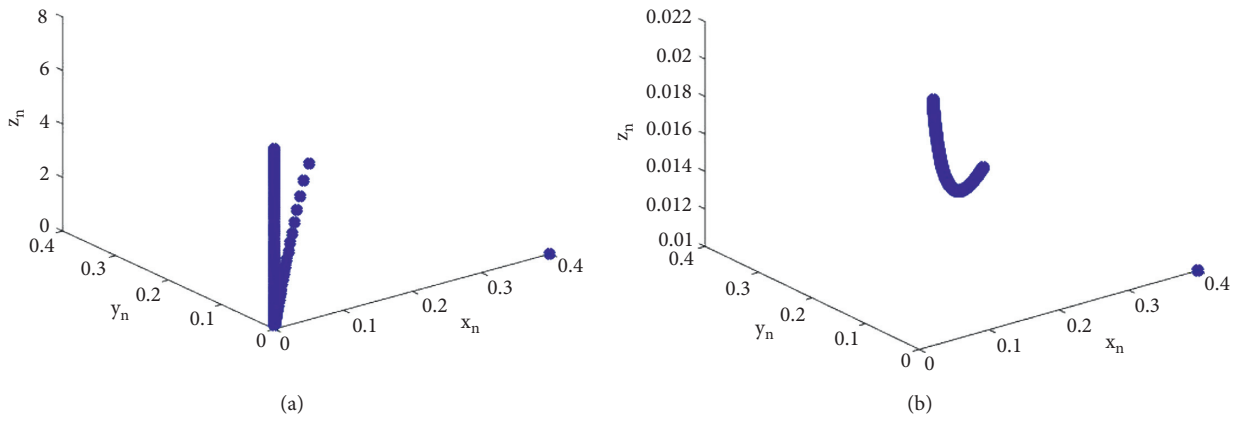


FIGURE 2: Phase portrait about P_2 .

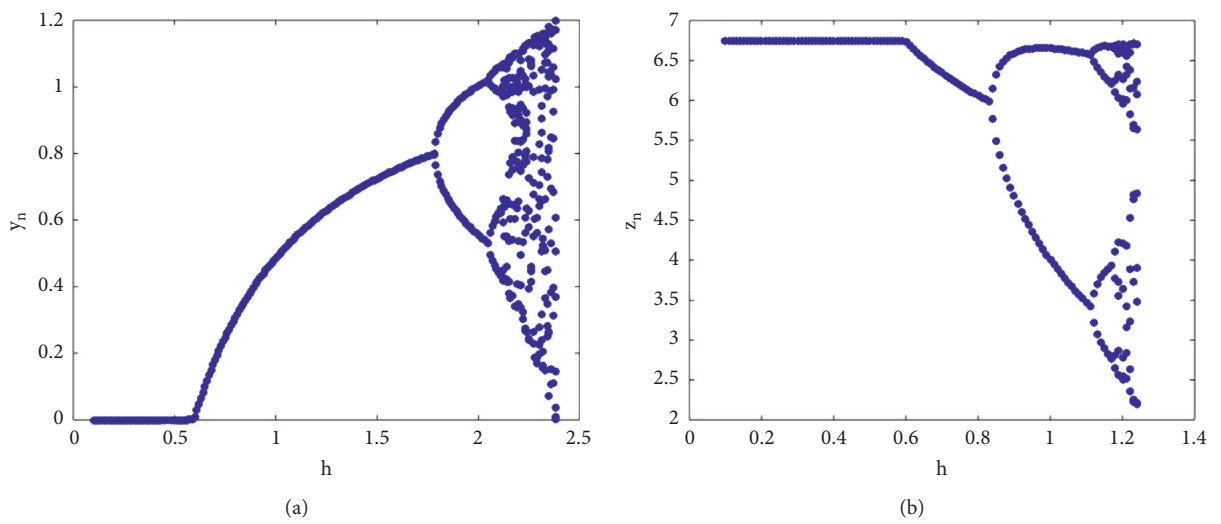


FIGURE 3: Continued.

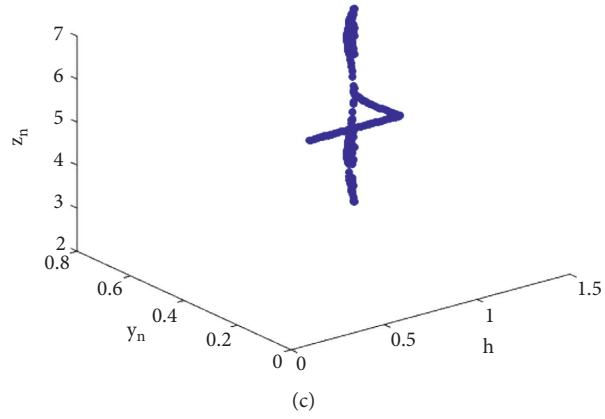


FIGURE 3: Flip bifurcation diagrams at P_2 , where $h \in [0.1, 6.4]$.

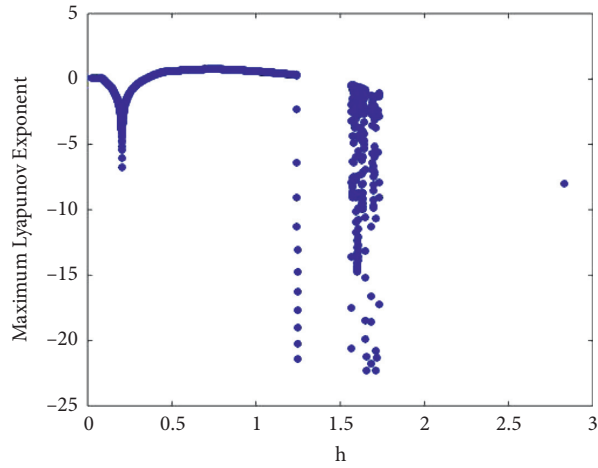


FIGURE 4: Maximum Lyapunov exponents corresponding to Figure 3.

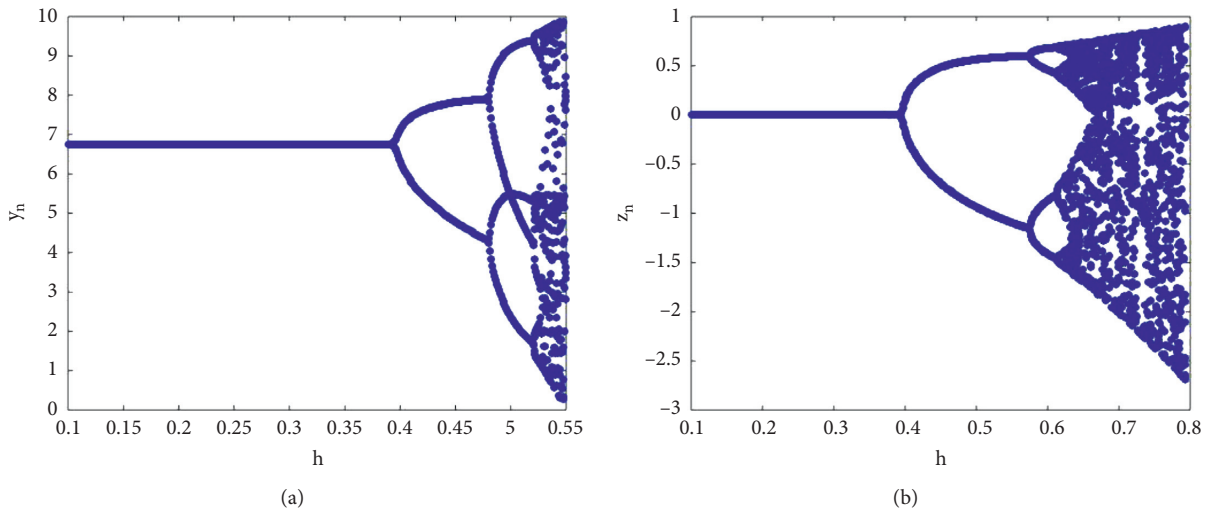


FIGURE 5: Continued.

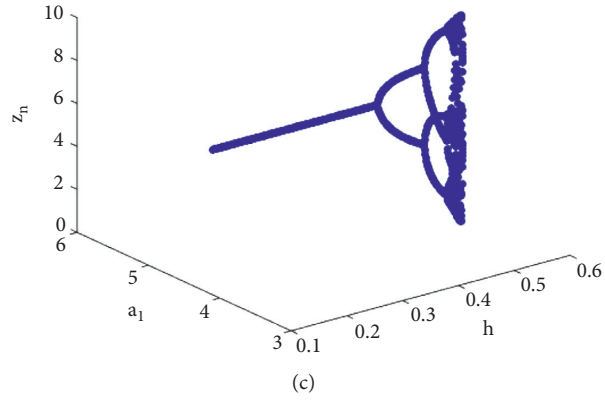


FIGURE 5: Flip bifurcation diagrams at P_3 , where $h \in [0.1, 1.4]$.

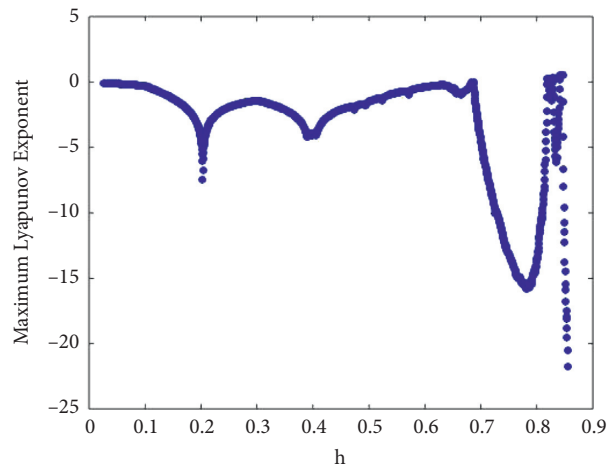


FIGURE 6: Maximum Lyapunov exponents corresponding to Figure 5.

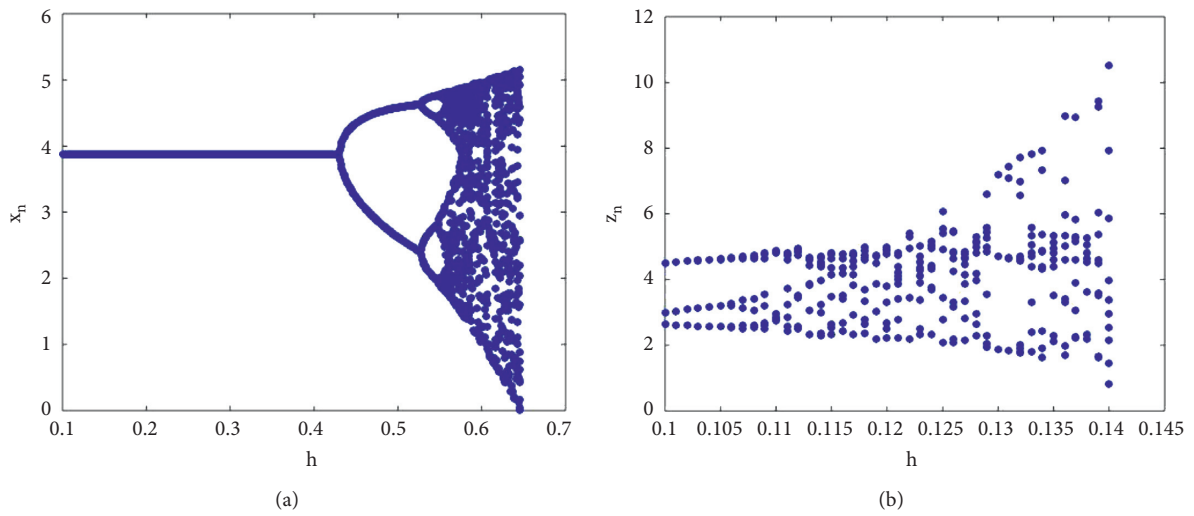


FIGURE 7: Continued.

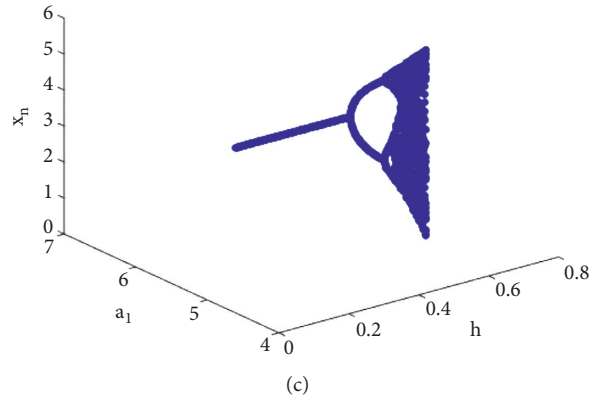


FIGURE 7: Flip bifurcation diagrams at P_4 , where $h \in [0; 1; 1:4]$.

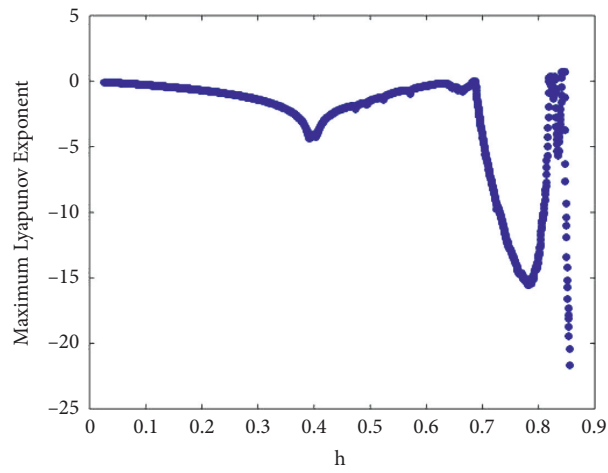


FIGURE 8: Maximum Lyapunov exponents corresponding to Figure 7.

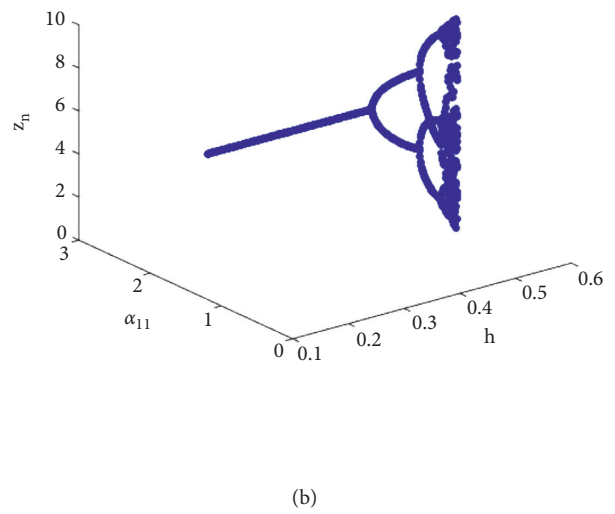
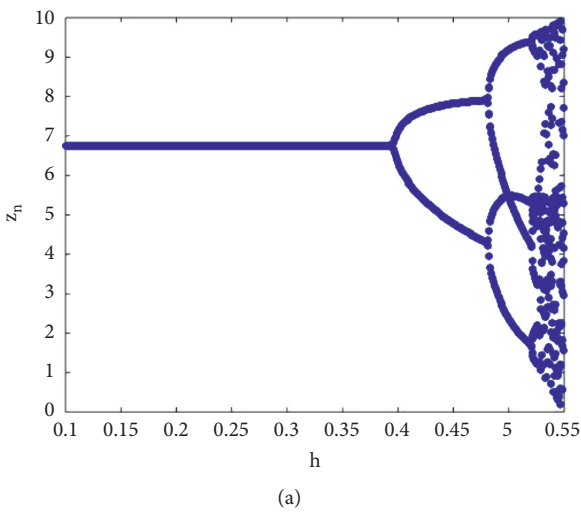


FIGURE 9: Continued.

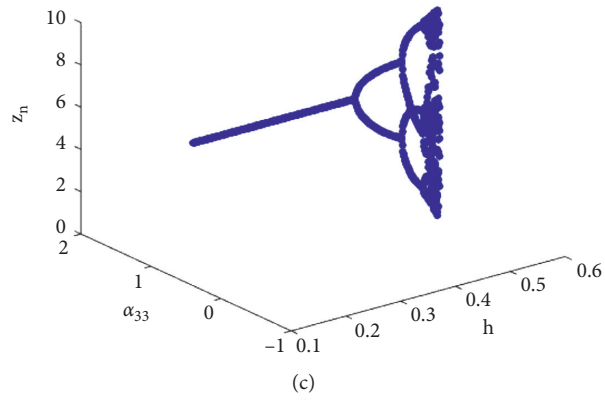


FIGURE 9: Flip bifurcation diagrams at P_5 , where $h \in [0.1, 1.4]$.

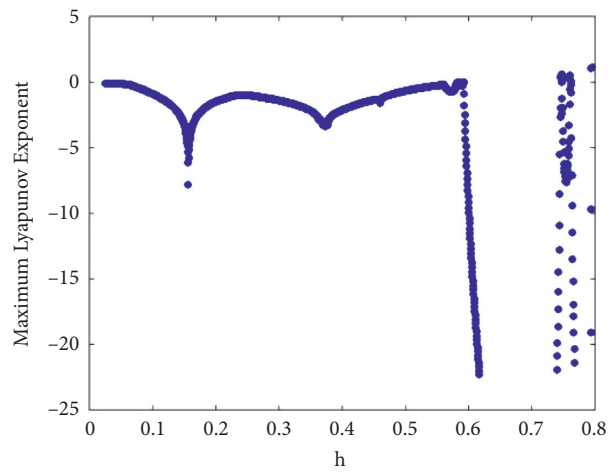


FIGURE 10: Maximum Lyapunov exponents corresponding to Figure 9.

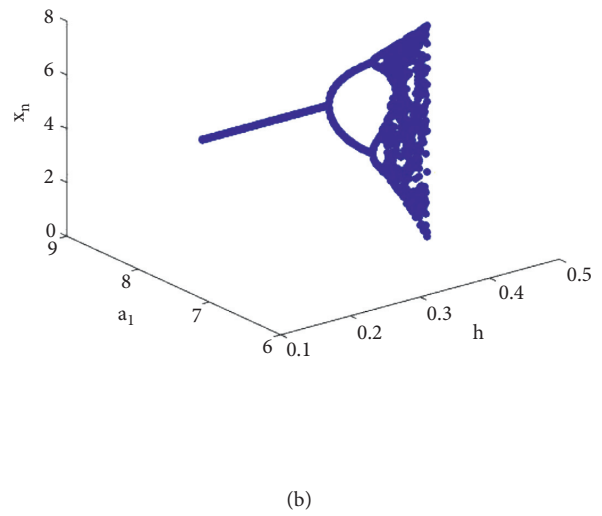
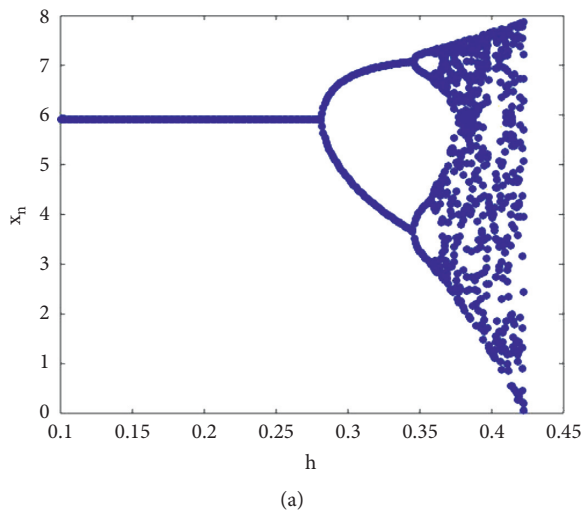


FIGURE 11: Continued.

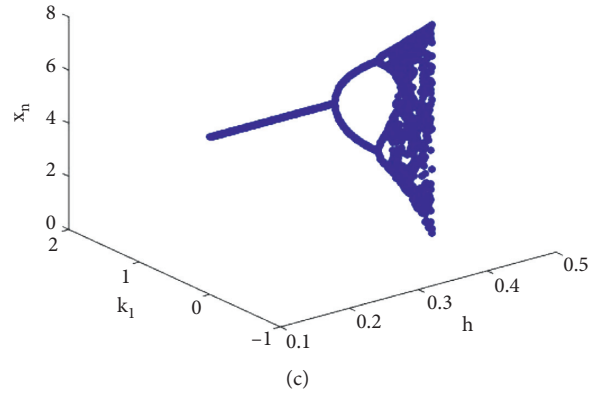


FIGURE 11: Flip bifurcation diagrams at P_6 , where $h \in [0.1, 1.4]$.

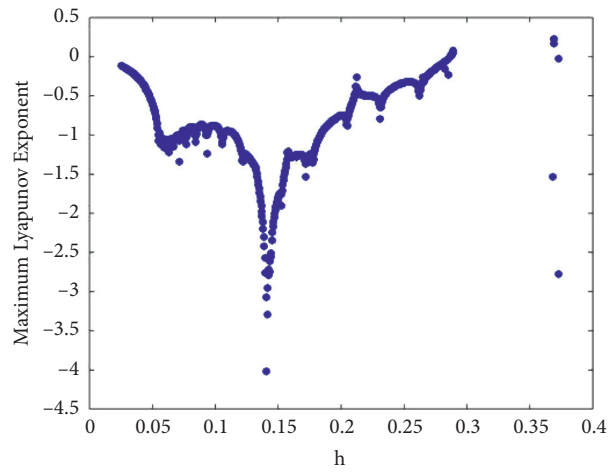


FIGURE 12: Maximum Lyapunov exponents corresponding to Figure 11.

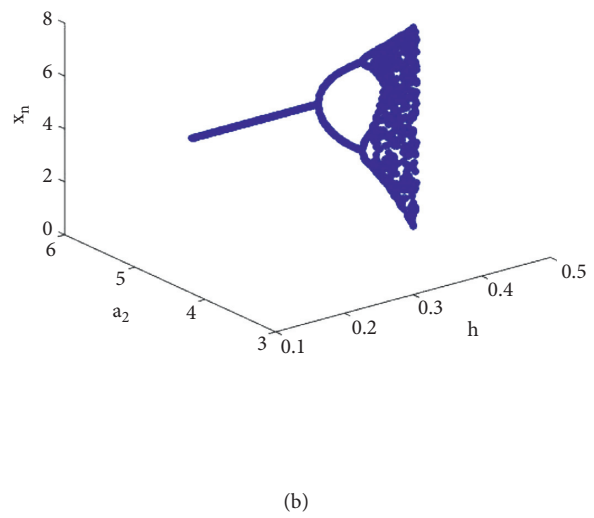
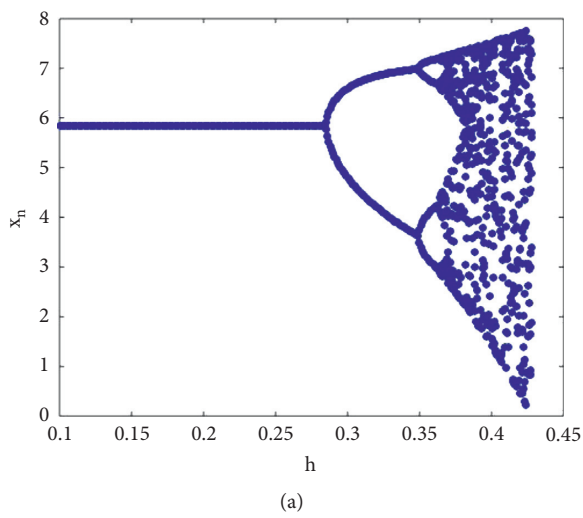


FIGURE 13: Continued.

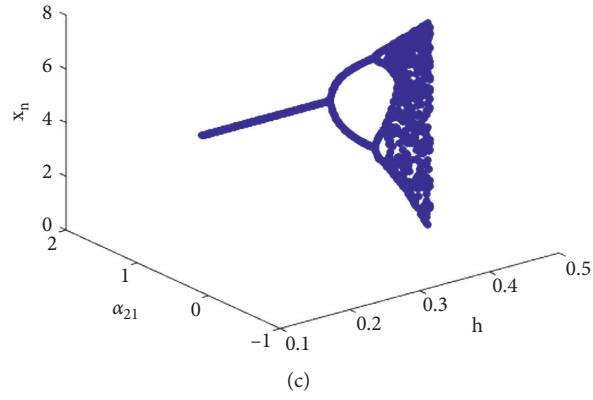


FIGURE 13: Flip bifurcation diagrams at P_7 , where $h \in [0.1, 1.0]$.

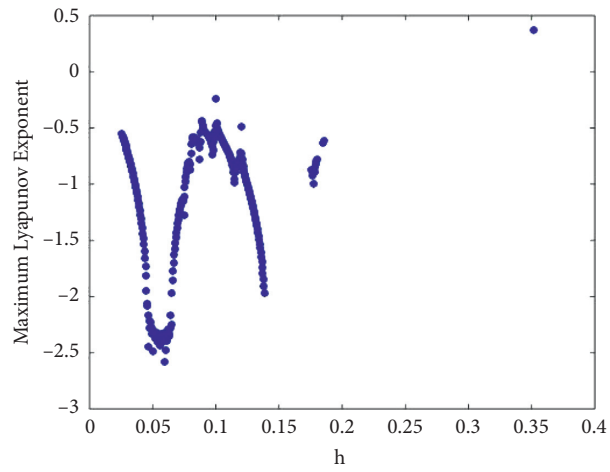


FIGURE 14: Maximum Lyapunov exponents corresponding to Figure 13.

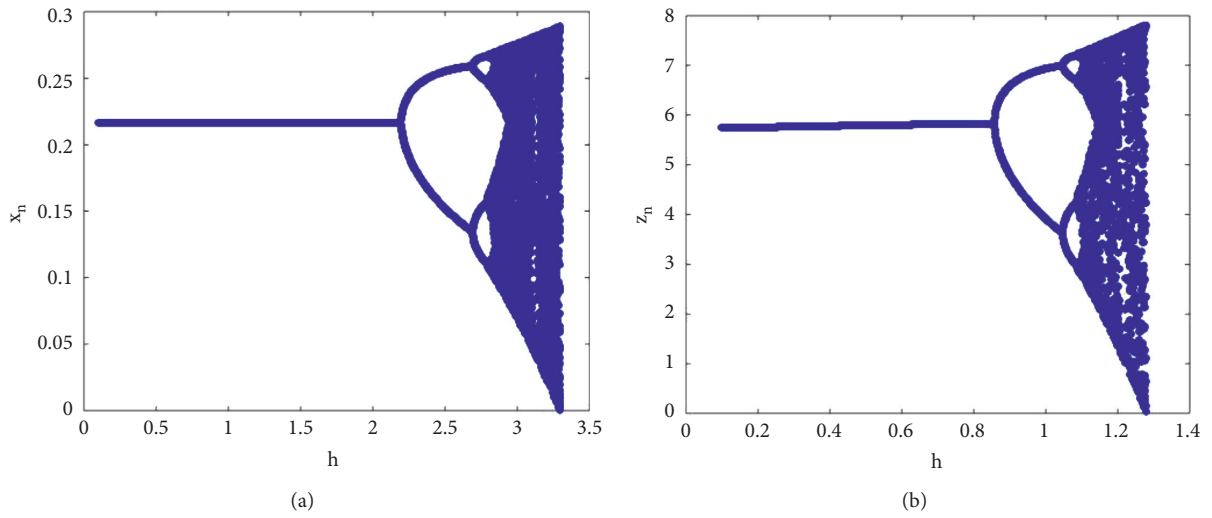


FIGURE 15: Continued.

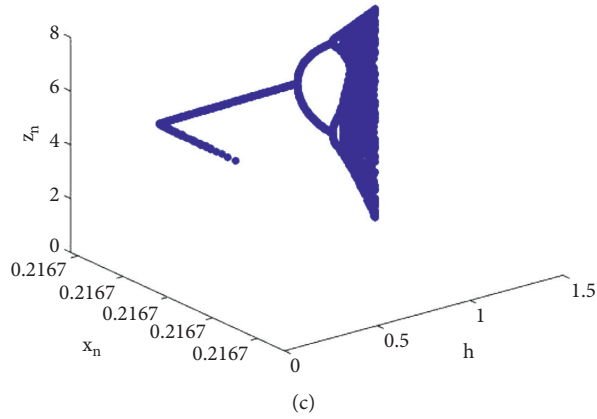


FIGURE 15: Flip bifurcation diagrams at P_8 , where $h \in [0.1, 4.2]$.

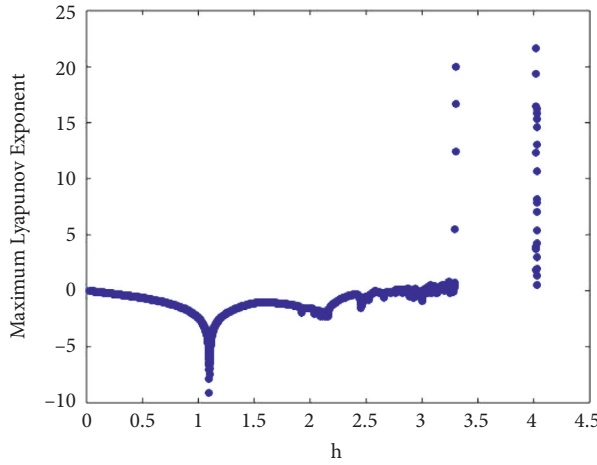


FIGURE 16: Maximum Lyapunov exponents corresponding to Figure 15.

TABLE 1: Dynamical classifications around fixed points of model (15).

Fixed points	Corresponding behavior
P_1	Not sink; source if $0 < h < \min\{2/a_1(k_1 - 1), 2/a_2(k_2 - 1)\}$; saddle if $h > \max\{2/a_1(k_1 - 1), 2/a_2(k_2 - 1)\}$; nonhyperbolic if $h = 2/a_1(k_1 - 1)$ or $h = 2/a_2(k_2 - 1)$
P_2	Sink if $h > \max\{2/a_1(k_1 - 1), 2/a_2(k_2 - 1)\}$ and $0 < h < (2/a_3)$ Source if $0 < h < \min\{2/a_1(k_1 - 1), 2/a_2(k_2 - 1)\}$ and $h > (2/a_3)$ Saddle if $0 < h < \min\{2/a_1(k_1 - 1), 2/a_2(k_2 - 1)\}$ and $0 < h < (2/a_3)$ Nonhyperbolic if $h = (2/a_3)$ or $h = (2/a_1(k_1 - 1))$ or $h = (2/a_2(k_2 - 1))$
P_3	Sink if $h > \max\{2/a_1(k_1 - 1), 2\alpha_{22}/(a_2\alpha_{32}(1 - k_2) - a_3\alpha_{22})\}$ and $0 < h < 2/a_2(1 - k_2)$ Source if $0 < h < \min\{2/a_1(k_1 - 1), 2\alpha_{22}/(a_2\alpha_{32}(1 - k_2) - a_3\alpha_{22})\}$ and $h > 2/a_2(1 - k_2)$ Saddle if $h > \max\{2/a_1(k_1 - 1), 2/a_2(1 - k_2)\}$ and $0 < h < (2\alpha_{22}/(a_2\alpha_{32}(1 - k_2) - a_3\alpha_{22}))$ Nonhyperbolic if $h = 2/a_2(1 - k_2)$ or $h = 2/a_1(k_1 - 1)$ or $h = 2\alpha_{22}/(a_2\alpha_{32}(1 - k_2) - a_3\alpha_{22})$
P_4	Not sink; source if $h > \max\{2/a_1(1 - k_1), 2/a_2(k_2 - 1)\}$ Saddle if $0 < h < \min\{2/a_1(1 - k_1), 2/a_2(k_2 - 1)\}$ Nonhyperbolic if $h = (2/a_1(1 - k_1))$ or $h = (2/a_2(k_2 - 1))$
P_5	Sink if $h > \max\{2/a_1(k_1 - 1), 2\alpha_{22}/(a_3\alpha_{22} - a_2\alpha_{32}(1 - k_2))\}$ and $0 < h < 2/a_2(1 - k_2)$ Source if $0 < h < \min\{2/a_1(k_1 - 1), 2\alpha_{22}/(a_3\alpha_{22} - a_2\alpha_{32}(1 - k_2))\}$ and $h > 2/a_2(1 - k_2)$ Saddle if $h > \max\{2/a_1(k_1 - 1), 2\alpha_{22}/(a_3\alpha_{22} - a_2\alpha_{32}(1 - k_2))\}$ and $h > 2/a_2(1 - k_2)$ Nonhyperbolic if $h = 2/a_1(k_1 - 1)$ or $h = (a_3\alpha_{22} - 2\alpha_{22})/a_2\alpha_{32}(1 - k_2)$ or $h = 2/a_2(1 - k_2)$

TABLE 1: Continued.

Fixed points	Corresponding behavior
P_6	Sink if $0 < h < \min\{2/a_1(1-k_1), 2/a_3\}$ and $h > 2\alpha_{11}/(a_1\alpha_{21}(1-k_1) - a_2\alpha_{11}(1-k_2))$; source if $h > \max\{2/a_1(1-k_1), 2/a_3\}$ and $0 < h < 2\alpha_{11}/(a_1\alpha_{21}(1-k_1) - a_2\alpha_{11}(1-k_2))$; saddle if $0 < h < \min\{2/a_1(1-k_1), 2/a_3\}$ and $0 < h < 2\alpha_{11}/(a_1\alpha_{21}(1-k_1) - a_2\alpha_{11}(1-k_2))$; nonhyperbolic if $h = 2/a_1(1-k_1)$ or $h = (2/a_3)$ or $h = 2\alpha_{11}/(a_1\alpha_{21}(1-k_1) - a_2\alpha_{11}(1-k_2))$.
P_7	Sink if $0 < h < \min\{2/a_1(1-k_1), 2\alpha_{11}/(a_2\alpha_{11}(1-k_2) - 2a_1\alpha_{21}(1-k_1))\}$ and $h > 2\alpha_{11}\alpha_{22}/(a_3\alpha_{11}\alpha_{22} - a_2\alpha_{11}\alpha_{32}(1-k_2) + a_1\alpha_{21}\alpha_{32}(1-k_1))$ Source if $h > \max\{2/a_1(1-k_1), 2\alpha_{11}/(a_2\alpha_{11}(1-k_2) - 2a_1\alpha_{21}(1-k_1))\}$ and $0 < h < 2\alpha_{11}\alpha_{22}/(a_3\alpha_{11}\alpha_{22} - a_2\alpha_{11}\alpha_{32}(1-k_2) + a_1\alpha_{21}\alpha_{32}(1-k_1))$ Saddle if $0 < h < \min\{2/a_1(1-k_1), 2\alpha_{11}/(a_2\alpha_{11}(1-k_2) - 2a_1\alpha_{21}(1-k_1))\}$ and $h < 2\alpha_{11}\alpha_{22}/(a_3\alpha_{11}\alpha_{22} - a_2\alpha_{11}\alpha_{32}(1-k_2) + a_1\alpha_{21}\alpha_{32}(1-k_1))$ Nonhyperbolic if $h = 2/a_1(1-k_1)$ or $h = 2\alpha_{11}/(a_2\alpha_{11}(1-k_2) - 2a_1\alpha_{21}(1-k_1))$ or $h = 2\alpha_{11}\alpha_{22}/(a_3\alpha_{11}\alpha_{22} - a_2\alpha_{11}\alpha_{32}(1-k_2) + a_1\alpha_{21}\alpha_{32}(1-k_1))$
P_8	Sink if $0 < h < \min\{2/a_1(1-k_1), 2\alpha_{11}/(a_2\alpha_{11}(1-k_2) - 2a_1\alpha_{21}(1-k_1)), 2\alpha_{11}\alpha_{22}/(a_3\alpha_{11}\alpha_{22} - a_2\alpha_{11}\alpha_{32}(1-k_2) + a_1\alpha_{21}\alpha_{32}(1-k_1))\}$ Source if $h > \max\{2/a_1(1-k_1), 2\alpha_{11}/(a_2\alpha_{11}(1-k_2) - 2a_1\alpha_{21}(1-k_1)), 2\alpha_{11}\alpha_{22}/(a_3\alpha_{11}\alpha_{22} - a_2\alpha_{11}\alpha_{32}(1-k_2) + a_1\alpha_{21}\alpha_{32}(1-k_1))\}$ Saddle if $0 < h < \min\{2/a_1(1-k_1), 2\alpha_{11}/(a_2\alpha_{11}(1-k_2) - 2a_1\alpha_{21}(1-k_1))\}$ and $h > 2\alpha_{11}\alpha_{22}/(a_3\alpha_{11}\alpha_{22} - a_2\alpha_{11}\alpha_{32}(1-k_2) + a_1\alpha_{21}\alpha_{32}(1-k_1))$ Nonhyperbolic if $h = 2/a_1(1-k_1)$ or $h = \frac{2\alpha_{11}}{a_2\alpha_{11}(1-k_2) - 2a_1\alpha_{21}(1-k_1)}$ or $h = 2\alpha_{11}\alpha_{22}/(a_3\alpha_{11}\alpha_{22} - a_2\alpha_{11}\alpha_{32}(1-k_2) + a_1\alpha_{21}\alpha_{32}(1-k_1))$

Case VI: if $a_1 = 7.1, a_2 = 4.2, a_3 = 2.7, k_1 = 0.0009, k_2 = 1.6, \alpha_{11} = 1.2, \alpha_{22} = 1.4, \alpha_{21} = 1.9, \alpha_{32} = 0.9, \alpha_{33} = 0.4$ then from (61) one gets: $h = 0.2819438903463822$. Hence P_6 is stable if $h < 0.2819438903463822$, and exchange stability if $h = 0.2819438903463822$ and in fact flip bifurcation takes place by Theorem 14. Therefore the flip bifurcation diagrams with initial value $(0.1, 0, 0.1)$ are presented in Figure 11. Finally maximum Lyapunov exponents corresponding to Figure 11 are drawn in Figure 12.

Case VII: If $a_1 = 9.1, a_2 = 4.2, a_3 = 2.7, k_1 = 0.23, k_2 = 4.6, \alpha_{11} = 1.2, \alpha_{22} = 1.4, \alpha_{21} = 0.099, \alpha_{32} = 5.9$, and $\alpha_{33} = 2.4$, then, from (68), one gets $h = 0.2854288568574283$. Hence, P_7 is stable if $h < 0.2854288568574283$, and exchange stability is $h = 0.2854288568574283$, and in fact, flip bifurcation takes place by Theorem 15. Therefore, the flip bifurcation diagrams with initial value $(0.2, 0.1, 0)$ are presented in Figure 13. Finally, maximum Lyapunov exponents corresponding to Figure 13 are drawn in Figure 14.

Case VIII: if $a_1 = 9.1, a_2 = 1.2, a_3 = 2.7, k_1 = 0.9, k_2 = 0.006, \alpha_{11} = 4.2, \alpha_{22} = 1.4, \alpha_{21} = 4.9, \alpha_{32} = 1.9$, and $\alpha_{33} = 0.4$, then, from (75), one gets $h = 2.1978021978021984$. Hence, $P_7 = (0.2166666666666666, 0.0936666666666666, 6.305083333333333)$ is stable if $h < 2.1978021978021984$, and exchange stability is $h = 2.1978021978021984$, and in fact, flip bifurcation takes place by Theorem 16. Therefore, flip bifurcation diagrams with $(0.2, 0.2, 0.4)$ are presented in Figure 15 which indicates that period-2 points bifurcate from P_8 are stable, since $\Omega_2 = (h\alpha_{11}d_{11} + 2\alpha_{11}d_{11})^2 = 310.844023668 > 0$. Finally, maximum Lyapunov exponents corresponding to Figure 15 are drawn in Figure 16.

8. Conclusion

The work is about the existence of fixed points, topological classifications around fixed points, periodic points, and bifurcations of a three-species discrete food chain model with harvesting in the region: $\mathbb{R}_+^3 = \{(x, y, z): x, y, z \geq 0\}$. We proved that, for all parametric values $h, a_1, a_2, a_3, k_1, k_2, \alpha_{11}, \alpha_{22}, \alpha_{21}, \alpha_{32}$, and α_{33} , model (15) has trivial fixed point: $P_1 = (0, 0, 0)$; boundary fixed points: $P_2 = (0, 0, a_3/\alpha_{33}) \forall a_3, \alpha_{33} > 0$; $P_3 = (0, (1-k_2)a_2/\alpha_{22}, 0)$ if $k_2 < 1$; $P_4 = ((1-k_1)a_1/\alpha_{11}, 0, 0)$ if $k_1 < 1$; $P_5 = (0, (1-k_2)a_2/\alpha_{22}, ((a_3\alpha_{22} - \alpha_{32}(1-k_2)a_2)/\alpha_{22}\alpha_{33}))$ if $a_3 > (\alpha_{32}(1-k_2)a_2/\alpha_{22})$ with $k_2 < 1$; $P_6 = ((1-k_1)a_1/\alpha_{11}, 0, a_3/\alpha_{33})$ if $k_1 < 1$; $P_7 = ((1-k_1)a_1/\alpha_{11}, (a_2(1-k_2)\alpha_{11} - a_1(1-k_1)\alpha_{21})/\alpha_{11}\alpha_{22}, 0)$ if $a_2 > (a_1(1-k_1)\alpha_{21}/(1-k_2)\alpha_{11})$ with $k_1, k_2 < 1$. We also proved that if $k_1 < 1, a_2 > (a_1(1-k_1)\alpha_{21}/(1-k_2)\alpha_{11})$ and $a_3 > (a_2(1-k_2)\alpha_{11}\alpha_{32} - a_1(1-k_1)\alpha_{21}\alpha_{32})/\alpha_{11}\alpha_{22}$, then, $P_8 = (((1-k_1)a_1/\alpha_{11}), (a_2(1-k_2)\alpha_{11} - a_1(1-k_1)\alpha_{21})/\alpha_{11}\alpha_{22}, (a_3\alpha_{11}\alpha_{22} - a_2(1-k_2)\alpha_{11}\alpha_{32} + a_1(1-k_1)\alpha_{21}\alpha_{32})/\alpha_{11}\alpha_{22}\alpha_{33})$ is an interior equilibrium point of (15). Furthermore, we studied the local stability with different topological classifications around each fixed points whose main findings are presented in Table 1. Next, for under consideration model (15), we also studied existence of periodic points by existing theory. Furthermore, we explored the existence of possible bifurcations about each fixed points in order to understand dynamics of model (15) deeply. It is proved that (i) around P_1 model undergoes no flip bifurcation if $\Omega \in \mathcal{F}|_{P_1} = \{\Omega: h = 2/a_1(k_1 - 1)\}$, (ii) around P_2 model undergoes flip bifurcation if $\Omega \in \mathcal{F}|_{P_2} = \{\Omega: h = 2/a_3\}$, (iii) around P_3 model undergoes flip bifurcation if $\Omega \in \mathcal{F}|_{P_3} = \{\Omega: h = 2/a_2(1-k_2)\}$, (iv) around P_4 model undergoes flip bifurcation if $\Omega \in \mathcal{F}|_{P_4} = \{\Omega: h = 2/a_1(1-k_1)\}$, (v) around P_5 model undergoes flip bifurcation if $\Omega \in \mathcal{F}|_{P_5} = \{\Omega: h = 2/a_1(k_1 - 1)\}$, (vi) around P_6 model undergoes flip

bifurcation if $\Omega \in \mathcal{F}|_{P_6} = \{\Omega: h = 2/a_1(1 - k_1)\}$, (vii) around P_7 model undergoes flip bifurcation if $\Omega \in \mathcal{F}|_{P_7} = \{\Omega: h = 2/a_1(1 - k_1)\}$, and (viii) around P_8 model undergoes flip bifurcation if $\Omega \in \mathcal{F}|_{P_8} = \{\Omega: h = 2/a_1(1 - k_1)\}$. Finally, obtained results are verified numerically. This research can provide a framework for theoretical basis and help for the research in different aspects of biology specifically in the field of ecology.

Data Availability

All the data used in this study are included within the article and the sources from where they were adopted are cited accordingly.

Conflicts of Interest




The authors declare that they have no conflicts of interest.

References

- [1] A. J. Lotka, *Elements of Physical Biology*, Williams & Wilkins, Philadelphia, PA, USA, 1925.
- [2] V. Volterra, *Leconsen la theory of mathematique de leitte pou lavi*, Gauthier-Villars, Paris, France, 1931.
- [3] J. R. Beddington, C. A. Free, and J. H. Lawton, "Dynamic complexity in predator-prey models framed in difference equations," *Nature*, vol. 255, no. 5503, pp. 58–60, 1975.
- [4] F. Chen, "Permanence and global attractivity of a discrete multispecies Lotka-Volterra competition predator-prey systems," *Applied Mathematics and Computation*, vol. 182, no. 1, pp. 3–12, 2006.
- [5] N. Fang and X. X. Chen, "Permanence of a discrete multispecies Lotka-Volterra competition predator-prey system with delays," *Nonlinear Analysis: Real World Applications*, vol. 9, no. 5, pp. 2185–2195, 2008.
- [6] Q. Fang, X. Li, and M. Cao, "Dynamics of a discrete predator-prey system with Beddington-DeAngelis function response," *Applied Mathematics*, vol. 3, no. 4, pp. 389–394, 2012.
- [7] H. N. Agiza, E. M. Elabbasy, H. El-Metwally, and A. A. Elsadany, "Chaotic dynamics of a discrete prey-predator model with Holling type II," *Nonlinear Analysis: Real World Applications*, vol. 10, no. 1, pp. 116–129, 2009.
- [8] H. F. Huo and W. T. Li, "Stable periodic solution of the discrete periodic Leslie-Gower predator-prey model," *Mathematical and Computer Modelling*, vol. 40, no. 3-4, pp. 261–269, 2004.
- [9] C. Lu and L. Zhang, "Permanence and global attractivity of a discrete semi-ratio dependent predator-prey system with Holling II type functional response," *Journal of Applied Mathematics and Computing*, vol. 33, no. 1, pp. 125–135, 2010.
- [10] M. Zhao and L. Zhang, "Permanence and chaos in a host-parasitoid model with prolonged diapause for the host," *Communications in Nonlinear Science and Numerical Simulation*, vol. 14, no. 12, pp. 4197–4203, 2009.
- [11] M. Zhao, L. Zhang, and J. Zhu, "Dynamics of a host-parasitoid model with prolonged diapause for parasitoid," *Communications in Nonlinear Science and Numerical Simulation*, vol. 16, no. 1, pp. 455–462, 2011.
- [12] S. M. Salman, A. M. Yousef, and A. A. Elsadany, "Stability, bifurcation analysis and chaos control of a discrete predator-prey system with square root functional response," *Chaos, Solitons & Fractals*, vol. 93, pp. 20–31, 2016.
- [13] X. Liu and D. Xiao, "Complex dynamic behaviors of a discrete-time predator-prey system," *Chaos, Solitons & Fractals*, vol. 32, no. 1, pp. 80–94, 2007.
- [14] K. A. Hasan and M. F. Hama, "Complex dynamics behaviors of a discrete prey-predator model with Beddington-Deangelis functional response," *International Journal of Contemporary Mathematical Sciences*, vol. 7, no. 45, pp. 2179–2195, 2012.
- [15] D. Wu and H. Zhang, "Bifurcation analysis of a two-species competitive discrete model of plankton allelopathy," *Advances in Difference Equations*, vol. 2014, no. 1, pp. 1–10, 2014.
- [16] S. M. Rana, "Chaotic dynamics and control of discrete ratio-dependent predator-prey system," *Discrete Dynamics in Nature and Society*, vol. 2017, Article ID 4537450, 13 pages, 2017.
- [17] S. M. Rana and U. Kulsum, "Bifurcation analysis and chaos control in a discrete-time predator-prey system of Leslie type with simplified Holling type IV functional response," *Discrete Dynamics in Nature and Society*, vol. 2017, Article ID 9705985, 11 pages, 2017.
- [18] J. Guckenheimer and P. Holmes, *Nonlinear Oscillations, Dynamical Systems and Bifurcation of Vector Fields*, Springer-Verlag, New York, NY, USA, 1983.
- [19] Y. A. Kuznetsov, *Elements of Applied Bifurcation Theory*, Springer-Verlag, New York, NY, USA, 3rd edition, 2004.

Research Article

On a Unified Mittag-Leffler Function and Associated Fractional Integral Operator

Yanyan Zhang ¹, Ghulam Farid ², Zabidin Salleh ³ and Ayyaz Ahmad²

¹College of Basic Education, Nantong Institute of Technology, Nantong 226002, China

²Department of Mathematics, COMSATS University Islamabad, Attock Campus, Attock, Pakistan

³Special Interest Group on Modelling and Data Analytics, Faculty of Ocean Engineering Technology and Informatics, Universiti Malaysia Terengganu, Kuala Nerus 21030, Terengganu, Malaysia

Correspondence should be addressed to Yanyan Zhang; joicezyy@sina.com and Zabidin Salleh; zabidin@umt.edu.my

Received 10 July 2021; Accepted 6 September 2021; Published 13 October 2021

Academic Editor: Abdelalim Elsadany

Copyright © 2021 Yanyan Zhang et al. This is an open access article distributed under the Creative Commons Attribution License, which permits unrestricted use, distribution, and reproduction in any medium, provided the original work is properly cited.

The aim of this paper is to unify the extended Mittag-Leffler function and generalized Q function and define a unified Mittag-Leffler function. Both the extended Mittag-Leffler function and generalized Q function can be obtained from the unified Mittag-Leffler function. The Laplace, Euler beta, and Whittaker transformations are applied for this function, and generalized formulas are obtained. These formulas reproduce integral transformations of various deduced Mittag-Leffler functions and Q function. Also, the convergence of this unified Mittag-Leffler function is proved, and an associated fractional integral operator is constructed.

1. Introduction

The exponential function naturally exists in the solution of differential equations and plays a very vital role in solving real-world problems modeled in the form of differential mathematical systems. At the same time, the Mittag-Leffler function provides assistance in the formulation of solutions of complicated fractional dynamical systems. The aim of this paper is to unify two types of functions, namely, an extended generalized Mittag-Leffler function given in (7) and the Q function given in (8). We study Laplace, Euler beta, and Whittaker transformations of extended generalized Mittag-Leffler function given in (7) and the Q function given in (8) in the compact formulas. Also we will define a compact form of fractional integral operator.

First, we give some basic definitions and notations which will be helpful to understand later definitions. These include the Laplace transform, Euler beta transform, Whittaker transform, gamma function (Γ), beta function (B), p -beta function (B_p), Mittag-Leffler function ($E_{\alpha,\beta}$), extended Mittag-Leffler function ($E_{\alpha,\beta}^{\lambda,r,k,\theta}$), the fractional integral

operator associated with extended Mittag-Leffler function and generalized Q function ($Q_{\alpha,\beta,\gamma,\delta,\mu,\nu}^{\lambda,\rho,\theta,k,n}$).

Definition 1 (see [1]). Laplace transform of an integrable function f on $[0, \infty)$ is defined as follows:

$$L[f(t)] = \int_0^{\infty} e^{-st} f(t) dt, \quad (1)$$

where $s \in \mathbb{C}$ is the variable of the transform.

Definition 2 (see [2]). The Euler beta transform of a function f is defined by the following definite integral:

$$B[f(t); a, b] = \int_0^1 t^{a-1} (1-t)^{b-1} f(t) dt, \quad (2)$$

where a and b are any complex number with $\Re(a) > 0$ and $\Re(b) > 0$.

Definition 3 (see [2]). The Whittaker transform is defined by the following improper integral:

$$\int_0^{\infty} e^{-(t/2)} t^{\nu-1} \omega_{\lambda,\mu}(t) dt = \frac{\Gamma((1/2) + \mu + \nu) \Gamma((1/2) - \mu + \nu)}{\Gamma(1 - \lambda + \nu)}, \quad (3)$$

where $\Re(\mu \pm \nu) > -(1/2)$ and $\omega_{\lambda,\mu}$ is the Whittaker confluent hypergeometric function.

Definition 4 (see [3]). The gamma function is defined by the following improper integral:

$$\Gamma(z) = \int_0^{\infty} e^{-t} t^{z-1} dt, \quad (4)$$

where $\Re(z) > 0$.

Definition 5 (see [2]). The beta function is defined by a definite integral and is given by

$$B(m, n) = \int_0^1 t^{m-1} (1-t)^{n-1} dt, \quad (5)$$

where $\Re(m), \Re(n) > 0$.

Definition 6 (see [4]). The Mittag-Leffler function with two parameters is defined by the following series:

$$E_{\alpha,\beta}(z) = \sum_{l=0}^{\infty} \frac{z^l}{\Gamma(\alpha l + \beta)}, \quad (6)$$

where $\Re(\alpha) > 0$.

Definition 7 (see [5]). An extended and generalized Mittag-Leffler function ($E_{\alpha,\beta,\gamma}^{\delta,\mu,k,\nu}$) is defined by the following series:

$$E_{\alpha,\beta,\gamma}^{\lambda,r,k,\theta}(z; p) = \sum_{l=0}^{\infty} \frac{B_p(\lambda + lk, \theta - \lambda)(\theta)_{lk} z^l}{B(\lambda, \theta - \lambda)(\gamma)_{lr} \Gamma(\alpha l + \beta)}, \quad (7)$$

where $z, \alpha, \beta, \gamma, \theta, \lambda \in \mathbb{C}$, $\Re(\alpha), \Re(\beta), \Re(\gamma), \Re(\theta), \Re(\lambda) > 0$ with $p \geq 0, r > 0, 0 < k \leq r + \Re(\alpha)$, and $(\theta)_{lk} = (\Gamma(\theta + lk) / \Gamma(\theta))$.

Definition 8 (see [2]). A generalized Q function ($Q_{\alpha,\beta,\gamma,\delta,\mu,\nu}^{\lambda,\rho,\theta,k,n}$) is defined by the following series:

$$Q_{\alpha,\beta,\gamma,\delta,\mu,\nu}^{\lambda,\rho,\theta,k,n}(z; \underline{a}, \underline{b}) = \sum_{l=0}^{\infty} \frac{\prod_{i=1}^n B(b_i, l)(\lambda)_{\rho l} (\theta)_{kl} z^l}{\prod_{i=1}^n B(a_i, l)(\gamma)_{\delta l} (\mu)_{\nu l} \Gamma(\alpha l + \beta)}, \quad (8)$$

where $\underline{a} = (a_1, a_2, \dots, a_n), \underline{b} = (b_1, b_2, \dots, b_n), \alpha, \beta, \gamma, \delta, \mu, \nu, \lambda, \rho, \theta, a_i, b_i \in \mathbb{C}$, $\min\{\Re(\alpha), \Re(\beta), \Re(\gamma), \Re(\theta), \Re(\lambda), \Re(\delta), \Re(\rho)\} > 0, k \in (0, 1) \cup \mathbb{N}$.

The Mittag-Leffler function takes place naturally similar to that of the exponential function in the solutions of fractional integro-differential equations having the arbitrary order. The Mittag-Leffler functions have to gain more recognition due to their wide applications in diverse fields [5–9]. They are used to define new fractional integral operators, and the fractional integral operators are used to generalize mathematical inequalities, see [5, 8, 10–14].

Our motivation is to introduce the unified Mittag-Leffler function. In this paper, we unify the extended Mittag-Leffler function (7) and generalized Q function (8) in a single function named unified Mittag-Leffler function. We studied the Laplace, Euler beta, and Whittaker transformation of the unified Mittag-Leffler function and obtained the compact formulas which reproduce integral transformations of Mittag-Leffler function and generalized Q function. Furthermore, the convergence of unified Mittag-Leffler function is proved, associated fractional integral operator is defined, and its boundedness is provided.

In the next section, we give the definition of unified Mittag-Leffler function and deduce extended generalized Mittag-Leffler function and generalized Q functions.

2. Unified Mittag-Leffler Function

We define a Mittag-Leffler function (will be called the unified Mittag-Leffler function) which unifies the functions given in (7) and (8) as follows:

$$M_{\alpha,\beta,\gamma,\delta,\mu,\nu}^{\lambda,\rho,\theta,k,n}(z; \underline{a}, \underline{b}, \underline{c}, p) = \sum_{l=0}^{\infty} \frac{\prod_{i=1}^n B_p(b_i, a_i)(\lambda)_{\rho l} (\theta)_{kl} z^l}{\prod_{i=1}^n B(c_i, a_i)(\gamma)_{\delta l} (\mu)_{\nu l} \Gamma(\alpha l + \beta)}, \quad (9)$$

where $\underline{a} = (a_1, a_2, \dots, a_n), \underline{b} = (b_1, b_2, \dots, b_n), \underline{c} = (c_1, c_2, \dots, c_n), a_i, b_i, c_i \in \mathbb{C}; i = 1, \dots, n$ such that $\Re(a_i), \Re(b_i), \Re(c_i) > 0, \forall i$. Also let $\alpha, \beta, \gamma, \delta, \mu, \nu, \lambda, \rho, \theta, z \in \mathbb{C}$, $\min\{\Re(\alpha), \Re(\beta), \Re(\gamma), \Re(\delta), \Re(\lambda), \Re(\theta)\} > 0$, and $k \in (0, 1) \cup \mathbb{N}$ with $k + \Re(\rho) < \Re(\delta + \nu + \alpha)$, $\text{Im}(\rho) = \text{Im}(\delta + \nu + \alpha)$.

For $n = 1$, (9) will obtain the following form:

$$M_{\alpha,\beta,\gamma,\delta,\mu,\nu}^{\lambda,\rho,\theta,k,1}(z; \underline{a}, \underline{b}, \underline{c}, p) = \sum_{l=0}^{\infty} \frac{B_p(b_1, a_1)(\lambda)_{\rho l} (\theta)_{kl} z^l}{B(c_1, a_1)(\gamma)_{\delta l} (\mu)_{\nu l} \Gamma(\alpha l + \beta)}. \quad (10)$$

By setting $b_1 = c_1 + lk, a_1 = \theta - \lambda, c_1 = \lambda, \rho = \nu = 0, \delta > 0$ in (10), we will get (7). Also, by substituting $a_i = l, p = 0$ and $\Re(\rho) > 0$ in (9), we will obtain (8). Hence the newly defined Mittag-Leffler function provides different kinds of related functions by setting the specific values of the parameters. The functions defined in [2, 4–9, 15] are particular cases of this newly defined function.

2.1. Integral Transforms of Unified Mittag-Leffler Function.

Now we give the integral transforms of the unified Mittag-Leffler function. These transformations include the Laplace transform, Euler beta transform, and Whittaker transform.

2.1.1. Laplace Transform. First we give the Laplace transform of the unified Mittag-Leffler function.

Theorem 1. For $\underline{a} = (a_1, a_2, \dots, a_n), \underline{b} = (b_1, b_2, \dots, b_n), \underline{c} = (c_1, c_2, \dots, c_n), a_i, b_i, c_i \in \mathbb{C}; i = 1, \dots, n$ such that $\Re(a_i), \Re(b_i), \Re(c_i) > 0, \forall i$. Also let $\alpha, \beta, \gamma, \delta, \mu, \nu, \lambda, \rho, \theta, t \in \mathbb{C}$, $\min\{\Re(\alpha), \Re(\beta), \Re(\gamma), \Re(\delta), \Re(\lambda), \Re(\theta)\} > 0$, and $k \in (0, 1) \cup \mathbb{N}$ with $k + \Re(\rho) < \Re(\delta + \nu + \alpha)$, $\text{Im}(\rho) = \text{Im}(\delta + \nu + \alpha)$, and the Laplace transform of unified Mittag-Leffler function is given as follows:

$$L\left[M_{\alpha,\beta,\gamma,\delta,\mu,\nu}^{\lambda,\rho,\theta,k,n}(t; \underline{a}, \underline{b}, \underline{c}, p)\right] = s^{-1} M_{\alpha,\beta,\gamma,\delta,\mu,\nu}^{\lambda,\rho,\theta,k,1,n}(s^{-1}; \underline{a}, \underline{b}, \underline{c}, p). \tag{11}$$

Proof. By the definition of the Laplace transform of a function, we have

$$\begin{aligned} L\left[M_{\alpha,\beta,\gamma,\delta,\mu,\nu}^{\lambda,\rho,\theta,k,n}(t; \underline{a}, \underline{b}, \underline{c}, p)\right] &= \int_0^\infty e^{-st} \sum_{l=0}^\infty \frac{\prod_{i=1}^n B_p(b_i, a_i)(\lambda)_{\rho l}(\theta)_{kl}}{\prod_{i=1}^n B(c_i, a_i)(\gamma)_{\delta l}(\mu)_{\nu l}} \frac{t^l}{\Gamma(\alpha l + \beta)} dt \\ &= \sum_{l=0}^\infty \frac{\prod_{i=1}^n B_p(b_i, a_i)(\lambda)_{\rho l}(\theta)_{kl}}{\prod_{i=1}^n B(c_i, a_i)(\gamma)_{\delta l}(\mu)_{\nu l}} \frac{1}{\Gamma(\alpha l + \beta)} \frac{l!}{s^{l+1}} \\ &= \frac{1}{s} \sum_{l=0}^\infty \frac{\prod_{i=1}^n B_p(b_i, a_i)(\lambda)_{\rho l}(\theta)_{kl}}{\prod_{i=1}^n B(c_i, a_i)(\gamma)_{\delta l}(\mu)_{\nu l}} \frac{1}{\Gamma(\alpha l + \beta)} s^{-l} (1)_l. \end{aligned} \tag{12}$$

Hence the Laplace transform of the unified Mittag-Leffler function can be given as follows:

$$L\left[M_{\alpha,\beta,\gamma,\delta,\mu,\nu}^{\lambda,\rho,\theta,k,n}(t; \underline{a}, \underline{b}, \underline{c}, p)\right] = s^{-1} M_{\alpha,\beta,\gamma,\delta,\mu,\nu}^{\lambda,\rho,\theta,k,1,n}(s^{-1}; \underline{a}, \underline{b}, \underline{c}, p). \tag{13}$$

Corollary 1. For $a_i = l, p = 0$, and $\Re(\rho) > 0$, the Laplace transform of the unified Mittag-Leffler function will become

$$L\left[M_{\alpha,\beta,\gamma,\delta,\mu,\nu}^{\lambda,\rho,\theta,k,n}(t; \underline{a}, \underline{b}, \underline{c}, p)\right] = L\left[Q_{\alpha,\beta,\gamma,\delta,\mu,\nu}^{\lambda,\rho,\theta,k,n}(t; \underline{b}, \underline{c})\right]. \tag{14}$$

□ *Proof.* From Theorem 1, we have

$$L\left[M_{\alpha,\beta,\gamma,\delta,\mu,\nu}^{\lambda,\rho,\theta,k,n}(t; \underline{a}, \underline{b}, \underline{c}, p)\right] = s^{-1} \sum_{l=0}^\infty \frac{\prod_{i=1}^n B_p(b_i, a_i)(\lambda)_{\rho l}(\theta)_{kl}}{\prod_{i=1}^n B(c_i, a_i)(\gamma)_{\delta l}(\mu)_{\nu l}} \frac{(1)_l s^{-l}}{\Gamma(\alpha l + \beta)}. \tag{15}$$

For $p = 0, B_p(x, y) = B(x, y)$.

Therefore the above expression becomes

$$L\left[M_{\alpha,\beta,\gamma,\delta,\mu,\nu}^{\lambda,\rho,\theta,k,n}(t; \underline{a}, \underline{b}, \underline{c}, p)\right] = s^{-1} \sum_{l=0}^\infty \frac{\prod_{i=1}^n B(b_i, a_i)(\lambda)_{\rho l}(\theta)_{kl}}{\prod_{i=1}^n B(c_i, a_i)(\gamma)_{\delta l}(\mu)_{\nu l}} \frac{(1)_l s^{-l}}{\Gamma(\alpha l + \beta)}. \tag{16}$$

Putting $a_i = l$ and $\Re(\rho) > 0$, we get the following:

$$L\left[M_{\alpha,\beta,\gamma,\delta,\mu,\nu}^{\lambda,\rho,\theta,k,n}(t; \underline{a}, \underline{b}, \underline{c}, p)\right] = s^{-1} \sum_{l=0}^\infty \frac{\prod_{i=1}^n B(b_i, l)(\lambda)_{\rho l}(\theta)_{kl}}{\prod_{i=1}^n B(c_i, l)(\gamma)_{\delta l}(\mu)_{\nu l}} \frac{l! s^{-l}}{\Gamma(\alpha l + \beta)}. \tag{17}$$

Hence we get

$$L\left[M_{\alpha,\beta,\gamma,\delta,\mu,\nu}^{\lambda,\rho,\theta,k,n}(t; \underline{a}, \underline{b}, \underline{c}, p)\right] = L\left[Q_{\alpha,\beta,\gamma,\delta,\mu,\nu}^{\lambda,\rho,\theta,k,n}(t; \underline{b}, \underline{c})\right]. \tag{18}$$

Similarly for $n = 1, b_1 = c_1 + lk, a_1 = \theta - \lambda, c_1 = \lambda, \rho = \nu = 0$ and $\delta > 0$ one can have

$$L\left[M_{\alpha,\beta,\gamma,\delta,\mu,\nu}^{\lambda,\rho,\theta,k,n}(t; \underline{a}, \underline{b}, \underline{c}, p)\right] = L\left[E_{\alpha,\beta,\gamma}^{\lambda,\delta,k,\theta}(t; p)\right]. \tag{19}$$

□

2.1.2. Euler Beta Transform. The Euler beta transformation of the unified Mittag-Leffler function is given in the next theorem.

Theorem 2. For $\underline{a} = (a_1, a_2, \dots, a_n), \underline{b} = (b_1, b_2, \dots, b_n), \underline{c} = (c_1, c_2, \dots, c_n), a_i, b_i, c_i \in \mathbb{C}; i = 1, \dots, n$ such that $\Re(a_i), \Re(b_i), \Re(c_i) > 0, \forall i$. Also let $\alpha, \beta, \gamma, \delta, \mu, \nu, \lambda, \rho, \theta, t \in \mathbb{C}, \min\{\Re(\alpha), \Re(\beta), \Re(\gamma), \Re(\delta), \Re(\lambda), \Re(\theta)\} > 0$, and $k \in (0, 1) \cup \mathbb{N}$ with $k + \Re(\rho) < \Re(\delta + \nu + \alpha)$, $\text{Im}(\rho) = \text{Im}(\delta + \nu + \alpha)$, and the Euler beta transform of the unified Mittag-Leffler function is given as follows:

$$B \left[M_{\alpha, \beta, \gamma, \delta, \mu, \nu}^{\lambda, \rho, \theta, k, n} (t; \underline{a}, \underline{b}, \underline{c}, p); m, n \right] = \sum_{l=0}^{\infty} \frac{\prod_{i=1}^n B_p (b_i, a_i) (\lambda)_{\rho l} (\theta)_{kl}}{\prod_{i=1}^n B (c_i, a_i) (\gamma)_{\delta l} (\mu)_{\nu l}} \frac{B(l+m, n)}{\Gamma(\alpha l + \beta)}. \tag{20}$$

Proof. By the definition of beta transform of an integrable function, we have the following:

$$\begin{aligned} B \left[M_{\alpha, \beta, \gamma, \delta, \mu, \nu}^{\lambda, \rho, \theta, k, n} (t; \underline{a}, \underline{b}, \underline{c}, p); m, n \right] &= \int_0^1 t^{m-1} (1-t)^{n-1} \sum_{l=0}^{\infty} \frac{\prod_{i=1}^n B_p (b_i, a_i) (\lambda)_{\rho l} (\theta)_{kl}}{\prod_{i=1}^n B (c_i, a_i) (\gamma)_{\delta l} (\mu)_{\nu l}} \frac{t^l}{\Gamma(\alpha l + \beta)} dt \\ &= \sum_{l=0}^{\infty} \frac{\prod_{i=1}^n B_p (b_i, a_i) (\lambda)_{\rho l} (\theta)_{kl}}{\prod_{i=1}^n B (c_i, a_i) (\gamma)_{\delta l} (\mu)_{\nu l}} \frac{1}{\Gamma(\alpha l + \beta)} \int_0^1 t^{(l+m)-1} (1-t)^{n-1} dt \\ &= \sum_{l=0}^{\infty} \frac{\prod_{i=1}^n B_p (b_i, a_i) (\lambda)_{\rho l} (\theta)_{kl}}{\prod_{i=1}^n B (c_i, a_i) (\gamma)_{\delta l} (\mu)_{\nu l}} \frac{B(l+m, n)}{\Gamma(\alpha l + \beta)}. \end{aligned} \tag{21}$$

Corollary 2. For $a_i = l, p = 0$, and $\Re(\rho) > 0$, the Euler beta transform of unified Mittag-Leffler function will become

$$B \left[M_{\alpha, \beta, \gamma, \delta, \mu, \nu}^{\lambda, \rho, \theta, k, n} (t; \underline{a}, \underline{b}, \underline{c}, p) \right] = B \left[Q_{\alpha, \beta, \gamma, \delta, \mu, \nu}^{\lambda, \rho, \theta, k, n} (t; \underline{b}, \underline{c}) \right]. \tag{22}$$

Similarly for $n = 1, b_1 = c_1 + lk, a_1 = \theta - \lambda, c_1 = \lambda, \rho = \nu = 0$ and $\delta > 0$ one can have

$$B \left[M_{\alpha, \beta, \gamma, \delta, \mu, \nu}^{\lambda, \rho, \theta, k, n} (t; \underline{a}, \underline{b}, \underline{c}, p) \right] = B \left[E_{\alpha, \beta, \gamma}^{\lambda, \delta, k, \theta} (t; p) \right]. \tag{23}$$

2.1.3. Whittaker Transform. The Whittaker transformation of the unified Mittag-Leffler function is given in the next theorem.

Theorem 3. For $\underline{a} = (a_1, a_2, \dots, a_n), \underline{b} = (b_1, b_2, \dots, b_n), \underline{c} = (c_1, c_2, \dots, c_n), a_i, b_i, c_i \in \mathbb{C}; i = 1, \dots, n$ such that $\Re(a_i), \Re(b_i), \Re(c_i) > 0, \forall i$. Also let $\alpha, \beta, \gamma, \delta, \mu, \nu, \zeta, \rho$,

$\theta, t \in \mathbb{C}, \min\{\Re(\alpha), \Re(\beta), \Re(\gamma), \Re(\delta), \Re(\zeta), \Re(\theta)\} > 0$, and $k \in (0, 1) \cup \mathbb{N}$ with $k + \Re(\rho) < \Re(\delta + \nu + \alpha)$, $\text{Im}(\rho) = \text{Im}(\delta + \nu + \alpha)$, and we have

$$\begin{aligned} &\int_0^{\infty} e^{-(\phi t/2)} t^{\xi-1} \omega_{\lambda, \psi}(\phi t) M_{\alpha, \beta, \gamma, \delta, \mu, \nu}^{\zeta, \rho, \theta, k, n}(\omega t^\eta; \underline{a}, \underline{b}, \underline{c}, p) dt \\ &= \frac{\phi^{-\xi} (f-1)!}{(g-1)!} M_{\alpha, \beta, \gamma, \delta, \mu, \nu, g, \eta, 1}^{\zeta, \rho, \theta, k, f, \eta, n}(\omega \phi^{-\eta}; \underline{a}, \underline{b}, \underline{c}, p), \end{aligned} \tag{24}$$

where $f = (1/2) \pm \psi + \xi$ and $g = 1 - \lambda + \xi$.

Proof. Consider the following improper integral:

$$\int_0^{\infty} e^{-(\phi t/2)} t^{\xi-1} \omega_{\lambda, \psi}(\phi t) M_{\alpha, \beta, \gamma, \delta, \mu, \nu}^{\zeta, \rho, \theta, k, n}(\omega t^\eta; \underline{a}, \underline{b}, \underline{c}, p) dt. \tag{25}$$

By substituting $\phi t = q$ in the above integral, we obtain the following:

$$\begin{aligned} &\int_0^{\infty} e^{-(q/2)} \left(\frac{q}{\phi}\right)^{\xi-1} \omega_{\lambda, \psi}(q) M_{\alpha, \beta, \gamma, \delta, \mu, \nu}^{\zeta, \rho, \theta, k, n} \left(\omega \left(\frac{q}{\phi}\right)^\eta; \underline{a}, \underline{b}, \underline{c}, p\right) \frac{dq}{\phi} \\ &= \phi^{-\xi} \int_0^{\infty} e^{-(q/2)} q^{\xi-1} \omega_{\lambda, \psi}(q) \sum_{l=0}^{\infty} \frac{\prod_{i=1}^n B_p (b_i, a_i) (\zeta)_{\rho l} (\theta)_{kl}}{\prod_{i=1}^n B (c_i, a_i) (\gamma)_{\delta l} (\mu)_{\nu l}} \frac{\omega^l (q/\phi)^\eta}{\Gamma(\alpha l + \beta)} dq \\ &= \phi^{-\xi} \sum_{l=0}^{\infty} \frac{\prod_{i=1}^n B_p (b_i, a_i) (\zeta)_{\rho l} (\theta)_{kl}}{\prod_{i=1}^n B (c_i, a_i) (\gamma)_{\delta l} (\mu)_{\nu l}} \frac{\omega^l (1/\phi)^\eta}{\Gamma(\alpha l + \beta)} \int_0^{\infty} e^{-(q/2)} q^{(\xi+\eta l)-1} \omega_{\lambda, \psi}(q) dq. \end{aligned} \tag{26}$$

By using the definition of Whittaker transformation, we get

$$\begin{aligned}
 &= \phi^{-\xi} \sum_{l=0}^{\infty} \frac{\prod_{i=1}^n B_p(b_i, a_i) (\zeta)_{\rho l} (\theta)_{kl} \omega^l (1/\phi)^{\eta l}}{\prod_{i=1}^n B(c_i, a_i) (\gamma)_{\delta l} (\mu)_{\nu l} \Gamma(\alpha l + \beta)} \frac{\Gamma((1/2) + \psi + \xi + \eta l) \Gamma((1/2) - \psi + \xi + \eta l)}{\Gamma(1 - \lambda + \xi + \eta l)} \\
 &= \phi^{-\xi} \sum_{l=0}^{\infty} \frac{\prod_{i=1}^n B_p(b_i, a_i) (\zeta)_{\rho l} (\theta)_{kl} \omega^l (1/\phi)^{\eta l}}{\prod_{i=1}^n B(c_i, a_i) (\gamma)_{\delta l} (\mu)_{\nu l} \Gamma(\alpha l + \beta)} \frac{\Gamma((1/2) \pm \psi + \xi + \eta l)}{\Gamma(1 - \lambda + \xi + \eta l) \Gamma(1 + l)} \\
 &= \phi^{-\xi} \sum_{l=0}^{\infty} \frac{\prod_{i=1}^n B_p(b_i, a_i) (\zeta)_{\rho l} (\theta)_{kl} \omega^l (1/\phi)^{\eta l}}{\prod_{i=1}^n B(c_i, a_i) (\gamma)_{\delta l} (\mu)_{\nu l} \Gamma(\alpha l + \beta)} \frac{\Gamma(g) \Gamma(f + \eta l) \Gamma(f)}{\Gamma(g) \Gamma(g + \eta l) \Gamma(1 + l) \Gamma(f)} \tag{27} \\
 &= \phi^{-\xi} \sum_{l=0}^{\infty} \frac{\prod_{i=1}^n B_p(b_i, a_i) (\zeta)_{\rho l} (\theta)_{kl} \omega^l (1/\phi)^{\eta l}}{\prod_{i=1}^n B(c_i, a_i) (\gamma)_{\delta l} (\mu)_{\nu l} \Gamma(\alpha l + \beta)} \frac{(f - 1)! (f)_{\eta l}}{(g - 1)! (g)_{\eta l} (1)_l} \\
 &= \phi^{-\xi} \frac{(f - 1)!}{(g - 1)!} M_{\alpha, \beta, \gamma, \delta, \mu, \nu, g, \eta, 1}^{\zeta, \rho, \theta, k, f, \eta, n} (\omega \phi^{-\eta}; \underline{a}, \underline{b}, \underline{c}, p),
 \end{aligned}$$

where $f = (1/2) \pm \psi + \xi$ and $g = 1 - \lambda + \xi$, and the required result is obtained. \square

Corollary 3. For $a_i = l, p = 0$ and $\Re(\rho) > 0$, we have

$$\begin{aligned}
 &\int_0^{\infty} e^{-(\phi t/2)} t^{\xi-1} \omega_{\lambda, \psi}(\phi t) M_{\alpha, \beta, \gamma, \delta, \mu, \nu}^{\zeta, \rho, \theta, k, n}(\omega t^{\eta}; \underline{a}, \underline{b}, \underline{c}, p) dt \\
 &= \int_0^{\infty} e^{-(\phi t/2)} t^{\xi-1} \omega_{\lambda, \psi}(\phi t) Q_{\alpha, \beta, \gamma, \delta, \mu, \nu}^{\zeta, \rho, \theta, k, n}(\omega t^{\eta}; \underline{b}, \underline{c}) dt. \tag{28}
 \end{aligned}$$

Similarly for $n = 1, b_1 = c_1 + lk, a_1 = \theta - \lambda, c_1 = \lambda, \rho = \nu = 0$ and $\delta > 0$ one can have

$$\begin{aligned}
 &\int_0^{\infty} e^{-(\phi t/2)} t^{\xi-1} \omega_{\lambda, \psi}(\phi t) M_{\alpha, \beta, \gamma, \delta, \mu, \nu}^{\zeta, \rho, \theta, k, n}(\omega t^{\eta}; \underline{a}, \underline{b}, \underline{c}, p) dt \\
 &\int_0^{\infty} e^{-(\phi t/2)} t^{\xi-1} \omega_{\lambda, \psi}(\phi t) E_{\alpha, \beta, \gamma}^{\zeta, \delta, k, n}(\omega t^{\eta} p) dt. \tag{29}
 \end{aligned}$$

3. Convergence of Unified Mittag-Leffler Function

Before stating the theorem for the convergence of the unified Mittag-Leffler function, we give an important formula that will be used in the proof of our theorem.

Definition 9. The asymptotic formula for the gamma function is given in [5] the following:

$$\frac{\Gamma(a + z)}{\Gamma(b + z)} = z^{a-b} \left[1 + \frac{(a-b)(a+b-1)}{2z} + O\left(\frac{1}{z^2}\right) \right], \tag{30}$$

$$|z| \longrightarrow \infty, |\arg z| < \pi.$$

Theorem 4. The unified Mittag-Leffler function $(M_{\alpha, \beta, \gamma, \delta, \mu, \nu}^{\lambda, \rho, \theta, k, n})$ converges absolutely for all values of $t \in \mathbb{C}$ if $k + \Re(\rho) < \Re(\delta + \nu + \alpha)$ with $\text{Im}(\rho) = \text{Im}(\delta + \nu + \alpha)$.

Proof. By the definition of the unified Mittag-Leffler function, we have the following series:

$$\begin{aligned}
 &M_{\alpha, \beta, \gamma, \delta, \mu, \nu}^{\lambda, \rho, \theta, k, n}(t; \underline{a}, \underline{b}, \underline{c}, p) \\
 &= \sum_{l=0}^{\infty} \frac{\prod_{i=1}^n B_p(b_i, a_i) (\lambda)_{\rho l} (\theta)_{kl}}{\prod_{i=1}^n B(c_i, a_i) (\gamma)_{\delta l} (\mu)_{\nu l} \Gamma(\alpha l + \beta)} t^l \\
 &= \sum_{l=0}^{\infty} a_l t^l, \tag{31}
 \end{aligned}$$

where

$$\begin{aligned}
 a_l &= \frac{\prod_{i=1}^n B_p(b_i, a_i) (\lambda)_{\rho l} (\theta)_{kl}}{\prod_{i=1}^n B(c_i, a_i) (\gamma)_{\delta l} (\mu)_{\nu l} \Gamma(\alpha l + \beta)} \\
 \left| \frac{a_l}{a_{l+1}} \right| &= \left| \frac{(\lambda)_{\rho l}}{(\lambda)_{\rho l + \rho}} \cdot \frac{(\theta)_{kl}}{(\theta)_{kl+k}} \cdot \frac{(\gamma)_{\delta l + \delta}}{(\gamma)_{\delta l}} \cdot \frac{(\mu)_{\nu l + \nu}}{(\mu)_{\nu l}} \cdot \frac{\Gamma(\alpha l + \alpha + \beta)}{\Gamma(\alpha l + \beta)} \right|. \tag{32}
 \end{aligned}$$

Applying limit on both sides, we get the following:

$$\lim_{l \rightarrow \infty} \left| \frac{a_l}{a_{l+1}} \right| = \lim_{l \rightarrow \infty} \left| \frac{(\lambda)_{\rho l}}{(\lambda)_{\rho l + \rho}} \cdot \frac{(\theta)_{kl}}{(\theta)_{kl+k}} \cdot \frac{(\gamma)_{\delta l + \delta}}{(\gamma)_{\delta l}} \cdot \frac{(\mu)_{\nu l + \nu}}{(\mu)_{\nu l}} \cdot \frac{\Gamma(\alpha l + \alpha + \beta)}{\Gamma(\alpha l + \beta)} \right|. \tag{33}$$

Using (30), the fractions involving Pochhammer symbols and gamma function in (33) become the following:

$$\frac{(\lambda)_{\rho l}}{(\lambda)_{\rho l + \rho}} = (\rho l)^{-\rho} \left[1 - \frac{2\lambda + \rho - 1}{2l} + O\left(\frac{1}{(\rho l)^2}\right) \right], \quad (34)$$

$$\frac{(\theta)_{kl}}{(\theta)_{kl+k}} = (kl)^{-k} \left[1 - \frac{2\theta + k - 1}{2l} + O\left(\frac{1}{(kl)^2}\right) \right], \quad (35)$$

$$\frac{(\gamma)_{\delta l + \delta}}{(\gamma)_{\delta l}} = (\delta l)^{\delta} \left[1 + \frac{2\gamma + \delta - 1}{2l} + O\left(\frac{1}{(\delta l)^2}\right) \right], \quad (36)$$

$$\frac{(\mu)_{\nu l + \nu}}{(\mu)_{\nu l}} = (\nu l)^{\nu} \left[1 + \frac{2\mu + \nu - 1}{2l} + O\left(\frac{1}{(\nu l)^2}\right) \right], \quad (37)$$

$$\frac{\Gamma(\alpha l + \alpha + \beta)}{\Gamma(\alpha l + \beta)} = (\alpha l)^{\alpha} \left[1 + \frac{2\beta + \alpha - 1}{2l} + O\left(\frac{1}{(\alpha l)^2}\right) \right]. \quad (38)$$

Using (34)–(38) in (33), we get the following:

$$\begin{aligned} \lim_{l \rightarrow \infty} \left| \frac{a_l}{a_{l+1}} \right| &\approx \lim_{l \rightarrow \infty} |(\rho l)^{-\rho} \left[1 - \frac{2\lambda + \rho - 1}{2l} + O\left(\frac{1}{(\rho l)^2}\right) \right] \\ &\quad \times (kl)^{-k} \left[1 - \frac{2\theta + k - 1}{2l} + O\left(\frac{1}{(kl)^2}\right) \right] (\delta l)^{\delta} \left[1 + \frac{2\gamma + \delta - 1}{2l} + O\left(\frac{1}{(\delta l)^2}\right) \right] \\ &\quad \times (\nu l)^{\nu} \left[1 + \frac{2\mu + \nu - 1}{2l} + O\left(\frac{1}{(\nu l)^2}\right) \right] (\alpha l)^{\alpha} \left[1 + \frac{2\beta + \alpha - 1}{2l} + O\left(\frac{1}{(\alpha l)^2}\right) \right] |, \\ \lim_{l \rightarrow \infty} \left| \frac{a_l}{a_{l+1}} \right| &\approx \lim_{l \rightarrow \infty} \frac{\delta^{\delta} \nu^{\nu} \alpha^{\alpha}}{\rho^{\rho} k^k} \cdot l^{(\delta + \nu + \alpha) - (\rho + k)}. \end{aligned} \quad (39)$$

The formula for the radius of convergence of a series is

$$\lim_{l \rightarrow \infty} \left| \frac{a_l}{a_{l+1}} \right| = R. \quad (40)$$

Therefore, the function $M_{\alpha, \beta, \gamma, \delta, \mu, \nu}^{\lambda, \rho, \theta, k, n}$ converges absolutely for all values of t if $k + \Re(\rho) < \Re(\delta + \nu + \alpha)$ with $\text{Im}(\rho) = \text{Im}(\delta + \nu + \alpha)$. \square

Next, we give recurrence relations of unified Mittag-Leffler function.

Theorem 5. Let $\underline{a} = (a_1, a_2, \dots, a_n)$, $\underline{b} = (b_1, b_2, \dots, b_n)$, $\underline{c} = (c_1, c_2, \dots, c_n)$, $a_i, b_i, c_i \in \mathbb{C}$; $i = 1, \dots, n$ such that $\Re(a_i), \Re(b_i), \Re(c_i) > 0, \forall i$. Also let $\alpha, \beta, \gamma, \delta, \mu, \nu, \lambda, \rho$,

$\theta, t \in \mathbb{C}$, $\min\{\Re(\alpha), \Re(\beta), \Re(\gamma), \Re(\delta), \Re(\lambda), \Re(\theta)\} > 0$, and $k \in (0, 1) \cup \mathbb{N}$ with $k + \Re(\rho) < \Re(\delta + \nu + \alpha)$, $\text{Im}(\rho) = \text{Im}(\delta + \nu + \alpha)$, and then the difference of two consecutive unified Mittag-Leffler functions is given as follows:

$$\begin{aligned} M_{\alpha, \beta, \gamma, \delta, \mu, \nu}^{\lambda, \rho, \theta, k, n}(t; \underline{a}, \underline{b}, \underline{c}, p) - M_{\alpha, \beta, \gamma-1, \delta, \mu, \nu}^{\lambda, \rho, \theta, k, n}(t; \underline{a}, \underline{b}, \underline{c}, p) \\ = \frac{t\delta}{1-\gamma} \frac{d}{dt} M_{\alpha, \beta, \gamma, \delta, \mu, \nu}^{\lambda, \rho, \theta, k, n}(t; \underline{a}, \underline{b}, \underline{c}, p), \end{aligned} \quad (41)$$

with $\Re(\gamma) > 1$.

Proof. By the definition of the unified Mittag-Leffler function, we have

$$\begin{aligned} M_{\alpha, \beta, \gamma, \delta, \mu, \nu}^{\lambda, \rho, \theta, k, n}(t; \underline{a}, \underline{b}, \underline{c}, p) - M_{\alpha, \beta, \gamma-1, \delta, \mu, \nu}^{\lambda, \rho, \theta, k, n}(t; \underline{a}, \underline{b}, \underline{c}, p) \\ = \sum_{l=0}^{\infty} \frac{\prod_{i=1}^n B_p(b_i, a_i) (\lambda)_{\rho l} (\theta)_{kl}}{\prod_{i=1}^n B(c_i, a_i) (\mu)_{\nu l}} \frac{t^l}{\Gamma(\alpha l + \beta)} \left[\frac{1}{(\gamma)_{\delta l}} - \frac{1}{(\gamma-1)_{\delta l}} \right] \\ = \sum_{l=0}^{\infty} \frac{\prod_{i=1}^n B_p(b_i, a_i) (\lambda)_{\rho l} (\theta)_{kl}}{\prod_{i=1}^n B(c_i, a_i) (\mu)_{\nu l}} \frac{t^l}{\Gamma(\alpha l + \beta)} \frac{\Gamma(\gamma)}{\Gamma(\gamma + \delta l)} \frac{\delta l}{1-\gamma} \\ = \frac{\delta t}{1-\gamma} \sum_{l=0}^{\infty} \frac{\prod_{i=1}^n B_p(b_i, a_i) (\lambda)_{\rho l} (\theta)_{kl}}{\prod_{i=1}^n B(c_i, a_i) (\mu)_{\nu l} (\gamma)_{\delta l}} \frac{t^{l-1}}{\Gamma(\alpha l + \beta)} \\ = \frac{t\delta}{1-\gamma} \frac{d}{dt} M_{\alpha, \beta, \gamma, \delta, \mu, \nu}^{\lambda, \rho, \theta, k, n}(t; \underline{a}, \underline{b}, \underline{c}, p). \end{aligned} \quad (42)$$

\square

Theorem 6. For $m \in \mathbb{Z}^+$, $\underline{a} = (a_1, a_2, \dots, a_n)$, $\underline{b} = (b_1, b_2, \dots, b_n)$, $\underline{c} = (c_1, c_2, \dots, c_n)$, where $a_i, b_i, c_i \in \mathbb{C}; i = 1, \dots, n$ such that $\Re(a_i), \Re(b_i), \Re(c_i) > 0, \forall i$. Also let $\alpha, \beta, \gamma, \delta, \mu, \nu, \lambda, \rho, \theta, t \in \mathbb{C}$, $\min\{\Re(\alpha), \Re(\beta), \Re(\gamma), \Re$

$(\delta), \Re(\lambda), \Re(\theta)\} > 0$ and $k \in (0, 1) \cup \mathbb{N}$ with $k + \Re(\rho) < \Re(\delta + \nu + \alpha)$, $\text{Im}(\rho) = \text{Im}(\delta + \nu + \alpha)$, and m th derivative of unified Mittag-Leffler function is given by

$$\begin{aligned} & \left(\frac{d}{dt}\right)^m M_{\alpha, \beta, \gamma, \delta, \mu, \nu}^{\lambda, \rho, \theta, k, n}(t; \underline{a}, \underline{b}, \underline{c}, p) \\ &= \frac{(\lambda)_{mp} (\theta)_{mk} \sum_{l=0}^{\infty} \prod_{i=1}^n B_p(b_i, a_i) (\lambda + \rho m)_{\rho l} (\theta + km)_{kl}}{(\gamma)_{m\delta} (\mu)_{m\nu} \sum_{l=0}^{\infty} \prod_{i=1}^n B(c_i, a_i) (\gamma + \delta m)_{\delta l} (\mu + \nu m)_{\nu l}} \cdot \frac{(1+l)_m t^l}{\Gamma(\alpha(l+m) + \beta)}. \end{aligned} \tag{43}$$

Proof. Differentiating the unified Mittag-Leffler function m times, we get

$$\begin{aligned} & \left(\frac{d}{dt}\right)^m M_{\alpha, \beta, \gamma, \delta, \mu, \nu}^{\lambda, \rho, \theta, k, n}(t; \underline{a}, \underline{b}, \underline{c}, p) \\ &= \frac{\sum_{l=m}^{\infty} \prod_{i=1}^n B_p(b_i, a_i) (\lambda)_{\rho l} (\theta)_{kl} [(l-1), \dots, (l-(m-1))] t^{l-m}}{\prod_{i=1}^n B(c_i, a_i) (\gamma)_{\delta l} (\mu)_{\nu l} \Gamma(\alpha l + \beta)} \\ &= \frac{\sum_{l=0}^{\infty} \prod_{i=1}^n B_p(b_i, a_i) (\lambda)_{\rho(l+m)} (\theta)_{k(l+m)} [(l+m)(l+m-1), \dots, (l+1)] t^l}{\prod_{i=1}^n B(c_i, a_i) (\gamma)_{\delta(l+m)} (\mu)_{\nu(l+m)} \Gamma(\alpha l + \beta)}. \end{aligned} \tag{44}$$

We know that $(\theta)_{a+b} = (\theta+a)_b (\theta)_a$. Therefore, we obtain

$$\begin{aligned} & \left(\frac{d}{dt}\right)^m M_{\alpha, \beta, \gamma, \delta, \mu, \nu}^{\lambda, \rho, \theta, k, n}(t; \underline{a}, \underline{b}, \underline{c}, p) \\ &= \frac{(\lambda)_{mp} (\theta)_{mk} \sum_{l=0}^{\infty} \prod_{i=1}^n B_p(b_i, a_i) (\lambda + \rho m)_{\rho l} (\theta + km)_{kl}}{(\gamma)_{m\delta} (\mu)_{m\nu} \sum_{l=0}^{\infty} \prod_{i=1}^n B(c_i, a_i) (\gamma + \delta m)_{\delta l} (\mu + \nu m)_{\nu l}} \cdot \frac{(1+l)_m t^l}{\Gamma(\alpha(l+m) + \beta)}. \end{aligned} \tag{45}$$

Next, we give the definition of fractional integral operator with unified Mittag-Leffler (Mfunction) as the kernel.

Definition 10. Let $f \in L_1[a, b]$. Then $\forall \xi \in [a, b]$, the fractional integral operator with Mfunction as its kernel is defined as follows:

$$\begin{aligned} I_{a^+}^{\omega, \lambda, \rho, \theta, k, n} f(\xi; \underline{a}, \underline{b}, \underline{c}, p) &= \int_a^\xi (\xi - t)^{\beta-1} M_{\alpha, \beta, \gamma, \delta, \mu, \nu}^{\lambda, \rho, \theta, k, n}(\omega(\xi - t)^\alpha; \underline{a}, \underline{b}, \underline{c}, p) f(t) dt, \\ I_{b^-}^{\omega, \lambda, \rho, \theta, k, n} f(\xi; \underline{a}, \underline{b}, \underline{c}, p) &= \int_\xi^b (t - \xi)^{\beta-1} M_{\alpha, \beta, \gamma, \delta, \mu, \nu}^{\lambda, \rho, \theta, k, n}(\omega(t - \xi)^\alpha; \underline{a}, \underline{b}, \underline{c}, p) f(t) dt, \end{aligned} \tag{46}$$

with $\underline{a} = (a_1, a_2, \dots, a_n)$, $\underline{b} = (b_1, b_2, \dots, b_n)$, $\underline{c} = (c_1, c_2, \dots, c_n)$, where $a_i, b_i, c_i, \omega \in \mathbb{C}; i = 1, \dots, n$ such that $\Re(a_i), \Re(b_i), \Re(c_i) > 0, \forall i$. Also let $\alpha, \beta, \gamma, \delta, \mu, \nu, \lambda, \rho,$

$\theta, t \in \mathbb{C}$, $\min\{\Re(\alpha), \Re(\beta), \Re(\gamma), \Re(\delta), \Re(\lambda), \Re(\theta)\} > 0$, and $k \in (0, 1) \cup \mathbb{N}$ with $k + \Re(\rho) < \Re(\delta + \nu + \alpha)$, $\text{Im}(\rho) = \text{Im}(\delta + \nu + \alpha)$.

Remark 1. For $n = 1$, $b_1 = c_1 + lk$, $a_1 = \theta - \lambda$, $c_1 = \lambda$, $\rho = \nu = 0$, $\delta > 0$, we obtain the fractional integral operator containing extended generalized Mittag-Leffler function in its kernel and is given by [5];

$$\begin{aligned} \varepsilon_{a^+, \alpha, \beta, \gamma}^{\omega, \lambda, \delta, k, \theta} f(\xi, \rho) &= \int_a^\xi (\xi - t)^{\beta-1} E_{\alpha, \beta, \gamma}^{\lambda, \delta, k, \theta}(\omega(\xi - t)^\alpha, \rho) f(t) dt, \\ \varepsilon_{b^-, \alpha, \beta, \gamma}^{\omega, \lambda, \delta, k, \theta} f(\xi, \rho) &= \int_\xi^b (t - \xi)^{\beta-1} E_{\alpha, \beta, \gamma}^{\lambda, \delta, k, \theta}(\omega(t - \xi)^\alpha, \rho) f(t) dt. \end{aligned} \tag{47}$$

Now we give the proof of boundedness of the fractional integral operator defined above.

Theorem 7. Let $f \in L_1[a, b]$. If $\underline{a} = (a_1, a_2, \dots, a_n)$, $\underline{b} = (b_1, b_2, \dots, b_n)$, $\underline{c} = (c_1, c_2, \dots, c_n)$, where $a_i, b_i, c_i, \omega \in \mathbb{C}$; $i = 1, \dots, n$ such that $\Re(a_i), \Re(b_i), \Re(c_i) > 0, \forall i$. Also let $\alpha, \beta, \gamma, \delta, \mu, \nu, \lambda, \rho, \theta, t \in \mathbb{C}$, $\min\{\Re(\alpha), \Re(\beta), \Re(\gamma), \Re(\delta), \Re(\lambda), \Re(\theta)\} > 0$, and $k \in (0, 1) \cup \mathbb{N}$ with $k + \Re(\rho) < \Re(\delta + \nu + \alpha)$, $\text{Im}(\rho) = \text{Im}(\delta + \nu + \alpha)$, and then the fractional integral operator $I_{a^+, \alpha, \beta, \gamma, \delta, \mu, \nu}^{\omega, \lambda, \rho, \theta, k, n} f$ is bounded on $L_1[a, b]$.

Proof. Applying 1-norm to the fractional integral operator $I_{a^+, \alpha, \beta, \gamma, \delta, \mu, \nu}^{\omega, \lambda, \rho, \theta, k, n} f$, we get the following:

$$\begin{aligned} \|I_{a^+, \alpha, \beta, \gamma, \delta, \mu, \nu}^{\omega, \lambda, \rho, \theta, k, n} f\|_1 &= \int_a^b \left| \int_a^\xi (\xi - t)^{\beta-1} M_{\alpha, \beta, \gamma, \delta, \mu, \nu}^{\lambda, \rho, \theta, k, n}(\omega(\xi - t)^\alpha; \underline{a}, \underline{b}, \underline{c}, \rho) f(t) dt \right| d\xi \\ &\leq \int_a^b |f(t)| \left[\int_t^b (\xi - t)^{\Re(\beta)-1} \left| M_{\alpha, \beta, \gamma, \delta, \mu, \nu}^{\lambda, \rho, \theta, k, n}(\omega(\xi - t)^\alpha; \underline{a}, \underline{b}, \underline{c}, \rho) \right| d\xi \right] dt. \end{aligned} \tag{48}$$

By substituting $\xi - t = s$, we obtain the following inequality:

$$\begin{aligned} \|I_{a^+, \alpha, \beta, \gamma, \delta, \mu, \nu}^{\omega, \lambda, \rho, \theta, k, n} f\|_1 &\leq \int_a^b |f(t)| \left[\int_0^{b-t} s^{\Re(\beta)-1} \left| M_{\alpha, \beta, \gamma, \delta, \mu, \nu}^{\lambda, \rho, \theta, k, n}(\omega s^\alpha; \underline{a}, \underline{b}, \underline{c}, \rho) \right| ds \right] dt \\ &\leq \int_a^b |f(t)| \left[\int_0^{b-a} s^{\Re(\beta)-1} \left| M_{\alpha, \beta, \gamma, \delta, \mu, \nu}^{\lambda, \rho, \theta, k, n}(\omega s^\alpha; \underline{a}, \underline{b}, \underline{c}, \rho) \right| ds \right] dt \\ &\leq \left| \sum_{l=0}^\infty \frac{\prod_{i=1}^n B_p(b_i, a_i)(\lambda)_{\rho l}(\theta)_{kl}}{\prod_{i=1}^n B(c_i, a_i)(\gamma)_{\delta l}(\mu)_{\nu l}} \frac{\omega^l}{\Gamma(\alpha l + \beta)} \right| \\ &\quad \times \int_0^{b-a} s^{\Re(\alpha)l + \Re(\beta)-1} ds \|f\|_1 \\ &\leq \left| \sum_{l=0}^\infty \frac{\prod_{i=1}^n B_p(b_i, a_i)(\lambda)_{\rho l}(\theta)_{kl}}{\prod_{i=1}^n B(c_i, a_i)(\gamma)_{\delta l}(\mu)_{\nu l}} \frac{\omega^l}{\Gamma(\alpha l + \beta)} \frac{(b-a)^{\Re(\alpha)l}}{\Re(\alpha)l + \Re(\beta)} \right| \times (b-a)^{\Re(\beta)} \|f\|_1, \\ \|I_{a^+, \alpha, \beta, \gamma, \delta, \mu, \nu}^{\omega, \lambda, \rho, \theta, k, n} f\|_1 &\leq K \|f\|_1, \end{aligned} \tag{49}$$

where

$$K = \left| \frac{\prod_{i=1}^n B_p(b_i, a_i)(\lambda)_{\rho l}(\theta)_{kl}}{\prod_{i=1}^n B(c_i, a_i)(\gamma)_{\delta l}(\mu)_{\nu l}} \frac{\omega^l}{\Gamma(\alpha l + \beta)} \frac{(b-a)^{\Re(\alpha)l}}{\Re(\alpha)l + \Re(\beta)} \right| (b-a)^{\Re(\beta)}. \tag{50}$$

□

4. Conclusions

In this paper, we extended the Mittag-Leffler function and generalized Q function simultaneously. By applying the Laplace, Euler beta, and Whittaker transformations on the unified Mittag-Leffler function, compact formulas are

established from which formulas for generalized Q function and extended generalized Mittag-Leffler function are deduced. These formulas also reproduce integral transformations of various deduced Mittag-Leffler functions. Moreover, we proved the convergence of this unified Mittag-Leffler function and constructed the associated fractional integral operator. Our proposed unified Mittag-Leffler function and constructed fractional integral operator will give new directions to the researcher working in this field.

Data Availability

There are no additional data required for the finding of results of this paper.

Conflicts of Interest

It is declared that the authors have no conflicts of interests.

Authors' Contributions

All authors have equal contribution in this article.

Acknowledgments

This work was supported by Jiangsu Provincial Department of Education (2020SJA1632), Jiangsu Provincial Association of Higher Education (2020JDKT150), and the Blue Project of Colleges and Universities in Jiangsu Province.

References

- [1] P. K. Kythe, P. Puri, and M. R. Schäferkotter, *Partial Differential Equations and Boundary Value Problems with Mathematica*, CRC Press, Boca Raton, FL, USA, 2002.
- [2] D. Bhatnagar and R. M. Pandey, "A study of some integral transforms on Q function," *South East Asian Journal of Mathematics and Mathematical Sciences*, vol. 16, no. 1, pp. 99–110, 2020.
- [3] W. E. Deming: The gamma and beta functions, Graduate school, Department of agriculture, 1946.
- [4] A. Wiman, "Über den fundamentalsatz in der theorie der funktionen $E_a(x)$," *Acta Mathematica*, vol. 29, pp. 191–201, 1905.
- [5] M. Andrić, G. Farid, and J. Pečarić, "A further extension of mittag-leffler function," *Journal of Fractional Calculus and Applications*, vol. 21, no. 5, pp. 1377–1395, 2018.
- [6] A. K. Shukla and J. C. Prajapati, "On a generalization of mittag-leffler function and its properties," *Journal of Mathematical Analysis and Applications*, vol. 336, no. 2, pp. 797–811, 2007.
- [7] G. Rahman, D. Baleanu, M. Al Qurashi, S. D. Purohit, S. Mubeen, and M. Arshad, "The extended mittag-leffler function via fractional calculus," *The Journal of Nonlinear Sciences and Applications*, vol. 10, no. 08, pp. 4244–4253, 2017.
- [8] T. O. Salim and A. W. Faraj, "A generalization of mittag-leffler function and integral operator associated with fractional calculus," *Journal of Fractional Calculus and Applications*, vol. 3, no. 5, pp. 1–13, 2012.
- [9] T. R. Prabhakar, "A singular integral equation with a generalized mittag-leffler function in the kernel," *Yokohama Mathematical Journal*, vol. 19, pp. 7–15, 1971.
- [10] B. Meftah, A. Souahi, and A. Souahi, "Cebyšev inequalities for co-ordinated QC-convex and (s, QC)-convex," *Engineering and Applied Science Letters*, vol. 4, no. 1, pp. 14–20, 2021.
- [11] M. E. Omaba, L. O. Omenyi, and L. O. Omenyi, "Generalized fractional hadamard type inequalities for (Qs)-class functions of the second kind," *Open Journal of Mathematical Sciences*, vol. 5, no. 1, pp. 270–278, 2021.
- [12] D. Baleanu, P. O. Mohammed, and S. Zeng, "Inequalities of trapezoidal type involving generalized fractional integrals," *Alexandria Engineering Journal*, vol. 59, no. 5, pp. 2975–2984, 2020.
- [13] D. Nie, S. Rashid, A. O. Akdemir, D. Baleanu, and J.-B. Liu, "On some new weighted inequalities for differentiable exponentially convex and exponentially quasi-convex functions with applications," *Mathematics*, vol. 7, no. 8, p. 727, 2019.
- [14] G. Farid, K. Mahreen, and Y. M. Chu, "Study of inequalities for unified integral operators of generalized convex functions," *Open Journal of Mathematical Sciences*, vol. 5, no. 1, pp. 80–93, 2021.
- [15] G. Mittag-Leffler, "Sur la nouvelle fonction $E(x)$," *Comptes Rendus de l'Académie des Sciences*, vol. 137, pp. 554–558, 1903.

Research Article

Some New Kinds of Fractional Integral Inequalities via Refined $(\alpha, h - m)$ -Convex Function

Moquddsa Zahra,¹ Muhammad Ashraf,¹ Ghulam Farid ,² and Kamsing Nonlaopon ³

¹Department of Mathematics, University of Wah, Wah Cantt, Pakistan

²Department of Mathematics, COMSATS University Islamabad, Attock Campus, Attock, Pakistan

³Department of Mathematics, Faculty of Science, Khon Kaen University, Khon Kaen 40002, Thailand

Correspondence should be addressed to Kamsing Nonlaopon; nkamsi@kku.ac.th

Received 10 July 2021; Accepted 28 August 2021; Published 14 September 2021

Academic Editor: Amr Elsonbaty

Copyright © 2021 Moquddsa Zahra et al. This is an open access article distributed under the Creative Commons Attribution License, which permits unrestricted use, distribution, and reproduction in any medium, provided the original work is properly cited.

In this article, we present new integral inequalities for refined $(\alpha, h - m)$ -convex functions using unified integral operators (12) and (13). The established results provide the refinements of several well-known integral and fractional integral inequalities.

1. Introduction

Convex functions are important in diverse fields of mathematics, statistics, engineering, and optimization. Especially in the formation of inequalities, they play a very vital role. In the subject of mathematical analysis, inequalities provide a significant contribution in developing classical concepts and notions. For example, inequalities well known as Cauchy–Schwarz inequality, Chebyshev inequality, Minkowski inequality, Hadamard inequality, and Jensen inequality are utilized frequently in pure and applied mathematics. It is always a challenge to extend, generalize, and refine such inequalities by considering new classes of functions. In this era, researchers are working on classical inequalities concerning fractional integral and derivative operators. It can be observed that the Hadamard inequality is studied more for many kinds of fractional integral and derivative operators than any other classical inequality, see [1–7] for more details.

The aim of this paper is to study the refinements of Hadamard and other integral inequalities recently studied in [8–11]. The consequences of these inequalities also provide refinements of fractional integral inequalities connected with the integral inequalities studied in the recent past.

The article is organized as follows. In Section 2, we suggest some preliminaries. In Section 3, the bounds of unified integral operators are given using refined

$(\alpha, h - m)$ -convex functions. These are the refinements of bounds already obtained in the literature. In Section 4, some applications of the main results are given in the form of fractional integral inequalities and their refinements.

2. Preliminaries

In this section, we give definitions of different kinds of convex functions and integral operators which will be useful in formulating the results of this paper. Throughout the paper, all the functions are assumed to be real-valued functions until specified.

Definition 1 (see [12]). A function Ω is called convex if

$$\Omega(tx'_1 + (1-t)y'_1) \leq t\Omega(x'_1) + (1-t)\Omega(y'_1), \quad (1)$$

holds for all $x'_1, y'_1 \in I \subseteq \mathbb{R}$ and $t \in [0, 1]$.

Definition 2 (see [1]). A function Ω is called (s, m) -convex if for each $x'_1, y'_1 \in [0, v] \subseteq \mathbb{R}$, we have

$$\Omega(tx'_1 + m(1-t)y'_1) \leq t^s \Omega(x'_1) + m(1-t)^s \Omega(y'_1), \quad (2)$$

where $t \in [0, 1]$ and $(s, m) \in [0, 1]^2$.

Definition 3 (see [13]). A function Ω is called (α, m) -convex if for each $x'_1, y'_1 \in [0, \nu] \subseteq \mathbb{R}$, we have

$$\Omega(tx'_1 + m(1-t)y'_1) \leq t^\alpha \Omega(x'_1) + m(1-t^\alpha)\Omega(y'_1), \quad (3)$$

where $(\alpha, m) \in [0, 1]^2$ and $t \in [0, 1]$.

Definition 4 (see [4]). Let $h: J \rightarrow \mathbb{R}$ is a function with $h \equiv 0$ and $(0, 1) \subseteq J$. A function Ω is said to be $(h - m)$ -convex, if $\Omega, h \geq 0$ and for each $x'_1, y'_1 \in [0, \nu] \subseteq \mathbb{R}$, we have

$$\Omega(tx'_1 + m(1-t)y'_1) \leq h(t)\Omega(x'_1) + mh(1-t)\Omega(y'_1), \quad (4)$$

where $m \in [0, 1]$ and $t \in (0, 1)$.

Definition 5 (see [4]). Let $h: J \rightarrow \mathbb{R}$ is a function with $h \equiv 0$ and $(0, 1) \subseteq J$. A function Ω is said to be $(\alpha, h - m)$ -convex, if $\Omega, h \geq 0$ and for each $x'_1, y'_1 \in [0, \nu] \subseteq \mathbb{R}$, we have

$$\Omega(tx'_1 + m(1-t)y'_1) \leq h(t^\alpha)\Omega(x'_1) + mh(1-t^\alpha)\Omega(y'_1), \quad (5)$$

where $(\alpha, m) \in [0, 1]^2$ and $t \in (0, 1)$.

Definition 6 (see [14]). Let $h: J \rightarrow \mathbb{R}$ be a function with $h \equiv 0$ and $(0, 1) \subseteq J$. A function Ω is called refined $(\alpha, h - m)$ -convex function, if $\Omega, h \geq 0$ and for each $x'_1, y'_1 \in [0, \nu] \subseteq \mathbb{R}$, we have

$$\Omega(tx'_1 + m(1-t)y'_1) \leq h(t^\alpha)h(1-t^\alpha)(\Omega(x'_1) + m\Omega(y'_1)), \quad (6)$$

where $(\alpha, m) \in (0, 1]^2$ and $t \in (0, 1)$.

Inequality (6) gives refinements of several types of convexities when $0 < h(t) < 1$, see [14].

The need for integral operators in the study of fractional derivatives is of immense importance. In the recent era, integral operators are being used extensively for producing new results in the literature. For references, see [2, 4–6]. Next, we give some fundamental integral operators which are used in this paper.

Definition 7 (see [15]). Let $\Omega \in L_1[x'_1, y'_1]$ and Δ be positive and increasing function having a continuous derivative on (x'_1, y'_1) . The left and right fractional integrals of Ω with respect to Δ on $[x'_1, y'_1]$ of order κ are given by

$$\begin{aligned} {}_{\Delta}^{\kappa} I_{y'_1^+} \Omega(x) &= \frac{1}{\Gamma(\kappa)} \int_{x'_1}^x (\Delta(x) - \Delta(t))^{\kappa-1} \Delta'(t) \Omega(t) dt, \quad x > x'_1, \\ {}_{\Delta}^{\kappa} I_{y'_1^-} \Omega(x) &= \frac{1}{\Gamma(\kappa)} \int_x^{y'_1} (\Delta(t) - \Delta(x))^{\kappa-1} \Delta'(t) \Omega(t) dt, \quad x < y'_1, \end{aligned} \quad (7)$$

where $\Gamma(\cdot)$ is the gamma function and $\Re(\kappa) > 0$.

Definition 8 (see [16]). Let $\Omega \in L_1[x'_1, y'_1]$ and Δ be positive and increasing function having a continuous derivative on

(x'_1, y'_1) . The left and right k -fractional integrals of Ω with respect to Δ on $[x'_1, y'_1]$ of order κ are given by

$$\begin{aligned} {}_{\Delta}^{\kappa} I_{x'_1^-} \Omega(x) &= \frac{1}{k\Gamma_k(\kappa)} \int_{x'_1}^x (\Delta(x) - \Delta(t))^{(\kappa/k)-1} \Delta'(t) \Omega(t) dt, \quad x > x'_1, \\ {}_{\Delta}^{\kappa} I_{y'_1^+} \Omega(x) &= \frac{1}{k\Gamma_k(\kappa)} \int_x^{y'_1} (\Delta(t) - \Delta(x))^{(\kappa/k)-1} \Delta'(t) \Omega(t) dt, \quad x < y'_1, \end{aligned} \quad (8)$$

where $\Gamma_k(\cdot)$ is the k -gamma function and $\Re(\kappa), k > 0$.

Definition 9 (see [17]). Let $\Omega \in L_1[x'_1, y'_1]$ and $x \in [x'_1, y'_1]$, also let

$\sigma, \kappa, \alpha, \xi, \gamma, \iota \in \mathbb{C}, \Re(\kappa), \Re(\alpha), \Re(\xi) > 0, \Re(\iota) > \Re(\gamma) > 0$ with $p \geq 0, \delta > 0$, and $0 < k \leq \delta + \Re(\kappa)$, then the generalized fractional integral operators $e_{\kappa, \alpha, \xi, \sigma, x'_1^+}^{\gamma, \delta, k, \iota} \Omega$ and $e_{\kappa, \alpha, \xi, \sigma, y'_1^-}^{\gamma, \delta, k, \iota} \Omega$ are defined by

$$\begin{aligned} \left(e_{\kappa, \alpha, \xi, \sigma, x'_1^+}^{\gamma, \delta, k, \iota} \Omega \right) (x; p) &= \int_{x'_1}^x (x-t)^{\alpha-1} E_{\kappa, \alpha, \xi}^{\gamma, \delta, k, \iota}(\sigma(x-t)^\kappa; p) \Omega(t) dt, \\ \left(e_{\kappa, \alpha, \xi, \sigma, y'_1^-}^{\gamma, \delta, k, \iota} \Omega \right) (x; p) &= \int_x^{y'_1} (t-x)^{\alpha-1} E_{\kappa, \alpha, \xi}^{\gamma, \delta, k, \iota}(\sigma(t-x)^\kappa; p) \Omega(t) dt, \end{aligned} \quad (10)$$

where $E_{\kappa,\alpha,\xi}^{\gamma,\delta,k,t}(t; p)$ is the extended generalized Mittag–Leffler function defined as

$$E_{\kappa,\alpha,\xi}^{\gamma,\delta,k,t}(t; p) = \sum_{n=0}^{\infty} \frac{\rho_p(\gamma + nk, t - \gamma)}{\rho(\gamma, t - \gamma)} \frac{(t)_{nk}}{\Gamma(\kappa n + \alpha)} \frac{t^n}{(\xi)_{n\delta}}. \quad (11)$$

Definition 10 (see [16]). Let Ω, Δ be real-valued functions defined over $[x'_1, y'_1]$ with $0 < x'_1 < y'_1$, where Ω is positive and integrable and Δ is differentiable and strictly increasing. Also, let Y/x be an increasing function on $[x'_1, \infty)$ and $\alpha, \xi, \gamma, \iota \in \mathbb{C}, p, \kappa, \delta \geq 0$, and $0 < k \leq \delta + \kappa$. Then, for $x \in [x'_1, y'_1]$, the left and right integral operators are defined as

$$\left({}_{\Delta} \mathbb{F}_{\kappa,\alpha,\xi,x'_1}^{\Upsilon,\gamma,\delta,k,t} \Omega \right) (x, \sigma; p) = \int_{x'_1}^x J_x^{\gamma} \left(E_{\kappa,\alpha,\xi}^{\gamma,\delta,k,t}, \Delta; \Upsilon \right) \Delta'(y) \Omega(y) dy, \quad (12)$$

$$\left({}_{\Delta} \mathbb{F}_{\kappa,\alpha,\xi,y'_1}^{\Upsilon,\gamma,\delta,k,t} \Omega \right) (x, \sigma; p) = \int_x^{y'_1} J_y^{\gamma} \left(E_{\kappa,\alpha,\xi}^{\gamma,\delta,k,t}, \Delta; \Upsilon \right) \Delta'(y) \Omega(y) dy, \quad (13)$$

where

$$J_x^{\gamma} \left(E_{\kappa,\alpha,\xi}^{\gamma,\delta,k,t}, \Delta; \Upsilon \right) = \frac{\Upsilon(\Delta(x) - \Delta(y))}{\Delta(x) - \Delta(y)} E_{\kappa,\alpha,\xi}^{\gamma,\delta,k,t}(\sigma(\Delta(x) - \Delta(y))^{\kappa}; p). \quad (14)$$

Mittag–Leffler functions give several fractional integrals by assigning particular choice to the parameters involved in it, see Remarks 6 and 7 in [16].

3. Main Results

Throughout the paper, we use the following notation:

$$\int_0^1 h(u^\alpha) h(1 - u^\alpha) \Delta'(x - u(x - x'_1)) du = H_{x'}^{x'_1}(u^\alpha; h, \Delta). \quad (15)$$

Theorem 1. Let Ω be a positive, refined $(\alpha, h - m)$ -convex and integrable function defined over $[x'_1, y'_1]$. Also, let Y/x be an increasing function defined on $[x'_1, y'_1]$ and Δ be strictly increasing and differentiable function on (x'_1, y'_1) . Then, for $\beta, \xi, \gamma, \iota \in \mathbb{R}, p, \kappa, \vartheta, \delta \geq 0, 0 < k \leq \delta + \kappa$, and $0 < k \leq \delta + \vartheta$, the following result holds:

$$\begin{aligned} & \left({}_{\Delta} \mathbb{F}_{\kappa,\beta,\xi,y'_1}^{\Upsilon,\gamma,\delta,k,t} \Omega \right) (x, \sigma; p) + \left({}_{\Delta} \mathbb{F}_{\vartheta,\beta,\xi,x'_1}^{\Upsilon,\gamma,\delta,k,t} \Omega \right) (x, \sigma; p) \\ & \leq J_{x'}^{x'_1} \left(E_{\kappa,\beta,\xi}^{\gamma,\delta,k,t}, \Delta; \Upsilon \right) \left(\Omega(x'_1) + m\Omega\left(\frac{x}{m}\right) \right) (x - x'_1) H_{x'}^{x'_1}(u^\alpha; h, \Delta) \\ & \quad + J_{y'_1}^x \left(E_{\vartheta,\beta,\xi}^{\gamma,\delta,k,t}, \Delta; \Upsilon \right) \left(\Omega(y'_1) + m\Omega\left(\frac{x}{m}\right) \right) (y'_1 - x) H_{y'_1}^x(v^\alpha; h, \Delta). \end{aligned} \quad (16)$$

Proof. For the functions Y/x and Δ , the following inequality holds:

$$J_x^t \left(E_{\kappa,\beta,\xi}^{\gamma,\delta,k,t}, \Delta; \Upsilon \right) \Delta'(t) \leq J_{x'}^{x'_1} \left(E_{\kappa,\alpha,\xi}^{\gamma,\delta,k,t}, \Delta; \Upsilon \right) \Delta'(t). \quad (17)$$

Using refined $(\alpha, h - m)$ -convexity of Ω , one can have

$$\Omega(t) \leq h\left(\left(\frac{x-t}{x-x'_1}\right)^\alpha\right) h\left(1 - \left(\frac{x-t}{x-x'_1}\right)^\alpha\right) \left(\Omega(x'_1) + m\Omega\left(\frac{x}{m}\right)\right). \quad (18)$$

From (17) and (18), we have the following integral inequality:

$$\int_{x_1'}^x J_x^t \left(E_{\kappa, \beta, \xi}^{\gamma, \delta, k, t}, \Delta; \Upsilon \right) \Delta'(t) \Omega(t) dt \leq J_x^{x_1'} \left(E_{\kappa, \beta, \xi}^{\gamma, \delta, k, t}, \Delta; \Upsilon \right) \left(\Omega(x_1') + m \Omega\left(\frac{x}{m}\right) \right) \times \int_{x_1'}^x h\left(\left(\frac{x-t}{x-x_1'}\right)^\alpha\right) h\left(1 - \left(\frac{x-t}{x-x_1'}\right)^\alpha\right) \Delta'(t) dt. \quad (19)$$

Using (12) of Definition 10 on the left side of inequality (19) and making change of the variable by setting $u = x -$

$t/x - x_1'$ on the right-hand side of the above inequality, we obtain

$$\left({}_{\Delta} \mathbb{F}_{\kappa, \beta, \xi, y_1'}^{\Upsilon, \gamma, \delta, k, t} \Omega \right) (x, \sigma; p) \leq J_x^{x_1'} \left(E_{\kappa, \beta, \xi}^{\gamma, \delta, k, t}, \Delta; \Upsilon \right) (x - x_1') \left(\Omega(x_1') + m \Omega\left(\frac{x}{m}\right) \right) \times \int_0^1 h(u^\alpha) h(1 - u^\alpha) \Delta'(x - u(x - x_1')) du. \quad (20)$$

Thus, we obtain

$$\left({}_{\Delta} \mathbb{F}_{\kappa, \beta, \xi, y_1'}^{\Upsilon, \gamma, \delta, k, t} \Omega \right) (x, \sigma; p) \leq J_x^{x_1'} \left(E_{\kappa, \beta, \xi}^{\gamma, \delta, k, t}, \Delta; \Upsilon \right) (x - x_1') \left(\Omega(x_1') + m \Omega\left(\frac{x}{m}\right) \right) (x - x_1') H_x^{x_1'}(u^\alpha; h, \Delta). \quad (21)$$

Also, for $t \in (x, y_1']$ and $x \in (x_1', y_1')$, we can write

$$J_t^x \left(E_{\vartheta, \beta, \xi}^{\gamma, \delta, k, t}, \Delta; \Upsilon \right) \Delta'(t) \leq J_{y_1'}^x \left(E_{\vartheta, \beta, \xi}^{\gamma, \delta, k, t}, \Delta; \Upsilon \right) \Delta'(t). \quad (22)$$

and

$$\Omega(t) \leq h\left(\left(\frac{t-x}{y_1'-x}\right)^\alpha\right) h\left(1 - \left(\frac{t-x}{y_1'-x}\right)^\alpha\right) \left(\Omega(y_1') + m \Omega\left(\frac{x}{m}\right) \right). \quad (23)$$

From (22) and (23), we have the following integral inequality:

$$\int_x^{y_1'} J_t^x \left(E_{\vartheta, \beta, \xi}^{\gamma, \delta, k, t}, \Delta; \Upsilon \right) \Delta'(t) \Omega(t) dt \leq J_{y_1'}^x \left(E_{\vartheta, \beta, \xi}^{\gamma, \delta, k, t}, \Delta; \Upsilon \right) \left(\Omega(y_1') + m \Omega\left(\frac{x}{m}\right) \right) \times \int_x^{y_1'} h\left(\left(\frac{t-x}{y_1'-x}\right)^\alpha\right) h\left(1 - \left(\frac{t-x}{y_1'-x}\right)^\alpha\right) \Delta'(t) dt. \quad (24)$$

Using (13) of Definition 10 on the left-hand side and making change of the variable by setting $v = t - x/y_1' - x$ on the right-hand side of the above inequality, we obtain

$$\left({}_{\Delta} \mathbb{F}_{\vartheta, \beta, \xi, y_1'}^{\Upsilon, \gamma, \delta, k, t} \Omega \right) (x, \sigma; p) \leq J_{y_1'}^x \left(E_{\vartheta, \beta, \xi}^{\gamma, \delta, k, t}, \Delta; \Upsilon \right) \left(\Omega(y_1') + m \Omega\left(\frac{x}{m}\right) \right) (y_1' - x) \times \int_0^1 h(v^\alpha) h(1 - v^\alpha) \Delta'(x + v(y_1' - x)) dv \quad (25)$$

Therefore,

$$\begin{aligned} & \left({}_{\Delta} \mathbb{F}_{\vartheta, \beta, \xi, y_1'}^{\Upsilon, \gamma, \delta, k, t} \Omega \right) (x, \sigma; p) \\ & \leq J_{y_1'}^x \left(E_{\vartheta, \beta, \xi}^{\gamma, \delta, k, t}, \Delta; \Upsilon \right) \left(\Omega(y_1') + m \Omega \left(\frac{x}{m} \right) \right) (y_1' - x) H_{y_1'}^x (v^\alpha; h, \Delta). \end{aligned} \tag{26}$$

Combining (21) and (26), the required inequality (16) is obtained. Hence, the proof is completed.

Next, we give the refinement of Theorem 1. \square

Theorem 2. Under the assumptions of Theorem 1, if $0 < h(t) < 1$, then the following result holds:

$$\begin{aligned} & \left({}_{\Delta} \mathbb{F}_{\vartheta, \beta, \xi, y_1'}^{\Upsilon, \gamma, \delta, k, t} \Omega \right) (x, \sigma; p) + \left({}_{\Delta} \mathbb{F}_{\vartheta, \beta, \xi, y_1'}^{\Upsilon, \gamma, \delta, k, t} \Omega \right) (x, \sigma; p) \\ & \leq J_x^{x_1'} \left(E_{\kappa, \beta, \xi}^{\gamma, \delta, k, t}, \Delta; \Upsilon \right) \left(\Omega(x_1') + m \Omega \left(\frac{x}{m} \right) \right) (x - x_1') H_x^{x_1'} (u^\alpha; h, \Delta) \\ & \quad + J_{y_1'}^x \left(E_{\vartheta, \beta, \xi}^{\gamma, \delta, k, t}, \Delta; \Upsilon \right) \left(\Omega(y_1') + m \Omega \left(\frac{x}{m} \right) \right) (y_1' - x) H_{y_1'}^x (v^\alpha; h, \Delta) \\ & \leq J_x^{x_1'} \left(E_{\kappa, \beta, \xi}^{\gamma, \delta, k, t}, \Delta; \Upsilon \right) (x - x_1') \left(\Omega(x_1') H_x^{x_1'} (u^\alpha; h, \Delta) + m \Omega \left(\frac{x}{m} \right) H_x^{x_1'} (1 - u^\alpha; h, \Delta) \right) \\ & \quad + J_{y_1'}^x \left(E_{\vartheta, \beta, \xi}^{\gamma, \delta, k, t}, \Delta; \Upsilon \right) (y_1' - x) \left(\Omega(y_1') H_{y_1'}^x (v^\alpha; h, \Delta) + m \Omega \left(\frac{x}{m} \right) H_{y_1'}^x (1 - v^\alpha; h, \Delta) \right). \end{aligned} \tag{27}$$

Proof. From (18) and (23), one can see that, for $0 < h(t) < 1$,

$$\begin{aligned} \Omega(t) & \leq h \left(\left(\frac{x-t}{x-x_1'} \right)^\alpha \right) h \left(1 - \left(\frac{x-t}{x-x_1'} \right)^\alpha \right) \left(\Omega(x_1') + m \Omega \left(\frac{x}{m} \right) \right) \\ & \leq h \left(\left(\frac{x-t}{x-x_1'} \right)^\alpha \right) \Omega(x_1') + mh \left(1 - \left(\frac{x-t}{x-x_1'} \right)^\alpha \right) \Omega \left(\frac{x}{m} \right), \\ \Omega(t) & \leq h \left(\left(\frac{t-x}{y_1'-x} \right)^\alpha \right) h \left(1 - \left(\frac{t-x}{y_1'-x} \right)^\alpha \right) \left(\Omega(y_1') + m \Omega \left(\frac{x}{m} \right) \right) \\ & \leq h \left(\left(\frac{t-x}{y_1'-x} \right)^\alpha \right) \Omega(y_1') + mh \left(1 - \left(\frac{t-x}{y_1'-x} \right)^\alpha \right) \Omega \left(\frac{x}{m} \right). \end{aligned} \tag{28}$$

Hence, by following the proof of Theorem 1, one can obtain (27). Hence, the proof is completed. \square

Corollary 1. Under the assumptions of Theorem 1, (16) gives the following result:

$$\begin{aligned}
& \left({}_{\Delta} \mathbb{F}_{k, \beta, \xi, \gamma_1^+}^{\Upsilon, \gamma, \delta, k, t} \Omega \right) (x, \sigma; p) + \left({}_{\Delta} \mathbb{F}_{k, \beta, \xi, \gamma_1^-}^{\Upsilon, \gamma, \delta, k, t} \Omega \right) (x, \sigma; p) \\
& \leq J_x^{\alpha'} \left(E_{\kappa, \beta, \xi}^{\gamma, \delta, k, t}, \Delta; \Upsilon \right) (x - x_1') \left(\Omega(x_1') + m \Omega \left(\frac{x}{m} \right) \right) H_x^{\alpha'} (u^\alpha; h, \Delta) \\
& \quad + J_{y_1'}^{\alpha'} \left(E_{\kappa, \beta, \xi}^{\gamma, \delta, k, t}, \Delta; \Upsilon \right) (y_1' - x) \left(\Omega(y_1') + m \Omega \left(\frac{x}{m} \right) \right) H_{y_1'}^{\alpha'} (v^\alpha; h, \Delta).
\end{aligned} \tag{29}$$

Now, we give the refinement of Theorem 5 in [9] in the following corollary.

Corollary 2. *The following inequality for refined $(h - m)$ -convex function holds:*

$$\begin{aligned}
& \left({}_{\Delta} \mathbb{F}_{k, \beta, \xi, \gamma_1^+}^{\Upsilon, \gamma, \delta, k, t} \Omega \right) (x, \sigma; p) + \left({}_{\Delta} \mathbb{F}_{\vartheta, \beta, \xi, \gamma_1^-}^{\Upsilon, \gamma, \delta, k, t} \Omega \right) (x, \sigma; p) \\
& \leq \left(J_x^{\alpha'} \left(E_{\kappa, \beta, \xi}^{\gamma, \delta, k, t}, \Delta; \Upsilon \right) \left(\Omega(x_1') + m \Omega \left(\frac{x}{m} \right) \right) (\Delta(x) - \Delta(x_1')) \right. \\
& \quad \left. + J_{y_1'}^{\alpha'} \left(E_{\vartheta, \beta, \xi}^{\gamma, \delta, k, t}, \Delta; \Upsilon \right) \left(\Omega(y_1') + m \Omega \left(\frac{x}{m} \right) \right) (\Delta(y_1') - \Delta(x)) \right) \|h\|_{\infty}^2 \\
& \leq \left(J_x^{\alpha'} \left(E_{\kappa, \beta, \xi}^{\gamma, \delta, k, t}, \Delta; \Upsilon \right) \left(\Omega(x_1') + m \Omega \left(\frac{x}{m} \right) \right) (\Delta(x) - \Delta(x_1')) \right) \\
& \quad \left. + J_{y_1'}^{\alpha'} \left(E_{\vartheta, \beta, \xi}^{\gamma, \delta, k, t}, \Delta; \Upsilon \right) \left(\Omega(y_1') + m \Omega \left(\frac{x}{m} \right) \right) (\Delta(y_1') - \Delta(x)) \right) \|h\|_{\infty}.
\end{aligned} \tag{30}$$

Proof. Using $\alpha = 1$ and $h \in L_{\infty}[0, 1]$ in (27), we obtain inequality (30). \square

Remark 1

- (i) For $\Upsilon(x) = x^{\alpha/k} \Gamma(\alpha t) / k \Gamma_k(\alpha t)$, $\alpha t > k > 0$ with $p = \omega = 0$, inequality (16) coincides with Theorem 10 in [18]
- (ii) For $k = 1$ along with the conditions of (i), inequality (29) coincides with Theorem 6 in [18]
- (iii) For Δ as identity function along with the conditions of (i), inequality (29) coincides with Theorem 5 in [14]
- (iv) For Δ as identity function and $k = 1$ along with the conditions of (i), inequality (29) coincides with Theorem 1 in [14]
- (v) For $h(t) = t$ and $m = 1 = \alpha$, inequality (16) coincides with Theorem 4 in [19]
- (vi) For $h(t) = t$ and $m = 1 = \alpha$, inequality (29) coincides with Corollary 1 in [19]
- (vii) For $h(t) = t$ and $m = 1 = \alpha$ along with the conditions of (i), inequality (29) coincides with Theorem 3.1 in [20]
- (viii) For $h(t) \leq 1/\sqrt{2}$ along with the conditions of (iv), inequality (29) coincides with Theorem 2 in [14]
- (ix) For $h(t) = t$ and $m = 1 = \alpha$ along with the conditions of (iii), inequality (29) coincides with Corollary 8 in [14]

- (x) For $\alpha = 1$ and $h(t) = t$ along with the conditions of (iii), inequality (29) coincides with Corollary 14 in [14]
- (xi) For $h(t) = t^s$ and $\alpha = 1$ along with the conditions of (iii), inequality (29) coincides with Corollary 15 in [14]
- (xii) For $h(t) = t$ and $\alpha = 1$ along with the conditions of (iii), inequality (29) coincides with Corollary 16 in [14]
- (xiii) For $h(t) = t$ and $m = 1 = \alpha$ along with the conditions of (iv), inequality (29) coincides with Corollary 1 in [14]
- (xiv) For $\alpha = 1$ and $h(t) = t$ along with the conditions of (iv), inequality (29) coincides with Corollary 2 in [14]
- (xv) For $h(t) = t^s$ and $\alpha = 1$ along with the conditions of (iv), inequality (29) coincides with Corollary 4 in [14]
- (xvi) For $h(t) = t$ and $\alpha = 1$ along with the conditions of (iv), inequality (29) coincides with Corollary 5 in [14]

By using $0 < h(t) < 1$ and making different choices of functions h and Δ and the parameters in (16), one can get the refinements of many well-known inequalities for different classes of convex functions which are mentioned in Remark 3 in [9].

Next, we give a lemma which we will use in the proof of upcoming Theorem 3.

Lemma 1. Let $\Omega: [0, \infty) \rightarrow \mathbb{R}$ be a refined $(\alpha, h - m)$ -convex function. If $\Omega(x) = \Omega(x'_1 + y'_1 - x/m)$, $x \in [x'_1, y'_1]$, and $m \in (0, 1]$, then the following inequality holds:

$$\Omega\left(\frac{x'_1 + y'_1}{2}\right) \leq h\left(\frac{1}{2^\alpha}\right)h\left(\frac{2^\alpha - 1}{2^\alpha}\right)(m + 1)\Omega(x). \quad (31)$$

Proof. Since Ω is refined $(\alpha, h - m)$ -convex, then following inequality holds:

$$\begin{aligned} \Omega\left(\frac{x'_1 + y'_1}{2}\right) &\leq h\left(\frac{1}{2^\alpha}\right)h\left(\frac{2^\alpha - 1}{2^\alpha}\right) \\ &\times \left[\Omega\left(\frac{x - x'_1}{y'_1 - x'_1}y'_1 + \frac{y'_1 - x}{y'_1 - x'_1}x'_1\right) + m\Omega\left(\frac{(x - x'_1/y'_1 - x'_1)x'_1 + (y'_1 - x/y'_1 - x'_1)y'_1}{m}\right) \right] \\ &\leq h\left(\frac{1}{2^\alpha}\right)h\left(\frac{2^\alpha - 1}{2^\alpha}\right)\left(\Omega(x) + m\Omega\left(\frac{x'_1 + y'_1 - x}{m}\right)\right). \end{aligned} \quad (32)$$

Using $\Omega(x) = \Omega(x'_1 + y'_1 - x/m)$ in the above inequality, we obtain (31). This completes the proof. \square

(ii) For $0 < h(t) < 1$, (31) gives refinement of Lemma 1 in [9]

Remark 2.

(i) For $h(t) = t$ and $m = \alpha = 1$, (31) coincides with Lemma 1 in [19]

Theorem 3. Under the assumptions of Theorem 1, the following result holds for $\Omega(x) = \Omega(x'_1 + y'_1 - x/m)$:

$$\begin{aligned} &\frac{1}{h(1/2^\alpha)h(2^\alpha - 1/2^\alpha)(m + 1)}\Omega\left(\frac{x'_1 + y'_1}{2}\right) \\ &\times \left(\left({}_{\Delta} \mathbb{F}_{\vartheta, \beta, \xi, y'_1}^{\Upsilon, \gamma, \delta, k, t} 1 \right) (x'_1, \sigma; p) + \left({}_{\Delta} \mathbb{F}_{\vartheta, \beta, \xi, y'_1}^{\Upsilon, \gamma, \delta, k, t} 1 \right) (y'_1, \sigma; p) \right) \\ &\leq \left({}_{\Delta} \mathbb{F}_{\vartheta, \beta, \xi, y'_1}^{\Upsilon, \gamma, \delta, k, t} \Omega \right) (x'_1, \sigma; p) + \left({}_{\Delta} \mathbb{F}_{\vartheta, \beta, \xi, y'_1}^{\Upsilon, \gamma, \delta, k, t} \Omega \right) (y'_1, \sigma; p) \\ &\leq (y'_1 - x'_1) \left(\Omega(y'_1) + m\Omega\left(\frac{x'_1}{m}\right) \right) \left[J_{y'_1}^{x'_1} \left(E_{\vartheta, \beta, \xi}^{\Upsilon, \delta, k, t}, \Delta; \Upsilon \right) H_{y'_1}^{x'_1} (v^\alpha; h, \Delta) \right. \\ &\quad \left. + J_{y'_1}^{x'_1} \left(E_{\kappa, \beta, \xi}^{\Upsilon, \delta, k, t}, \Delta; \Upsilon \right) H_{y'_1}^{x'_1} (v^\alpha; h, \Delta) \right]. \end{aligned} \quad (33)$$

Proof. For the kernel defined in (14) and function Δ , the following inequality holds:

$$J_x^{x'_1} \left(E_{\vartheta, \beta, \xi}^{\Upsilon, \delta, k, t}, \Delta; \Upsilon \right) \Delta'(x) \leq J_{y'_1}^{x'_1} \left(E_{\vartheta, \beta, \xi}^{\Upsilon, \delta, k, t}, \Delta; \Upsilon \right) \Delta'(x), \quad x \in (x'_1, y'_1). \quad (34)$$

Using refined $(\alpha, h - m)$ -convexity of Ω , we have

$$\Omega(x) \leq h\left(\left(\frac{x - x'_1}{y'_1 - x'_1}\right)^\alpha\right)h\left(1 - \left(\frac{x - x'_1}{y'_1 - x'_1}\right)^\alpha\right)\left(\Omega(y'_1) + m\Omega\left(\frac{x'_1}{m}\right)\right). \quad (35)$$

From (34) and (35), we have the following integral inequality:

$$\begin{aligned} \int_{x'_1}^{y'_1} J_x^{x'_1} \left(E_{\vartheta, \beta, \xi}^{\Upsilon, \delta, k, t}, \Delta; \Upsilon \right) \Omega(x) \Delta'(x) dx &\leq J_{y'_1}^{x'_1} \left(E_{\vartheta, \beta, \xi}^{\Upsilon, \delta, k, t}, \Delta; \Upsilon \right) \left(\Omega(y'_1) + m\Omega\left(\frac{x'_1}{m}\right) \right) \\ &\times \int_{x'_1}^{y'_1} h\left(\left(\frac{x - x'_1}{y'_1 - x'_1}\right)^\alpha\right)h\left(1 - \left(\frac{x - x'_1}{y'_1 - x'_1}\right)^\alpha\right) \Delta'(x) dx. \end{aligned} \quad (36)$$

Using (13) of Definition 10 on the right-hand side and making change of the variable by setting $v = x - x'_1/y'_1 - x'_1$ on the right-hand side of the above inequality, we obtain

$$\begin{aligned} & \left({}_{\Delta} \mathbb{F}_{\vartheta, \beta, \xi, \gamma_1}^{\gamma, \delta, k, t} 1 \Omega \right) (x'_1, \sigma; p) \\ & \leq J_{\gamma_1}^{x'_1} \left(E_{\vartheta, \beta, \xi}^{\gamma, \delta, k, t}, \Delta; \Upsilon \right) (y'_1 - x'_1) \left(\Omega(y'_1) + m \Omega \left(\frac{x'_1}{m} \right) \right) H_{\gamma_1}^{x'_1} (v^\alpha; h, \Delta). \end{aligned} \tag{37}$$

The following inequality also holds true for $x \in (x'_1, y'_1)$:

$$J_{\gamma_1}^x \left(E_{\kappa, \beta, \xi}^{\gamma, \delta, k, t}, \Delta; \Upsilon \right) \Delta' (x) \leq J_{\gamma_1}^{x'_1} \left(E_{\kappa, \beta, \xi}^{\gamma, \delta, k, t}, \Delta; \Upsilon \right) \Delta' (x). \tag{38}$$

From (35) and (38), the following integral inequality is obtained:

$$\begin{aligned} \int_{x'_1}^{y'_1} J_{\gamma_1}^x \left(E_{\kappa, \beta, \xi}^{\gamma, \delta, k, t}, \Delta; \Upsilon \right) \Delta' (x) \Omega(x) dx & \leq J_{\gamma_1}^{x'_1} \left(E_{\kappa, \beta, \xi}^{\gamma, \delta, k, t}, \Delta; \Upsilon \right) \left(\Omega(y'_1) + m \Omega \left(\frac{x_1}{m} \right) \right) \\ & \times \int_{x'_1}^{y'_1} h \left(\left(\frac{x - x'_1}{y'_1 - x'_1} \right)^\alpha \right) h \left(1 - \left(\frac{x - x'_1}{y'_1 - x'_1} \right)^\alpha \right) \Delta' (x) dx. \end{aligned} \tag{39}$$

Using (12) of Definition 10 on the left-hand side and making change of the variable on the right-hand side of the above inequality, we obtain

$$\begin{aligned} & \left({}_{\Delta} \mathbb{F}_{\kappa, \beta, \xi, \gamma_1}^{\gamma, \delta, k, t} 1 \Omega \right) (y'_1, \sigma; p) \\ & \leq J_{\gamma_1}^{x'_1} \left(E_{\kappa, \beta, \xi}^{\gamma, \delta, k, t}, \Delta; \Upsilon \right) (y'_1 - x'_1) \left(\Omega(y'_1) + m \Omega \left(\frac{x'_1}{m} \right) \right) H_{\gamma_1}^{x'_1} (v^\alpha; h, \Delta). \end{aligned} \tag{40}$$

Now, using Lemma 1, we can write

$$\begin{aligned} & \frac{1}{h(1/2^\alpha)h(2^\alpha - 1/2^\alpha)(m + 1)} \Omega \left(\frac{x'_1 + y'_1}{2} \right) \left({}_{\Delta} \mathbb{F}_{\vartheta, \beta, \xi, \gamma_1}^{\gamma, \delta, k, t} 1 \right) (x'_1, \sigma; p) \\ & \leq \left({}_{\Delta} \mathbb{F}_{\vartheta, \beta, \xi, \gamma_1}^{\gamma, \delta, k, t} \Omega \right) (x'_1, \sigma; p). \end{aligned} \tag{42}$$

Again, using Lemma 1, we can write

$$\begin{aligned} & \Omega \left(\frac{x'_1 + y'_1}{2} \right) J_{\gamma_1}^{x'_1} \left(E_{\kappa, \beta, \xi}^{\gamma, \delta, k, t}, \Delta; \Upsilon \right) \Delta' (x) dx \\ & \leq h \left(\frac{1}{2^\alpha} \right) h \left(\frac{2^\alpha - 1}{2^\alpha} \right) (m + 1) \int_{x'_1}^{y'_1} J_{\gamma_1}^x \left(E_{\kappa, \beta, \xi}^{\gamma, \delta, k, t}, \Delta; \Upsilon \right) \Delta' (x) \Omega(x) dx, \end{aligned} \tag{43}$$

$$\begin{aligned} & \int_{x'_1}^{y'_1} \Omega \left(\frac{x'_1 + y'_1}{2} \right) J_x^{x'_1} \left(E_{\vartheta, \beta, \xi}^{\gamma, \delta, k, t}, \Delta; \Upsilon \right) \Delta' (x) dx \\ & \leq h \left(\frac{1}{2^\alpha} \right) h \left(\frac{2^\alpha - 1}{2^\alpha} \right) (m + 1) \int_{x'_1}^{y'_1} J_x^{x'_1} \left(E_{\vartheta, \beta, \xi}^{\gamma, \delta, k, t}, \Delta; \Upsilon \right) \Delta' (x) \Omega(x) dx, \end{aligned} \tag{41}$$

which by using (13) of Definition 10 gives the following integral inequality:

which by using (12) of Definition 10 gives the following fractional integral inequality:

$$\begin{aligned} & \frac{1}{h(1/2^\alpha)h(2^\alpha - 1/2^\alpha)(m + 1)} \Omega \left(\frac{x'_1 + y'_1}{2} \right) \left({}_{\Delta} \mathbb{F}_{\vartheta, \beta, \xi, \gamma_1}^{\gamma, \delta, k, t} 1 \right) (y'_1, \sigma; p) \\ & \leq \left({}_{\Delta} \mathbb{F}_{\vartheta, \beta, \xi, \gamma_1}^{\gamma, \delta, k, t} \Omega \right) (y'_1, \sigma; p). \end{aligned} \tag{44}$$

Inequality (33) will be obtained by using (37), (40), (42), and (44).

The following theorem is the refinement of Theorem 3. \square

Theorem 4. Under the assumptions of Theorem 3, if $0 < h(t) < 1$, then the following refinement holds:

$$\begin{aligned}
 & \frac{1}{h(1/2^\alpha)h(2^\alpha - 1/2^\alpha)(m+1)} \Omega\left(\frac{x'_1 + y'_1}{2}\right) \\
 & \quad \times \left(\left({}_{\Delta} \mathbb{F}_{\vartheta, \beta, \xi, y'_1}^{\Upsilon, \gamma, \delta, k, t} 1 \right) (x'_1, \sigma; p) + \left({}_{\Delta} \mathbb{F}_{\kappa, \beta, \xi, y'_1}^{\Upsilon, \gamma, \delta, k, t} 1 \right) (y'_1, \sigma; p) \right) \\
 & \leq \frac{1}{h(1/2^\alpha) + mh(2^\alpha - 1/2^\alpha)} \Omega\left(\frac{x'_1 + y'_1}{2}\right) \\
 & \quad \times \left(\left({}_{\Delta} \mathbb{F}_{\vartheta, \beta, \xi, y'_1}^{\Upsilon, \gamma, \delta, k, t} 1 \right) (x'_1, \sigma; p) + \left({}_{\Delta} \mathbb{F}_{\kappa, \beta, \xi, x'_1}^{\Upsilon, \gamma, \delta, k, t} 1 \right) (y'_1, \sigma; p) \right) \\
 & \leq \left({}_{\Delta} \mathbb{F}_{\kappa, \beta, \xi, y'_1}^{\Upsilon, \gamma, \delta, k, t} \Omega \right) (x'_1, \sigma; p) + \left({}_{\Delta} \mathbb{F}_{\vartheta, \beta, \xi, x'_1}^{\Upsilon, \gamma, \delta, k, t} \Omega \right) (y'_1, \sigma; p) \\
 & \leq (y'_1 - x'_1) \left(\Omega(y'_1) + m\Omega\left(\frac{x'_1}{m}\right) \right) \left[J_{y'_1}^{x'_1} \left(E_{\vartheta, \beta, \xi}^{\gamma, \delta, k, t}, \Delta; \Upsilon \right) H_{y'_1}^{x'_1} (v^\alpha; h, \Delta) \right. \\
 & \quad \left. + J_{y'_1}^{x'_1} \left(E_{\kappa, \beta, \xi}^{\gamma, \delta, k, t}, \Delta; \Upsilon \right) H_{y'_1}^{x'_1} (v^\alpha; h, \Delta) \right] \\
 & \leq (y'_1 - x'_1) \left(J_{y'_1}^{x'_1} \left(E_{\vartheta, \beta, \xi}^{\gamma, \delta, k, t}, \Delta; \Upsilon \right) + J_{y'_1}^{x'_1} \left(E_{\kappa, \beta, \xi}^{\gamma, \delta, k, t}, \Delta; \Upsilon \right) \right) \\
 & \quad \times \left(\Omega(y'_1) H_{y'_1}^{x'_1} (v^\alpha; h, \Delta) + m\Omega\left(\frac{x'_1}{m}\right) H_{y'_1}^{x'_1} (1 - v^\alpha; h, \Delta) \right).
 \end{aligned} \tag{45}$$

Proof. From (35), one can see that, for $0 < h(t) < 1$,

$$\begin{aligned}
 \Omega(x) & \leq h \left(\left(\frac{x - x'_1}{y'_1 - x'_1} \right)^\alpha \right) h \left(1 - \left(\frac{x - x'_1}{y'_1 - x'_1} \right)^\alpha \right) \left(\Omega(y'_1) + m\Omega\left(\frac{x'_1}{m}\right) \right) \\
 & \leq h \left(\left(\frac{x - x'_1}{y'_1 - x'_1} \right)^\alpha \right) \Omega(y'_1) + mh \left(1 - \left(\frac{x - x'_1}{y'_1 - x'_1} \right)^\alpha \right) \Omega\left(\frac{x'_1}{m}\right).
 \end{aligned} \tag{46}$$

Hence, by following the proof of Theorem 3, one can obtain (45). This completes the proof. \square

Corollary 3. Under the assumptions of Theorem 3, (33) gives the following result:

$$\begin{aligned}
 & \frac{1}{h(1/2^\alpha)h(2^\alpha - 1/2^\alpha)(m+1)} \Omega\left(\frac{x'_1 + y'_1}{2}\right) \left(\left({}_{\Delta} \mathbb{F}_{\kappa, \beta, \xi, y'_1}^{\Upsilon, \gamma, \delta, k, t} 1 \right) (x'_1, \sigma; p) \right. \\
 & \quad \left. + \left({}_{\Delta} \mathbb{F}_{\vartheta, \beta, \xi, y'_1}^{\Upsilon, \gamma, \delta, k, t} 1 \right) (y'_1, \sigma; p) \right) \leq \left({}_{\Delta} \mathbb{F}_{\kappa, \beta, \xi, y'_1}^{\Upsilon, \gamma, \delta, k, t} \Omega \right) (x'_1, \sigma; p) + \left({}_{\Delta} \mathbb{F}_{\vartheta, \beta, \xi, y'_1}^{\Upsilon, \gamma, \delta, k, t} \Omega \right) (y'_1, \sigma; p) \\
 & \leq 2(y'_1 - x'_1) \left(\Omega(y'_1) + m\Omega\left(\frac{x'_1}{m}\right) \right) J_{y'_1}^{x'_1} \left(E_{\kappa, \beta, \xi}^{\gamma, \delta, k, t}, \Delta; \Upsilon \right) H_{y'_1}^{x'_1} (v^\alpha; h, \Delta).
 \end{aligned} \tag{47}$$

Now, we give the refinement of Theorem 6 in [9] in the following corollary.

Corollary 4. The following inequality for refined $(h - m)$ -convex function holds:

$$\begin{aligned}
 & \frac{1}{h^2(1/2)(m+1)} \Omega\left(\frac{x'_1 + y'_1}{2}\right) \left(\left({}_{\Delta} \mathbb{F}_{\kappa, \alpha, \xi, y'_1}^{\gamma, \delta, k, \iota} 1 \right) (x'_1, \sigma; p) + \left({}_{\Delta} F_{\kappa, \alpha, \xi, x'_1}^{\gamma, \delta, k, \iota} 1 \right) (y'_1, \sigma; p) \right) \\
 & \leq \frac{1}{h(1/2)(m+1)} \Omega\left(\frac{x'_1 + y'_1}{2}\right) \left(\left({}_{\Delta} \mathbb{F}_{\kappa, \alpha, \xi, y'_1}^{\gamma, \delta, k, \iota} \Omega \right) (x'_1, \sigma; p) + \left({}_{\Delta} F_{\kappa, \alpha, \xi, x'_1}^{\gamma, \delta, k, \iota} \Omega \right) (y'_1, \sigma; p) \right) \\
 & \leq \left({}_{\Delta} \mathbb{F}_{\kappa, \beta, \xi, y'_1}^{\gamma, \delta, k, \iota} \Omega \right) (x'_1, \sigma; p) + \left({}_{\Delta} F_{\kappa, \beta, \xi, y'_1}^{\gamma, \delta, k, \iota} \Omega \right) (y'_1, \sigma; p) \tag{48} \\
 & \leq 2 \left(\Omega(y'_1) + m \Omega\left(\frac{x'_1}{m}\right) \right) J_{y'_1}^{x'_1} \left(E_{\kappa, \beta, \xi}^{\gamma, \delta, k, \iota}, \Delta; \Upsilon \right) (\Delta(y'_1) - \Delta(x'_1)) \|h\|_{\infty}^2 \\
 & \leq 2 \left(\Omega(y'_1) + m \Omega\left(\frac{x'_1}{m}\right) \right) J_{y'_1}^{x'_1} \left(E_{\kappa, \beta, \xi}^{\gamma, \delta, k, \iota}, \Delta; \Upsilon \right) (\Delta(y'_1) - \Delta(x'_1)) \|h\|_{\infty}.
 \end{aligned}$$

Proof. For $h \in L_{\infty}[0, 1]$ and $\alpha = 1$ in (45), one can obtain (48). \square

refinements of many well-known inequalities for different classes of convex functions which are mentioned in Remark 5 of [9].

Remark 3

- (i) For $h(t) = t$ and $m = 1 = \alpha$, inequality (33) coincides with Theorem 5 in [19]
- (ii) For $h(t) = t$ and $m = 1 = \alpha$, inequality (47) coincides with Corollary 2 in [19]

By using $0 < h(t) < 1$ and making different choices of functions h and Δ and the parameters in (33), one can get the

Theorem 5. Let Ω, Δ be differentiable functions such that $|\Omega'|$ is refined $(\alpha, h - m)$ -convex and Δ be strictly increasing over $[x'_1, y'_1]$ and differentiable over $[x'_1, y'_1]$. Also, Υ/x be an increasing function on $[x'_1, y'_1]$ and $\beta, \xi, \gamma, \iota \in \mathbb{R}, p, \kappa, \vartheta, \delta \geq 0, 0 < k \leq \delta + \kappa$, and $0 < k \leq \delta + \vartheta$. Then, for $x \in (x'_1, y'_1)$, we have

$$\begin{aligned}
 & \left| \left({}_{\Delta} \mathbb{F}_{\kappa, \beta, \xi, y'_1}^{\gamma, \delta, k, \iota} \Omega * \Delta \right) (x, \sigma; p) + \left({}_{\Delta} F_{\vartheta, \beta, \xi, y'_1}^{\gamma, \delta, k, \iota} \Omega * \Delta \right) (x, \sigma; p) \right| \\
 & \leq J_{x'}^{x'_1} \left(E_{\kappa, \beta, \xi}^{\gamma, \delta, k, \iota}, \Delta; \Upsilon \right) (x - x'_1) \left(|\Omega'(x'_1)| + m \left| \Omega'\left(\frac{x}{m}\right) \right| \right) H_{x'}^{x'_1} (u^{\alpha}; h, \Delta) \\
 & \quad + J_{y'_1}^x \left(E_{\vartheta, \beta, \xi}^{\gamma, \delta, k, \iota}, \Delta; \Upsilon \right) (y'_1 - x) \left(|\Omega'(y'_1)| + m \left| \Omega'\left(\frac{x}{m}\right) \right| \right) H_{y'_1}^x (v^{\alpha}; h, \Delta),
 \end{aligned} \tag{49}$$

where

$$\begin{aligned}
 \left({}_{\Delta} \mathbb{F}_{\kappa, \beta, \xi, y'_1}^{\gamma, \delta, k, \iota} \Omega * \Delta \right) (x, \sigma; p) &= \int_{x'_1}^x J_x^t \left(E_{\kappa, \beta, \xi}^{\gamma, \delta, k, \iota}, \Delta; \Upsilon \right) \Delta'(t) \Omega'(t) dt, \\
 \left({}_{\Delta} F_{\vartheta, \beta, \xi, y'_1}^{\gamma, \delta, k, \iota} \Omega * \Delta \right) (x, \sigma; p) &= \int_x^{y'_1} J_t^x \left(E_{\vartheta, \beta, \xi}^{\gamma, \delta, k, \iota}, \Delta; \Upsilon \right) \Delta'(t) \Omega'(t) dt.
 \end{aligned} \tag{50}$$

Proof. Using refined $(\alpha, h - m)$ -convexity of $|\Omega'|$ over $[x'_1, y'_1]$ implies

$$|\Omega'(t)| \leq h \left(\frac{x-t}{x-x_1'} \right)^\alpha h \left(1 - \frac{x-t}{x-x_1'} \right)^\alpha \left(|\Omega'(x_1')| + m \left| \Omega' \left(\frac{x}{m} \right) \right| \right). \tag{51}$$

Absolute value property implies the following relation:

$$\begin{aligned} & -h \left(\frac{x-t}{x-x_1'} \right)^\alpha h \left(1 - \frac{x-t}{x-x_1'} \right)^\alpha \left(|\Omega'(x_1')| + m \left| \Omega' \left(\frac{x}{m} \right) \right| \right) \leq \Omega'(t) \\ & \leq h \left(\frac{x-t}{x-x_1'} \right)^\alpha h \left(1 - \frac{x-t}{x-x_1'} \right)^\alpha \left(|\Omega'(x_1')| + m \left| \Omega' \left(\frac{x}{m} \right) \right| \right). \end{aligned} \tag{52}$$

From (17) and the second inequality of (52), we have the following inequality:

$$\begin{aligned} & \int_{x_1}^x J_x^t \left(E_{\kappa, \beta, \xi}^{\gamma, \delta, k, t}, \Delta; \Upsilon \right) \Delta'(t) \Omega'(t) dt \leq J_x^{x_1'} \left(E_{\kappa, \beta, \xi}^{\gamma, \delta, k, t}, \Delta; \Upsilon \right) \left(|\Omega'(x_1')| + m \left| \Omega' \left(\frac{x}{m} \right) \right| \right) \\ & \times \int_{x_1'}^x h \left(\frac{x-t}{x-x_1'} \right)^\alpha h \left(1 - \frac{x-t}{x-x_1'} \right)^\alpha \Delta'(t) dt, \end{aligned} \tag{53}$$

which leads to the following fractional integral inequality:

$$\begin{aligned} & \left({}_{\Delta} \mathbb{F}_{\kappa, \beta, \xi, y_1^+}^{\Upsilon, \gamma, \delta, k, t} \Omega * \Delta \right) (x, \sigma; p) \\ & \leq J_x^{x_1'} \left(E_{\kappa, \beta, \xi}^{\gamma, \delta, k, t}, \Delta; \Upsilon \right) (x - x_1') \left(|\Omega'(x_1')| + m \left| \Omega' \left(\frac{x}{m} \right) \right| \right) H_x^{x_1'} (u^\alpha; h, \Delta). \end{aligned} \tag{54}$$

Also, inequality (17) and the first inequality of (52) give the following fractional integral inequality:

$$\begin{aligned} & \left({}_{\Delta} \mathbb{F}_{\kappa, \beta, \xi, y_1^+}^{\Upsilon, \gamma, \delta, k, t} \Omega * \Delta \right) (x, \sigma; p) \\ & \geq -J_x^{x_1'} \left(E_{\kappa, \beta, \xi}^{\gamma, \delta, k, t}, \Delta; \Upsilon \right) (x - x_1') \left(|\Omega'(x_1')| + m \left| \Omega' \left(\frac{x}{m} \right) \right| \right) H_x^{x_1'} (u^\alpha; h, \Delta). \end{aligned} \tag{55}$$

Again, using refined $(\alpha, h - m)$ -convexity of $|\Omega'|$ over $[x_1', y_1']$, we can write

$$|\Omega'(t)| \leq h \left(\frac{t-x}{y_1'-x} \right)^\alpha h \left(1 - \frac{t-x}{y_1'-x} \right)^\alpha \left(m \left| \Omega' \left(\frac{x}{m} \right) \right| + |\Omega'(y_1')| \right). \tag{56}$$

and

$$\begin{aligned}
& h\left(\left(\frac{t-x}{y_1'-x}\right)^\alpha\right)h\left(1-\left(\frac{t-x}{y_1'-x}\right)^\alpha\right)\left(m\left|\Omega'\left(\frac{x}{m}\right)\right|+|\Omega'(y_1')|\right)\leq\Omega'(t) \\
& \leq h\left(\left(\frac{t-x}{y_1'-x}\right)^\alpha\right)h\left(1-\left(\frac{t-x}{y_1'-x}\right)^\alpha\right)\left(m\left|\Omega'\left(\frac{x}{m}\right)\right|+|\Omega'(y_1')|\right).
\end{aligned} \tag{57}$$

From (22) and the second inequality of (57), the following fractional integral inequality is obtained:

$$\begin{aligned}
& \left({}_{\Delta}\mathbb{F}_{\vartheta,\beta,\xi,y_1'}^{\Upsilon,\gamma,\delta,k,t}\Omega*\Delta\right)(x,\sigma;p) \\
& \leq J_{y_1'}^x\left(E_{\vartheta,\beta,\xi}^{\gamma,\delta,k,t},\Delta;\Upsilon\right)(y_1'-x)\left(|\Omega'(y_1')|+m\left|\Omega'\left(\frac{x}{m}\right)\right|\right)H_{y_1'}^x(v^\alpha;h,\Delta),
\end{aligned} \tag{58}$$

and (22) and the first inequality of (57) give the following fractional integral inequality:

$$\begin{aligned}
& \left({}_{\Delta}\mathbb{F}_{\vartheta,\beta,\xi,y_1'}^{\Upsilon,\gamma,\delta,k,t}\Omega*\Delta\right)(x,\sigma;p) \\
& \geq -J_{y_1'}^x\left(E_{\vartheta,\beta,\xi}^{\gamma,\delta,k,t},\Delta;\Upsilon\right)(y_1'-x)\left(|\Omega'(y_1')|+m\left|\Omega'\left(\frac{x}{m}\right)\right|\right)H_{y_1'}^x(v^\alpha;h,\Delta).
\end{aligned} \tag{59}$$

Inequality (49) will be obtained by using (54), (55), (58), and (59). Hence, the proof is completed.

Next, we give refinement of Theorem 5 in the following theorem. \square

Theorem 6. Under the assumptions of Theorem 5, if $0 < h(t) < 1$, then the following refinement holds:

$$\begin{aligned}
& \left| \left({}_{\Delta}\mathbb{F}_{\kappa,\beta,\xi,y_1'}^{\Upsilon,\gamma,\delta,k,t}\Omega*\Delta\right)(x,\sigma;p) + \left({}_{\Delta}\mathbb{F}_{\vartheta,\beta,\xi,y_1'}^{\Upsilon,\Omega*\gamma,\delta,k,t}\Delta\right)(x,\sigma;p) \right| \\
& \leq J_x^{x_1'}\left(E_{\kappa,\beta,\xi}^{\gamma,\delta,k,t},\Delta;\Upsilon\right)(x-x_1')\left(|\Omega'(x_1')|+m\left|\Omega'\left(\frac{x}{m}\right)\right|\right)H_x^{x_1'}(u^\alpha;h,\Delta) \\
& \quad + J_{y_1'}^x\left(E_{\vartheta,\beta,\xi}^{\gamma,\delta,k,t},\Delta;\Upsilon\right)(y_1'-x)\left(|\Omega'(y_1')|+m\left|\Omega'\left(\frac{x}{m}\right)\right|\right)H_{y_1'}^x(v^\alpha;h,\Delta) \\
& \leq J_x^{x_1'}\left(E_{\kappa,\beta,\xi}^{\gamma,\delta,k,t},\Delta;\Upsilon\right)(x-x_1')\left(|\Omega'(x_1')|H_x^{x_1'}(u^\alpha;h,\Delta)\right. \\
& \quad \left.+ m\left|\Omega'\left(\frac{x}{m}\right)\right|H_x^{x_1'}(1-u^\alpha;h,\Delta)\right) + J_{y_1'}^x\left(E_{\vartheta,\beta,\xi}^{\gamma,\delta,k,t},\Delta;\Upsilon\right)(y_1'-x) \\
& \quad \times \left(|\Omega'(y_1')|H_{y_1'}^x(v^\alpha;h,\Delta) + m\left|\Omega'\left(\frac{x}{m}\right)\right|H_{y_1'}^x(1-v^\alpha;h,\Delta)\right).
\end{aligned} \tag{60}$$

Proof. From (51), one can see that, for $0 < h(t) < 1$,

$$\begin{aligned}
 |\Omega'(t)| &\leq h\left(\left(\frac{x-t}{x-x'_1}\right)^\alpha\right)h\left(1-\left(\frac{x-t}{x-x'_1}\right)^\alpha\right)\left(|\Omega'(x'_1)|+m\left|\Omega'\left(\frac{x}{m}\right)\right|\right) \\
 &\leq h\left(\left(\frac{x-t}{x-x'_1}\right)^\alpha\right)|\Omega'(x'_1)|+mh\left(1-\left(\frac{x-t}{x-x'_1}\right)^\alpha\right)\left|\Omega'\left(\frac{x}{m}\right)\right|.
 \end{aligned}
 \tag{61}$$

Hence, by following the proof of Theorem 5, one can obtain (60). This completes the proof. \square

Corollary 5. Under the assumptions of Theorem 5, (49) gives the following result:

$$\begin{aligned}
 &\left|\left({}_{\Delta}\mathbb{F}_{\kappa,\beta,\xi,y_1^+}^{\gamma,\delta,k,t}\Omega * \Delta\right)(x,\sigma;p)+\left({}_{\Delta}\mathbb{F}_{\kappa,\beta,\xi,y_1^-}^{\gamma,\delta,k,t}\Omega * \Delta\right)(x,\sigma;p)\right| \\
 &\leq J_x^{x'_1}\left(E_{\kappa,\beta,\xi}^{\gamma,\delta,k,t},\Delta;\Upsilon\right)(x-x'_1)\left(|\Omega'(x'_1)|+m\left|\Omega'\left(\frac{x}{m}\right)\right|\right)H_x^{x'_1}(u^\alpha;h,\Delta) \\
 &\quad + J_{y_1^x}\left(E_{\kappa,\beta,\xi}^{\gamma,\delta,k,t},\Delta;\Upsilon\right)(y_1^x-x)\left(|\Omega'(y_1^x)|+m\left|\Omega'\left(\frac{x}{m}\right)\right|\right)H_{y_1^x}^x(v^\alpha;h,\Delta).
 \end{aligned}
 \tag{62}$$

The following corollary presents the refinement of Theorem 7 in [9].

Corollary 6. The following inequality for refined $(h-m)$ -convex function holds:

$$\begin{aligned}
 &\left|\left({}_{\Delta}\mathbb{F}_{\kappa,\beta,\xi,y_1^+}^{\gamma,\delta,k,t}\Omega * \Delta\right)(x,\sigma;p)+\left({}_{\Delta}\mathbb{F}_{\vartheta,\beta,\xi,y_1^-}^{\gamma,\delta,k,t}1\Omega * g\right)(x,\sigma;p)\right| \\
 &\leq \left[J_x^{x'_1}\left(E_{\kappa,\beta,\xi}^{\gamma,\delta,k,t},\Delta;\Upsilon\right)(\Delta(x)-\Delta(x'_1))\left(|\Omega'(x'_1)|+m\left|\Omega'\left(\frac{x}{m}\right)\right|\right)\right. \\
 &\quad \left.+ J_{y_1^x}\left(E_{\vartheta,\beta,\xi}^{\gamma,\delta,k,t},\Delta;\Upsilon\right)(\Delta(y_1^x)-\Delta(x))\left(|\Omega'(y_1^x)|+m\left|\Omega'\left(\frac{x}{m}\right)\right|\right)\right]\|h\|_\infty^2 \\
 &\leq \left[J_x^{x'_1}\left(E_{\kappa,\beta,\xi}^{\gamma,\delta,k,t},\Delta;\Upsilon\right)(\Delta(x)-\Delta(x'_1))\left(|\Omega'(x'_1)|+m\left|\Omega'\left(\frac{x}{m}\right)\right|\right)\right. \\
 &\quad \left.+ J_{y_1^x}\left(E_{\vartheta,\beta,\xi}^{\gamma,\delta,k,t},\Delta;\Upsilon\right)(\Delta(y_1^x)-\Delta(x))\left(|\Omega'(y_1^x)|+m\left|\Omega'\left(\frac{x}{m}\right)\right|\right)\right]\|h\|_\infty.
 \end{aligned}
 \tag{63}$$

Proof. For $h \in L_\infty[0, 1]$ and $\alpha = 1$ in (60), we obtain (63). \square

classes of convex functions which are mentioned in Remark 6 of [9].

Remark 4

- (i) For $h(t) = t$ and $m = 1 = \alpha$, inequality (49) coincides with Theorem 6 in [19]
- (ii) For $h(t) = t$ and $m = 1 = \alpha$, inequality (62) coincides with Corollary 3 in [19]

By using $0 < h(t) < 1$ and making different choices of functions h and Δ and the parameters in (49), one can get the refinements of many well-known inequalities for different

4. Inequalities for Fractional Integral Operators

In this section, we present the bounds of some of the fractional integral operators which will be deduced from the results of Section 3.

Proposition 1. Under the assumptions of Theorem 1, the following result holds:

$$\begin{aligned} & \Gamma(\beta) \left(\left({}_{\Delta}^{\beta} I_{x_1^+} \Omega \right) (x) + \left({}_{\Delta}^{\beta} I_{y_1^-} \Omega \right) (x) \right) \\ & \leq (\Delta(x) - \Delta(x_1'))^{\beta-1} \left(\Omega(x_1') + m\Omega\left(\frac{x}{m}\right) \right) (x - x_1') H_x^{x_1'}(u^\alpha; h, \Delta) \\ & \quad + (\Delta(y_1') - \Delta(x))^{\beta-1} \left(\Omega(y_1') + m\Omega\left(\frac{x}{m}\right) \right) (y_1' - x) H_{y_1'}^{x_1'}(v^\alpha; h, \Delta). \end{aligned} \tag{64}$$

Proof. For $Y(t) = t^\beta, \beta > 0$, and $p = \sigma = 0$ in the proof of Theorem 1, we obtain (64). \square

Proposition 2. Under the assumptions of Theorem 1, the following inequality holds:

$$\begin{aligned} & \Gamma(\beta) \left(\left({}_{x_1^+} I_Y \Omega \right) (x) + \left({}_{y_1^+} I_Y \Omega \right) (x) \right) \\ & \leq Y(x - x_1') \left(\Omega(x_1') + m\Omega\left(\frac{x}{m}\right) \right) \int_0^1 h(u^\alpha) h(1 - u^\alpha) du \\ & \quad + Y(y_1' - x) \left(\Omega(y_1') + m\Omega\left(\frac{x}{m}\right) \right) \int_0^1 h(v^\alpha) h(1 - v^\alpha) dv. \end{aligned} \tag{65}$$

$$\begin{aligned} & k\Gamma_k(\beta) \left[\left({}_{\Delta}^{\beta} I_{x_1^+}^k \Omega \right) (x) + \left({}_{\Delta}^{\beta} I_{y_1^-}^k \Omega \right) (x) \right] \\ & \leq (\Delta(x) - \Delta(x_1'))^{(\beta/k)-1} \left(\Omega(x_1') + m\Omega\left(\frac{x}{m}\right) \right) (x - x_1') H_x^{x_1'}(u^\alpha; h, \Delta) \\ & \quad + (\Delta(y_1') - \Delta(x))^{(\beta/k)-1} \left(\Omega(y_1') + m\Omega\left(\frac{x}{m}\right) \right) (y_1' - x) H_{y_1'}^{x_1'}(v^\alpha; h, \Delta). \end{aligned} \tag{66}$$

Remark 5. For $0 < h(t) < 1$, (66) gives refinement of Corollary 8 in [9].

Corollary 8. Using $Y(t) = t^\beta$ and Δ as identity function for $\beta \geq 1$ along with $p = \sigma = 0$, (12) and (13) give fractional integral ${}_{x_1^+}^{\beta} I \Omega(x)$ and ${}_{y_1^-}^{\beta} I \Omega(x)$ defined in [15], which satisfy the following upper bound:

$$\begin{aligned} & \Gamma(\beta) \left(\left({}_{\Delta}^{\beta} I_{x_1^+} \Omega \right) (x) + \left({}_{\Delta}^{\beta} I_{y_1^-} \Omega \right) (x) \right) \\ & \leq (x - x_1')^\beta \left(\Omega(x_1') + m\Omega\left(\frac{x}{m}\right) \right) \int_0^1 h(u^\alpha) h(1 - u^\alpha) du \\ & \quad + (y_1' - x)^\beta \left(\Omega(y_1') + m\Omega\left(\frac{x}{m}\right) \right) \int_0^1 h(v^\alpha) h(1 - v^\alpha) dv. \end{aligned} \tag{67}$$

Corollary 9. Using $Y(t) = \Gamma(\beta)t^{\beta/k}/k\Gamma_k(\beta)$ and Δ as identity function along with $p = \sigma = 0$, (12) and (13) reduce to the

Proof. Using Δ as identity function with $\sigma = p = 0$ in the proof of Theorem 1, we obtain the required result. \square

Corollary 7. For $Y(t) = \Gamma(\beta)t^{\beta/k}/k\Gamma_k(\beta)$ with $\beta > k$ and $p = \sigma = 0$, (12) and (13) reduce to the fractional integral operators (8) and (9), which satisfy the following upper bound:

fractional integral operators ${}_{x_1^+}^{\beta} I_{x_1^+}^k \Omega(x)$ and ${}_{y_1^-}^{\beta} I_{y_1^-}^k \Omega(x)$ given in [21], which satisfy the following upper bound:

$$\begin{aligned} & \left({}_{x_1^+}^{\beta} I_{x_1^+}^k \Omega \right) (x) + \left({}_{y_1^-}^{\beta} I_{y_1^-}^k \Omega \right) (x) \\ & \leq \frac{1}{k\Gamma_k(\beta)} \left[(x - x_1')^{\beta/k} \left(\Omega(x_1') + m\Omega\left(\frac{x}{m}\right) \right) \right. \\ & \quad \times \int_0^1 h(u^\alpha) h(1 - u^\alpha) du + (y_1' - x)^{\beta/k} \left(\Omega(y_1') + m\Omega\left(\frac{x}{m}\right) \right) \\ & \quad \left. \times \int_0^1 h(v^\alpha) h(1 - v^\alpha) dv \right]. \end{aligned} \tag{68}$$

Remark 6. For $0 < h(t) < 1$, (68) gives refinement of Corollary 10 in [9].

Corollary 10. For $k = 1$ in Corollary 9, the following upper bound for Riemann–Liouville fractional integral is satisfied:

$$\begin{aligned} & \left({}^\beta I_{x_1^+} \Omega \right) (x) + \left({}^\beta I_{y_1^+} \Omega \right) (x) \leq \frac{1}{\Gamma(\beta)} \left[(x - x_1')^\beta \left(\Omega(x_1') + m\Omega\left(\frac{x}{m}\right) \right) \right. \\ & \times \int_0^1 h(u)^\alpha h(1 - u^\alpha) du + (y_1' - x)^\beta \left(\Omega(y_1') + m\Omega\left(\frac{x}{m}\right) \right) \\ & \left. \times \int_0^1 h(v)^\alpha h(1 - v^\alpha) dv \right]. \end{aligned} \tag{69}$$

Remark 7. For $0 < h(t) < 1$, (69) gives refinement of Corollary 11 in [9].

Similar bounds can be obtained for Theorems 3 and 5, which we leave for the reader.

5. Conclusions

This article is about the bounds of unified integral operators via refined $(\alpha, h - m)$ -convexity. The obtained results are the refinements of some already published results. Moreover, some deducible fractional integral operators and their related bounds are also given.

Data Availability

No data were used to support this study.

Conflicts of Interest

The authors declare that they have no conflicts of interest.

References

- [1] G. A. Anastassiou, “Generalized fractional Hermite-Hadamard inequalities involving m -convexity and (s, m) -convexity,” *Series Mathematics and Informatics*, vol. 28, no. 2, pp. 107–126, 2013.
- [2] M. Bombardelli and S. Varošaneć, “Properties of h -convex functions related to the Hermite-Hadamard-Fejér inequalities,” *Computers & Mathematics with Applications*, vol. 58, no. 9, pp. 1869–1877, 2009.
- [3] H. Chen and U. N. Katugampola, “Hermite-Hadamard and Hermite-Hadamard-Fejér type inequalities for generalized fractional integrals,” *Journal of Mathematical Analysis and Applications*, vol. 446, no. 2, pp. 1274–1291, 2017.
- [4] G. Farid, A. U. Rehman, and Q. U. Ain, “ k -fractional integral inequalities of Hadamard type for $(h - m)$ -convex functions,” *Computational Methods for Differential Equations*, vol. 8, no. 1, pp. 119–140, 2020.
- [5] S. Hussain, M. I. Bhatti, and M. Iqbal, “Hadamard-type inequalities for s -convex functions,” *Jurnal Matematika*, vol. 41, pp. 51–60, 2009.
- [6] M. E. Özdemir, M. Avci, and E. Set, “On some inequalities of Hermite-Hadamard type via m -convexity,” *Applied Mathematics Letters*, vol. 23, pp. 1065–1070, 2010.
- [7] M. E. Özdemir, A. O. Akdemri, and E. Set, “On (h, m) -convexity and hadamard type inequalities,”

Transylvanian Journal of Mathematics and Mechanics, vol. 8, no. 1, pp. 51–58, 2016.

- [8] L. Chen, G. Farid, S. I. But, and S. B. Akbar, “Boundedness of fractional integral operators containing Mittag-Leffler functions,” *Turkish Journal of Inequalities*, vol. 4, no. 1, pp. 14–24, 2020.
- [9] G. Farid, K. Mahreen, K. Mahreen, and Y.-M. Chu, “Study of inequalities for unified integral operators of generalized convex functions,” *Open Journal of Mathematical Sciences*, vol. 5, no. 1, pp. 80–93, 2021.
- [10] G. Farid, W. Nazeer, M. Saleem, S. Mehmood, and S. Kang, “Bounds of Riemann-Liouville fractional integrals in general form via convex functions and their applications,” *Mathematics*, vol. 6, no. 11, p. 248, 2018.
- [11] Y. C. Kwun, G. Farid, S. M. Kang, B. K. Bangash, and S. Ullah, “Derivation of bounds of several kinds of operators via (s, m) -convexity,” *Advances in Differential Equations*, vol. 2020, p. 5, 2020.
- [12] A. W. Roberts and D. E. Varberg, *Convex Functions*, Academic Press, New York, NY, USA, 1973.
- [13] V. G. Mihesan, “A generalization of the convexity, seminar on functional equations, approx. and convex,” 1993.
- [14] G. Farid and M. Zahra, “On fractional integral inequalities for reimann-liouville integrals of refined $(\alpha, h - m)$ -convex functions,” 2021.
- [15] A. A. Kilbas, H. M. Srivastava, and J. J. Trujillo, *Theory and Applications of Fractional Differential Equations*, Elsevier, Amsterdam, Netherlands, North-Holland Mathematics Studies 204, 2006.
- [16] Y. C. Kwun, G. Farid, S. Ullah, W. Nazeer, K. Mahreen, and S. M. Kang, “Inequalities for a unified integral operator and associated results in fractional calculus,” *IEEE Access*, vol. 7, pp. 126283–126292, 2019.
- [17] M. Andrić, G. Farid, and J. Pečarić, “A further extension of Mittag-Leffler function,” *Fractional Calculus and Applied Analysis*, vol. 21, no. 5, pp. 1377–1395, 2018.
- [18] C. Y. Jung, G. Farid, H. Yasmeen, Y.-P. Lv, and J. Pečarić, “Refinements of some fractional integral inequalities for refined $(\alpha, h - m)$ -convex function,” *Advances in Difference Equations*, vol. 2021, no. 1, p. 391, 2021.
- [19] G. Farid and M. Zahra, “Some integral inequalities involving Mittag-Leffler functions for tgs-convex functions,” *Computational Methods in Applied Mathematics*, vol. 3, no. 5, 2021.
- [20] M. Tunc, E. Gav, and U. Şanal, “On tgs-convex function and their inequalities,” *Series Mathematics and Informatics*, vol. 30, no. 5, pp. 679–691, 2015.
- [21] S. Mubeen and G. M. Habibullah, “ k -fractional integrals and applications,” *International Journal of Contemporary Mathematical Sciences*, vol. 7, pp. 89–94, 2012.

Research Article

Novel Stability Results for Caputo Fractional Differential Equations

Abdellatif Ben Makhoulf  and El-Sayed El-Hady 

Mathematics Department, College of Science, Jouf University, P.O. Box 2014, Sakaka, Saudi Arabia

Correspondence should be addressed to Abdellatif Ben Makhoulf; abmakhoulf@ju.edu.sa

Received 8 May 2021; Accepted 19 June 2021; Published 1 July 2021

Academic Editor: Amr Elsonbaty

Copyright © 2021 Abdellatif Ben Makhoulf and El-Sayed El-Hady. This is an open access article distributed under the Creative Commons Attribution License, which permits unrestricted use, distribution, and reproduction in any medium, provided the original work is properly cited.

Modelling some diseases with large mortality rates worldwide, such as COVID-19 and cancer is crucial. Fractional differential equations are being extensively used in such modelling stages. However, exact analytical solutions for the solutions of such kind of equations are not reachable. Therefore, close exact solutions are of interests in many scientific investigations. The theory of stability in the sense of Ulam and Ulam–Hyers–Rassias provides such close exact solutions. So, this study presents stability results of some Caputo fractional differential equations in the sense of Ulam–Hyers, Ulam–Hyers–Rassias, and generalized Ulam–Hyers–Rassias. Two examples are introduced at the end to show the validity of our results. In this way, we generalize several recent interesting results.

1. Introduction and Preliminaries

Fractional calculus provides a powerful tool in both theoretical frameworks and practical aspects. In many disciplines, fractional modelling is much more suitable than the classical one. This is because of the nice modelling tools that are available only in fractional calculus (see e.g., [1, 2]). In particular, fractional calculus has been used extensively in the modelling stages in the fields of economics, chemistry, aerodynamics, physics, and polymer rheology. It should be remarked also that a certain kind of fractional derivative has been used recently to model Ebola virus (see [3]) and HIV (see [4]). Fractional differential equations with Caputo and Caputo–Fabrizio derivatives are used recently by the authors in [5] for the model of cancer-immune system.

The stability issue has gained substantially important attention in several research fields through applications. There are many kinds of stability; one of them is the stability introduced by Ulam in 1940. Since then, the problem is known as Ulam–Hyers stability or simply Ulam stability (see e.g., [6], for more details). Its applications for many types of equations have been investigated by many researchers. For

more details on this concept, the readers can see the interesting works [7–10]. The stability problem that is introduced by Ulam can be stated as follows.

Assume that \mathbb{G}_1 is a group and (\mathbb{G}_2, χ) a metric group. Given some $\varepsilon^* > 0$, does there exist $\delta^* > 0$ such that if $F: \mathbb{G}_1 \rightarrow \mathbb{G}_2$ satisfies

$$\chi(F(x_1 x_2), F(x_1)F(x_2)) < \delta^*, \quad (1)$$

for all $x_1, x_2 \in \mathbb{G}_1$, then a homomorphism $F^*: \mathbb{G}_1 \rightarrow \mathbb{G}_2$ exists such that

$$\chi(F(x_1), F^*(x_1)) < \varepsilon^*, \quad (2)$$

for all $x_1 \in \mathbb{G}_1$?

Ulam's problem has been extended in many directions for interesting settings. In particular, Rassias (see [11]) generalized Ulam's result for Banach spaces. The nice result of Rassias reads as follows (see [11]).

Theorem 1. Consider Banach spaces \mathbb{B} and \mathbb{B}^* , and suppose a mapping $Y: \mathbb{B} \rightarrow \mathbb{B}^*$ such that the function $t \mapsto Y(tx)$ from \mathbb{R} into \mathbb{B}^* is continuous for each fixed $x \in \mathbb{B}$. Assume that there are some $\beta \geq 0$ and $\omega \in [0, 1)$, fulfilling

$$\|Y(x_1 + x_2) - Y(x_1) - Y(x_2)\| \leq \beta(\|x_1\|^\omega + \|x_2\|^\omega), \quad x_1, x_2 \in \mathbb{B} \setminus \{0\}. \quad (3)$$

Then, a unique solution exists $Y^*: \mathbb{B} \rightarrow \mathbb{B}^*$ of the Cauchy equation ($F(x_1 + x_2) = F(x_1) + F(x_2)$) with

$$\|Y(x_1) - Y^*(x_1)\| \leq \frac{2\beta\|x_1\|^\omega}{|2 - 2^\omega|}, \quad x_1 \in \mathbb{B} \setminus \{0\}. \quad (4)$$

The theorem of Rassias (see [11]) is nowadays known as the Hyers–Ulam–Rassias stability.

Throughout the study, we denote the set of reals by \mathbb{R} , the set of nonzero reals by \mathbb{R}^* , and the set of complex numbers by \mathbb{C} , and we fix an interval $I := [\nu, \nu + T]$ for some reals ν, T with $T > 0$.

Definition 1. Let $\tilde{\lambda} > 0, \chi \in \mathbb{C}$. The Mittag–Leffler function (MLF) (see e.g., [2]) $\mathbb{E}_{\tilde{\lambda}}^-$ is defined as

$$\mathbb{E}_{\tilde{\lambda}}^-(\chi) := \sum_{n=0}^{\infty} \frac{\chi^n}{\Gamma(\tilde{\lambda}n + 1)}. \quad (5)$$

Similar to the exponential function, the function $h(s) = \mathbb{E}_{\tilde{\lambda}}^-(M(s - c)^{\tilde{\lambda}})$ satisfies ${}^C D_{c,s}^{\tilde{\lambda}} h(s) = Mh(s)$ and $I_c^{\tilde{\lambda}} h(s) = (1/M)(h(s) - 1)$, where $M \in \mathbb{R}^*$.

Remark 1. Authors in [12–15] obtained some stability results by using the MLF.

Now, we present the notion of generalized metric as follows. Let Z be a nonempty set.

Definition 2. A mapping $\vartheta: Z \times Z \rightarrow [0, \infty]$ is called a generalized metric on Z if and only if ϑ satisfies the following:

- G1 $\vartheta(\xi_1, \xi_2) = 0$ if and only if $\xi_1 = \xi_2$
- G2 $\vartheta(\xi_1, \xi_2) = \vartheta(\xi_2, \xi_1)$ for all $\xi_1, \xi_2 \in Z$
- G3 $\vartheta(\xi_1, \xi_3) \leq \vartheta(\xi_1, \xi_2) + \vartheta(\xi_2, \xi_3)$ for all $\xi_1, \xi_2, \xi_3 \in Z$

The notion of stability in the sense of Ulam–Hyers (UH), Ulam–Hyers–Rassias (UHR), and generalized UHR of fractional differential equations can be introduced as follows (see e.g., [16]). We consider the following fractional differential equation:

$$H\left(t, \kappa, {}^C D_{\nu,t}^{\tilde{\lambda}} \kappa(t)\right) = 0, \quad (6)$$

and the following three inequalities:

$$\left|H\left(t, \kappa, {}^C D_{\nu,t}^{\tilde{\lambda}} \kappa(t)\right)\right| \leq \varepsilon, \quad (7)$$

$$\left|H\left(t, \kappa, {}^C D_{\nu,t}^{\tilde{\lambda}} \kappa(t)\right)\right| \leq \varrho(t), \quad (8)$$

$$\left|H\left(t, \kappa, {}^C D_{\nu,t}^{\tilde{\lambda}} \kappa(t)\right)\right| \leq \varepsilon \varrho(t), \quad (9)$$

We define the stability of (6) as follows.

Definition 3. Equation (6) is called stable in the sense of UH if for a given $\varepsilon > 0$ and a function κ which satisfies (7), and there exists a solution κ_0 of (6) such that

$$|\kappa(t_1) - \kappa_0(t_1)| \leq c\varepsilon. \quad (10)$$

Definition 4. Equation (6) is called UHR stable if, for some $\varepsilon > 0$ and a function κ satisfying (9), there exists a solution κ_0 of (6) such that

$$|\kappa(t_1) - \kappa_0(t_1)| \leq c\varepsilon \varrho(t_1), \quad (11)$$

where $\varrho(t_1)$ is some positive, nondecreasing, and continuous function.

Definition 5. Equation (6) is called generalized UHR stable if, for some $\varepsilon > 0$ and a function κ satisfying (8), there exists a solution κ_0 of (6) such that

$$|\kappa(t_1) - \kappa_0(t_1)| \leq c\varrho(t_1). \quad (12)$$

The theorem below represents a basic well-known fixed point theory (see [17]). This theorem plays a fundamental role in our study.

Theorem 2. Assume that (P, R) is a metric space that is generalized completely. Let $M: P \rightarrow P$ be a strictly contractive operator. If there is an integer $u \geq 0$ with $R(M^{u+1}d, M^u d) < \infty$ for some $d \in P$, therefore,

- (a) $\lim_{l \rightarrow +\infty} M^l d = d^*$, where d^* is the unique fixed point of M in

$$P^* := \{d_1 \in P: R(M^u d, d_1) < \infty\}. \quad (13)$$

- (b) If $d_1 \in P^*$, then $R(d_1, d^*) \leq (1/(1 - \tilde{K}))R(Md_1, d_1)$.

Define the space X as $X := C(I, \mathbb{R})$.

Lemma 1. Define a metric $d: X \times X \rightarrow [0, \infty]$ in such a way that

$$d(\kappa_1, \kappa_2) = \inf \left\{ \tilde{D} \in [0, \infty]: \frac{|\kappa_1(s) - \kappa_2(s)|}{\mathbb{E}_{\tilde{\lambda}}^-(\tilde{\eta}(s - \nu)^{\tilde{\lambda}})} \leq \tilde{D}\beta(s), s \in I \right\}, \quad (14)$$

where $\tilde{\eta} > 0$ and $\beta \in C(I, (0, +\infty))$. Then, (X, d) is a generalized complete metric space.

Remark 2. Note that the authors in [18] proved the existence and uniqueness of global solutions using the norm:

$$\|\kappa\|_\gamma = \sup_{t \in [0, \vartheta]} \frac{\|\kappa(t)\|}{\mathbb{E}_{\tilde{\lambda}}^-(\gamma t^{\tilde{\lambda}})}, \quad \text{for } \kappa \in C([0, \vartheta], \mathbb{R}^d). \quad (15)$$

This contribution is considered as a generalized version of the interesting results in [19–21]. Our contribution is original for many reasons. First, the metric used is a function of the Mittag–Leffler function. Second, the obtained results are in a complete generalized metric space. Third, the tool

used is a version of Banach fixed point theory. The main purpose of this study is to study the stability of the following initial value problem:

$$\begin{aligned} {}^C D_{\nu, \omega}^{\tilde{\lambda}} y(\omega) &= G(\omega, y(\omega)), \\ y(\nu) &= y_\nu, \end{aligned} \tag{16}$$

in the sense depicted in Definitions 3–5, where $\tilde{\lambda} \in (0, 1)$, ${}^C D_{\nu, \omega}^{\tilde{\lambda}}$ is the Caputo fractional derivative, and $G: I \times \mathbb{R} \rightarrow \mathbb{R}$ is a given function. It should be noted that the solution of the initial value problem (16) is given by

$$y(\omega) = y_\nu + \frac{1}{\Gamma(\tilde{\lambda})} \int_\nu^\omega (\omega - \varsigma)^{\tilde{\lambda}-1} G(\varsigma, y(\varsigma)) d\varsigma. \tag{17}$$

2. Stability Results

In this section, we present our main results. In other words, we prove that, under certain conditions, functions that satisfy (16) approximately (in some sense) are close (in some way) to the solutions of (16). We have done this in both UH sense and also in UHR sense. The following theorem represents the stability of (16) in the sense of UHR.

Theorem 3. Assume $G: I \times \mathbb{R} \rightarrow \mathbb{R}$ is continuous and satisfies

$$|G(\omega, \kappa_1) - G(\omega, \kappa_2)| \leq L_G |\kappa_1 - \kappa_2|, \tag{18}$$

for all $\omega \in I, \kappa_i \in \mathbb{R}, i = 1, 2$, and for some $L_G > 0$. If an absolutely continuous function $x: I \rightarrow \mathbb{R}$ satisfies

$$\left| {}^C D_{\nu, \omega}^{\tilde{\lambda}} x(\omega) - G(\omega, x(\omega)) \right| \leq \varepsilon(\omega), \tag{19}$$

for all $\omega \in I$, where $\varepsilon > 0$ and $\varrho(\omega)$ is a positive, nondecreasing, and continuous function, then there is a solution x^* of (16) such that

$$|x(\omega) - x^*(\omega)| \leq \left(\frac{L_G + \delta}{\delta} \right) \frac{M \mathbb{E}_{\tilde{\lambda}}\left((L_G + \delta)T^{\tilde{\lambda}}\right)}{\Gamma(\tilde{\lambda} + 1)}, \quad \varepsilon \varrho(\omega), \tag{20}$$

where

$$M = \sup_{s \in [\nu, \nu+T]} \left(\frac{(s - \nu)^{\tilde{\lambda}}}{\mathbb{E}_{\tilde{\lambda}}\left((L_G + \delta)(s - \nu)^{\tilde{\lambda}}\right)} \right), \tag{21}$$

and δ is any positive constant.

Proof. Define the metric d on X in this way:

$$d(x_1, x_2) = \inf \left\{ D \in [0, \infty) : \frac{|x_1(\omega) - x_2(\omega)|}{\mathbb{E}_{\tilde{\lambda}}\left((L_G + \delta)(\omega - \nu)^{\tilde{\lambda}}\right)} \leq D \varrho(\omega), \forall \omega \in I \right\}. \tag{22}$$

Now, define the operator $\mathcal{A}: X \rightarrow X$ such that

$$(\mathcal{A}y)(\omega) := x(\nu) + \frac{1}{\Gamma(\tilde{\lambda})} \int_\nu^\omega (\omega - s)^{\tilde{\lambda}-1} G(s, y(s)) ds. \tag{23}$$

It is easy to see that $d(\mathcal{A}y_0, y_0) < \infty$, and $\{y \in X: d(y_0, y) < \infty\} = X, \forall y_0 \in X$.

Now, we prove that the operator \mathcal{A} is a strictly contractive operator:

$$\begin{aligned} |(\mathcal{A}y_1)(\omega) - (\mathcal{A}y_2)(\omega)| &\leq \left| \int_\nu^\omega \frac{(\omega - \varsigma)^{\tilde{\lambda}-1}}{\Gamma(\tilde{\lambda})} \{G(\varsigma, y_1(\varsigma)) - G(\varsigma, y_2(\varsigma))\} d\varsigma \right| \\ &\leq \frac{1}{\Gamma(\tilde{\lambda})} \int_\nu^\omega (\omega - \varsigma)^{\tilde{\lambda}-1} |G(\varsigma, y_1(\varsigma)) - G(\varsigma, y_2(\varsigma))| d\varsigma \\ &\leq L_G \int_\nu^\omega (\omega - \varsigma)^{\tilde{\lambda}-1} \frac{|y_1(\varsigma) - y_2(\varsigma)|}{\Gamma(\tilde{\lambda})} d\varsigma \\ &\leq \frac{L_G}{\Gamma(\tilde{\lambda})} \int_\nu^\omega (\omega - \varsigma)^{\tilde{\lambda}-1} \frac{|y_1(\varsigma) - y_2(\varsigma)|}{\mathbb{E}_{\tilde{\lambda}}\left((L_G + \delta)(\varsigma - \nu)^{\tilde{\lambda}}\right)} \mathbb{E}_{\tilde{\lambda}}\left((L_G + \delta)(\varsigma - \nu)^{\tilde{\lambda}}\right) d\varsigma \\ &\leq \frac{L_G d(y_1, y_2)}{\Gamma(\tilde{\lambda})} \int_\nu^\omega (\omega - \varsigma)^{\tilde{\lambda}-1} \varrho(\varsigma) \mathbb{E}_{\tilde{\lambda}}\left((L_G + \delta)(\varsigma - \nu)^{\tilde{\lambda}}\right) d\varsigma, \quad \text{for all } \omega \in I. \end{aligned} \tag{24}$$

Since ϱ is nondecreasing, therefore,

$$\begin{aligned} |(\mathcal{A}y_1)(\omega) - (\mathcal{A}y_2)(\omega)| &\leq \frac{L_G d(y_1, y_2)}{\Gamma(\tilde{\lambda})} \varrho(\omega) \int_{\nu}^{\omega} (\omega - \varsigma)^{\tilde{\lambda}-1} \mathbb{E}_{\tilde{\lambda}}^{-}((L_G + \delta)(\varsigma - \nu)^{\tilde{\lambda}}) d\varsigma \\ &\leq \frac{L_G d(y_1, y_2)}{L_G + \delta} \left(\mathbb{E}_{\tilde{\lambda}}^{-}((L_G + \delta)(\omega - \nu)^{\tilde{\lambda}}) - 1 \right) \varrho(\omega) \\ &\leq \frac{L_G d(y_1, y_2)}{L_G + \delta} \left(\mathbb{E}_{\tilde{\lambda}}^{-}((L_G + \delta)(\omega - \nu)^{\tilde{\lambda}}) \right) \varrho(\omega), \quad \text{for all } \omega \in I, \end{aligned} \tag{25}$$

so that

$$d(\mathcal{A}y_1, \mathcal{A}y_2) \leq \frac{L_G}{L_G + \delta} d(y_1, y_2), \tag{26}$$

which means that the operator \mathcal{A} is a strictly contractive operator. Now, since we have

$$\left| {}^C D_{\nu, \omega}^{\tilde{\lambda}} x(\omega) - G(\omega, x(\omega)) \right| \leq \varepsilon \varrho(\omega), \tag{27}$$

then,

$$|x(\omega) - \mathcal{A}x(\omega)| \leq \frac{\varepsilon}{\Gamma(\tilde{\lambda})} \int_{\nu}^{\omega} (\omega - \varsigma)^{\tilde{\lambda}-1} \varrho(\varsigma) d\varsigma, \tag{28}$$

which implies that

$$\begin{aligned} \frac{|x(\omega) - \mathcal{A}x(\omega)|}{\mathbb{E}_{\tilde{\lambda}}^{-}((L_G + \delta)(\omega - \nu)^{\tilde{\lambda}})} &\leq \frac{\varepsilon}{\Gamma(\tilde{\lambda} + 1)} \varrho(\omega) \frac{(\omega - \nu)^{\tilde{\lambda}}}{\mathbb{E}_{\tilde{\lambda}}^{-}((L_G + \delta)(\omega - \nu)^{\tilde{\lambda}})} \\ &\leq \frac{\varepsilon M}{\Gamma(\tilde{\lambda} + 1)} \varrho(\omega). \end{aligned} \tag{29}$$

Therefore,

$$d(x, \mathcal{A}x) \leq \varepsilon \frac{M}{\Gamma(\tilde{\lambda} + 1)}. \tag{30}$$

By employing Theorem 2, there is a solution x^* of (16) such that

$$d(x, x^*) \leq \varepsilon \left(\frac{L_G + \delta}{\delta} \right) \frac{M}{\Gamma(\tilde{\lambda} + 1)}, \tag{31}$$

so that

$$|x(\omega) - x^*(\omega)| \leq \left(\frac{L_G + \delta}{\delta} \right) \frac{M \mathbb{E}_{\tilde{\lambda}}^{-}((L_G + \delta)T^{\tilde{\lambda}})}{\Gamma(\tilde{\lambda} + 1)}, \quad \varepsilon \varrho(\omega), \tag{32}$$

for all $\omega \in I$.

The following theorem represents the stability of (16) in the sense of UH. \square

Theorem 4. Assume $G: I \times \mathbb{R} \rightarrow \mathbb{R}$ is continuous and satisfies

$$|G(\omega, \kappa_1) - G(\omega, \kappa_2)| \leq L_G |\kappa_1 - \kappa_2|, \quad \forall \omega \in I, \kappa_i \in \mathbb{R}, i = 1, 2. \tag{33}$$

If an absolutely continuous function $x: I \rightarrow \mathbb{R}$ satisfies

$$\left| {}^C D_{\nu, \omega}^{\tilde{\lambda}} x(\omega) - G(\omega, x(\omega)) \right| \leq \varepsilon, \tag{34}$$

for all $\omega \in I$ and some $\varepsilon > 0$, then there is a solution x^* of (16) such that

$$|x(\omega) - x^*(\omega)| \leq \varepsilon \left(\frac{L_G + \delta}{\delta} \right) \frac{M \mathbb{E}_{\tilde{\lambda}}^{-}((L_G + \delta)T^{\tilde{\lambda}})}{\Gamma(\tilde{\lambda} + 1)}, \tag{35}$$

where

$$M = \sup_{s \in [\nu, \nu+T]} \left(\frac{(s - \nu)^{\tilde{\lambda}}}{\mathbb{E}_{\tilde{\lambda}}^{-}((L_G + \delta)(s - \nu)^{\tilde{\lambda}})} \right), \tag{36}$$

and δ is any positive constant.

Proof. The proof is similar to Theorem 3. \square

Remark 3. It should be noted that, in our analysis, we do not assume any condition on the constant L_G , unlike the case of Theorem 4.1 in [20], where the condition $0 < (L_G r^{\lambda} / (\Gamma(\tilde{\lambda} + 1))) < 1$ was a basic condition.

Remark 4. Note that our results of the UH stability are some generalizations of the results obtained in [19].

The following theorem represents the stability of (16) in the sense of generalized UHR.

Theorem 5. Assume $G: I \times \mathbb{R} \rightarrow \mathbb{R}$ is continuous and satisfies

$$|G(\omega, \kappa_1) - G(\omega, \kappa_2)| \leq L_G |\kappa_1 - \kappa_2|, \quad (37)$$

for all $\omega \in I, \kappa_i \in \mathbb{R}, i = 1, 2$, and for some $L_G > 0$. If an absolutely continuous function $x: I \rightarrow \mathbb{R}$ satisfies

$$\left| {}^C D_{\nu, \omega}^{\tilde{\lambda}} x(\omega) - G(\omega, x(\omega)) \right| \leq \varrho(\omega), \quad (38)$$

for all $\omega \in I$, where $\varrho(\omega)$ is a positive, nondecreasing, and continuous function, then there is a solution x^* of (16) such that

$$|x(\omega) - x^*(\omega)| \leq \left(\frac{L_G + \delta}{\delta} \right) \frac{M \mathbb{E}_{\tilde{\lambda}}^-((L_G + \delta)T^{\tilde{\lambda}})}{\Gamma(\tilde{\lambda} + 1)} \varrho(\omega), \quad (39)$$

where

$$M = \sup_{s \in [\nu, \nu+T]} \left(\frac{(s - \nu)^{\tilde{\lambda}}}{\mathbb{E}_{\tilde{\lambda}}^-((L_G + \delta)(s - \nu)^{\tilde{\lambda}})} \right), \quad (40)$$

and δ is any positive constant.

Proof. The proof is similar to Theorem 3. □

Remark 5. Notice that, in our study of the generalized UHR stability, we do not assume any condition on L_G , unlike the case in Theorem 3.1 in [20].

Remark 6. Note that, in [19], the authors obtained stability results for differential equations with integer-order derivatives, while in our case, it is for fractional-order derivatives. In this sense, we generalized the interesting results in [19].

3. Examples

Two illustrative examples are given to show the validity of results.

Example 1. Consider equation (16) for $\tilde{\lambda} = 0.6, \nu = 0, T = 9$, and $G(\omega, \kappa) = \omega^2 \sin(\kappa)$.

We have

$$|\omega^2 \sin(\kappa_1) - \omega^2 \sin(\kappa_2)| \leq 81 |\kappa_1 - \kappa_2|, \quad \forall \omega \in [0, 9], \kappa_1, \kappa_2 \in \mathbb{R}. \quad (41)$$

Then, $L_G = 81$.

Suppose that x satisfies

$$\left| {}^C D_{0, \omega}^{0.6} x(\omega) - \omega^2 \sin(x(\omega)) \right| \leq 0.01(\omega + 2), \quad (42)$$

for all $\omega \in [0, 9]$.

Here, $\varepsilon = 0.01$ and $\psi(\omega) = \omega + 2$. Using Theorem 3, there is a solution x^* of the fractional differential equation and $M > 0$ such that

$$|x(\omega) - x^*(\omega)| \leq 0.01M(\omega + 2), \quad \forall \omega \in [0, 9]. \quad (43)$$

Example 2. Consider equation (16) for $\tilde{\lambda} = 0.4, \nu = 0, T = 2$, and $G(\omega, \kappa) = \omega^4 \cos(\kappa)$.

We have

$$|\omega^4 \cos(\kappa_1) - \omega^4 \cos(\kappa_2)| \leq 16 |\kappa_1 - \kappa_2|, \quad \forall \omega \in [0, 2], \kappa_1, \kappa_2 \in \mathbb{R}. \quad (44)$$

Then, $L_G = 16$.

Suppose that x satisfies

$$\left| {}^C D_{0, \omega}^{0.4} x(\omega) - \omega^4 \cos(x(\omega)) \right| \leq 0.01, \quad (45)$$

for all $\omega \in [0, 2]$.

Here, $\varepsilon = 0.01$. Using Theorem 4, there is a solution x^* of the fractional differential equation and $M > 0$ such that

$$|x(\omega) - x^*(\omega)| \leq 0.01M, \quad \forall \omega \in [0, 2]. \quad (46)$$

4. Conclusion

It is known that, for the majority of fractional differential problems, a widely applicable general approach to determine the analytical solutions is not available. In this paper, we used a version of Banach fixed point theorem to prove that, under certain conditions, functions that satisfy some Caputo fractional differential equations approximately are close in some sense to the exact solutions of such kind of equations. In other words, we presented stability results for some Caputo fractional differential equations in the sense of UH, UHR, and generalized UHR. In our analysis, we used a new metric as a function of the Mittag-Leffler function. We end up with two examples that show the validity of our results.

Data Availability

No data were used to support this study.

Disclosure

An earlier version of this work has been presented as preprint in Authorea.

Conflicts of Interest

The authors declare that they have no conflicts of interest.

Acknowledgments

The authors extend their appreciation to the Deanship of Scientific Research at Jouf University for funding this work through research Grant no. DSR-2021-03-0121.

References

- [1] I. Podlubny, “Fractional differential equations,” *Mathematics in Science and Engineering*, Vol. 198, Academic Press, San Diego, CA, USA, 1999.
- [2] A. A. Kilbas, H. M. Srivastava, and J. J. Trujillo, *Theory and Applications of Fractional Differential Equations*, Vol. 204, Elsevier, Amsterdam, Netherlands, 2006.
- [3] I. Koca, “Modelling the spread of Ebola virus with atangana-baleanu fractional operators,” *European Physical Journal Plus*, vol. 133, no. 3, pp. 1–11, 2018.
- [4] D. Baleanu, H. Mohammadi, and S. Rezapour, “Analysis of the model of HIV-1 infection of $CD4^+$ T-cell with a new approach of fractional derivative,” *Advances in Difference Equations*, vol. 2020, no. 1, 17 pages, Article ID 71, 2020.
- [5] E. Uçar and N. Özdemir, “A fractional model of cancer-immune system with caputo and caputo-fabrizio derivatives,” *European Physical Journal Plus*, vol. 136, no. 1, pp. 43–17, 2021.
- [6] N. Brillouët-Belluot, J. Brzdek, and K. Ciepliński, “On some recent developments in ulam’s type stability,” *Abstract and Applied Analysis*, vol. 2012, Article ID 716936, 41 pages, 2012.
- [7] S. András and A. R. Mészáros, “Ulam-Hyers stability of dynamic equations on time scales via picard operators,” *Applied Mathematics and Computation*, vol. 219, no. 9, pp. 4853–4864, 2013.
- [8] D. S. Cimpean and D. Popa, “Hyers-Ulam stability of Euler’s equation,” *Applied Mathematics Letters*, vol. 24, no. 9, pp. 1539–1543, 2011.
- [9] B. Hegyi and S.-M. Jung, “On the stability of Laplace’s equation,” *Applied Mathematics Letters*, vol. 26, no. 5, pp. 549–552, 2013.
- [10] S.-M. Jung, “Hyers-Ulam stability of linear differential equations of first order,” *Applied Mathematics Letters*, vol. 17, no. 10, pp. 1135–1140, 2004.
- [11] T. M. Rassias, “On the stability of the linear mapping in Banach spaces,” *Proceedings of the American Mathematical Society*, vol. 72, no. 2, pp. 297–300, 1978.
- [12] A. Ahmadova and N. I. Mahmudov, “Ulam-Hyers stability of caputo type fractional stochastic neutral differential equations,” *Statistics & Probability Letters*, vol. 168, p. 108949, 2021.
- [13] A. Ben Makhlouf, “Stability with respect to part of the variables of nonlinear caputo fractional differential equations,” *Mathematical Communications*, vol. 23, no. 1, pp. 119–126, 2018.
- [14] N. Eghbali, V. Kalvandi, and J. M. Rassias, “A fixed point approach to the Mittag-Leffler-Hyers-Ulam stability of a fractional integral equation,” *Open Mathematics*, vol. 14, no. 1, pp. 237–246, 2016.
- [15] J. Wang and Y. Zhou, “Mittag-Leffler-Ulam stabilities of fractional evolution equations,” *Applied Mathematics Letters*, vol. 25, no. 4, pp. 723–728, 2012.
- [16] J. Wang, L. Lv, and Y. Zhou, “Ulam stability and data dependence for fractional differential equations with caputo derivative,” *Electronic Journal of Qualitative Theory of Differential Equations*, vol. 63, pp. 1–10, 2011.
- [17] J. B. Diaz and B. Margolis, “A fixed point theorem of the alternative, for contractions on a generalized complete metric space,” *Bulletin of the American Mathematical Society*, vol. 74, no. 2, pp. 305–310, 1968.
- [18] T. S. Doan and P. E. Kloeden, “Semi-dynamical systems generated by autonomous caputo fractional differential equations,” *Vietnam Journal of Mathematics*, pp. 1–11, 2019.
- [19] Y. Başı, A. Misir, and S. Ögrekçi, “On the stability problem of differential equations in the sense of Ulam,” *Results Math*, vol. 75, no. 1, pp. 1–13, 2020.
- [20] J. Wang, L. Lv, and Y. Zhou, “New concepts and results in stability of fractional differential equations,” *Communications in Nonlinear Science and Numerical Simulation*, vol. 17, no. 6, pp. 2530–2538, 2012.
- [21] E. El-hady and S. Ögrekçi, “On Hyers-Ulam-Rassias stability of fractional differential equations with caputo derivative,” *Journal of Mathematics and Computer Science*, vol. 22, pp. 325–332, 2021.

Research Article

Dynamics and Solutions' Expressions of a Higher-Order Nonlinear Fractional Recursive Sequence

Abeer Alshareef,¹ Faris Alzahrani,¹ and Abdul Qadeer Khan²

¹Department of Mathematics, Faculty of Science, King Abdulaziz University, P. O. Box 80203, Jeddah 21589, Saudi Arabia

²Department of Mathematics, University of Azad Jammu and Kashmir, Muzaffarabad 13100, Pakistan

Correspondence should be addressed to Abdul Qadeer Khan; abdulqadeerkhan1@gmail.com

Received 19 April 2021; Accepted 20 May 2021; Published 9 June 2021

Academic Editor: Abdelalim Elsadany

Copyright © 2021 Abeer Alshareef et al. This is an open access article distributed under the Creative Commons Attribution License, which permits unrestricted use, distribution, and reproduction in any medium, provided the original work is properly cited.

The principle purpose of this article is to examine some stability properties for the fixed point of the below rational difference equation $U_{n+1} = \xi U_{n-8} + (\varepsilon U_{n-8}^2 / (\mu U_{n-8} + \kappa U_{n-17}))$ where $\xi, \varepsilon, \mu,$ and κ are arbitrary real numbers. Moreover, solutions for some special cases of the proposed difference equation are introduced.

1. Introduction

In recent years, many researchers have tended to use difference equations in mathematical models to explain the problems in different sciences since they have a lot of features such as they enable the scientists to introduce the predictions of their study and it gives more accurate results. In addition, there are various types of nonlinear difference equations that can be studied; one of the most commonly used is rational nonlinear difference equations. However, the research studies in the area of difference equations have two directions: first one is the analysis of the behavior of solutions. Therefore, there are a huge number of articles published to investigate the stability of the equilibrium points and the existence of the periodic solutions for the nonlinear difference equations (see, for example, [1–5]). The second direction is to obtain the expressions of the solution if it is possible since there is no explicit and enough methods to find the solution of nonlinear difference equations (see, for example, [6–11]).

Saleh and Farhat [12] investigated the stability properties and the period two solutions of all nonnegative solutions of the difference equation:

$$V_{n+1} = \frac{a_1 V_n + a_2 V_{n-k}}{A + B V_{n-k}}. \quad (1)$$

In [13], Jia studied the solutions' behavior of the high-order fuzzy difference equation:

$$V_{n+1} = \frac{A_1 V_{n-1} V_{n-2}}{B_2 + \sum_{i=3}^k D_i V_{n-i}}. \quad (2)$$

Kerker et al. [14] investigated the global behavior of the rational difference equation:

$$V_{n+1} = \frac{a_n + V_n}{a_n + V_{n-k}}. \quad (3)$$

Khaliq and Elsayed [15] examined the dynamics behavior and existence of the periodic solution of the difference equation:

$$V_{n+1} = \alpha_1 V_{n-2} + \frac{\alpha_2 V_{n-2}^2}{\gamma_1 V_{n-2} + \gamma_2 V_{n-5}}. \quad (4)$$

In [16], Saleh et al. studied the properties' stability for a nonlinear rational difference equation of a higher order:

$$V_{n+1} = \frac{\beta_1 + \beta_2 V_n + \beta_3 V_{n-k}}{B_1 V_n + B_2 V_{n-k}}. \quad (5)$$

Sadiq and Kalim [17] obtained the solution behavior of the difference equation:

$$V_{n+1} = \alpha_1 V_{n-9} + \frac{\alpha_2 V_{n-19}^2}{\alpha_3 V_{n-9} + \alpha_4 V_{n-19}}. \quad (6)$$

To see more related work on the nonlinear difference equation, refer to [18–43]. Our aim of this article is to investigate the dynamics of the solution for the below difference equation:

$$U_{n+1} = \xi U_{n-8} + \frac{\varepsilon U_{n-8}^2}{\mu U_{n-8} + \kappa U_{n-17}}, \quad (7)$$

where ξ, ε, μ , and κ are arbitrary real numbers with initial conditions U_j for $j = -17, -16, \dots, 0$.

This paper is collected as follows: in Section 2, the boundedness of the solution is presented, and we prove that the periodic solution of period two does not exist in the next section. Following that, we state the conditions of the local and global stability of the equilibrium point in Sections 4 and 5, respectively. Then, we introduce the solutions' forms for some special cases in Section 6. Finally, we give some numerical examples in order to illustrate the behavior of the solutions.

2. Boundedness of Solution

Theorem 1. *If the following condition*

$$\left(\xi + \frac{\varepsilon}{\mu}\right) < 1, \quad (8)$$

is true, then every solution of (7) is bounded.

Proof. Assume that $\{U_n\}_{n=-17}^\infty$ is a solution of (7). Then, from (7), we have

$$U_{n+1} = \xi U_{n-8} + \frac{\varepsilon U_{n-8}^2}{\mu U_{n-8} + \kappa U_{n-17}} \leq \xi U_{n-8} + \frac{\varepsilon U_{n-8}^2}{\mu U_{n-8}} = \left(\xi + \frac{\varepsilon}{\mu}\right) U_{n-8}. \quad (9)$$

Hence,

$$U_{n+1} \leq U_{n-8}, \quad \forall n \geq 0. \quad (10)$$

Implies that the subsequences $\{U_{9n-8}\}_{n=-17}^\infty, \{U_{9n-7}\}_{n=-17}^\infty, \{U_{9n-6}\}_{n=-17}^\infty, \{U_{9n-5}\}_{n=-17}^\infty, \{U_{9n-4}\}_{n=-17}^\infty, \{U_{9n-3}\}_{n=-17}^\infty, \{U_{9n-2}\}_{n=-17}^\infty, \{U_{9n-1}\}_{n=-17}^\infty$ and $\{U_{9n}\}_{n=-17}^\infty$ are nonincreasing. Thus, they are bounded from above by U_{max} , where $U_{max} = \max\{U_{-17}, U_{-16}, U_{-15}, U_{-14}, U_{-13}, U_{-12}, U_{-11}, U_{-10}, U_{-9}, U_{-8}, U_{-7}, U_{-6}, U_{-5}, U_{-4}, U_{-3}, U_{-2}, U_{-1}, U_0\}$. \square

3. Periodicity of the Solution

Theorem 2. *For nonlinear difference equation (7), there is no periodic solution of period two.*

Proof. To prove Theorem 2, suppose that (7) has a positive prime period two solutions presented as \dots, e, f, e, f, \dots . Then,

$$e = \xi f + \frac{\varepsilon f^2}{\mu f + \kappa e},$$

$$e = \frac{\xi \mu f^2 + \xi \kappa e f + \varepsilon f^2}{\mu f + \kappa e}, \quad (11)$$

$$(\xi \mu + \varepsilon) f^2 = (\mu - \xi \kappa) e f + \kappa e^2.$$

Similarly,

$$f = \xi e + \frac{\varepsilon e^2}{\mu e + \kappa f},$$

$$f = \frac{\xi \mu e^2 + \xi \kappa e f + \varepsilon e^2}{\mu e + \kappa f}, \quad (12)$$

$$(\xi \mu + \varepsilon) e^2 = (\mu - \xi \kappa) f e + \kappa f^2.$$

Subtracting (11) from (12), we get

$$\kappa(e^2 - f^2) + (\xi \mu + \varepsilon)(e^2 - f^2) = 0, \quad (13)$$

$$(\kappa + \xi \mu + \varepsilon)(e^2 - f^2) = 0.$$

Since $(\kappa + \xi \mu + \varepsilon) \neq 0$, thus $e = f$, and this contradicts the fact that $e \neq f$. \square

4. The Equilibrium Point and Local Stability

The fixed points of (7) are given by

$$\bar{U} = \xi \bar{U} + \frac{\varepsilon \bar{U}^2}{\mu \bar{U} + \kappa \bar{U}},$$

$$(1 - \xi) \bar{U} = \frac{\varepsilon \bar{U}^2}{(\mu + \kappa) \bar{U}} \quad (14)$$

$$((1 - \xi)(\mu + \kappa) - \varepsilon) \bar{U}^2 = 0.$$

If $(1 - \xi)(\mu + \kappa) \neq \varepsilon$, then (7) has only one equilibrium point which is $\bar{U} = 0$.

Assume $g: (0, \infty)^2 \rightarrow (0, \infty)$ is a continuously differentiable function defined by

$$g(v, w) = \xi v + \frac{\varepsilon v^2}{\mu v + \kappa w}. \quad (15)$$

Therefore,

$$\frac{\partial g}{\partial v} = \xi + \frac{\varepsilon \mu v^2 + 2 \varepsilon \kappa v w}{(\mu v + \kappa w)^2}, \quad (16)$$

$$\frac{\partial g}{\partial w} = \frac{-\kappa \varepsilon v^2}{(\mu v + \kappa w)^2}.$$

Then,

$$\frac{\partial g}{\partial v} \Big|_{v=w=\bar{U}} = \xi + \frac{\varepsilon\mu + 2\varepsilon\kappa}{(\mu + \kappa)^2}, \quad \mu(1 - \xi) \neq \varepsilon. \tag{17}$$

$$\frac{\partial g}{\partial w} \Big|_{v=w=\bar{U}} = \frac{-\varepsilon\kappa}{(\mu + \kappa)^2}.$$

Hence,

$$x_{n+1} - \left(\xi + \frac{\varepsilon\mu + 2\varepsilon\kappa}{(\mu + \kappa)^2} \right) x_n + \left(\frac{\varepsilon\kappa}{(\mu + \kappa)^2} \right) x_{n-1} = 0. \tag{18}$$

Theorem 3. *The fixed point $\bar{U} = 0$ is said to be a locally asymptotically stable if the relation*

$$\varepsilon(\mu + 3\kappa) < (1 - \xi)(\mu + \kappa)^2, \tag{19}$$

is satisfied.

Proof. From Theorem 5.10 in [44], it follows that \bar{U} is asymptotically stable if

$$|P_0| + |P_1| < 1, \tag{20}$$

where $P_0 = \xi + ((\varepsilon\mu + 2\varepsilon\kappa)/(\mu + \kappa)^2)$ and $P_1 = (-\varepsilon\kappa/(\mu + \kappa)^2)$. Then,

$$\left| \xi + \frac{\varepsilon\mu + 2\varepsilon\kappa}{(\mu + \kappa)^2} \right| + \left| \frac{-\varepsilon\kappa}{(\mu + \kappa)^2} \right| < 1, \tag{21}$$

$$\xi + \frac{\varepsilon\mu + 3\varepsilon\kappa}{(\mu + \kappa)^2} < 1.$$

Hence,

$$\varepsilon(\mu + 3\kappa) < (1 - \xi)(\mu + \kappa)^2. \tag{22}$$

Finally, the proof is done. □

5. Global Attractivity of the Fixed Point

Theorem 4. *The fixed point \bar{U} of (7) has to be a global attracting when*

$$U_{-17}, U_{-16}, U_{-15}, U_{-14}, U_{-13}, U_{-12}, U_{-11}, U_{-10}, U_{-9}, U_{-8}, U_{-7}, U_{-6}, U_{-5}, U_{-4}, U_{-3}, U_{-2}, U_{-1}, \tag{29}$$

and U_0 are arbitrary real numbers.

6.1. *First Equation.* We solve the equation

Proof. From (16), we see that the function $g(v, w)$, which defined in (15), is increasing in v and decreasing in w . Let (ρ, τ) be a solution of the system:

$$\begin{aligned} \tau &= g(\tau, \rho), \\ \rho &= g(\rho, \tau), \\ \tau &= \xi\tau + \frac{\varepsilon\tau^2}{\mu\tau + \kappa\rho}, \\ \rho &= \xi\rho + \frac{\varepsilon\rho^2}{\mu\rho + \kappa\tau}. \end{aligned} \tag{24}$$

Therefore,

$$\mu(1 - \xi)\tau^2 + \kappa(1 - \xi)\tau\rho = \varepsilon\tau^2, \tag{25}$$

$$\mu(1 - \xi)\rho^2 + \kappa(1 - \xi)\tau\rho = \varepsilon\rho^2. \tag{26}$$

Subtracting (25) from (26), we get

$$(\mu(1 - \xi) - \varepsilon)(\tau^2 - \rho^2) = 0, \tag{27}$$

and then, $\rho = \tau$ if $\mu(1 - \xi) \neq \varepsilon$. Thus, from Theorem 5.20 in [44], we observe that there exists only one solution for (7) and it is a global attractor if $\mu(1 - \xi) \neq \varepsilon$. □

6. Special Cases

Now, we present the solutions' expressions for special cases of (7):

$$U_{n+1} = U_{n-8} \pm \frac{U_{n-8}^2}{U_{n-8} \pm U_{n-17}}, \tag{28}$$

where the initial conditions are

$$U_{n+1} = U_{n-8} + \frac{U_{n-8}^2}{U_{n-8} + U_{n-17}}. \tag{30}$$

Theorem 5. Assume $\{U_n\}_{n=-17}^{\infty}$ is a solution of (30); thus, for $n = 0, 1, \dots$,

$$\begin{aligned}
 U_{9n-8} &= U_{-8} \prod_{i=1}^n \left(\frac{F_{2i+1}U_{-8} + F_{2i}U_{-17}}{F_{2i}U_{-8} + F_{2i-1}U_{-17}} \right), \\
 U_{9n-4} &= U_{-4} \prod_{i=1}^n \left(\frac{F_{2i+1}U_{-4} + F_{2i}U_{-13}}{F_{2i}U_{-4} + F_{2i-1}U_{-13}} \right), \\
 U_{9n-7} &= U_{-7} \prod_{i=1}^n \left(\frac{F_{2i+1}U_{-7} + F_{2i}U_{-16}}{F_{2i}U_{-7} + F_{2i-1}U_{-16}} \right), \\
 U_{9n-3} &= U_{-3} \prod_{i=1}^n \left(\frac{F_{2i+1}U_{-3} + F_{2i}U_{-12}}{F_{2i}U_{-3} + F_{2i-1}U_{-12}} \right), \\
 U_{9n-6} &= U_{-6} \prod_{i=1}^n \left(\frac{F_{2i+1}U_{-6} + F_{2i}U_{-15}}{F_{2i}U_{-6} + F_{2i-1}U_{-15}} \right), \\
 U_{9n-2} &= U_{-2} \prod_{i=1}^n \left(\frac{F_{2i+1}U_{-2} + F_{2i}U_{-11}}{F_{2i}U_{-2} + F_{2i-1}U_{-11}} \right), \\
 U_{9n-5} &= U_{-5} \prod_{i=1}^n \left(\frac{F_{2i+1}U_{-5} + F_{2i}U_{-14}}{F_{2i}U_{-5} + F_{2i-1}U_{-14}} \right), \\
 U_{9n-1} &= U_{-1} \prod_{i=1}^n \left(\frac{F_{2i+1}U_{-1} + F_{2i}U_{-10}}{F_{2i}U_{-1} + F_{2i-1}U_{-10}} \right), \\
 U_{9n} &= U_0 \prod_{i=1}^n \left(\frac{F_{2i+1}U_0 + F_{2i}U_{-9}}{F_{2i}U_0 + F_{2i-1}U_{-9}} \right),
 \end{aligned} \tag{31}$$

where $\{F_i\}_{i=1}^{\infty} = \{1, 1, 2, 3, 5, \dots\}$ is the Fibonacci sequence.

Proof. We show that the expressions in (31) are solutions of (30) by applying mathematical induction. First, the results hold for $n = 0$. Second, we suppose that the forms are satisfied for $n - 1$ and $n - 2$. Now, we prove that the results are satisfied for n :

$$\begin{aligned}
 U_{9n-17} &= U_{-8} \prod_{i=1}^{n-1} \left(\frac{F_{2i+1}U_{-8} + F_{2i}U_{-17}}{F_{2i}U_{-8} + F_{2i-1}U_{-17}} \right), \\
 U_{9n-13} &= U_{-4} \prod_{i=1}^{n-1} \left(\frac{F_{2i+1}U_{-4} + F_{2i}U_{-13}}{F_{2i}U_{-4} + F_{2i-1}U_{-13}} \right), \\
 U_{9n-16} &= U_{-7} \prod_{i=1}^{n-1} \left(\frac{F_{2i+1}U_{-7} + F_{2i}U_{-16}}{F_{2i}U_{-7} + F_{2i-1}U_{-16}} \right), \\
 U_{9n-12} &= U_{-3} \prod_{i=1}^{n-1} \left(\frac{F_{2i+1}U_{-3} + F_{2i}U_{-12}}{F_{2i}U_{-3} + F_{2i-1}U_{-12}} \right),
 \end{aligned}$$

$$\begin{aligned}
 U_{9n-15} &= U_{-6} \prod_{i=1}^{n-1} \left(\frac{F_{2i+1}U_{-6} + F_{2i}U_{-15}}{F_{2i}U_{-6} + F_{2i-1}U_{-15}} \right), \\
 U_{9n-11} &= U_{-2} \prod_{i=1}^{n-1} \left(\frac{F_{2i+1}U_{-2} + F_{2i}U_{-11}}{F_{2i}U_{-2} + F_{2i-1}U_{-11}} \right), \\
 U_{9n-14} &= U_{-5} \prod_{i=1}^{n-1} \left(\frac{F_{2i+1}U_{-5} + F_{2i}U_{-14}}{F_{2i}U_{-5} + F_{2i-1}U_{-14}} \right), \\
 U_{9n-10} &= U_{-1} \prod_{i=1}^{n-1} \left(\frac{F_{2i+1}U_{-1} + F_{2i}U_{-10}}{F_{2i}U_{-1} + F_{2i-1}U_{-10}} \right), \\
 U_{9n-9} &= U_0 \prod_{i=1}^{n-1} \left(\frac{F_{2i+1}U_0 + F_{2i}U_{-9}}{F_{2i}U_0 + F_{2i-1}U_{-9}} \right), \\
 U_{9n-18} &= U_0 \prod_{i=1}^{n-2} \left(\frac{F_{2i+1}U_0 + F_{2i}U_{-9}}{F_{2i}U_0 + F_{2i-1}U_{-9}} \right), \\
 U_{9n-26} &= U_{-8} \prod_{i=1}^{n-2} \left(\frac{F_{2i+1}U_{-8} + F_{2i}U_{-17}}{F_{2i}U_{-8} + F_{2i-1}U_{-17}} \right), \\
 U_{9n-22} &= U_{-4} \prod_{i=1}^{n-2} \left(\frac{F_{2i+1}U_{-4} + F_{2i}U_{-13}}{F_{2i}U_{-4} + F_{2i-1}U_{-13}} \right), \\
 U_{9n-25} &= U_{-7} \prod_{i=1}^{n-2} \left(\frac{F_{2i+1}U_{-7} + F_{2i}U_{-16}}{F_{2i}U_{-7} + F_{2i-1}U_{-16}} \right), \\
 U_{9n-21} &= U_{-3} \prod_{i=1}^{n-2} \left(\frac{F_{2i+1}U_{-3} + F_{2i}U_{-12}}{F_{2i}U_{-3} + F_{2i-1}U_{-12}} \right), \\
 U_{9n-24} &= U_{-6} \prod_{i=1}^{n-2} \left(\frac{F_{2i+1}U_{-6} + F_{2i}U_{-15}}{F_{2i}U_{-6} + F_{2i-1}U_{-15}} \right), \\
 U_{9n-20} &= U_{-2} \prod_{i=1}^{n-2} \left(\frac{F_{2i+1}U_{-2} + F_{2i}U_{-11}}{F_{2i}U_{-2} + F_{2i-1}U_{-11}} \right), \\
 U_{9n-23} &= U_{-5} \prod_{i=1}^{n-2} \left(\frac{F_{2i+1}U_{-5} + F_{2i}U_{-14}}{F_{2i}U_{-5} + F_{2i-1}U_{-14}} \right), \\
 U_{9n-19} &= U_{-1} \prod_{i=1}^{n-2} \left(\frac{F_{2i+1}U_{-1} + F_{2i}U_{-10}}{F_{2i}U_{-1} + F_{2i-1}U_{-10}} \right).
 \end{aligned} \tag{32}$$

From (30), it follows that

$$\begin{aligned}
 U_{9n-1} &= U_{9n-10} + \frac{U_{9n-10}^2}{U_{9n-10} + U_{9n-19}}, \\
 &= U_{9n-10} \left(1 + \frac{U_{9n-10}}{U_{9n-10} + U_{9n-19}} \right), \\
 &= U_{9n-10} \left(1 + \frac{U_{-1} \prod_{i=1}^{n-1} ((F_{2i+1}U_{-1} + F_{2i}U_{-10}) / (F_{2i}U_{-1} + F_{2i-1}U_{-10}))}{U_{-1} \prod_{i=1}^{n-1} ((F_{2i+1}U_{-1} + F_{2i}U_{-10}) / (F_{2i}U_{-1} + F_{2i-1}U_{-10})) + U_{-1} \prod_{i=1}^{n-2} ((F_{2i+1}U_{-1} + F_{2i}U_{-10}) / (F_{2i}U_{-1} + F_{2i-1}U_{-10}))} \right), \\
 &= U_{9n-10} \left(1 + \frac{U_{-1} \prod_{i=1}^{n-2} ((F_{2i+1}U_{-1} + F_{2i}U_{-10}) / (F_{2i}U_{-1} + F_{2i-1}U_{-10})) [(F_{2n-1}U_{-1} + F_{2n-2}U_{-10}) / (F_{2n-2}U_{-1} + F_{2n-3}U_{-10})]}{U_{-1} \prod_{i=1}^{n-2} ((F_{2i+1}U_{-1} + F_{2i}U_{-10}) / (F_{2i}U_{-1} + F_{2i-1}U_{-10})) [(F_{2n-1}U_{-1} + F_{2n-2}U_{-10}) / (F_{2n-2}U_{-1} + F_{2n-3}U_{-10} + 1)]} \right), \\
 &= U_{9n-10} \left(1 + \frac{[(F_{2n-1}U_{-1} + F_{2n-2}U_{-10}) / (F_{2n-2}U_{-1} + F_{2n-3}U_{-10})]}{[(F_{2n-1}U_{-1} + F_{2n-2}U_{-10}) / (F_{2n-2}U_{-1} + F_{2n-3}U_{-10} + 1)]} \right), \\
 &= U_{9n-10} \left(1 + \frac{F_{2n-1}U_{-1} + F_{2n-2}U_{-10}}{F_{2n-1}U_{-1} + F_{2n-2}U_{-10} + F_{2n-2}U_{-1} + F_{2n-3}U_{-10}} \right), \\
 &= U_{9n-10} \left(1 + \frac{F_{2n-1}U_{-1} + F_{2n-2}U_{-10}}{(F_{2n-1} + F_{2n-2})U_{-1} + (F_{2n-2} + F_{2n-3})U_{-10}} \right), \\
 &= U_{9n-10} \left(1 + \frac{F_{2n-1}U_{-1} + F_{2n-2}U_{-10}}{F_{2n}U_{-1} + F_{2n-1}U_{-10}} \right), \\
 &= U_{9n-10} \left(\frac{(F_{2n-1} + F_{2n})U_{-1} + (F_{2n-2} + F_{2n-1})U_{-10}}{F_{2n}U_{-1} + F_{2n-1}U_{-10}} \right), \\
 &= U_{9n-10} \left(\frac{F_{2n+1}U_{-1} + F_{2n}U_{-10}}{F_{2n}U_{-1} + F_{2n-1}U_{-10}} \right), \\
 &= \left(U_{-1} \prod_{i=1}^{n-1} \left(\frac{F_{2i+1}U_{-1} + F_{2i}U_{-10}}{F_{2i}U_{-1} + F_{2i-1}U_{-10}} \right) \right) \left(\frac{F_{2n+1}U_{-1} + F_{2n}U_{-10}}{F_{2n}U_{-1} + F_{2n-1}U_{-10}} \right), \\
 &= U_{-1} \prod_{i=1}^n \left(\frac{F_{2i+1}U_{-1} + F_{2i}U_{-10}}{F_{2i}U_{-1} + F_{2i-1}U_{-10}} \right).
 \end{aligned}$$

(33)

Therefore,

$$\begin{aligned}
 U_{9n-1} &= U_{-1} \\
 &\cdot \prod_{i=1}^n \left(\frac{F_{2i+1}U_{-1} + F_{2i}U_{-10}}{F_{2i}U_{-1} + F_{2i-1}U_{-10}} \right). \quad (34)
 \end{aligned}$$

Similarly, one can investigate other expressions. The proof is done. \square

6.2. *Second Equation.* In this section, we introduce the solution of the following equation:

$$U_{n+1} = U_{n-8} + \frac{U_{n-8}^2}{U_{n-8} - U_{n-17}}. \quad (35)$$

Theorem 6. Let $\{U_n\}_{n=-17}^{\infty}$ be a solution of (35); then, for $n = 0, 1, \dots$,

$$\begin{aligned}
U_{9n-8} &= U_{-8} \prod_{i=1}^n \left(\frac{F_{2i+1}U_{-8} - F_{2i}U_{-17}}{F_{2i}U_{-8} - F_{2i-1}U_{-17}} \right), \\
U_{9n-4} &= U_{-4} \prod_{i=1}^n \left(\frac{F_{2i+1}U_{-4} - F_{2i}U_{-13}}{F_{2i}U_{-4} - F_{2i-1}U_{-13}} \right), \\
U_{9n-7} &= U_{-7} \prod_{i=1}^n \left(\frac{F_{2i+1}U_{-7} - F_{2i}U_{-16}}{F_{2i}U_{-7} - F_{2i-1}U_{-16}} \right), \\
U_{9n-3} &= U_{-3} \prod_{i=1}^n \left(\frac{F_{2i+1}U_{-3} - F_{2i}U_{-12}}{F_{2i}U_{-3} - F_{2i-1}U_{-12}} \right), \\
U_{9n-6} &= U_{-6} \prod_{i=1}^n \left(\frac{F_{2i+1}U_{-6} - F_{2i}U_{-15}}{F_{2i}U_{-6} - F_{2i-1}U_{-15}} \right), \\
U_{9n-2} &= U_{-2} \prod_{i=1}^n \left(\frac{F_{2i+1}U_{-2} - F_{2i}U_{-11}}{F_{2i}U_{-2} - F_{2i-1}U_{-11}} \right), \\
U_{9n-5} &= U_{-5} \prod_{i=1}^n \left(\frac{F_{2i+1}U_{-5} - F_{2i}U_{-14}}{F_{2i}U_{-5} - F_{2i-1}U_{-14}} \right), \\
U_{9n-1} &= U_{-1} \prod_{i=1}^n \left(\frac{F_{2i+1}U_{-1} - F_{2i}U_{-10}}{F_{2i}U_{-1} - F_{2i-1}U_{-10}} \right), \\
U_{9n} &= U_0 \prod_{i=1}^n \left(\frac{F_{2i+1}U_0 - F_{2i}U_{-9}}{F_{2i}U_0 - F_{2i-1}U_{-9}} \right),
\end{aligned} \tag{36}$$

where $\{F_i\}_{i=-1}^{\infty} = \{1, 0, 1, 1, 2, 3, 5, \dots\}$ is the Fibonacci sequence.

Proof. The proof will be the same as proof of Theorem 5, so it is therefore omitted. \square

6.3. Third Equation. In this section, we present the solution of the following equation:

$$U_{n+1} = U_{n-8} - \frac{U_{n-8}^2}{U_{n-8} + U_{n-17}}. \tag{37}$$

Theorem 7. Let $\{U_n\}_{n=-17}^{\infty}$ be a solution of (37); then, for $n = 0, 1, \dots$,

$$\begin{aligned}
U_{9n-8} &= \frac{U_{-8}U_{-17}}{F_nU_{-8} + F_{n+1}U_{-17}}, \\
U_{9n-4} &= \frac{U_{-4}U_{-13}}{F_nU_{-4} + F_{n+1}U_{-13}}, \\
U_{9n-7} &= \frac{U_{-7}U_{-16}}{F_nU_{-7} + F_{n+1}U_{-16}}, \\
U_{9n-3} &= \frac{U_{-3}U_{-12}}{F_nU_{-3} + F_{n+1}U_{-12}},
\end{aligned}$$

$$\begin{aligned}
U_{9n-6} &= \frac{U_{-6}U_{-15}}{F_nU_{-6} + F_{n+1}U_{-15}}, \\
U_{9n-2} &= \frac{U_{-2}U_{-11}}{F_nU_{-2} + F_{n+1}U_{-11}}, \\
U_{9n-5} &= \frac{U_{-5}U_{-14}}{F_nU_{-5} + F_{n+1}U_{-14}}, \\
U_{9n-1} &= \frac{U_{-1}U_{-10}}{F_nU_{-1} + F_{n+1}U_{-10}}, \\
U_{9n} &= \frac{U_0U_{-9}}{F_nU_0 + F_{n+1}U_{-9}},
\end{aligned} \tag{38}$$

where $\{F_i\}_{i=-1}^{\infty} = \{1, 0, 1, 1, 2, 3, 5, \dots\}$.

Proof. By using mathematical induction, we prove that (38) are solutions of (37). First, the results for $n = 0$ are true. Second, assume that the assumption holds for $n - 2$ and $n - 1$.

$$\begin{aligned}
U_{9n-17} &= \frac{U_{-8}U_{-17}}{F_{n-1}U_{-8} + F_nU_{-17}}, \\
U_{9n-13} &= \frac{U_{-4}U_{-13}}{F_{n-1}U_{-4} + F_nU_{-13}}, \\
U_{9n-16} &= \frac{U_{-7}U_{-16}}{F_{n-1}U_{-7} + F_nU_{-16}}, \\
U_{9n-12} &= \frac{U_{-3}U_{-12}}{F_{n-1}U_{-3} + F_nU_{-12}}, \\
U_{9n-15} &= \frac{U_{-6}U_{-15}}{F_{n-1}U_{-6} + F_nU_{-15}}, \\
U_{9n-11} &= \frac{U_{-2}U_{-11}}{F_{n-1}U_{-2} + F_nU_{-11}}, \\
U_{9n-14} &= \frac{U_{-5}U_{-14}}{F_{n-1}U_{-5} + F_nU_{-14}}, \\
U_{9n-10} &= \frac{U_{-1}U_{-10}}{F_{n-1}U_{-1} + F_nU_{-10}}, \\
U_{9n-9} &= \frac{U_0U_{-9}}{F_{n-1}U_0 + F_nU_{-9}}, \\
U_{9n-18} &= \frac{U_0U_{-9}}{F_{n-2}U_0 + F_{n-1}U_{-9}}, \\
U_{9n-26} &= \frac{U_{-8}U_{-17}}{F_{n-2}U_{-8} + F_{n-1}U_{-17}}, \\
U_{9n-22} &= \frac{U_{-4}U_{-13}}{F_{n-2}U_{-4} + F_{n-1}U_{-13}},
\end{aligned}$$

$$\begin{aligned}
 U_{9n-25} &= \frac{U_{-7}U_{-16}}{F_{n-2}U_{-7} + F_{n-1}U_{-16}}, \\
 U_{9n-21} &= \frac{U_{-3}U_{-12}}{F_{n-2}U_{-3} + F_{n-1}U_{-12}}, \\
 U_{9n-24} &= \frac{U_{-6}U_{-15}}{F_{n-2}U_{-6} + F_{n-1}U_{-15}}, \\
 U_{9n-20} &= \frac{U_{-2}U_{-11}}{F_{n-2}U_{-2} + F_{n-1}U_{-11}}, \\
 U_{9n-23} &= \frac{U_{-5}U_{-14}}{F_{n-2}U_{-5} + F_{n-1}U_{-14}}, \\
 U_{9n-19} &= \frac{U_{-1}U_{-10}}{F_{n-2}U_{-1} + F_{n-1}U_{-10}}.
 \end{aligned} \tag{39}$$

Now, from (37), we have

$$\begin{aligned}
 U_{9n-1} &= U_{9n-10} - \frac{U_{9n-10}^2}{U_{9n-10} + U_{9n-19}}, \\
 &= U_{9n-10} \left(1 - \frac{U_{9n-10}}{U_{9n-10} + U_{9n-19}} \right), \\
 &= U_{9n-10} \left(1 - \frac{(U_{-1}U_{-10}/(F_{n-1}U_{-1} + F_nU_{-10}))}{(U_{-1}U_{-10}/(F_{n-1}U_{-1} + F_nU_{-10})) + (U_{-1}U_{-10}/(F_{n-2}U_{-1} + F_{n-1}U_{-10}))} \right), \\
 &= U_{9n-10} \left(1 - \frac{(U_{-1}U_{-10}/(F_{n-1}U_{-1} + F_nU_{-10}))}{(U_{-1}U_{-10}/(F_{n-1}U_{-1} + F_nU_{-10})) [1 + (F_{n-1}U_{-1} + F_nU_{-10}/F_{n-2}U_{-1} + F_{n-1}U_{-10})]} \right), \\
 &= U_{9n-10} \left(1 - \frac{1}{[1 + (F_{n-1}U_{-1} + F_nU_{-10}/F_{n-2}U_{-1} + F_{n-1}U_{-10})]} \right), \\
 &= U_{9n-10} \left(1 - \frac{F_{n-2}U_{-1} + F_{n-1}U_{-10}}{[F_{n-2}U_{-1} + F_{n-1}U_{-10} + F_{n-1}U_{-1} + F_nU_{-10}]} \right) \tag{40} \\
 &= U_{9n-10} \left(1 - \frac{F_{n-2}U_{-1} + F_{n-1}U_{-10}}{F_nU_{-1} + F_{n+1}U_{-10}} \right), \\
 &= U_{9n-10} \left(\frac{(F_n - F_{n-2})U_{-1} + (F_{n+1} - F_{n-1})U_{-10}}{F_nU_{-1} + F_{n+1}U_{-10}} \right), \\
 &= U_{9n-10} \left(\frac{F_{n-1}U_{-1} + F_nU_{-10}}{F_nU_{-1} + F_{n+1}U_{-10}} \right), \\
 &= \left(\frac{U_{-1}U_{-10}}{F_{n-1}U_{-1} + F_nU_{-10}} \right) \left(\frac{F_{n-1}U_{-1} + F_nU_{-10}}{F_nU_{-1} + F_{n+1}U_{-10}} \right), \\
 &= \frac{U_{-1}U_{-10}}{F_nU_{-1} + F_{n+1}U_{-10}}.
 \end{aligned}$$

Thus,

$$U_{9n-1} = \frac{U_{-1}U_{-10}}{F_n U_{-1} + F_{n+1} U_{-10}}. \quad (41)$$

Similarly, one can see that the other forms are true. The proof is complete. \square

6.4. Fourth Equation. We study the following equation:

$$\begin{aligned} & \{U_{-17}, U_{-16}, U_{-15}, U_{-14}, U_{-13}, U_{-12}, U_{-11}, U_{-10}, U_{-9}, U_{-8}, U_{-7}, \\ & U_{-6}, U_{-5}, U_{-4}, U_{-3}, U_{-2}, U_{-1}, U_0, \frac{U_{-8}U_{-17}}{U_{-8} - U_{-17}}, \frac{U_{-7}U_{-16}}{U_{-7} - U_{-16}}, \frac{U_{-6}U_{-15}}{U_{-6} - U_{-15}}, \frac{U_{-5}U_{-14}}{U_{-5} - U_{-14}}, \\ & -\frac{U_{-4}U_{-13}}{U_{-4} - U_{-13}}, -\frac{U_{-3}U_{-12}}{U_{-3} - U_{-12}}, -\frac{U_{-2}U_{-11}}{U_{-2} - U_{-11}}, -\frac{U_{-1}U_{-10}}{U_{-1} - U_{-10}}, -\frac{U_0U_{-9}}{U_0 - U_{-9}}, -U_{-17}, -U_{-16}, \\ & -U_{-15}, -U_{-14}, -U_{-13}, -U_{-12}, -U_{-11}, -U_{-10}, \\ & -U_{-9}, -U_{-8}, -U_{-7}, -U_{-6}, -U_{-5}, -U_{-4}, -U_{-3}, -U_{-2}, -U_{-1}, -U_0, \\ & \frac{U_{-8}U_{-17}}{U_{-8} - U_{-17}}, \frac{U_{-7}U_{-16}}{U_{-7} - U_{-16}}, \frac{U_{-6}U_{-15}}{U_{-6} - U_{-15}}, \frac{U_{-5}U_{-14}}{U_{-5} - U_{-14}}, \frac{U_{-4}U_{-13}}{U_{-4} - U_{-13}}, \frac{U_{-3}U_{-12}}{U_{-3} - U_{-12}}, \frac{U_{-2}U_{-11}}{U_{-2} - U_{-11}}, \frac{U_{-1}U_{-10}}{U_{-1} - U_{-10}}, \\ & \frac{U_0U_{-9}}{U_0 - U_{-9}}, U_{-17}, U_{-16}, U_{-15}, U_{-14}, U_{-13}, U_{-12}, U_{-11}, U_{-10}, \\ & U_{-9}, U_{-8}, U_{-7}, U_{-6}, U_{-5}, U_{-4}, U_{-3}, U_{-2}, U_{-1}, U_0, \dots\}. \end{aligned} \quad (43)$$

Proof. The proof of this case will be the same as the proof presented for Theorem 7 and will be omitted therefore. \square

7. Numerical Examples

To illustrate the solution behavior of (7) for various cases, we present some numerical examples.

Example 1. To show the stability of (7), we set two groups for the values of the coefficients: (i) $\xi = 0.5$, $\varepsilon = 0.1$, $\mu = 1.6$, and $\kappa = 0.2$ and (ii) $\xi = 0.5$, $\varepsilon = 5$, $\mu = 10$, and $\kappa = 0.001$, and the initial conditions are

$$\begin{aligned} U_{-17} &= 0.1, \\ U_{-16} &= 0.2, \\ U_{-15} &= 0.3, \\ U_{-14} &= 0.4, \\ U_{-13} &= 0.5, \\ U_{-12} &= 0.6, \\ U_{-11} &= 0.7, \\ U_{-10} &= 0.8, \end{aligned}$$

$$\begin{aligned} U_{-9} &= 0.9, \\ U_{-8} &= 1.2, \\ U_{-7} &= 1.5, \\ U_{-6} &= 2.2, \\ U_{-5} &= 2.3, \\ U_{-4} &= 2.5, \\ U_{-3} &= 4.2, \\ U_{-2} &= 4.6, \\ U_{-1} &= 4.8, \end{aligned} \quad (44)$$

and $U_0 = 5.2$. The result is obtained in Figure 1. It is clear that (i) condition (23) is satisfied, which implies that the solution tends to the fixed point $\bar{U} = 0$, while the solution moves away from the fixed point for (ii) since condition (23) failed.

The following examples have explained the solutions of special case equations (30)–(42).

Example 2. We choose the initial conditions as

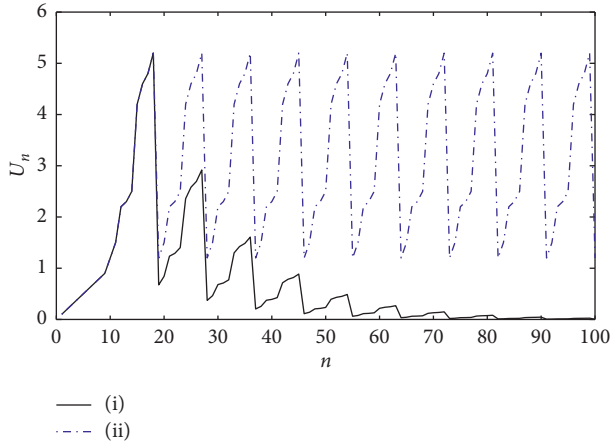


FIGURE 1: Plotting the solution of $U_{n+1} = \xi U_{n-8} + (\epsilon U_{n-8}^2 / \mu U_{n-8} + \kappa U_{n-17})$.

$$\begin{aligned}
 U_{-17} &= 0.01, \\
 U_{-16} &= 0.02, \\
 U_{-15} &= 0.03, \\
 U_{-14} &= 0.04, \\
 U_{-13} &= 0.05, \\
 U_{-12} &= 0.06, \\
 U_{-11} &= 0.07, \\
 U_{-10} &= 0.08, \\
 U_{-9} &= 0.09, \\
 U_{-8} &= 1.02, \\
 U_{-7} &= 1.05, \\
 U_{-6} &= 2.02, \\
 U_{-5} &= 2.03, \\
 U_{-4} &= 2.05, \\
 U_{-3} &= 4.02, \\
 U_{-2} &= 4.06, \\
 U_{-1} &= 4.08,
 \end{aligned}$$

(45)

and $U_0 = 5.02$. The solution is given in Figure 2.

Example 3. In Figure 3, we set the initial conditions:

$$\begin{aligned}
 U_{-17} &= 0.01, \\
 U_{-16} &= 0.02, \\
 U_{-15} &= 0.03, \\
 U_{-14} &= 0.04, \\
 U_{-13} &= 0.05, \\
 U_{-12} &= 0.06,
 \end{aligned}$$

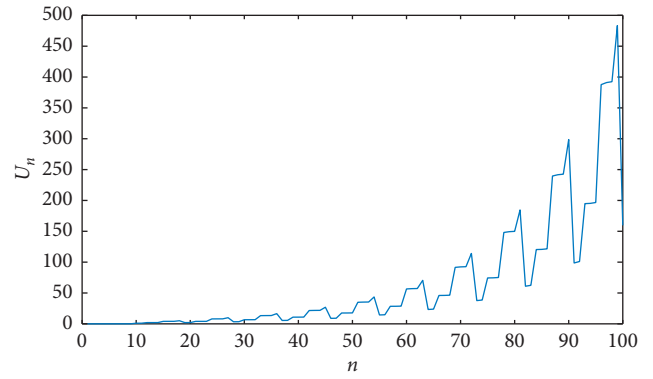


FIGURE 2: Plotting of the solution of $U_{n+1} = U_{n-8} + (U_{n-8}^2 / U_{n-8} + U_{n-17})$.

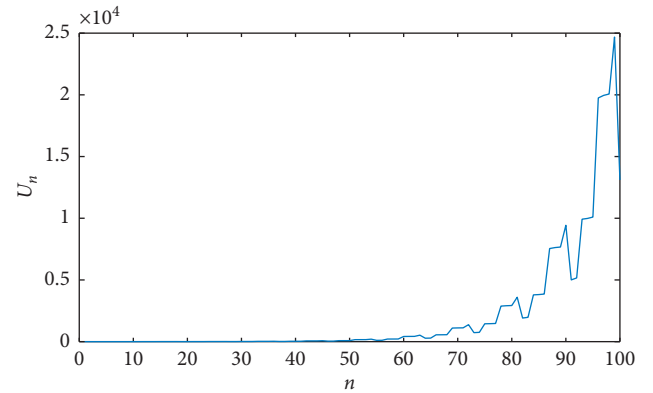


FIGURE 3: The solution behavior of $U_{n+1} = U_{n-8} + (U_{n-8}^2 / U_{n-8} - U_{n-17})$.

$$\begin{aligned}
 U_{-11} &= 0.07, \\
 U_{-10} &= 0.08, \\
 U_{-9} &= 0.09, \\
 U_{-8} &= 1.02, \\
 U_{-7} &= 1.05, \\
 U_{-6} &= 2.02, \\
 U_{-5} &= 2.03, \\
 U_{-4} &= 2.05, \\
 U_{-3} &= 4.02, \\
 U_{-2} &= 4.06, \\
 U_{-1} &= 4.08, \\
 U_0 &= 5.02.
 \end{aligned}$$

(46)

Example 4. For (37), we choose the initial conditions as

$$\begin{aligned}
 U_{-17} &= 2, \\
 U_{-16} &= 2.1, \\
 U_{-15} &= 2.2, \\
 U_{-14} &= 2.3, \\
 U_{-13} &= 2.4, \\
 U_{-12} &= 2.5, \\
 U_{-11} &= 2.6, \\
 U_{-10} &= 2.7, \\
 U_{-9} &= 2.8, \\
 U_{-8} &= 3, \\
 U_{-7} &= 3.1, \\
 U_{-6} &= 3.2, \\
 U_{-5} &= 3.3, \\
 U_{-4} &= 3.4, \\
 U_{-3} &= 3.5, \\
 U_{-2} &= 3.6, \\
 U_{-1} &= 3.7, \\
 U_0 &= 3.8,
 \end{aligned}$$

(47)

and then, the result is shown in Figure 4.

Example 5. We set the values

$$\begin{aligned}
 U_{-17} &= 0.01, \\
 U_{-16} &= 0.02, \\
 U_{-15} &= 0.03, \\
 U_{-14} &= 0.04, \\
 U_{-13} &= 0.05, \\
 U_{-12} &= 0.06, \\
 U_{-11} &= 0.07, \\
 U_{-10} &= 0.08, \\
 U_{-9} &= 0.09, \\
 U_{-8} &= 1.02, \\
 U_{-7} &= 1.05, \\
 U_{-6} &= 2.02, \\
 U_{-5} &= 2.03, \\
 U_{-4} &= 2.05, \\
 U_{-3} &= 4.02, \\
 U_{-2} &= 4.06, \\
 U_{-1} &= 4.08, \\
 U_0 &= 5.02.
 \end{aligned}$$

(48)

The solution is given in Figure 5. Clearly, the solution is periodic that means the result conforms with Theorem 8.

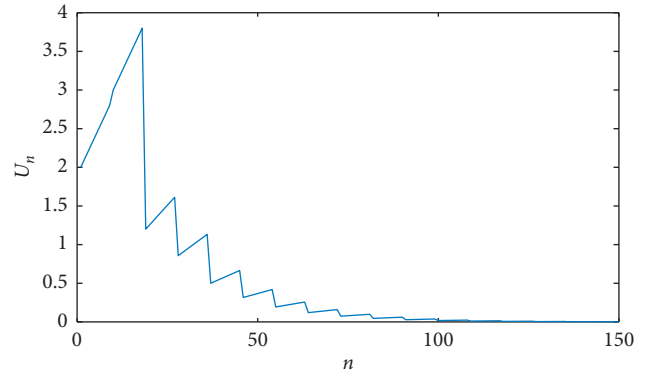


FIGURE 4: The solution behavior of $U_{n+1} = U_{n-8} - (U_{n-8}^2 / (U_{n-8} + U_{n-17}))$.

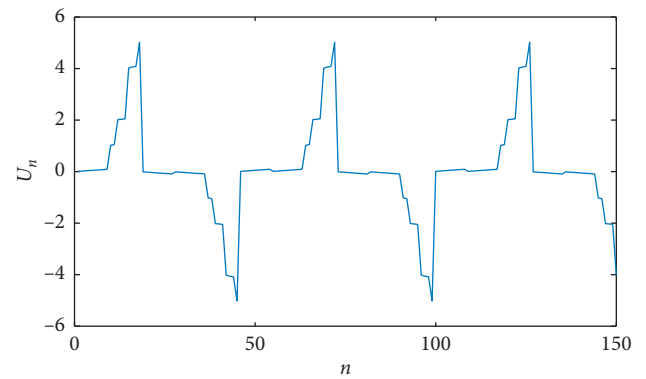


FIGURE 5: Plotting the solution of $U_{n+1} = U_{n-8} - (U_{n-8}^2 / (U_{n-8} - U_{n-17}))$.

Data Availability

The data used to support the findings of the study are included within the article.

Conflicts of Interest

The authors declare that they have no conflicts of interest.

References

- [1] M. Dayeh, G. Livadiotis, and S. Elaydi, "A discrete mathematical model for the aggregation of β -Amyloid," *Plos One*, vol. 135, pp. 1-13, 2018.
- [2] S. Georgiev, "Asymptotic behaviour of the solutions of a class of $(k + 1)$ -order rational difference equations," *Sarajevo Journal of Mathematics*, vol. 16, pp. 237-244, 2020.
- [3] M. Kerker and A. Bouaziz, "On the global behavior of a higher-order nonautonomous rational difference equation," *Electronic Journal of Mathematical Analysis and Applications*, vol. 9, pp. 302-309, 2021.
- [4] S. Moranjkic and Z. Nurkanovic, "Local and global dynamics of certain second-order rational difference equations containing quadratic terms," *Advances in Dynamical Systems and Applications*, vol. 12, pp. 123-157, 2017.
- [5] K. Liu, P. Li, F. Han, and W. Zhong, "Global dynamics of nonlinear difference equation $x_{n+1} = A + (x_n/x_{n-1}x_{n-2})$,"

- Journal of Computational Analysis and Applications*, vol. 24, pp. 1125–1132, 2018.
- [6] E. M. Elsayed, F. Alzahrani, F. Abbas, and N. H. Alotaibi, “Dynamical behavior and solution of nonlinear difference equation via Fibonacci sequence,” *Journal of Applied Analysis & Computation*, vol. 10, no. 1, pp. 282–296, 2020.
 - [7] M. Kara and Y. Yazlik, “On a solvable system of non-linear difference equations with variable coefficients,” *Journal of Science and Arts*, vol. 21, no. 1, pp. 145–162, 2021.
 - [8] F. Şahinkaya, İ. Yaşınkaya, and D. Tollu, “A solvable system of nonlinear difference equations,” *Ikonion Journal of Mathematics*, vol. 2, pp. 10–20, 2020.
 - [9] S. Stević, “New class of solvable systems of difference equations,” *Applied Mathematics Letters*, vol. 63, pp. 137–144, 2017.
 - [10] S. Stević, “Solvability of a general class of two-dimensional hyperbolic-cotangent-type systems of difference equations,” *Advances in Difference Equations*, vol. 294, pp. 1–34, 2019.
 - [11] D. T. Tollu, Y. Yazlik, and N. Taşkara, “On a solvable non-linear difference equation of higher order,” *Turkish Journal of Mathematics*, vol. 42, no. 4, pp. 1765–1778, 2018.
 - [12] M. Saleh and A. Farhat, “Global asymptotic stability of the higher order equation $x_{n+1} = \frac{ax_n + bx_{n-k}}{A + Bx_n + Cx_{n-k}}$,” *Journal of Applied Mathematics and Computing*, vol. 55, no. 1-2, pp. 135–148, 2017.
 - [13] L. Jia, “Dynamic behaviors of a class of high-order fuzzy difference equations,” *Journal of Mathematics*, vol. 2020, Article ID 1737983, 13 pages, 2020.
 - [14] M. A. Kerker, E. Hadidi, and A. Salmi, “Qualitative behavior of a higher-order nonautonomous rational difference equation,” *Journal of Applied Mathematics and Computing*, vol. 64, no. 1-2, pp. 399–409, 2020.
 - [15] A. Khaliq and E. Elsayed, “Qualitative properties of difference equation of order six,” *Mathematics*, vol. 24, pp. 1–14, 2016.
 - [16] M. Saleh, N. Alkouni, and A. Farhat, “On the dynamics of a rational difference equation $x_{n+1} = ((\alpha + \beta x_n + \gamma x_{n-k}) / (Bx_n + Cx_{n-k}))$,” *Chaos, Solitons and Fractals*, vol. 96, pp. 76–84, 2017.
 - [17] S. Sadiq and M. Kalim, “Global attractivity of a rational difference equation of order twenty,” *International Journal of Advanced and Applied Sciences*, vol. 5, no. 2, pp. 1–7, 2018.
 - [18] R. Abo-Zeid, “Behavior of solutions of a second order rational difference equation,” *Mathematica Moravica*, vol. 23, no. 1, pp. 11–25, 2019.
 - [19] M. Abu Alhalawa and M. Saleh, “Dynamics of higher order rational difference equation $x_{n+1} = ((\alpha + \beta x_n) / (A + Bx_n + Cx_{n-k}))$,” *International Journal of Nonlinear Analysis and Application*, vol. 8 2, pp. 363–379, 2017.
 - [20] H. Alayachi, M. Noorani, and E. Elsayed, “Qualitative analysis of a fourth difference equation,” *Journal of Applied Analysis and Computation*, vol. 10 4, pp. 343–1354, 2020.
 - [21] A. Asiri, M. El-Dessoky, and E. Elsayed, “Solution of a third order fractional system of difference equations,” *Journal of Computational Analysis and Applications*, vol. 243, pp. 444–453, 2018.
 - [22] E. M. Elsayed, “Dynamics and behavior of a higher order rational difference equation,” *Journal of Nonlinear Sciences and Applications*, vol. 09, no. 04, pp. 1463–1474, 2016.
 - [23] E. M. Elsayed and A. M. Ahmed, “Dynamics of a three-dimensional systems of rational difference equations,” *Mathematical Methods in The Applied Sciences*, vol. 39, no. 5, pp. 1026–1038, 2016.
 - [24] E. Elsayed, A. Alotaibi, and H. Almaylubi, “On a solutions of fourth order rational systems of difference equations,” *Journal of Computational Analysis and Applications*, vol. 227, pp. 1298–1308, 2017.
 - [25] E. M. Elsayed, F. Alzahrani, and F. Alzahrani, “Periodicity and solutions of some rational difference equations systems,” *Journal of Applied Analysis & Computation*, vol. 9, no. 6, pp. 2358–2380, 2019.
 - [26] E. Elsayed, F. Alzahrani, and H. Alayachi, “Formulas and properties of some class of nonlinear difference equations,” *Journal of Computational Analysis and Applications*, vol. 24, pp. 1517–1531, 2018.
 - [27] E. Elsayed, F. Alzahrani, and H. Alayachi, “Global attractivity and the periodic nature of third order rational difference equation,” *Journal of Computational Analysis and Applications*, vol. 237, pp. 1230–1241, 2017.
 - [28] M. Gumus, R. Abo-Zeid, and O. Ocalan, “Dynamical behavior of a third-order difference equation with arbitrary powers,” *Kyungpook Mathematical Journal*, vol. 57, pp. 251–263, 2017.
 - [29] Y. Halim and J. F. T. Rabago, “On the solutions of a second-order difference equation in terms of generalized Padovan sequences,” *Mathematica Slovaca*, vol. 68, no. 3, pp. 625–638, 2018.
 - [30] L. Huang, G. Wu, D. Baleanu, and H. Wang, “Discrete fractional calculus for interval-valued systems,” *Fuzzy Sets and Systems*, vol. 404, pp. 141–158, 2021.
 - [31] A. Khaliq and E. Elsayed, “Qualitative study of a higher order rational difference equation,” *Hacettepe Journal of Mathematics and Statistics*, vol. 47, pp. 1128–1143, 2018.
 - [32] A. Q. Khan and S. M. Qureshi, “Dynamical properties of some rational systems of difference equations,” *Mathematical Methods in the Applied Sciences*, vol. 44, pp. 3485–3508, 2021.
 - [33] M. Kulenovic, S. Moranjkic, M. Nurkanovic, and Z. Nurkanovic, “Global asymptotic stability and Naimark-Sacker bifurcation of certain mix monotone difference equation,” *Discrete Dynamics in Nature and Society*, vol. 2018, Article ID 7052935, 22 pages, 2018.
 - [34] O. Moaaz, G. Chatzarakis, D. Chalishajar, and O. Bazighifan, “Dynamics of general class of difference equations and population model with two age classes,” *Mathematics*, vol. 516, pp. 1–13, 2020.
 - [35] S. H. Saker, M. M. Abuelwafa, A. M. Zidan, and D. Baleanu, “On Cesàro and Copson sequence spaces with weights,” *Journal of Inequalities and Applications*, vol. 2021, pp. 1–23, 2021.
 - [36] A. Sanbo, E. M. Elsayed, and F. Alzahrani, “Dynamics of the nonlinear rational difference equation $x_{n+1} = \frac{A\{x_{n-\alpha}\}x_{n-\beta} + B\{x_{n-\gamma}\}}{C\{x_{n-\alpha}\}x_{n-\beta} + D\{x_{n-\gamma}\}}$,” *Indian Journal of Pure and Applied Mathematics*, vol. 50, no. 2, pp. 385–401, 2019.
 - [37] D. Simsek, B. Ogul, and C. Cinar, “Solution of the rational difference equation $x_{n+1} = (x_{n-17} / (1 + x_{n-5}x_{n-11}))$,” *Filomat*, vol. 33, pp. 1353–1359, 2019.
 - [38] D. Simsek, B. Ogul, and F. Abdullayev, “Solutions of the rational difference equations $x_{n+1} = x_n - 11 + x_n - 2x_n - 5x_n - 8$,” in *Proceedings of the International Conference “Functional Analysis in Interdisciplinary Applications” (FAIA2017)*, Astana, Kazakhstan, October 2017.
 - [39] S. Stević, M. Alghamdi, A. Alotaibi, and E. Elsayed, “On a class of solvable higher-order difference equations,” *Filomat*, vol. 31, no. 2, pp. 461–477, 2017.
 - [40] N. Taskara, D. Tollu, N. Touafek, and Y. Yazlik, “A solvable system of difference equations,” *Communications of The Korean Mathematical Society*, vol. 35, pp. 301–319, 2020.
 - [41] E. Tasdemir, “On the global asymptotic stability of a system of difference equations with quadratic terms,” *Journal of Applied Mathematics and Computing*, vol. 66, 2020.

- [42] Y. Yazlik and M. Kara, "On a solvable system of difference equations of higher-order with period two coefficients," *Communications Faculty Of Science University of Ankara Series Mathematics and Statistics*, vol. 68, pp. 1675–1693, 2019.
- [43] B. Ogul and D. Simsek, "Solution of rational difference equation," *Journal of Mathematical Analysis*, vol. 11, pp. 32–43, 2020.
- [44] S. Elaydi, "An introduction to difference equation," *Undergraduate Texts in Mathematics*, Springer, New York, NY, USA, 2005.